

NASA Contractor Report 168277

(NASA-CR-168277) DEPOSIT FORMATION AND HEAT
TRANSFER IN HYDROCARBON ROCKET FUELS Final
Progress Report, Jul. 1982 - May 1983
(United Technologies Corp.) 170 p
HC A08/MF A01

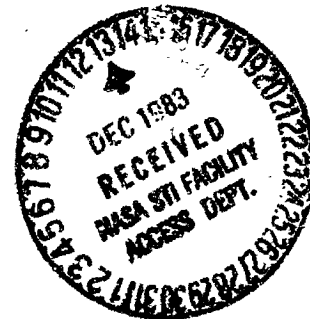
N84-12225

Unclass

CSCD 21H G3/20 42556

Deposit Formation and Heat Transfer in Hydrocarbon Rocket Fuels

Anthony J. Giovanetti
Louis J. Spadaccini
Eugene J. Szetela



UNITED TECHNOLOGIES RESEARCH CENTER
East Hartford, CT 06108

October 1983



National Aeronautics and
Space Administration

Lewis Research Center
Cleveland, Ohio 44135

1. Report No. NASA CR-168277	2. Government Accession No.	3. Recipient's Catalog No.	
4. Title and Subtitle Deposit Formation and Heat Transfer in Hydrocarbon Rocket Fuels		5. Report Date October 1983	
		6. Performing Organization Code	
7. Author(s) Anthony J. Giovanetti, Louis J. Spadaccini, Eugene I. Szerels		8. Performing Organization Report No. R83-956152-10	
		10. Work Unit No.	
9. Performing Organization Name and Address United Technologies Research Center Silver Lane East Hartford, CT 06108		11. Contract or Grant No. NAS3-23344	
		13. Type of Report and Period Covered Final Progress Report 7/82-5/83	
12. Sponsoring Agency Name and Address National Aeronautics and Space Administration Washington, D.C. 20546		14. Sponsoring Agency Code YOS8912	
		15. Supplementary Notes NASA-Lewis Research Center, Cleveland, OH 44135 Project Manager, Philip A. Masters	
16. Abstract An experimental research program was undertaken to investigate the thermal stability and heat transfer characteristics of several hydrocarbon fuels under conditions that simulate high-pressure, rocket engine cooling systems. The rates of carbon deposition in heated copper and nickel-plated copper tubes were determined for RP-1, propane, and natural gas using a continuous flow test apparatus which permitted independent variation and evaluation of the effect on deposit formation of wall temperature, fuel pressure, and fuel velocity. In addition, the effects of fuel additives and contaminants, cryogenic fuel temperatures, and extended duration testing with intermittent operation were examined. Parametric tests to map the thermal stability characteristics of RP-1, commercial-grade propane, and natural gas were conducted at pressures of 6.9 to 13.8 MPa, bulk fuel velocities of 30 to 90 m/s, and tube wall temperatures in the range of 230 to 810 K. Also, tests were run in which propane and natural gas fuels were chilled to 230 and 160 K, respectively. Corrosion of the copper tube surface was detected for all fuels tested. Plating the inside of the copper tubes with nickel reduced deposit formation and eliminated tube corrosion in most cases. The lowest rates of carbon deposition were obtained for natural gas, and the highest rates were obtained for propane. For all fuels tested, the forced-convection heat transfer film coefficients were satisfactorily correlated using a Nusselt-Reynolds-Prandtl number equation.			
17. Key Words (Suggested by Author(s)) Thrust chamber cooling; hydrocarbon rocket coolants; hydrocarbon fuel thermal decomposition; hydrocarbon rocket fuel stability; deposit formation; carbon formation rates; heat transfer.		18. Distribution Statement Unclassified-Unlimited	
19. Security Classif. (of this report) Unclassified	20. Security Classif. (of this page) Unclassified	21. No. of Pages 166	22. Price*

* For sale by the National Technical Information Service, Springfield, Virginia 22161

Deposit Formation and Heat Transfer in Hydrocarbon Rocket Fuels

TABLE OF CONTENTS

	<u>Page</u>
FOREWORD	i
SUMMARY	1
INTRODUCTION	3
BACKGROUND	5
Mechanisms for Deposit Formation	5
Chemistry of Deposit Forming Processes	5
Empirical Correlations	8
Catalytic Effect of Metals	9
Background Summary	9
EXPERIMENTAL APPARATUS AND TEST PROCEDURES	11
Fuels Characterization and Pretreatment	11
Test Facility and Test Procedures	13
Data Analysis	19
EXPERIMENTAL RESULTS AND DISCUSSION	24
RP-1 Tests	24
Propane Tests	27
Natural Gas Tests	32
Deposit Morphology	35
Heat Transfer Correlation Analyses	38
Hydrostatic Burst Tests	39
CONCLUDING REMARKS	41
REFERENCES	43
LIST OF SYMBOLS	46
TABLES	
FIGURES	
APPENDIX A - TABULATED TEST DATA	A-1

FOREWORD

This research was conducted under Contract NAS3-23344 from NASA-Lewis Research Center, Philip A. Masters, Project Manager. Additional support for heat transfer correlation analyses was provided by United Technologies Research Center as part of a Corporate-sponsored IR&D program. The authors acknowledge research engineer John TeVelde and laboratory technicians Bruce S. True and David Terza for their assistance in this program.

Deposit Formation and Heat Transfer in Hydrocarbon Rocket Fuels

A. J. Giovanetti
L. J. Spaccini
E. J. Szetela

SUMMARY

An experimental research program was undertaken to investigate the thermal stability and heat transfer characteristics of several hydrocarbon fuels under conditions that simulate high-pressure, rocket engine cooling systems. The rates of carbon deposition in heated copper and nickel-plated copper tubes were determined for RP-1, propane, and natural gas using a continuous flow test apparatus which permitted independent variation and evaluation of the effect on deposit formation of wall temperature, fuel pressure, and fuel velocity. In addition, the effects of fuel additives and contaminants, cryogenic fuel temperatures, and extended duration testing with intermittent operation were examined.

Parametric tests to map the thermal stability characteristics of RP-1, commercial-grade propane, and natural gas were conducted at pressures of 6.9 to 13.8 MPa, bulk fuel velocities of 30 to 90 m/s, and tube wall temperatures in the range of 230 to 810 K. Tests were performed in which RP-1 base fuel was either doped with an additive designed to inhibit copper migration, or contaminated with two representative sulfur compounds. Also, tests were run in which propane and natural gas fuels were chilled to 230 and 160 K, respectively.

Corrosion of the copper tube surface was detected for all fuels tested, possibly due to reactions with the trace sulfur impurities present in the fuel. Plating the inside of the copper tubes with nickel reduced deposit formation and eliminated tube corrosion in most cases. Doping RP-1 fuel with a commercially-produced metal deactivator resulted in a significant reduction in the levels of deposit formed. Also, for short test durations (< 30 min), the rates of deposit formation decreased as test time increased. Chilling the propane fuel prior to entry into the heated tube significantly reduced deposit

formation rates. Cryogenic cooling of natural gas (97 percent methane) did not significantly reduce deposit formation. At a given wall temperature and fuel velocity, carbon deposition rates for propane in copper tubes were highest and ranged from 300 to 580 $\mu\text{g}/\text{cm}^2\text{-hr}$ at wall temperatures between 400 and 580 K. The lowest rates of carbon deposition were obtained for natural gas in copper tubes and did not exceed 80 $\mu\text{g}/\text{cm}^2\text{-hr}$ at wall temperatures between 500 and 650 K. Carbon deposition rates of 200 to 320 $\mu\text{g}/\text{cm}^2\text{-hr}$ were typical for RP-1 in copper tubes at wall temperatures between 560 and 750 K.

For all fuels tested, multiple linear regression correlation analyses were performed to correlate experimentally-measured fuel-side heat transfer film coefficients with Nusselt-Reynolds-Prandtl number expressions for a Nusselt number range of 100 to 10,000. In addition, total deposit thermal resistances which ranged from 0.001 to 1.0 $\text{K}\text{-cm}^2/\text{W}$ were computed at the end of each test. Together, these two pieces of information can be used to predict the heat transfer characteristics of a rocket engine cooling system in the presence of deposit formation.

INTRODUCTION

In an effort to increase the performance of hydrocarbon/liquid oxygen rocket engines for space booster or orbit transportation systems, (i.e., to reduce weight and increase specific impulse) combustion pressures as high as practical are desirable. However, increased combustion pressure leads to a nearly proportionate increase in wall heat flux in the thrust chamber, and therefore, greater stress is placed on the design of the regenerative cooling system. Regenerative cooling with hydrocarbon fuels is feasible up to a point where the coolant wall temperature reaches a limit defined by a thermal decomposition or "coking" temperature. Deposit formation on the coolant wall surface, which usually occurs when the thermal decomposition temperature is reached, causes an increased thermal resistance, leading to a progressively increasing wall temperature and, ultimately, failure.

In the previous phase of this program (Ref. 1), an experimental effort was initiated to study deposit formation in hydrocarbon fuels under flow conditions that exist in high-pressure, rocket engine cooling systems. A fuel coking test apparatus was designed and developed and was used to evaluate the carbon deposition rates in heated copper tubes for two hydrocarbon rocket fuels, RP-1 and commercial-grade propane. Also, tests were conducted using JP-7 and chemically-pure propane as being representative of more refined cuts of the baseline fuels. The results indicated that substantial deposit formation occurred in ten minute tests with RP-1 fuel at wall temperatures between 600 and 800 K, with peak deposit formation occurring at wall temperatures near 700 K. Relatively high carbon deposition rates of between 200 and 600 $\mu\text{g}/\text{cm}^2\text{-hr}$ were observed for RP-1, and the rate of deposit formation increased slightly with pressure over the range 13.8 to 34.5 MPa. In preliminary tests, plating the inside wall of the tubes with nickel was found to significantly reduce carbon deposition rates for RP-1 fuel. No improvements were obtained when deoxygenated JP-7 fuel was substituted for RP-1.

The carbon deposition rates for the propane fuels were generally higher than those obtained for either of the kerosene fuels at any given wall temperature. Deposits were found with propane at a wall temperature as low as 420 K. However, the migration and interdiffusion of copper and carbon in the form of dendritic formations which appeared to grow out of the copper surface improved heat transfer from the tube to the fuel and suppressed any significant thermal resistance buildup. Severe wall temperature instability was experienced when the heat flux was raised to increase the wall temperature above 420 K, allowing the bulk temperature of the propane to pass through a value corresponding to the maximum point of inflection in the specific heat

vs. temperature curve. There appeared to be little difference between commercial-grade and chemically-pure propane with regard to type and quantity of deposit for wall temperatures between 400 and 600 K.

The objective of this investigation was to extend the available data base for deposit formation in hydrocarbon fuels under conditions that exist in high-pressure rocket engine cooling systems. Experiments were conducted to evaluate the rates of carbon deposition in electrically-heated tubes for RP-1, commercial propane, and natural gas for a range of fuel pressures, flow velocities, and tube wall temperatures. In addition, the effects on fuel thermal stability of variations in tube material, extended duration testing with intermittent operation, fuel additives and contaminants, and cryogenic fuel temperatures were examined. The method of approach to accomplish these tasks consisted of (1) characterizing each test fuel with respect to its chemical composition and physical properties, (2) modifying and fabricating components for an existing heated-tube test facility, (3) thermally stressing each test fuel in accordance with a prescribed matrix of operating conditions, and (4) characterizing the deposit thermal resistance and levels of carbon deposition observed in the experiments.

The organization of this report is as follows: First, a background section is presented which discusses possible mechanisms for deposit formation and the empirical correlations used to relate deposit formation rate with fuel composition. The experimental apparatus and procedures used in this program are then presented, followed by presentation and discussion of the experimental results. The last section of this report summarizes the important conclusions drawn from the program. A complete listing of all the test data acquired, including calculated parameters, is presented in the Appendix.

BACKGROUND

Mechanisms for Deposit Formation

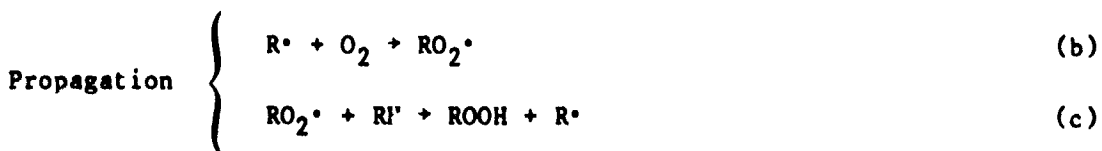
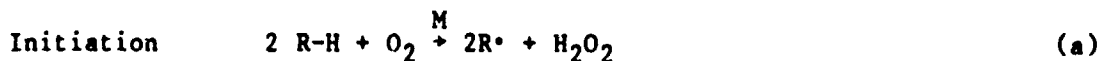
The rate of formation of deposits on heated walls in contact with flowing hydrocarbon fuels has been found by a number of investigators (Ref. 2) to vary with temperature in a unique manner as shown in Fig. 1. The Region A is characterized by the presence of oxidation products in the fuel stream and oxygen in the deposits. The Region B is characterized by the pyrolysis of hydrocarbon molecules and the scission of hydrogen. The reaction mechanism in the region between A and B, which is characterized by a decreasing deposit formation rate, is not well understood, and any effort to explain the behavior of fuel in that region would prove to be conjecture. Most of the available deposit formation data obtained from kerosene-type fuels flowing in tubes falls into either Region A or the negative-slope region between A and B. Furthermore, reactions can be accelerated if the passage surfaces are made of reactive or catalytic metals.

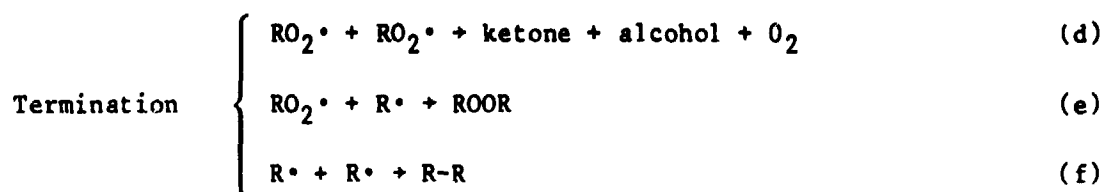
In the previous phase of this program (Ref. 1), deposit thermal resistance were shown to be strong functions of wall temperature in Region A. Also, deposit formation rate and thermal resistance decreased with increasing velocity. These trends indicate that the deposit forming mechanisms tend to be limited by the chemical kinetics of the deposition reaction rather than by diffusion. The higher shear resulting from increased velocity may have served only to promote washing away of deposit from the tube wall.

Chemistry of Deposit-Forming Processes

The detailed chemical reactions that result in fuel deposits are very complex and not well understood at present. It is widely agreed, however, that they usually begin with oxidation of the fuel, which is promoted by dissolved air. The fuel/oxygen reaction, which involves free radical chains, is termed autoxidation. Common impurities such as compounds of sulfur, nitrogen, and metals enter and accelerate the reactions.

The following chain reaction mechanism is usually cited to describe hydrocarbon autoxidation (Ref. 3):





Reaction (a) forms an alkyl free radical (R•), in most cases with the aid of a surface. The propagation steps (b) and (c) carry the chain to a stable product, a hydroperoxide. Reaction (b) is relatively fast and Reaction (c) is normally rate controlling. At low oxygen concentrations (1 to 20 ppm), however, Reaction (b) may be rate controlling. Termination reaction rates also depend on oxygen concentration, with Reaction (d) predominating at high oxygen concentrations and Reaction (f) at low concentrations.

The rates of the reactions in autoxidation are dependent upon temperature, hydrocarbon structure, and oxygen concentration. Catalysts and free radical initiators can also materially alter rates, particularly that for step (a).

If sufficient oxygen is present, the hydroperoxide concentration will reach a limiting concentration. Hydroperoxide decomposition ensues and additional free radical reactions occur. Alcohols and ketones are the major products in the initial stages of this process, but the more extensive oxidation which follows yields acids, hydroxyketones, and esters. If the oxygen supply is limited but the temperature is raised, hydroperoxide will decompose. The major products are alcohols, ketones, and small hydrocarbons.

The importance of autoxidation reactions may be their ability to generate a spectrum of free radical intermediates which can accelerate other reactions such as oxidative polymerization (Ref. 4). Vranos (Ref. 5) has postulated that it is the simultaneous formation of olefins and free radicals which ultimately leads to the formation of polymeric deposits, and he has constructed a scheme for describing how polymer formation proceeds in a n-alkane/oxygen system.

Effect of Hydrocarbon Type

Taylor (Ref. 6) has studied the effect of hydrocarbon type on fuel thermal stability and, as shown in the table below, has normalized his results relative to deposit formation in n-dodecane.

EFFECTS OF HYDROCARBON TYPE
ON DEPOSIT FORMATION (REF. 6)

<u>HYDROCARBON TYPE</u>	<u>DEPOSITS RELATIVE TO n-DODECANE = 1.0</u>
n-C ₁₂	1.0
n-C ₁₀	0.8
n-C ₁₆	1.5
n-C ₁₂	2.3
AROMATICS (PURE)	1 to 5
AROMATICS (10% BLEND)	0.1 to 0.8
OLEFINS	3 to 50
NAPHTHENES	0.5 to 0.8

In the range of C₁₀ to C₁₆, the n-alkanes produced fewer deposits at a given temperature. Hydrocarbon chain branching increased the rate of deposit formation. Pure aromatics produced more deposits than n-alkanes, but actually seemed to inhibit deposit formation when blended with n-alkanes. Naphthenes behaved much as did aromatics in these studies, and olefins were quite deleterious to fuel stability. The most reactive species were diolefins with non-conjugated terminal double bonds.

Effect of Impurities and Dissolved Oxygen

Nitrogen and sulfur compounds and certain metals play a major role in the oxidation process by catalyzing the formation and decomposition of hydroperoxides for the free radical autoxidative polymerization. The following discussion of the effects of sulfur and nitrogen compounds and dissolved oxygen was taken from the CRC Literature Survey on the Thermal Oxidation Stability of Jet Fuel (Ref. 3).

The only major study on the role of sulfur in thermal oxidation stability was made by Taylor (Ref. 7). In this study, pure sulfur compounds were added at the 1000 ppm S level to a sulfur-free jet fuel. Experiments were conducted in the Esso kinetic unit at temperatures between 366 to 709 K. Of 12 sulfur compounds examined, two--diphenyl sulfide and dibenzothiophene--produced slight effects. Disulfides, thiols, and other sulfides exhibited significant increases, in some cases up to twentyfold. This effect increased as the temperature was raised. Deposit formation appeared to increase proportional to the square root of the sulfur concentration.

Much less is known about the effect of nitrogen compounds on thermal oxidation stability. Indole, 2-ethylpyridine and 2,5-dimethylpyrrole increased deposit formation rates four- to ten-fold in the kinetic unit when added at the 1000 ppm nitrogen level (Ref. 8). This effect, which was tested in the 379 to 422 K range, was more pronounced at higher temperatures. Other tests with the pyrrole at lower concentrations demonstrated that this compound increased deposits even at the 10 ppm N level.

As discussed above, dissolved molecular oxygen participates in complex free-radical chain reactions which have been shown ultimately to result in the formation of sediments, gum, and deposits. This suggests that fuel stability can be enhanced by suppressing these autoxidative deposit forming reactions via removal of dissolved oxygen.

The effect of deoxygenation was investigated (Ref. 4) with a spectrum of jet fuels whose quality ranged from very good to poor. The fuels were evaluated on both an air-saturated and deoxygenated basis (<1 ppm O₂) at 7.0 MPa. The ranking of these fuels on an air-saturated basis agreed well with previous evaluations. Total deposits were markedly reduced by the removal of molecular oxygen with all fuels except the poorest quality fuel. It was concluded that although deoxygenation has the potential for a marked reduction in deposit formation rate, deoxygenation by itself does not guarantee such a reduction, and the composition of the fuel in a deoxygenated system is equally important for reduced deposit formation rates.

Empirical Correlations

Because of the complexity of the deposit formation problem, empirical correlations offer the best possibility of formulating generalized relationships between deposit rate and the environment in which a deposit forms. An example of a correlating equation relating JFTOT breakpoint temperature (i.e., the temperature at which deposit level is considered significant based on a visual comparative test) to the quantity of certain fuel constituents (Ref. 9) is shown below:

$$T = 255 + 259(S)^{-0.024} (N)^{-0.00415} (Na)^{-0.0149} (OL)^{-0.082} (Ar)^{-0.067}$$

The percentages of the materials are denoted by the following symbols: S - Sulfur, N - Nitrogen, Na - Naphthalenes, OL - Olefins, and Ar - Aromatics; and T is the breakpoint temperature in degrees Fahrenheit.

The utility of such equations is limited to the fuels tested and by the range of applicability of the empirically-determined constants. Not unexpectedly, recent data (Ref. 10) with pyridene, ethylpyridene, indole, pyrrole, and quinoline indicates that the particular type of nitrogen compound has a greater effect on breakpoint temperature than the total nitrogen concentration in the fuel. Other data (Ref. 11) obtained in a JFTOT indicate that benzene (aromatic) yielded less deposit than Jet A while 1-hexene (olefin) yielded more deposit than Jet A.

Catalytic Effect of Metals

It has been widely shown in the literature that both soluble and insoluble metals can catalyze reactions involved in autoxidation. For example, a concentration of only 0.01 ppm of elemental copper in jet fuel can significantly decrease its thermal stability and result in excessive deposit formation. Low allowable metal contaminate concentration thresholds have also been reported for iron, zinc, lead, and vanadium (Ref. 12).

Studies of the catalytic effects produced by various tube wall materials have indicated that copper and copper-alloy surfaces cause high deposit formation rates while aluminum, titanium, and nickel surfaces result in low rates of formation. Deposit formation on stainless steel is generally low, particularly for type 316; however, higher deposit rates have been reported for type 304.

Baker (Ref. 13) has suggested that nickel can also be very reactive, particularly with light hydrocarbons, and can promote a greater degree of fuel pyrolysis and deposit formation than copper. Copper alloys are also considered to be very reactive. Gold may be the only metal that can be considered unreactive and a continuous, pore-free coating might protect copper. Although pure methane is not likely to form deposits, impurities commonly found in natural gas such as olefins (e.g., ethylene, propylene) and sulfur are likely to be very reactive.

Background Summary

Experiments conducted with kerosene-type fuels have shown deposit formation on metal surfaces, such as stainless steel in the temperature range of 400 to 600 K, depends upon the formation of oxidation products. Oxygen is often present in the deposits. If oxygen is removed from the fuel, deposit

formation is reduced. Some metal surfaces accelerate these reactions; copper has been found to be very reactive. The presence of copper may even overshadow the effect of oxygen. Certain sulfur and nitrogen compounds in the fuel result in increased deposits on some metal surfaces. A high concentration of certain hydrocarbons, particularly olefins, also result in increased deposits.

The chemistry involved in deposit formation at temperatures above 800 K, where the effects of oxygen are no longer important, includes cracking of the hydrocarbon and the production of carbon. The carbon may migrate into the metal surface and even remove some of the metal from the surface. Some metals are quite reactive and can be considered to be catalytic at elevated temperatures, e.g., nickel. The effect of copper at temperatures above 800 K has not yet been adequately documented.

Although the chemistry of fuel deposit formation continues to be studied, in the near term, empirical correlations of data offer the best possibility of formulating generalized relationships between deposit rate and the environment in which a deposit occurs. Where deposit formation measurements include thermal resistance, these correlations can be extended to include the heat transfer effects of deposit formation.

EXPERIMENTAL APPARATUS AND TEST PROCEDURES

Experiments were conducted to evaluate the rates of carbon deposition for RP-1, commercial-grade propane, and natural gas under flow conditions that exist in high-pressure rocket engine cooling systems. The fuel characteristics, test facility, and data analysis procedures are discussed in the following sections.

Fuels Characterization and Pretreatment

The base fuels which were tested during this program were RP-1 rocket fuel (MIL-P-25576), commercial-grade propane, and natural gas (a simulant for methane). Both the propane and natural gas fuels were acquired from local commercial suppliers, and RP-1 was supplied by the Government. In addition, two samples of stock RP-1 fuel were pretreated with additives to study the effects of altering fuel composition on thermal stability and carbon deposition rate. These modified fuels were produced by (1) doping with a commercially-produced additive designed to inhibit copper migration into the fuel, and (2) contaminating with two selected organic sulfur compounds to raise the sulfur concentration in RP-1 to the specification limit (i.e., 0.05 wt%). These modifications were made immediately prior to a test run and no special storage or handling facilities were required for the fuel.

The chemical compositions of the test fuels were obtained by utilizing a combination of available Government-furnished information and independent analytical laboratory facilities; that is, a certificate of analysis for the RP-1 fuel used in this program was supplied by the Government (Ref. 14), and the propane and natural gas fuels were analyzed at an independent laboratory (Refs. 15 and 16). Selected results of the RP-1, propane, and natural gas fuel analyses are summarized in Tables I to III, respectively. Thermophysical and transport properties of each fuel as functions of temperature and pressure were obtained from several sources (Refs. 1, 17 to 20). Tables IV to VI summarize the variation of viscosity, specific heat, thermal conductivity, density, and specific enthalpy as a function of pressure and temperature for RP-1, propane, and methane, respectively.

Fuel Treatment with Metal Deactivator

The tendency of the copper tube material to migrate into the fuel was inhibited by treatment of the test fuel with DuPont Metal Deactivator (DMD), an 80 percent (by weight) solution of N,N'-disalicylidene-1,2,-propanediamine in xylene (Ref. 21). When added to the fuel in proper concentrations, DMD acts to combine with dissolved copper to form a stable chelate of copper.

Because DMD was developed to increase long term storage stability and to reduce gum formation in liquid hydrocarbon fuels at moderate temperatures, it was unknown whether it would have a positive effect in reducing carbon deposition and improving fuel thermal stability at the elevated temperatures characteristic of the heated-tube tests. DMD is a liquid at room temperature. When heated above a temperature of 422 K, DMD begins to break down. At 556 K, the material boils and decomposes rapidly to lower boiling point compounds, including phenol.

DuPont recommends that the concentration of DMD be approximately five times the concentration of the copper dissolved in the fuel, and not exceed 0.005 percent by weight for optimum benefit. The concentration of copper in the RP-1 fuel is normally less than 0.01 ppm by weight (Ref. 1). However, because it was believed that additional copper would dissolve into the fuel when passed through the copper test tube, it was decided to add the maximum recommended amount of DMD. A concentrated stock solution of RP-1 and DMD was accurately prepared and, prior to test, it was added to a preweighed quantity of RP-1 to produce an effective concentration of 0.005 percent DMD in RP-1. In order to ensure thorough mixing of the RP-1 and DMD, the contents of the drum were recirculated using a fuel transfer pump until approximately ten times the volume had passed through the pump.

Fuel Treatment with Sulfur Compounds

The maximum concentration of sulfur permitted in RP-1 in accordance with the applicable military specification is 0.05 percent by weight; however, the RP-1 fuel used in this test program was analyzed and found to contain only 0.007 percent sulfur by weight (see Table I). Therefore, a batch of the as-delivered fuel was treated with enough thianaphthene, $C_6H_4C_2SH_2$, and benzyl disulfide $(C_6H_5CH_2)_2S_2$, to raise its sulfur concentration to the specification limit, i.e., from 0.007 to 0.05 percent by weight. The selection of thianaphthene and benzyl disulfide compounds as the sulfur-containing species was based on typical analyses of the crude oil performed by the refiner. These analyses indicate that nearly two-thirds of the sulfur is bound in the form of thiophenes and one-third is bound in the form of disulfides (Ref. 22). Also, the solubility of each of these compounds in RP-1 had been previously verified in the laboratory.

The same experimental techniques followed for doping RP-1 fuel with metal deactivator were followed in the sulfur treatment test; that is, a concentrated stock solution of thianaphthene and benzyl disulfide dissolved in RP-1 was prepared and mixed with a preweighed quantity of RP-1 just prior to test. The net effect was to raise the sulfur concentration of the test fuel to 0.05 percent by weight.

In order to verify proper treatment of the stock RP-1 fuel with sulfur, a sample was drawn and its composition analyzed (Ref. 23). The results of this analysis are shown in Table VII. The certified analysis confirmed that the appropriate amount of sulfur had been added to the stock fuel to bring it to the specification maximum of 0.05 percent by weight.

Test Facility and Test Procedures

Experimental Apparatus

The test program was conducted in an existing self-contained combustion test facility which consists of a concrete test cell and a separate control room housing operating personnel and the data acquisition system. The facility and test apparatus employed in this experiment are capable of continuous operation over a range of conditions including fuel flow velocities up to 100 m/s, fuel pressures up to 13.8 MPa, and tube wall temperatures up to 866 K. An electrical power supply capable of delivering 4000 amp at 40 kVA a-c was used to provide power for heating the test tubes while flowing fuel. The experimental facility is capable of handling both gaseous and liquid fuels.

The test apparatus, shown schematically in Fig. 2, consists of the following major components: (1) a fuel supply tank, (2) a zeolite-type molecular sieve used to remove water, carbon dioxide, and sulfur from the natural gas, (3) a fuel delivery system consisting of four piston-type accumulators having a total volume of 0.35 m³ and used to drive fuel through the test section, (4) a cryogenic heat exchanger to cool the propane and natural gas in selected tests to temperatures of 230 K and 160 K, respectively, (5) a resistance-heated test tube connected to a 40 kVA high-amperage power supply, (6) an in-line nylon-membrane filter (0.45 μ m) for collecting any solid particles which might form in the bulk flow or break off from the tube wall during a test, (7) a fuel cooler, (8) an electrically-driven metering valve to control the fuel flow through the test section, (9) turbine and venturi flowmeters, (10) a fuel dump tank, and (11) an air-driven ejector and exhaust stack used when testing with natural gas. A photograph of the facility is presented as Fig. 3.

The heat exchanger, provided to cool the propane and methane, is part of the cryogenic fuel delivery system depicted schematically in Fig. 4. The basic components of this system include: (1) three nested, double spiral, heat exchanger coils fabricated from 0.95-cm OD stainless steel tubing, each approximately 36-m long; (2) a 76-l vented dewar flask filled with liquid nitrogen; (3) a liquid nitrogen level sensor and level control unit; (4) a flexible, stainless steel liquid nitrogen transfer line attached to a porous, sintered-bronze phase separator; (5) a cryogenic solenoid valve; and (6) a low

pressure, insulated liquid nitrogen supply vessel to replenish the liquid nitrogen that is vaporized in the dewar.

The stainless steel heat exchanger coils were immersed in the vented dewar flask of liquid nitrogen. Natural gas or propane entered the coils at approximately 290 K and 13.8 MPa. All three coils, connected in parallel, were required to cool the natural gas to the temperature of 160 K, whereas, a single coil was sufficient to lower the temperature of the propane to 230 K. An electronic control unit and liquid-level sensor element were used to actuate a solenoid valve in the transfer line to enable automatic transfer of liquid nitrogen from the supply vessel to the dewar, as required. The phase separator, attached to the discharge end of the transfer line, minimized flashing of liquid nitrogen into vapor during filling of the dewar. A photograph of the heat exchanger, liquid nitrogen supply vessel, and zeolite molecular sieve is provided as Fig. 5.

Since it was not possible to reclaim the natural gas used in this program, a special mixer/diffuser was fabricated to dilute the natural gas below its flammability limit. The gas/air exhaust system consisted of a compressed-air-driven ejector installed approximately 6 m above ground. The ejector primary nozzle and mixing sections were designed to yield an entrainment ratio of 3.3 (using the data in Ref. 24) and to dilute the natural gas with air, resulting in a natural gas mass fraction at the exhaust of approximately 0.008; a value well below both the flammability limit and the level affecting pulmonary function.

Heated Test Tube Fabrication and Characterization

The heated test tube assembly and a cross-sectional view of the tube configuration are shown schematically in Fig. 6. The test tube comprised a duplex arrangement formed by an inner 0.196-cm ID x 0.348-cm OD, 99.99 percent pure copper tube and an outer 0.348-cm ID x 0.475-cm OD Inconel 600 tube. The Inconel sheath provided the necessary high-temperature tensile strength while the inner copper tube provided the desired test material and surface condition for studying fuel deposit formation in rocket engine cooling systems. The test tubes were designed to withstand continuous operation at maximum outer wall temperatures up to 866 K and fuel pressures up to 13.8 MPa. While the structural load was carried by the outer Inconel sheath, the major electrical power fraction (approximately 95 percent) was carried by the higher conductivity copper tube. Therefore, the induced radial temperature gradient was small.

The duplex tubes were fabricated by inserting the copper tubing into oversize Inconel tubing and drawing the assembly through a die, thereby reducing the tube diameters and creating a mechanical bond. Prior to fabrication, the manufacturer cleaned both the Inconel and copper tube components

using a special cleaning procedure designed to ensure against the existence of any significant electrical or thermal resistance at the interface of the two metals, which could stem from contamination or oxidation. The cleaning procedure adopted for the copper tubing consisted of immersing the tubing in a solution of 10 percent sulphuric acid and 90 percent water for a period of 10 to 15 min, followed by a thorough water rinse to remove all traces of acid residue. The Inconel tubing was degreased by immersing in acetone for a period of 5 to 10 min.

After fabrication, the integrity of the Inconel/copper bond in the test tubes was ascertained by testing a sample length. These tests consisted of metallographic examinations made with a scanning-electron microscope and elemental analysis at the tube interface made utilizing a scanning-electron microprobe. Microscopic examination of the interface showed that the mechanical bond was satisfactory. The microprobe analysis comprised searches for carbon, oxygen, sulfur, and chlorine. These analyses indicated that the interface region was clean and free of constituents which would affect the tube heat transfer characteristics.

The test tube interior surface finish was characterized using a Bendix type AD, Model 17 profilometer. A tracing speed of 0.25 cm/s was used. The measured interior surface roughness height (i.e., the average deviation from the mean surface) of the tube was from 0.25 to 0.30 μm , slightly smoother than the 0.63 to 0.84 μm finish tube tested in the previous program (Ref. 1).

In an effort to passivate the normally reactive copper surface, several test tubes were plated with nickel by a vendor who used an electroless process. Phosphorous is a major constituent in the electroless plating solution and was found present in the nickel plate (Ref. 1). After the plating process, selected tube specimens were split longitudinally to verify that there was complete coverage of the copper with nickel. In addition, in order to determine the thickness of nickel deposited on the copper surface, a longitudinal specimen of plated tubing was polished and examined microscopically. The average thickness of the nickel plating was 6 μm .

Test tube assemblies depicted in Fig. 6 were cut from 1.9-m lengths of duplex tubing and brazed to copper bus rings, which in turn were bolted to copper ring adapters. In order to avoid excessive heating of the test tube, a 95/5 percent cadmium/silver solder having a solidus of 611 K and a liquidus of 667 K was used in this operation. Ten chromel-alumel thermocouples were spot welded to the Inconel sheath at 2.54-cm intervals, starting at 1.27 cm from the electrical bus ring. The surface of the Inconel tube was coated with Sauereisen cement at the thermocouple junctions, to electrically insulate the thermocouple lead wires from the tube, and the wire was wrapped once around

the tube and coated with additional Sauereisen cement to ensure good thermal contact and thereby minimize heat conduction from the junction.

The test section mounting arrangement is also shown in the photograph in Fig. 7. The test tube assembly was mounted on teflon-lined cradles designed to accommodate the bus rings and to permit thermal expansion by providing a smooth sliding surface. The teflon also acted as an electrical insulator to prevent grounding of the test tube. In addition, nonconductive flexible hose was installed at the entrance and exit of the test tube assembly to allow thermal expansion and to electrically isolate the tube from the other components of the test apparatus. The test tube assembly was connected to the power supply using a rigid connector and flexible water-cooled cable. The flexible cable permitted thermal expansion of the test section. Adjustable wall anchors and adjustable transformer connections were used to assist in aligning the test section prior to a run.

Instrumentation and Data Acquisition System

The locations of the principal instrumentation elements are shown in the schematic of the test apparatus in Fig. 2. All test data were recorded using a calculating data-logger microprocessor (Ref. 25). When set at standard resolution, the data system is capable of a scan rate of up to 35 channels per second. The data system converts the output signals from thermocouples, pressure transducers, current transducers, voltage transducers, and flow meters to precisely scaled d-c voltages for measurement, but displays the data in engineering units as specified by the operator through built-in linear scaling functions. A cathode-ray tube displays key operating variables, thereby providing a continuous visual check of up to 13 channels. If a measured test parameter exceeds a specified setpoint, an alarm message is displayed, and a contact may be closed to terminate the experiment. The raw data are logged on paper tape either by demand logging or by programmed interval logging. In addition, a magnetic tape drive coupled to the data system is used to store test data for subsequent processing on a high-speed digital computer.

During the RP-1 and propane tests, the primary fuel flow measurement was made using a turbine-type flow meter located downstream of the test section. In addition, a redundant fuel flow measurement was made downstream of the test section with a venturi and a differential pressure transducer. Generally, the turbine meter and venturi flow rate measurements agreed within four percent. The natural gas flow rates were established by utilizing an appropriately sized critical-flow venturi that was installed in the same location downstream of the test section. The pressure drop between the venturi inlet and throat was monitored continuously to verify critical flow conditions at the throat.

Other pertinent data parameters monitored and recorded during each test included: the outer wall temperature of the test tube at ten axial locations, the temperature of the fuel entering and exiting the test tube, the fuel pressure at the test tube inlet, the drop in fuel pressure across the test tube, the voltage applied to the test tube, and the current through the test tube. Since piercing the heated test section to measure bulk temperatures is not considered to be good practice (because of possible fuel leakage, insertion of preferential sites for deposition, and electrical discontinuities), only inlet and exit fuel temperature measurements were made. However, theoretical predictions of the axial variation of fuel temperature suggest that the distribution is nearly linear. Fuel pressure measurements were made using strain-gauge-type pressure transducers and all temperature measurements were made using chromel-alumel thermocouples. The a-c current was measured using a commercially-produced inductive pickup and current transmitter.

Test Matrix and Test Operation

The test matrix, shown in Table VIII, comprised twenty-four tests for RP-1, commercial-grade propane, and natural gas fuels that were conducted at the nominal conditions consisting of a fuel delivery pressure of 13.8 MPa, a fuel delivery temperature of 290 K, maximum initial inner wall temperatures of 589, 700, and 811 K, and for a test duration of 10 min. Also, a calibration test for RP-1 and three additional tests (one for each fuel) were conducted during the course of the program. The RP-1 and propane tests were performed to extend the data base that was acquired under the previous phase of this program (Ref. 1). The experimental program began with a sequence of calibrations using RP-1 fuel to establish operating procedures and to verify proper performance of the data acquisition system.

Referring to Table VIII, the initial series of tests (Runs 1 to 4) used RP-1 fuel. Run 1 provided data for a copper tube in which the nominal fuel inlet velocity was 61 m/s; Run 2 explored the effect of nickel plating on deposit formation for RP-1 at a nominal fuel velocity of 30 m/s; and Runs 3 and 4 made use of copper test tubes to evaluate the effects of (1) doping the fuel with metal-deactivating agent, and (2) increasing the sulfur content of the fuel to the RP-1 specification limit of 0.05 percent by weight, respectively.

The second series of tests (Runs 5 to 12) used commercial-grade propane fuel. Runs 5 to 8 were conducted for ambient temperature propane, while Runs 9 to 12 explored the effects of cooling the fuel to a nominal delivery temperature of 233 K. With the exception of Runs 5 and 11, all tests used nickel-plated copper tubes. In Run 5, the effect of a nominal fuel inlet velocity of 61 m/s on carbon deposition in a copper tube was explored. In Run 7, fuel pressure was reduced to a nominal value of 6.9 MPa. In Run 8, which

was performed using ambient temperature propane in a nickel-coated tube, the tube was operated intermittently; that is the power and fuel flow were cycled on and off eight times. Each power on cycle was approximately three minutes in duration. Between power-on cycles, fuel flow was maintained long enough to cool the tube wall to about 310 K. Once the tube wall had been sufficiently cooled, the power was reset to the previous level and the cycle was repeated. The total time for which the tube was heated was 24 min.

The third series of tests (Runs 13 to 24) were conducted using natural gas as a simulant for methane. Runs 13 to 20 were conducted using ambient temperature natural gas, and Runs 21 to 24 were conducted using cryogenic natural gas. Both copper and nickel-plated copper tubes were used. Runs 17 and 18 were performed at nominal fuel inlet velocities of 61 and 91 m/s, respectively and at a fuel pressure of 6.9 MPa. As in the case of Run 8 with propane, Run 20 was designed to explore the effect of intermittent operation on carbon deposition. Total run time at high temperature was 24.5 min, comprising eight cycles with power on and eight cycles with power off. Runs 21 to 24 were conducted using cryogenic natural gas cooled to a nominal inlet temperature of 160 K at 13.8 MPa delivery pressure. An additional test coded as Run 220 is listed at the bottom of Table VIII. This run was a first attempt at Run 22, but was repeated because there were large fluctuations in the fuel inlet temperature.

Prior to running a test, the interior surface of each test tube assembly was degreased and cleansed. The cleaning procedure adopted consisted of the following steps:

1. Swab several times with pipe cleaners dipped in acetone, and rinse with distilled water.
2. Swab several times with pipe cleaners dipped in an aqueous solution comprised of 3 g citric acid dissolved in 50 ml of hot distilled water and 10 ml of 3 percent by volume hydrogen peroxide.
3. Rinse with distilled water and dry with nitrogen.

To ensure that no contaminants were present on the test surface, scanning-electron-microprobe analyses were conducted to verify that the cleaning procedure adopted was successful in removing the trace quantities of contaminant species found on the uncleaned copper surface (e.g., chlorine, sulfur, and phosphorous).

Routine pretest facility preparation consisted of installing a clean test tube and particle filter, charging the accumulators with an appropriate quantity of fuel, activating the data acquisition system and closed-circuit

television monitor, and checking all transducer calibrations and thermocouple junctions. After pressurizing the accumulators with nitrogen, the entire system was inspected for leaks by flowing fuel momentarily. Provided there were no leaks, the test was initiated by opening the electrically-powered fuel shutoff valve and adjusting the downstream metering valve until the desired flow rate was obtained. The electric powerstats were then activated and set to a relatively low power level (e.g., wall temperatures in the range of 350 to 450 K). This was done to verify proper operation of all the thermocouples. The electric powerstats were then rapidly advanced to heat the tube to the desired wall temperature (transient time was about 15 sec for RP-1 and methane and 1 min for propane), and data logging was commenced. At high electrical power settings, wall temperature was very sensitive to powerstat setting, and it was difficult to set the maximum initial wall temperature accurately; hence the slight deviation from nominal values (Table VIII). Data were usually recorded every 30 sec. The test was continued for the specified duration or until the maximum wall temperature exceeded 866 K. After the test was completed, power was turned off and fuel flow was maintained for a brief period (approximately 15 sec) to cool the test tube to about 310 to 340 K. The test tube and particulate filter were then removed from the facility and set aside for post-test analysis.

A slightly modified run procedure was adopted for the tests utilizing cryogenic fuels. The fuel flow and the liquid nitrogen flow to the cryogenic heat exchanger were started simultaneously. Typically, a ten minute system cooldown period was allowed to achieve a steady-state temperature prior to starting the test. During the system cooldown period, a low level of electrical power was supplied to the test section, to maintain the fuel discharge temperature above cryogenic levels and thereby simplify the apparatus downstream of the test section. Once the desired fuel inlet temperature was attained, the normal run procedure was begun. The start-up procedure was especially critical in the case of natural gas. Here, a trace amount of carbon dioxide remaining in the fuel after it passed through the zeolite filter would crystallize and block the heat exchanger coils if a low fuel flow rate was not maintained at all times.

Data Analysis

Test data were recorded on magnetic tape and subsequently transferred to a high-speed digital computer for further processing. A data reduction program was developed for calculating additional parameters of interest, such as Reynolds number, fuel-side heat transfer coefficients, friction factors, and deposit thermal resistances.

Thermal Data Analysis

The local inner wall temperatures of the test tube (i.e., temperatures at interface between deposit layer and tube wall) were computed from the measured outer wall temperatures using results from a numerical heat transfer simulation known as TCAL. In this analysis, a finite difference representation of the heat conduction equation (a time-dependent version of Laplace's equation) is solved by a relaxation technique. The temperature at the interface between the fuel and the deposit layer which forms inside the tube equals the initial inner wall temperature, provided the convective heat transfer coefficient remains constant (i.e., constant heat flux and flow rate). The local value of the forced-convection heat transfer coefficient was determined based on the assumption of a linear bulk fuel temperature profile. A more rigorous analysis (Ref. 1) has verified that this assumption is a reasonable one for RP-1 at the conditions of interest.

Two measures of the effect of carbon formation on heat transfer were employed in the data reduction analysis. The deposit thermal resistance (t/k), defined as the ratio of deposit thickness to deposit thermal conductivity was computed from

$$t/k = \left(\frac{1}{U} - \frac{1}{U_0} \right) \quad (1)$$

where U is the instantaneous overall inside wall heat transfer coefficient. It is defined as

$$U = \frac{Q/A}{T_{w_i} - T_f} \quad (2)$$

where Q/A is the instantaneous heat flux, T_{w_i} is the calculated local inside wall temperature, and T_f is the local bulk fuel temperature. Notice that as defined, U incorporates the resistance due to deposit formation. However, at time zero when the tube is clean, U reduces to the heat transfer film coefficient U_0 .

In addition, the thermal resistance buildup rate (\dot{R}_c) is given by

$$R_c = \frac{\Delta T_{w_o}}{(Q/A) \Delta t} \quad (3)$$

where ΔT_{w_o} is the observed rise in outer wall temperature and Δt is the elapsed time for which the tube was heated. The latter definition assumes linearity over the time period Δt . It is a simple matter to prove that t/k equals $R_c \cdot \Delta t$, provided the heat flux and bulk fuel temperature profiles do not change with time.

Analyses were performed to correlate the experimentally-derived heat transfer film coefficients (U_o) for each fuel with a Nusselt-Reynolds-Prandtl number expression (Ref. 26) given by

$$\frac{Nu}{Pr^c [1 + 2/(x/D)]} = A Re^b \left(\frac{\rho}{\rho_w}\right)^d \left(\frac{\mu}{\mu_w}\right)^e \left(\frac{k}{k_w}\right)^f \left(\frac{\bar{C}_p}{C_p}\right)^g \left(\frac{P}{P_{crit}}\right)^h \quad (4)$$

where Nu is the Nusselt number, Re is the Reynolds number, Pr is the Prandtl number, ρ , μ , k , C_p , and P are local values of the fuel density, absolute viscosity, thermal conductivity, specific heat, and pressure, respectively. \bar{C}_p is the average value of specific heat computed from the inside wall temperature and the fuel bulk temperature, and x/D is the axial distance to diameter ratio. The subscript w denotes evaluation of the fuel property at the wall temperature. All other fuel properties are evaluated at the bulk temperature. In this analysis, it was assumed that $c = 0.4$.

The unknown coefficient A and exponents b, d, e, f, g, and h were determined using a multiple linear regression and correlation analysis computer program. The above equation is of the form

$$Y = a B^b D^d E^e F^f G^g H^h. \quad (5)$$

Taking the natural logarithm of each side of the latter equation and denoting the natural logarithm of a quantity by (*) gives a linear equation of the form

$$Y^* = a^* + bB^* + dD^* + eE^* + fF^* + gG^* + hH^*. \quad (6)$$

The regression analysis operates to make the standard deviation

$$\sigma = \left(\frac{\sum_n (Y^*_{\text{exp}} - Y^*_{\text{calc}})^2}{n-m} \right)^{1/2} \quad (7)$$

a minimum, where n is the total number of data points, m is the total number of regression coefficients (e.g., seven), and the subscripts exp and calc indicate that the value of Y^* is derived from experiment or calculated from the correlation equation. The standard deviation is an absolute measure of dispersion of the data about the fitted curve.

At the same time, the regression analysis maximizes the correlation coefficient

$$R = \left(\frac{\sum_n (Y^*_{\text{exp}} - \bar{Y}^*_{\text{exp}})^2 - \sum_n (Y^*_{\text{exp}} - Y^*_{\text{calc}})^2}{\sum_n (Y^*_{\text{exp}} - \bar{Y}^*_{\text{exp}})^2} \right)^{1/2} \quad (8)$$

where an overbar denotes a mean value. The correlation coefficient is a relative measure of the closeness of fit of the correlating equation to the experimental data, and its square (the coefficient of determination) may be interpreted as the percentage of the total variation in the dependent variable that is associated with variation in the independent variables. The correlation coefficient takes on values between 0 and 1, with perfect correlation occurring for $R = 1$.

In addition to solving for the unknown coefficient and exponents for the assumed correlating equation, the regression and correlation analysis computer program incorporated a statistical significance test (Student's t test, 95 percent confidence) which automatically deleted the least significant independent variables from the original correlating equation and recomputed new values of the coefficient and exponents for the remaining terms.

Deposit Characterization

The quantity of carbon on the test tube surface was determined by burning off the deposit in oxygen with analysis of the evolved CO and CO_2 . As shown in Fig. 8, four equally-spaced sections (each approximately 3.81-cm long) were cut from each test tube and used for the burnoff tests. The four tube sections represent approximately 60 percent of the total surface area of the

tube; the remainder of the tube was cut into longitudinal sections which were examined microscopically. A special fixture and jewelers saw were used to section the tubes. Prior to the burnoff procedure, the test tube sections were dried in a vacuum oven at 390 K for 24 to 48 hours to evaporate any residual liquid fuel. To acquire the deposit formation rate data, a metered flow of oxygen was passed at a constant rate through the inside of a heated section of the test tube (see Fig. 9). The product gases from the burnoff were passed through an Infrared Industries, Inc. Model IR-702 nondispersive infrared (NDIR) analyzer which measured the concentrations of CO and CO₂ in the test tube effluent. The analyzer was calibrated before each series of burnoff tests using nitrogen for setting the instrument zero level and a N₂/CO₂ or N₂/CO gas mixture of certified concentration for establishing the appropriate scale factor. Output from the analyzer was recorded continuously to give a time trace of the percentage of CO₂ and CO evolved during burnoff of the deposit. Integration of the data over the total burnoff time yielded the total volumes of CO₂ and CO evolved, from which a carbon weight and deposition rate were calculated. The catalyst bed shown in Fig. 9 was used to convert any CO evolved to CO₂, thereby simplifying the calculation. The carbon deposition rate is defined as the mass of carbon deduced from the burnoff analysis divided by the product of the inside lateral surface area of the tube section and the total test time, and is expressed in units of $\mu\text{g}/\text{cm}^2\text{-hr}$. In this program, carbon deposition rates are reported as both tube local and tube average quantities. The local rate is computed for a single 3.81-cm long tube section whereas the average rate is the arithmetic mean value from four of these sections.

The accuracy of the burnoff procedure was verified periodically by oxidizing a known mass of solid carbon in the apparatus, measuring the concentrations of CO₂ and CO in the effluent gases, and computing the mass of carbon. Typically, the computed and measured values of carbon mass agreed to within 6 percent. Also, burnoff tests were conducted for clean, unused copper and nickel tube specimens to compensate for any tare carbon mass present. All deposit masses and deposit formation rates reported in this program include a tare adjustment.

In selected cases, the longitudinal tube sections shown in Fig. 6, were scanned optically and the deposit was characterized qualitatively in terms of its type and uniformity. A Scanning-Electron Microscope (SEM) was used to elucidate the morphology of the deposit; limited elemental analysis of the deposit was performed using a Scanning-Electron Microprobe (SEMP). This procedure involved a qualitative scan of elements present in the deposit (e.g., carbon, copper, sulfur, oxygen, and nitrogen) within a detectability limit of approximately 200 ppm. X-ray emission imagery of the selected element (indicated by clusters of white dots on a black background) was matched to standard photomicrographs of the sample deposits. In addition, a computer algorithm was used to process the X-ray map data and to quantify the elemental composition of the deposit on a mass fraction basis.

EXPERIMENTAL RESULTS AND DISCUSSION

In this section, the data for the heated-tube tests conducted for RP-1, commercial-grade propane, and natural gas are presented. In addition, a summary of the results of the deposit characterizations, including the burnoff data and deposit morphology, is provided. The extent of corrosion within a test tube due to the carbon deposition process is quantified through results of hydrostatic burst tests on selected tube specimens. A complete listing of all the on-line test data acquired, including calculated parameters, is presented in the Appendix. A summary of the tube burnoff data for the three fuels is found in Tables IX to XI.

RP-1 Tests

Calibration Tests

In order to characterize the test tube input power requirements for RP-1 fuel, a series of calibration tests was conducted. The fuel inlet velocity was fixed and the electrical power supplied to the tube was varied incrementally to produce peak inside wall temperatures between 400 and 800 K. These tests were conducted at a nominal fuel inlet pressure of 13.8 MPa. Operating conditions were held constant only momentarily so that data could be recorded at each power setting in the absence of significant deposit formation. The inner wall temperature distributions and corresponding power levels for fuel inlet velocities of 21, 44, and 65 m/s are shown in Fig. 10. Inlet Reynolds number at these velocities are 14-, 21-, and 43×10^3 , respectively. As reported in Ref. 1, at high inlet Reynolds numbers, the wall temperature profiles indicate no apparent entrance effects associated with a developing thermal boundary layer. At the lower power levels for the range of velocity explored, wall temperature is nearly uniform along the tube. At higher power levels, wall temperature decreases slightly from the tube entrance to the tube exit. This characteristic profile stems from the variation of bulk fuel properties with temperature and was explained in detail in Ref. 1.

Effect of Fuel Velocity on Carbon Deposition and Thermal Resistance

As discussed in Ref. 1, the rate of carbon deposition is affected by changes in fuel velocity. In Fig. 11, which is based on data acquired in the previous phase of this program, the rate of carbon deposition for RP-1 in copper tubes is plotted as a function of the initial inner wall temperature for several fuel inlet velocities. The data are based on tube-averaged quantities; that is, an average temperature and an average carbon deposition rate have been computed for each tube. The figure shows that along a curve of constant fuel velocity, there is a maximum value of the rate of carbon deposition. As fuel velocity increases, the maximum rates of carbon deposition

shift to higher wall temperatures. Also, the rates of carbon deposition decrease as fuel velocity increases. In order to further explore these trends, two tests were conducted to extend the existing data base for copper and nickel-plated tubes. Fuel inlet velocity was set at 58 m/s for the copper tube and 30 m/s for the nickel-plated tube. Both tests were run at 13.8 MPa fuel inlet pressure. Composite plots summarizing the burnoff data from Ref. 1 and from this program and describing the effects of fuel velocity on carbon deposition for copper and nickel-plated tubes are shown in Figs. 12 and 13, respectively.

In Fig. 12, the rate of carbon deposition is plotted as a function of fuel inlet velocity and grouped into two bands enclosing initial inner wall temperature data less than 640 K and greater than or equal to 640 K, as suggested by the trends in Fig. 11. For wall temperatures less than 640 K, the rate of carbon deposition decreases as fuel velocity increases from 7 to 30 m/s. However, when wall temperature is greater than or equal to 640 K, the rate of carbon deposition exhibits a reverse trend and increases with increasing fuel velocity in the range of 7 to 58 m/s. Also, at low fuel velocities (e.g., 7 to 15 m/s) the rates of carbon deposition for wall temperatures less than 640 K exceed those rates for wall temperatures greater than 640 K.

The opposing trends observed for the effect of fuel velocity on carbon deposition for the two wall temperature ranges shown may be explained as follows. At low wall temperatures (e.g., less than 640 K) the rate of deposit formation may be limited by the kinetics of the carbon deposition processes, so that the additional fuel supplied to the hot surface (corresponding to an increase in fuel velocity) is not reacted. The slight decrease in the rate of carbon deposition associated with an increase in fuel velocity at these temperatures may be due to increased flaking of deposit from the tube surface. However, at high wall temperatures (e.g., greater than or equal to 640 K), the carbon deposition kinetics are accelerated so that in the limit, the rate at which deposit forms is governed only by the rate at which fuel is supplied to the hot tube surface. Thus, at the higher temperature the increase in fuel mass flow rate associated with an increase in fuel velocity promotes further deposit formation.

The higher rates of carbon deposition shown for wall temperatures less than 640 K at fuel velocities between 7 and 15 m/s may be due to the observation that the rate of carbon deposition reaches a maximum at an intermediate value of wall temperature and decreases thereafter for further increases in wall temperature (cf., Fig. 11). Previously, this value was determined experimentally to be between 550 and 600 K at a fluid velocity of 7 m/s (Ref. 1). Carbon deposition rates decreased rapidly when wall temperature exceeded these values.

In the case of nickel-plated tubes, Fig. 13 summarizes the results of the rate of carbon deposition as a function of initial inner wall temperature for fuel inlet velocities of 6, 18, and 30 m/s. Open symbols correspond to data derived from a particular section of a tube; whereas solid symbols correspond to data based on tube-averaged quantities. The plot shows that the carbon deposition rates for velocities 6 and 18 m/s (Ref. 1) fall in a band significantly below that data corresponding to 30 m/s (Run 2). In the range of wall temperatures tested, an increase in fuel velocity is accompanied by a significant increase in the rate of carbon deposition. This increase in the rate of carbon deposition cannot be attributed solely to the increased fuel flow at higher velocity. Also, a comparison of Figs. 13 and 11 shows that for fuel velocities between 6 and 13 m/s, the rates of carbon deposition for nickel tubes are approximately one-fifth of those for copper.

The effect of fuel velocity on the thermal resistance buildup rate (\dot{R}) defined earlier was explored for copper tubes. Previously, it was determined that, for fuel velocities between 7 and 30 m/s, the thermal resistance buildup rate reached a maximum at an initial wall temperature in the range 650 to 700 K and decreased thereafter for further increases in wall temperature (Ref. 1). In addition, the thermal resistance buildup rates decreased as fuel velocity increased. In order to summarize this trend for the data compiled in Ref. 1 and in this program, a plot of maximum thermal resistance buildup rate as a function of fuel inlet velocity is shown in Fig. 14. These rates were calculated for tube locations where thermocouple measurements exhibited an overall rise for the full test duration. In Fig. 14, the thermal resistance buildup rate is shown to decrease by a factor of five with an increase in fuel velocity from 8 to 58 m/s; a trend that cannot be explained by a reduction in the level of deposit produced (cf., Fig. 12). Therefore, the reduction in the thermal resistance buildup rate is attributed to enhancement of the local heat transfer coefficient due to increased velocity and/or roughening of the tube wall during the carbon deposition process. Also, it is postulated that as the mass of deposit increases, its porosity decreases, and its thermal conductivity increases from a value representative of the fuel to a value typical of amorphous carbon. Consequently, the higher deposit loadings observed for an increase in fuel velocity could improve heat transfer and reduce the thermal resistance buildup rate.

Effect of Fuel Composition on Carbon Deposition

Two heated-tube tests were conducted to explore the effects of (a) doping RP-1 base fuel with a metal deactivator designed to inhibit copper migration and (b) contaminating the fuel with compounds to increase the total sulfur concentration to the specification maximum of 0.05 percent by weight. A composite plot comparing the data for the fuel composition modification tests with those obtained for RP-1 base fuel is shown in Fig. 15. Here the rate

of carbon deposition is plotted as a function of initial inner wall temperature and a curve is drawn through the data for the RP-1 base fuel.

Based on the tube-averaged data, there is a significant reduction in the rate of carbon deposition when RP-1 is doped with metal deactivator. At an initial wall temperature of about 670 K, this reduction is approximately a factor of two. With regard to the data obtained for the sulfur-doped fuel, the tube-averaged data suggests no significant increase in the rate of carbon deposition when compared to RP-1 base fuel. However, as will be discussed later, significant loss of deposit caused by flaking from the tube surface because of corrosion of the copper was characteristic for most of this tube. In general, the deposit appeared thicker than that obtained for RP-1 base fuel and the peak deposit rate of $970 \mu\text{g}/\text{cm}^2\text{-hr}$ at a wall temperature of 725 K (a threefold increase relative to the base fuel) may be more representative of the tube-averaged level that would be obtained had flaking not occurred. The results of the sulfur-doped fuel test indicate that high concentrations of fuel-bound sulfur (e.g., 0.05 wt % S) accelerate deposit formation and tube corrosion. However, further work utilizing fuels with naturally-occurring high sulfur concentrations is necessary before a definitive conclusion can be reached.

Propane Tests

Effect of Fuel Velocity on Carbon Deposition

The effects of fuel velocity on carbon deposition in copper tubes for propane fuel, were explored by comparing the results of Ref. 1 with those of a test in which the fuel inlet velocity was set at 49 m/s. Nominal fuel inlet pressure and temperature were maintained at 13.8 MPa and 290 K, respectively. A plot summarizing the burnoff data from Ref. 1 and that from this program is shown in Fig. 16 where the rate of carbon deposition is plotted as a function of fuel inlet velocity and the data are grouped in three bands enclosing initial inner wall temperature data less than 400 K, between 400 and 560 K, and greater than 560 K. The data points shown on the figure are for tube-averaged deposition rates. The temperature bands were selected on the basis of a natural grouping of the data. Along a band of initial inner wall temperatures, the rate of carbon deposition decreases with increases in fuel inlet velocity in the range of 6 to 50 m/s. In addition, for most fuel velocities, an increase in initial wall temperature produces an increase in the rate of carbon deposition.

The trends exhibited by these curves in Fig. 16 are consistent with the hypothesis that the rate of deposit formation is limited by the kinetics of the carbon deposition reaction. An increase in wall temperature accelerates the reaction kinetics, but an increase in fuel velocity, which corresponds to

an increase in fuel supplied to the hot tube wall, does not promote additional deposit formation. As in the case for RP-1 fuel, the decrease in the rate of carbon deposition associated with an increase in fuel velocity along a band of wall temperatures may be due to increased washing of the deposit from the tube surface at higher velocities. However, as will be discussed later and in contrast to the results for RP-1, deposit coverage of the tube surface appeared to be uniform and local flaking of deposit was not visible.

Effect of Tube Surface Material on Carbon Deposition

Tests were conducted using nickel-plated tubes and ambient temperature propane (290 K) to explore the effects of tube surface material on carbon deposition. As shown in Fig. 17 (a SEMP photograph which is taken from Ref. 1), extensive degradation of the tube wall, manifested in the form of dendrite structures, was characteristic for propane flowing through a copper tube. The SEMP analysis showed the dendrite to contain a high concentration of copper, suggesting that tube material was forced up and away from the surface. Some carbon was evident at the base of the tree-like deposit structure. A very low concentration of sulfur was also detected, but no oxygen was observed. The objective of the nickel tube experiments was to determine if this phenomenon could be mitigated. Nominal fuel inlet velocity was 30 m/s for each test at nominal inlet pressures of 13.8 and 6.9 MPa.

The carbon deposition data for copper tubes, reported in Ref. 1, and the data for nickel tubes tested in this phase of the program are summarized in Fig. 18, with all data corresponding to ten minute test durations. In the figure, the rate of carbon deposition is plotted as a function of initial inner wall temperature. Lines are drawn through the two groups of tube data to indicate the trends. The plot shows that at relatively low wall temperatures (e.g., 400 K) the rates of carbon deposition for copper and nickel tubes are similar. However, as wall temperature increases, the rate of carbon deposition for copper tubes increases while that for nickel tubes remains nearly constant. At 580 K, the highest common value of wall temperature tested, the rate of carbon deposition on copper tubes exceeds that of nickel by a factor of four. In addition, as noted in Fig. 18, the tube surface degradation that is characteristic for copper tubes does not occur for nickel tubes in the range of conditions explored. Also, there appears to be no significant effect of fuel pressure on carbon deposition for the nickel-tube tests.

The differing trends exhibited by the rates of deposition for copper as compared with nickel tubes may be related to the tube surface degradation process. As reported in Ref. 1 and as will be discussed later, the size of the dendrite structures which form on the copper surface appear to be a function of tube wall temperature. Microscopic examination of several tube sections revealed that at higher wall temperatures, dendrite size is visibly

larger than that found at lower temperatures. Therefore, at higher wall temperatures more copper metal is pushed out from the tube and the surface area exposed to fuel is increased. Consequently, additional carbon deposit is formed around the base of a dendrite, and scanning-electron-microprobe analyses done in Ref. 1 support this conclusion. This mechanism is not present in nickel tubes as witnessed by the absence of visible dendrites. Also, at low wall temperatures, (e.g., $T_{\text{wall}} < 400 \text{ K}$) dendrite formation (i.e., corrosive attack) on copper is not as prevalent, and the rates of carbon deposition for copper and nickel tubes are similar as the data of Fig. 18 indicate.

Effect of Intermittent Operation and Test Time on Carbon Deposition

A test in which a nickel tube was heated intermittently for eight 3-min cycles was performed to determine the effects of intermittent operation and test duration on carbon deposition. The motivation for intermittent testing derives from a desire to simulate a number of operating cycles for a reusable rocket engine application. A summary of the carbon deposition rates acquired for several tests are shown in Fig. 19.

In Fig. 19, the rate of carbon deposition is plotted as a function of test time (i.e., the total time for which heat was applied) for nickel tubes. Note that the longer test corresponds to intermittent operation. Nominal inlet pressure, velocity, and temperature of the propane fuel were 13.8 MPa, 30 m/s, and 290 K, respectively. All data plotted correspond to tests having the same range of initial inner wall temperatures (i.e., 490 to 590 K). Based on the data in Fig. 19, the rate of carbon deposition decreases as test time (no. of cycles) increases. This result is consistent with that obtained for continuous tests with copper tubes (Ref. 1). An explanation for decreasing deposit formation rate with increasing test time may be that the deposit breaks away from the tube surface as test time increases (this effect would be intensified by intermittent operation), or due to a suppression of the deposit formation rate owing to passivation of the tube surface resulting from the buildup of deposit over the longer operating period.

Effect of Fuel Chilling on Carbon Deposition

A series of tests was performed to study the effects on carbon deposition in copper and nickel tubes of prechilling the propane to 233 K. The motivation for fuel prechilling was an attempt to reduce fuel temperatures and thereby avoid wall temperature instabilities that limited the data of Ref. 1. Nominal fuel inlet pressure was either 6.9 or 13.8 MPa; fuel inlet velocity was 30 m/s; and fuel inlet temperature was 233 K. The carbon deposition rates

determined from these tests and from those of Ref. 1 are plotted in Fig. 20, wherein the results obtained for ambient temperature and for chilled propane are compared. The ambient temperature curves for copper and nickel tubes that were previously presented in Fig. 18 are represented in Fig. 20, as are the individual data points and corresponding curves for the data representing the chilled fuel tests.

As indicated in Fig. 20, chilling the fuel results in a substantial reduction in the rate of carbon deposition for wall temperatures in the range 400 to 600 K for both copper and nickel tubes. Chilling the propane to 233 K reduces deposit formation by a factor of three for nickel tubes and by over two orders of magnitude for copper tubes. Because of the narrow range of wall temperature which resulted during the single copper tube test, it is not clear whether or not the rate of carbon deposition increases with increasing wall temperature as shown earlier for the ambient temperature fuel. Furthermore, although the rates of carbon deposition for chilled propane on copper tubes are lower than those for chilled propane on nickel tubes, the differences may not be significant due to the inherent scatter in the data at these low deposit rates. However, as will be discussed later, a similar phenomenon occurred for natural gas. As before, there is no apparent effect of fuel inlet pressure on deposit formation for the range of conditions tested.

The reduction in the rates of carbon deposition observed for chilled commercial-grade propane may be due to freezing and removal of trace sulfur impurities present in the fuel. As shown in Table II, chemical analysis of the propane showed a total sulfur concentration of 25 ppm. This sulfur is usually in the form of corrosive compounds such as methyl mercaptan (CH_3SH), hydrogen sulfide (H_2S), and carbonyl sulfide (COS) (Ref. 27). Adsorption of these compounds onto the tube wall could be a mechanism for carbon deposit formation. Because of nucleate boiling, the inside wall temperature of the cryogenic heat exchanger was close to the liquid nitrogen boiling point of 77 K at 0.1 MPa. The melting points of CH_3SH , H_2S , and COS , are 150, 189, and 135 K, respectively (Ref. 28). Therefore, it is likely that some fraction of these impurities was frozen and retained inside the cryogenic heat exchanger. Consequently, the chilled propane fuel entering the heated test tube probably contained lower concentrations of sulfur impurities, which should have resulted in a reduced amount of adsorption onto the tube wall and a lower rate of carbon deposition. It is unlikely that the slight reduction in the fuel bulk temperatures for the chilled propane tests had a significant effect on the carbon deposition processes.

As in the case of ambient temperature propane, tube wall corrosion in the form of dendrites was evident on the copper tube for the chilled propane test. However, contrary to the previous results, after one of the chilled propane tests for a nickel tube (Run 12, $T_{\text{wall}} = 785 \text{ K}$), copper dendrites were

visible pushing through the nickel plating. The dendrites appeared to start at a location one-third of the way in from the tube entrance, and they extended to the tube exit. Tubes tested at lower wall temperatures (Runs 9 and 10) did not show any deterioration of the nickel plating or the presence of copper dendrites.

The deterioration of the nickel plating and appearance of copper dendrites on the tube used for Run 12 may be a consequence of mechanical rather than chemical phenomena. It is unlikely that the nickel plating on that tube was defective due to the manufacturing process since all tubes were plated simultaneously in the same plating bath. It is more likely that the nickel plating may have fractured as a result of the extreme temperatures and severe gradients that the tube sustained. Initially, cold propane fuel was flowed through the tube, and thereafter electrical power was applied. Because of the different coefficients of thermal expansion between copper and nickel (i.e., a 25 percent difference), the nickel coating may not have expanded as rapidly as the copper during the tube heating process, and it may have cracked. Once the protective nickel coating was broken, propane may have come in contact with the copper and formed dendrites. As will be discussed, cracking of the nickel coating was also observed for tubes subjected to cryogenic natural gas. A more detailed discussion of the appearance and behavior of nickel tubes subjected to high wall temperature conditions will be presented later.

Thermal Resistance

For those thermocouples exhibiting a temperature rise over the test period, the thermal resistance buildup rate (\dot{R}_c) and thermal resistance (t/k) were computed. The results are summarized in Figs. 21 and 22 for \dot{R}_c and t/k as functions of reciprocal initial inner wall temperature. Nominal fuel inlet velocity was 30 m/s and fuel pressures were 6.9 and 13.8 MPa for all data shown. The data (acquired in this program) are for a 10-min run duration and include copper and nickel tubes, ambient temperature fuel (290 K), and chilled fuel (230 K) tests. Although there is scatter in the data, the smooth curves drawn in both figures are based on trends exhibited by kerosene-type fuels in Refs. 1 and 20. The peak thermal resistance buildup rates for propane are of the same order of magnitude as those determined for RP-1 at comparable test conditions.

Natural Gas Tests

Wall Temperature Distributions and Thermal Resistance

Figures 23 and 24 summarize typical inner wall temperature and bulk fuel temperature distributions as a function of tube axial position for natural gas in copper and nickel tubes, respectively. Each figure presents results from two tests; the upper plot corresponds to ambient temperature fuel and the lower plot to cryogenic fuel. Temperature distributions measured at the start of a test and after 10 min are shown.

As is evident in Fig. 24, the wall temperatures for natural gas in nickel tubes increase monotonically from the tube entrance to the tube exit. This was characteristic of all tests using nickel tubes. However, as shown in Fig. 23, the wall temperature distributions for copper tubes exhibited points of inflection characterized by steep positive and negative gradients. At the same time, occasional wall temperature instabilities were common for the copper tubes during early stages of the tests. The exact reasons for these phenomena are not known. Possible explanations include large variations in the energy transport properties of the fuel as the bulk temperature nears the critical temperature (191 K), and/or superficial effects owing to deterioration of the inner tube wall due to corrosion by the sulfur impurities in the fuel.

The thermal resistance buildup rate and thermal resistance were computed, and the results are summarized in Figs. 25 and 26 for 10-min tests. Data from copper tube, nickel tube, ambient temperature (290 K), and cryogenic (160 K) fuel tests are shown. Both the thermal resistance buildup rate and thermal resistance reach their maximum values at a wall temperature of approximately 430 K ($1/T_{wI} = 2.3 \times 10^{-3} \text{ (K)}^{-1}$). There appears to be no effect of either tube material or bulk fuel temperature on thermal resistance or thermal resistance buildup rates. Peak thermal resistance buildup rates (as well as thermal resistances) for natural gas are about an order of magnitude higher than those found for RP-1 (cf., Fig. 14). As will be shown in the next section, carbon deposition rates for natural gas are well below those for RP-1. This apparent anomaly between the thermal resistance buildup and carbon deposition rates for the two fuels may be explained through differences in the surface condition of the deposit (e.g., roughness) and/or thermal conductivity.

Effect of Tube Surface Material on Carbon Deposition

Figures 27 and 28 summarize the rate of carbon deposition data for natural gas on copper and nickel tubes, respectively. In each figure, the rate of carbon deposition is plotted as a function of initial inner wall temperature on an absolute basis ($\mu\text{g}/\text{cm}^2\text{-hr}$) and on a normalized basis ($\text{ppm}/\text{cm}^2\text{-hr}$) where the mass of deposit has been divided by the total mass of fuel which flowed through the tube during the test period. Data for both ambient temperature and cryogenic natural gas are displayed. Arrows are shown on the plots to designate which data points correspond to a given fuel temperature.

On Figs. 27a and 28a, a trend of decreasing rates of carbon deposition with increasing wall temperature is evident for copper and nickel tubes. Contrary to the previous results for RP-1 and propane, on average, the carbon deposition rates for nickel tubes exceed those for copper tubes. As discussed earlier using information cited from Ref. 13, deposit formation on nickel resulting from pyrolysis of light hydrocarbon gases is often greater than that on copper. Also, research done for methane (Ref. 29) showed the rate of deposit formation on nickel to be several times greater than that on copper. The highest rates of carbon deposition occur at wall temperatures in the range of 300 to 500 K, and correspond to those tests using cryogenic fuel. Because of the possibility that this trend due to the difference in fuel flow rates (density) between ambient temperature (gaseous) and cryogenic (compressed liquid) fuels (a factor of four), the rates of carbon deposition were normalized relative to the total mass of fuel passed through the test tube. These plots are summarized as Figs. 27b and 28b. A trend of decreasing rates of carbon deposition with increasing wall temperature may still exist, but the relative magnitude of this decrease is obviously not nearly as great as it first appears when comparisons are made on an absolute basis. Of course, differences due to surface material are unaffected by normalizing the data.

Similar to observations with propane, most natural gas tests using copper tubes show deterioration of the surface manifested in the form of copper dendrites. However, the size and number of these dendrites appear to be significantly less than observed for a typical propane test. For tests using ambient temperature natural gas, the nearly uniform formation of dendrites at all axial locations between the tube entrance and tube exit is typical. However, for cryogenic fuel tests, dendrites form only at those sections closest to the tube exit (i.e., near the maximum wall temperature). Dendrite formation is greatest on tube sections with initial inner wall temperatures between 500 and 700 K. The only copper tube not to show any evidence of copper dendrites was that of Run 16, which also has zero deposit. This test

was for a relatively high maximum initial wall temperature (i.e., 824 K). This observation is consistent with the hypothesis that carbon deposition in natural gas may be due to adsorption of mercaptans (corrosive hydrocarbon-sulfur impurities) in the fuel on the tube wall. As wall temperature increases, the rate at which the adsorption mechanism proceeds decreases, thereby decreasing deposit formation and tube corrosion. Also, deposit formation owing to pyrolysis reactions (i.e., cracking of the hydrocarbon fuel molecule) which normally occur at high temperature for fuel molecules having more than a single carbon atom are nonexistent for methane. Thus, it may be possible to minimize deposit formation in natural gas by operation at high wall temperatures.

All nickel tube tests using cryogenic natural gas showed evidence of breakdown of the nickel plate and formation of copper dendrites at axial locations near the tube exit. Initial inner wall temperatures for these tube sections were between 700 and 800 K. However, no deterioration of the nickel plating occurred at these wall temperatures for ambient temperature natural gas. As explained earlier for chilled propane, fracturing of the nickel plating may be a consequence of the different coefficients of thermal expansion between nickel and copper and the rapid change in wall temperature during test start-up as electrical power is applied to the tube.

As reported in Table III, the sample of natural gas used in this program contained 4 ppm total sulfur. Typically, an odorant called tertiary-butyl mercaptan $[(\text{CH}_3)_3\text{CSH}]$ is added to natural gas at the refinery to give a total sulfur concentration of between 4 and 5 ppm (Ref. 30). Therefore, it is logical to assume that all of the sulfur contained in natural gas is in the form of $[(\text{CH}_3)_3\text{CSH}]$. The melting point of $[(\text{CH}_3)_3\text{CSH}]$ is 274 K (Ref. 28).

As will be discussed later, a scanning-electron-microprobe analysis of a typical natural gas deposit in a copper tube showed sulfur present. The concentration of sulfur in the deposit, the degradation of the copper tube, and the increase in the rate of deposit formation with a decrease in tube wall temperature may be explained through the adsorption mechanism described earlier. A decrease in the rate of carbon deposition with an increase in wall temperature could be due to a decrease in the rate of adsorption of mercaptan on the tube wall. Also, at wall temperatures above 700 K and wall temperatures below 500 K, dendrite formation was visibly less than that occurring between 500 and 700 K. When the inside tube wall is below the melting point of the mercaptan, tube corrosion is reduced because in a solid state, the mercaptan is unable to react with the copper wall. At very high wall temperatures a corrosive agent such as mercaptan cannot condense onto the tube surface. Consequently, corrosion is reduced.

Effect of Fuel Velocity on Carbon Deposition

In order to explore the effects of fuel velocity on carbon deposition for natural gas, copper tube tests were performed at two additional fuel inlet velocities (65 and 98 m/s) above the baseline value (30 m/s). Nominal inlet pressure and temperature were 6.9 MPa and 290 K, respectively. A plot summarizing the rates of deposition and describing the effects of fuel velocity on carbon deposition is shown in Fig. 29. In the figure, carbon deposition rates corresponding to the three fuel velocities are shown for initial inner wall temperatures between 550 and 625 K. Although there is scatter, the data indicate the rate of carbon deposition is nearly constant with fuel velocity. Based on these experiments, it is reasonable to conclude that there is no effect of fuel velocity on carbon deposition suggesting deposit formation may be limited by the kinetics of the deposition processes for natural gas.

Effect of Intermittent Operation and Test Time on Carbon Deposition

Similar to what was done for propane, a longer duration test was performed in which a nickel tube was heated intermittently for eight 3-min cycles to determine the effects of intermittent operation and test duration on carbon deposition. A summary of the carbon deposition rates acquired for two test durations is shown in Fig. 30. Nominal fuel inlet pressure, velocity, and temperature of the natural gas were 13.8 MPa, 30 m/s, and 290 K, respectively. The data plotted correspond to initial inner wall temperatures between 550 and 620 K. As the line drawn through the data points suggests, there appears to be no effect of intermittent operation or test time on the carbon deposition rates for the range of conditions shown. Recall earlier for propane, there was a trend of decreasing carbon deposition rates with increasing test time. However, since carbon deposition rates for natural gas are low (i.e., less than $100 \mu\text{g}/\text{cm}^2\text{-hr}$) and because of data scatter, differences associated with test time may not be discernible.

Deposit Morphology

Deposit Appearance

Longitudinal sections of copper test tubes were photographed at low magnification (8x) to document the macrostructure of deposits formed from RP-1, commercial-grade propane, and natural gas. These photographs are presented in Fig. 31. The sections correspond to a point on the tube approximately 1.9 cm downstream of the entrance (i.e., Section 2, Fig. 8). A section of a clean, unused copper tube is also shown in the figure and serves as a reference for comparison. The test conditions corresponding to each tube section are listed in Table VIII for the indicated run number.

As shown in the photograph for the RP-1 base fuel, there is a nonuniform coverage of the tube surface by a black deposit, and there is evidence of flaking of the deposit layer. These flakes of deposit were collected on a nylon-membrane filter downstream of the test section and subsequently examined under a low-power microscope. There was evidence in the deposit collected that copper had been stripped from the tube wall, presumably as a consequence of the flaking action. Because of the obvious difficulties associated with recovering or accurately weighing such small particles, no attempt was made to quantify the amount of deposit or copper collected on the filter. In addition, the tube surface appears to have been roughened by this flaking action.

The effect of doping RP-1 with metal deactivator (0.005% by weight) is shown in Fig. 31. Although the tube is discolored, the amount of deposit on the tube is visibly less than that shown for the base fuel. As before, deposit flaking and erosion of the copper wall are evident. Recall that on average, carbon deposition rates obtained for this test were lower than those obtained for RP-1.

The deposits formed from RP-1 doped with sulfur additives (0.05% sulfur by weight), shown in Fig. 31 are noticeably thicker in appearance than those obtained for the RP-1 base fuel. In addition, a greater degree of flaking of deposit accompanied by roughening of the tube surface is apparent. Copper dendrites breaking through the deposit were evident on tube mid and exit sections (i.e., Sections 6 and 10, not shown). The characteristics of these dendrites will be discussed further in the next section.

The appearance of propane deposits on copper is significantly different from that of RP-1. As shown in Fig. 31, the tube is covered with a uniform layer of black deposit and at the same time, copper dendrites are visible. Examination of the entire tube showed the size and number of dendrites to increase from the tube entrance to exit (i.e., as wall temperature increases). The dendrites could be easily removed by scraping, leaving a depression in the tube. The roughening of the tube surface associated with formation of dendrites is a possible explanation for the significant drop in fuel pressure with axial location for heated-tube tests exhibiting dendrites. The natural gas deposits are similar in appearance to those obtained with propane; that is, the tube surface shown in Fig. 31 is covered with a nearly uniform layer of loose deposit and copper dendrites were visible on sections near the tube exit. However, the dendrites appeared smaller and were not as numerous as those seen for propane. Although a layer of black deposit is clearly visible on this tube, the burnoff tests indicated negligible carbon deposit levels across the tube. Low-magnification color photographs taken of deposits on nickel tubes were not helpful because of the difficulty in discriminating black deposits on the dark-colored nickel surface.

Some additional comments relative to the appearance of deposits on tube surfaces are in order. Although sections of the nickel tube that was tested with RP-1 (Run 2) appeared clean under low-power magnification, high levels of carbon were detected by the burnoff analyses. In contrast to this, a black layer of carbonaceous deposit always formed with propane (ambient and chilled) in copper tubes for all wall temperatures investigated. Thus, there was often no correlation between the appearance of the deposit on the tube and the amount of carbon present (cf., Fig. 20). For propane (ambient and chilled) in nickel tubes at wall temperatures below 450 K, the surface of the tube always appeared clean (as though it were unused); however, X-ray scans and the burn-off analyses detected significant levels of carbon. For wall temperatures above 450 K, the nickel surface was covered with a layer of black deposit, and this deposit contained a relatively high concentration of oxygen (as detected by X-ray mapping).

For natural gas in copper tubes, the tube surface was covered with a black deposit layer at wall temperatures between 230 and 700 K. The color of this layer changed to gray at wall temperatures above 700 K. In addition, carbon deposit levels were negligible at wall temperatures above 600 K. For natural gas in nickel tubes, high levels of carbon deposit were found at wall temperatures below 700 K (tube appeared clean); whereas carbon deposit levels above 700 K were negligible (tube had a layer of black deposit). The apparently non-carbonaceous deposits which form on nickel tubes at wall temperatures above 700 K may be oxide layers produced from impurities (i.e., introduced in the electroless plating process).

Deposit Composition

Quantitative scanning-electron-microprobe analyses were done for representative deposits formed in copper tubes to determine the approximate relative elemental concentrations of carbon, copper, sulfur, oxygen, and nitrogen present in the deposit. Copper was a major constituent for all deposit samples analyzed. In general, those deposits exhibiting significant copper dendrite formation (i.e., Runs 4 and 5) showed the highest levels of copper. Also, the concentrations of oxygen and nitrogen were significant in all cases, and they generally exceeded those of carbon and sulfur. Presumably, the oxygen and nitrogen in the deposit originated from trace concentrations present in the fuel.

Scanning-electron-microscope photographs of deposit formed from RP-1 doped with sulfur were taken to document the degree of tube deterioration and to relate it to that reported for propane in Ref. 1. Photographs of different aspects of the deposit are shown in Fig. 32. Four typically different regions are shown and are labelled A, B, C, and D. In conjunction with the scanning-

electron-microscope photographs, a scanning-electron microprobe incorporating an X-ray energy dispersive spectrometer was used to produce a qualitative scan of the elements having atomic numbers greater than 11. Carbon (atomic number 6) escapes detection by this technique. As expected, Region A which corresponds to the copper tube wall was found to contain only copper. Region B which appears to be a layer of deposit immediately adjacent to the tube wall was rich in copper and sulfur and contained traces of silicon and aluminum. Region C, which is adjacent to Region B, was similar in composition to Region B. Because Regions B and C appear black, it is reasonable to assume they contain carbon; however, the concentrations of sulfur suggest compounds such as copper sulfide (e.g., Cu_2S or CuS). Finally, Region D (i.e., dendrites) was found to contain only copper. As shown in Fig. 32a, these dendrites have broken through layers of deposit. Another view of a dendrite forming and piercing the layers of deposit is shown as Fig. 32b. This phenomenon is similar to that observed for propane. However, fewer dendrites formed in the RP-1 and sulfur test in comparison to the number found after a typical propane test.

Heat Transfer Correlation Analyses

The forced-convection heat transfer data acquired in this program and in the previous phase (Ref. 1) were correlated using the expression defined earlier in Eq. (4), and best-fit empirical relations were determined for clean tubes. Nusselt number was correlated as a function of Reynolds number, Prandtl number, and fuel properties and expressions were developed for each of the test fuels (RP-1, chemically-pure propane, commercial-grade propane, and natural gas) within the range of experimental conditions. In addition, the forced-convection data from several of these fuels were commingled, and a generalized expression was developed for liquid hydrocarbons. The results of the heat transfer correlation analyses are summarized in Table XII.

As shown in Table XII, an attempt was made to simplify the correlating equations by eliminating some of the fuel properties terms. For RP-1 and propane (chemically pure and commercial grades), the simple Dittus-Boelter form of the equation was found to be satisfactory for correlating the data; that is, there was no significant reduction in the correlation coefficient when the fuel properties ratios were deleted. Therefore, the major effects on the heat transfer coefficient are accounted for by the Reynolds and Prandtl number terms, and this dependence is illustrated graphically in Fig. 33. Because of the wide variations in the thermophysical properties of natural gas over the test temperature range, which extended well below and well above the critical temperature (191 K), it was not possible to obtain a satisfactory correlation without retaining the fuel properties terms. This is illustrated

in Table XII by the failure to obtain a suitably accurate Dittus-Boelter type correlation of the natural gas data. However, as shown in the table, it is possible to simplify the overall natural gas correlation by eliminating the term $(P/P_{crit})^h$ using a statistical significance test (Student's t) that is included as part of the regression analysis computer program.

A correlating expression for each fuel was selected from Table XII and used to calculate a value of Nusselt number at each data point. The calculated Nusselt numbers are compared to the experimentally-derived values in Figs. 34 to 37, with the imposed bandwidth of ± 30 percent illustrating the extent of the departure. For each fuel, the valid ranges of Reynolds and Prandtl numbers for which the correlation was developed are shown. As shown in these figures, the agreement between the experimentally-derived and calculated Nusselt numbers is satisfactory; that is, the bandwidth of ± 30 percent encloses 94 percent of the data for RP-1, 97 percent for chemically-pure propane, 78 percent for commercial-grade propane, and 97 percent for natural gas. The commingled correlation for RP-1 and propane, shown in Fig. 38, encloses 82 percent of the data within a bandwidth of ± 30 percent. In addition, there is very good agreement between the correlation for RP-1 plotted in Fig. 34 and a RP-1 expression generated at Rocketdyne (Ref. 31).

Hydrostatic Burst Tests

The extent of corrosion damage incurred by a test tube owing to the carbon deposition process is of interest. Considerable surface degradation resulted from heated copper-tube tests conducted with RP-1 fuel having a high sulfur content and with commercial-grade propane. This surface degradation manifested itself in the form of fibrous dendritic or tree-like structures which appeared to grow out of the copper surface. In order to assess whether the mechanical strength of the copper tube was significantly reduced as a consequence of this phenomenon, hydrostatic burst tests were conducted on two 3.81-cm-long tube specimens. A specimen from a clean copper tube, not subjected to test conditions, served as a control. The test specimen was evaluated after burnoff analysis and corresponded to a typical propane test (Run 5, Section 7). Copper dendrite structures were clearly visible along the entire length of the longitudinal sections upstream and downstream of the test specimen.

For each specimen, the outer Inconel sheath was removed from the inner copper tube using a specially developed technique to ensure that the copper tube would not be damaged during the removal process. The procedure involved machining the diameter of the outer Inconel tube on a lathe and threading the

specimen through a die to engrave a spiral pattern in the sheath. Using a pair of needle-nosed pliers, the Inconel sheath, now sufficiently weakened by the turning and threading operations, was easily stripped away from the copper core tube.

The theoretical burst pressure at room temperature for the thick-wall copper tubes used in this investigation was estimated to be of 115 MPa. Because a pressure source of only 69 MPa was available, the tests were conducted at elevated temperature to reduce the ultimate tensile strength of the copper and consequently the burst pressure. Therefore, each tube was heated in an oven and pressurized with oil supplied from a positive-displacement pump. Results of these experiments which were conducted at 820 K showed the control tube and the tube subjected to the deposit test to burst at 36.0 MPa and 33.2 MPa, respectively. The theoretical burst pressure of the control tube was approximately 40 MPa. Based on the accuracy of the instrumentation used and the anticipated variation in tube samples, it was concluded that no significant reduction in mechanical strength resulted from the corrosive effects observed in the heated-tube deposit test.

CONCLUDING REMARKS

Thermal stability and deposit heat transfer characteristics were investigated for RP-1, commercial-grade propane, and natural gas in heated copper and nickel-plated copper tubes. In addition, the effects of fuel additives and contaminants, cryogenic fuel temperatures, and extended duration testing with intermittent operation were examined. The continuous flow test apparatus used in the experiments permitted independent variation and evaluation of the effects of wall temperature, fuel pressure, and fuel velocity on deposit formation.

Corrosion of the copper tube surface was detected for all fuels tested, possibly due to reactions with the trace sulfur impurities present in the fuel. Plating the inside of the copper tubes with nickel reduced deposit formation and eliminated tube corrosion in most cases. However, cracking of the nickel plating did occur when subjected to cryogenic natural gas at 160 K. For natural gas in copper tubes, operation above wall temperatures of 700 K produced a significant reduction in deposit formation on an absolute basis and a complete elimination of tube corrosion.

Doping RP-1 fuel with a commercially-produced metal deactivator resulted in a significant reduction in the levels of deposit formed. However contaminating the RP-1 fuel with organic sulfur compounds in order to increase its sulfur concentration to the specification maximum resulted in significantly greater deposit formation and tube corrosion.

For short test durations (< 30 min), the rates of deposit formation were found to decrease as test time increased.

Chilling the propane fuel prior to entry into the heated tube significantly reduced deposit formation rates. However, cryogenic cooling of natural gas (97 percent methane) did not significantly reduce deposit formation.

The effect of fuel velocity on deposit formation was varied. For RP-1 and propane in copper tubes at wall temperatures below 650 K, increases in fuel velocity resulted in decreases in the rate of carbon deposition. However, counter trends were observed for RP-1 in copper tubes at wall temperatures above 650 K and RP-1 in nickel tubes. No effect of fuel velocity on the rates of carbon deposition was detected for natural gas.

For all fuels investigated, formation of deposit did not always coincide with a rise in wall temperature. Total deposit thermal resistances ranged from 0.001 to 1.0 K-cm²/W. For RP-1, peak thermal resistance buildup rates were found to decrease rapidly as fuel velocity increased.

For RP-1, propane, and natural gas, multiple linear regression correlation analyses were performed to correlate experimentally-measured fuel-side heat transfer film coefficients with Nusselt-Reynolds-Prandtl number expressions for Nusselt numbers between 100 and 10,000. The agreement between the experimentally-derived and calculated Nusselt number was good and, in most cases, better than 90 percent of all data fell within a bandwidth of ± 30 percent.

A plot summarizing the variation of the rates of carbon deposition in copper and nickel tubes for RP-1, commercial-grade propane, and natural gas as a function of wall temperature is shown in Fig. 39. In most cases, the three fuels are compared at a common test condition corresponding to a fuel inlet pressure, temperature, and velocity of 13.8 MPa, 290 K, and 30 m/s, respectively. The data for RP-1 in nickel tubes were obtained at velocities of 6 and 18 m/s. Carbon deposition rates for propane in copper tubes were highest and ranged from 300 to 580 $\mu\text{g}/\text{cm}^2\text{-hr}$ at wall temperatures between 400 and 580 K. The lowest rates of carbon deposition were obtained for natural gas in copper tubes, and they did not exceed 80 $\mu\text{g}/\text{cm}^2\text{-hr}$ at wall temperatures between 500 and 650 K. Carbon deposition rates of 200 to 320 $\mu\text{g}/\text{cm}^2\text{-hr}$ were typical for RP-1 in copper tubes at wall temperatures between 560 and 750 K. For natural gas, the unexpected trend of increasing carbon deposition rates (approaching those of RP-1) with decreasing wall temperature was explained as being possibly due to wall adsorption of mercaptans present in the fuel in trace concentrations. It is postulated that at higher fuel temperatures, this mechanism did not exist.

Based on the results of this program, the following conclusions can be made:

1. Natural gas is an attractive rocket fuel with regard to thermal stability.
2. Metallic coatings on the insides of the copper cooling tubes are an effective way to reduce deposit formation and tube corrosion.
3. Cryogenic cooling of the fuel may be a means to remove some of the impurities which are detrimental to thermal stability.

The key benefit derived from this program is the quantitative assessment of the carbon deposition and the associated thermal resistance rate as a function of wall temperature for several fuels. Measureable deposits occur for all the candidate hydrocarbon fuels over the temperature range tested and the data generated serve as a basis for the specification of cooling system design criteria.

REFERENCES

1. Roback, R., E. J. Szetela, and L. J. Spadaccini: Deposit Formation in Hydrocarbon Rocket Fuels. NASA CR-165405, August 1981. Also Journal of Engineering for Power, Trans. ASME, Vol. 105, pp. 59-65, January 1983.
2. Szetela, E. J.: Deposits from Heated Gas Turbine Fuels. ASME Paper No. 76-GT-9, 1976.
3. ANON: CRC Literature Survey on the Thermal Oxidation Stability of Jet Fuel. CRC Report No. 590, Coordinating Research Council, Inc., Atlanta, GA. April 1979.
4. Taylor, W. F.: Deposit Formation from Deoxygenated Hydrocarbons, Part I - General Features. Ind. and Eng. Chem., Prod. Res. and Devel., Vol. 13, No. 2, pp. 133-138, 1974.
5. Szetela, E. J., and A. Vranos: Deposits from Heated Fuel-An Information Study. United Technologies Research Laboratories Report R75-214388-1, December 1975.
6. Taylor, W. F.: Kinetics of Deposit Formation from Hydrocarbons. Ind. and Eng. Chem., Prod. Res. and Devel., Vol. 8, No. 375, 1969.
7. Taylor, W. F. and T. J. Wallace: Kinetics of Deposit Formation from Hydrocarbons - Effects of Trace Sulfur Compounds. Ind. and Eng. Chem., Prod. Res. and Devel., Vol. 7, No. 198, 1968.
8. Taylor, W. F.: Mechanisms of Deposit Formation in Wing Tanks. SAE Transactions, Vol. 76, No. 2811, 1968.
9. Lohmann, R. P., E. J. Szetela, and A. Vranos: Analytical Evaluation of the Impact of Broad Specification Fuels on High Bypass Turbofan Engine Combustors. NASA CR-159454, December 1978.
10. Antoine, A.: Effect of Some Nitrogen Compounds on Thermal Stability of Jet A. NASA TM-82908, June 1982.
11. Wong, E. L. and D. A. Bittker: Effect of Hydrocarbon Fuel Type on Fuel Thermal Stability. NASA TM-82916, June 1982.
12. Meehan, R., W. Carson, and R. Morgan: Determine the Effects of Various Metals on the Thermal Stability of Jet Fuel. Pratt & Whitney Aircraft Materials Development Laboratory Work Request, No. 13230, July 1968.

REFERENCES (Cont'd)

13. Baker, R. T. K. and P. S. Harris: The Formation of Filamentous Carbon. Chemistry and Physics of Carbon, Vol. 14. P. L. Walker and P. A. Throver Ed. Marcel Dekker, Inc., New York 1978.
14. McIntosh, L. V.: Fuels Test Report for RP-1 (MIL-P-25576), No. 81-P-48, Aerospace Fuels Laboratory, Mukiteo, WA. December 17, 1981.
15. Winfrey, J. C.: Certificate of Analysis No. 104727, Sample of Liquid Propane, Southern Petroleum Laboratories, Inc., Houston, TX. February 25, 1983.
16. Winfrey, J. C.: Certificate of Analysis No. 105674, Sample of Natural Gas, Southern Petroleum Laboratories, Inc., Houston, TX. March 30, 1983.
17. ANON: Technical Data Book - Petroleum Refining Chapters 7-14, Second Edition. American Petroleum Institute, Division of Refining, Port City Press, Inc., Baltimore, MD. 1971.
18. Goodwin, R. D. and W. M. Haynes: Thermophysical Properties of Propane from 85 to 700 K at Pressures to 70 MPa. Thermophysical Properties Division, National Bureau of Standards, Boulder, CO. NBS Monograph 170.
19. Hendriks, R. C. and A. K. Baron: GASP - A Computer Code for Calculating the Thermodynamic and Transport Properties for Ten Fluids: Parahydrogen, Helium, Neon, Methane, Nitrogen, Carbon Monoxide, Oxygen, Fluorine, Argon, and Carbon Dioxide. NASA TN D-7808, February 1975.
20. TeVelde, J., L. J. Spadaccini, E. J. Szetela, and M. R. Glickstein: Thermal Stability of Alternative Aircraft Fuels, AIAA Paper No. 83-143, June 1983.
21. ANON: DuPont Metal Deactivator. Product Brochure A-7984, Petroleum Chemicals Division, E.I. DuPont de Nemours & Co., Inc., Wilmington, DE.
22. Strigler, Bert. (Technical Services Manager, Conoco): private communication to the author.
23. Winfrey, J. C.: Certificate of Analysis No. 103758, Sample of RP-1 Kerosene Fuel, Southern Petroleum Laboratories, Inc., Houston, TX. February 4, 1983.

REFERENCES (Cont'd)

24. Peschke, W.: Advanced Ejector Thrust Augmentation Study - Mass Entrainment of Axisymmetric and Rectangular Free Jets. Bell Aerospace, Technical Report AFFDL-TR-73-55, April 1973.
25. Bloom, K.: Autodata Ten/10 Calculating Datalogger Operation and Installation Manual, Acurex Corporation, Mountain View, CA. April 1980.
26. Masters, P. A. and C. A. Aukerman: Deposit Formation in Hydrocarbon Rocket Fuels with an Evaluation of a Propane Heat Transfer Correlation. NASA TM-82911, June 1982.
27. Gabel, Robert (Sales Representative, Matheson): private communication to the author.
28. Handbook of Chemistry and Physics, 63rd Edition, 1982-83, CRC Press, Inc., Boca Raton, FL, 1982.
29. Nishiyama, Y. and Y. Tamai: Wall Effects During Thermal Reactions. Chemtech Journal, November 1980.
30. Braker, W. and A. L. Mossman: Matheson Gas Data Book, Sixth Edition, Matheson, Lyndhurst, NJ, 1980.
31. Hines, W. S.: Turbulent Forced Convection Heat Transfer to Liquids at Very High Heat Fluxes and Flowrates. Rocketdyne Research Report 61-41, 1961.

LIST OF SYMBOLS

A	experimentally-determined constant
C_p	specific heat at constant pressure
D	inside tube diameter
E	electrical power
EB	energy balance
f	friction factor
h	specific enthalpy
I	current
k	thermal conductivity
L	tube length
\dot{m}	mass flow rate
Nu	Nusselt number, $U_o D/k$
P	pressure
Pr	Prandtl number, $C_p \mu/k$
Q/A	heat flux
R	correlation coefficient
\dot{R}_c	thermal resistance buildup rate
Re _D	Reynolds number based on tube diameter, $\rho v D/\mu$
T	temperature
t	thickness
Δt	elapsed time

LIST OF SYMBOLS (Cont'd)

t/k	thermal resistance
U	overall inside wall heat transfer coefficient
U_o	inside wall film coefficient
V	voltage
v	velocity
x/D	axial distance to diameter ratio
μ	absolute viscosity
ρ	density
σ	standard deviation

Subscripts

calc	calculated
crit	critical point
exp	experimental
f	fuel
i	inner; initial
max	maximum
o	outer
w	wall
1	tube entrance
2	tube exit

TABLE I

CERTIFIED CHEMICAL ANALYSIS OF RP-1 SPECIFICATION FUEL

Distillation (K)	
Initial boiling point	461
10% evaporated	471
50% evaporated	487
90% evaporated	512
Final boiling point	532
Residue, vol%	1.3
Loss, vol%	0.7
Gravity, °API	43.6
Existent Gum, mg/100ml	2.0
Total sulfur, wt%	0.007
Mercaptan sulfur, wt%	0.0002
Aromatics, vol%	1.26
Olefins, vol%	0.3

PRECEDING PAGE BLANK NOT FILMED

TABLE II

CERTIFIED CHEMICAL ANALYSIS OF COMMERCIAL-GRADE PROPANE

Propane, mol%	94.00
Ethane, mol%	4.27
Iso-Butane, mol%	0.78
Propylene, mol%	0.61
n-Butane, mol%	0.26
Methane, mol%	0.07
Nitrogen, mol%	0.01
Sulfur, ppm	25
Organic Chloride, ppm	<1
Ethylene, mol% in ethane	0.01

TABLE III

CERTIFIED CHEMICAL ANALYSIS OF NATURAL GAS

Methane, mol%	96.508
Ethane, mol%	1.542
Nitrogen, mol%	0.826
Carbon Dioxide, mol%	0.571
Propane, mol%	0.254
Heptanes, mol%	0.096
Iso-Butane, mol%	0.063
n-Butane, mol%	0.062
Iso-Pentane, mol%	0.028
n-Pentane, mol%	0.025
Hexanes, mol%	0.025
Sulfur, ppm	4
Organic Chloride, ppm	<1
Olefins	No. Detected

TABLE IV

THERMODYNAMIC AND TRANSPORT PROPERTIES OF RP-1

T	C_p	ρ	μ	k
(K)	(kJ/kg·K)	(kg/m ³)	(kg/m·s) x10 ⁴	(W/m·K)
256	1.64	847	51.85	0.133
283	1.77	824	24.51	0.126
300	2.00	801	15.63	0.0885
325	2.10	782	10.87	0.0911
350	2.20	763	7.52	0.0942
375	2.36	744	5.42	0.0967
400	2.41	724	4.26	0.0974
425	2.52	704	3.51	0.0982
450	2.63	682	2.98	0.0971
475	2.73	660	2.56	0.0958
500	2.84	637	2.23	0.0942
525	2.95	612	1.90	0.0922
550	3.06	583	1.74	0.0898
575	3.17	552	1.54	0.0871
600	3.28	515	1.36	0.0837
625	3.40	472	1.21	0.0798
650	3.50	405	1.04	0.0730

$P_{crit} = 2.20$ MPa

$T_{crit} = 666$ K

TABLE V
THERMODYNAMIC AND TRANSPORT PROPERTIES OF PROPANE

T (K)	7.0 MPa					13.0 MPa				
	C_p (kJ/kg·K)	ρ (kg/m ³)	μ (kg/m·s) $\times 10^4$	k (W/m·K)	h (kJ/kg)	C_p (kJ/kg·K)	ρ (kg/m ³)	μ (kg/m·s) $\times 10^4$	k (W/m·K)	h (kJ/kg)
180	2.05	641.7	3.74	0.166	194.9	2.043	645.6	3.74	0.166	201.6
200	2.11	621.4	2.81	0.150	236.6	2.093	626.0	2.81	0.150	243.2
220	2.17	600.6	2.19	0.136	279.8	2.152	606.1	2.19	0.136	286.0
240	2.25	579.0	1.76	0.123	324.7	2.223	585.6	1.76	0.123	330.4
260	2.34	556.3	1.43	0.111	371.2	2.307	564.3	1.43	0.111	376.4
280	2.46	532.1	1.17	0.100	419.7	2.406	542.1	1.17	0.100	423.9
300	2.60	505.8	0.95	0.091	470.3	2.524	518.7	0.95	0.091	473.2
320	2.79	476.7	0.77	0.082	523.5	2.662	493.7	0.77	0.082	524.3
340	3.04	443.0	0.60	0.073	580.2	2.821	466.8	0.60	0.073	577.7
360	3.40	401.5	0.42	0.066	642.2	2.976	437.4	0.42	0.066	633.6
380	4.44	342.6	0.27	0.034	715.4	3.334	404.8	0.27	0.043	693.0
400	5.76	240.0	0.18	0.036	821.3	3.447	368.2	0.18	0.044	760.5
420	4.21	164.3	0.12	0.038	920.8	3.615	327.6	0.12	0.045	831.2
440	3.43	131.3	0.07	0.042	995.8	3.686	285.6	0.07	0.048	904.5

$P_{crit} = 4.26 \text{ MPa}$

$T_{crit} = 370 \text{ K}$

TABLE VI
THERMODYNAMIC AND TRANSPORT PROPERTIES OF METHANE

		6.895 MPa						13.790 MPa					
T	(K)	C _p	ρ	μ	k	h	C _p	ρ	μ	k	h		
		(kJ/kg·K)	(kg/m ³)	(kg/m·s) x10 ⁴	(W/m·K)	(kJ/kg)	(kJ/kg·K)	(kg/m ³)	(kg/m·s) x10 ⁴	(W/m·K)	(kJ/kg)		
120		3.545	417.2	1.095	0.1873	324.5	3.486	423.4	1.198	0.1954	334.6		
140		3.555	387.8	0.7548	0.1557	395.3	3.429	396.8	0.8412	0.1652	403.6		
160		3.889	353.3	0.5345	0.1267	471.4	3.600	367.4	0.6121	0.1385	475.9		
180		4.756	307.4	0.3776	0.09787	553.9	3.901	333.4	0.4578	0.1141	548.3		
200		10.06	215.8	0.2362	0.06196	682.6	4.403	291.8	0.3474	0.09174	630.8		
220		5.639	102.2	0.1277	0.03943	862.6	4.986	240.7	0.2779	0.07229	725.0		
240		3.695	75.86	0.1185	0.03747	951.2	4.932	188.1	0.2158	0.05905	825.7		
260		3.114	63.32	0.1189	0.03792	1018	4.275	149.2	0.1806	0.05283	918.1		
280		2.858	55.36	0.1219	0.03923	1078	3.693	124.2	0.1645	0.05067	997.4		
300		2.732	49.64	0.1258	0.04104	1134	3.328	107.5	0.1577	0.05048	1067		
320		2.673	45.23	0.1302	0.04321	1188	3.115	95.63	0.1555	0.05135	1132		
340		2.554	41.09	0.1348	0.04562	1241	2.995	86.63	0.1556	0.05284	1192		
360		2.662	38.75	0.1394	0.04822	1294	2.934	79.52	0.1572	0.05473	1252		
380		2.688	36.26	0.1441	0.05101	1347	2.910	73.70	0.1595	0.05695	1310		
400		2.726	34.10	0.1488	0.05394	1402	2.912	68.83	0.1624	0.05943	1368		
420		2.773	32.22	0.1535	0.05701	1457	2.932	64.66	0.1657	0.06210	1427		
440		2.826	30.56	0.1582	0.06019	1512	2.963	61.05	0.1692	0.06494	1486		
460		2.880	29.00	0.1629	0.06347	1570	3.000	57.87	0.1728	0.06791	1545		
480		2.934	27.74	0.1675	0.06683	1628	3.040	55.05	0.1767	0.07100	1606		
500		2.984	26.54	0.1722	0.07026	1687	3.078	52.53	0.1806	0.07419	1667		
520		3.026	25.44	0.1769	0.07376	1747	3.112	50.25	0.1847	0.07747	1729		
540		3.059	24.43	0.1816	0.07731	1808	3.137	48.18	0.1889	0.08082	1791		
560		3.079	23.51	0.1853	0.08091	1869	3.149	46.30	0.1922	0.08424	1854		
580		3.082	22.66	0.1896	0.08455	1931	3.146	44.57	0.1961	0.08771	1917		
600		3.064	21.87	0.1939	0.08823	1992	3.124	42.97	0.2000	0.09124	1980		

P_{crit} = 4.64 MPa

T_{crit} = 191 K

TABLE VII

CERTIFIED CHEMICAL ANALYSIS OF SULFUR-DOPED RP-1

Carbon, wt%	86.34
Hydrogen, wt%	13.26
Oxygen, wt%	<0.5
Sulfur, wt%	0.050
Nitrogen, wt%	0.043
Naptha and Paraffins, vol%	>99.0
Aromatics, vol%	1.20

TABLE VIII

SUMMARY OF TEST CONDITIONS

Run	Fuel	Tube ⁽¹⁾ Mat'l	Duration (min)	Fuel ⁽²⁾	Fuel ⁽²⁾	Fuel ⁽²⁾	Max. Init. Inner Wall Temp. (K)
				Inlet Temp. (K)	Inlet Velocity (m/s)	Inlet Pressure (MPa)	
1	RP-1	Cu	10.1	279	58	13.7	682
2	+	Ni	10.4	289	30	13.2	701
3	RP-1 & DMD ⁽³⁾	Cu	10.2	291	30	13.6	693
4	RP-1 & S ⁽⁴⁾	Cu	9.9	287	29	13.2	821
5	Propane ↓	Cu	10.0	284	49	13.2	629
6		Ni	9.0	281	34	13.9	589
7		Ni	10.5	287	30	7.44	691
8		Ni	24.0 ⁽⁵⁾	289	32	13.6	590
9		Ni	10.0	234	32	14.5	670
10		Ni	10.2	231	31	7.22	694
11		Cu	9.6	236	30	7.16	683
12		Cu	10.1	229	30	7.40	785
13	Nat. Gas ↓	Ni	10.3	292	31	13.2	596
14		Ni	10.2	292	32	13.6	692
15		Cu	10.4	291	31	13.1	753
16		Cu	9.8	289	31	13.0	813
17		Cu	10.3	292	65	7.30	700
18		Cu	10.3	291	98	7.48	723
19		Ni	10.3	296	32	14.2	804
20		Ni	24.5 ⁽⁵⁾	293	32	14.3	698
21		Ni	10.0	168	34	13.3	694
22		Ni	8.2	173	35	13.0	843
23		Cu	10.0	156	32	13.4	683
24		Cu	10.0	157	33	13.7	862
Calib.	RP-1	Cu	-	varied	varied	13.8	varied
220	Nat. Gas	Ni	10.4	133	29	14.2	793

(1) Cu = Copper; Ni = Nickel-plated copper

(2) At midpoint of run

(3) RP-1 and DuPont Metal Deactivator

(4) RP-1 and sulfur additives

(5) Intermittent operation

TABLE IX

DEPOSIT BURNOFF DATA FOR RP-1

Kun-Section	Tube Material	Duration (min)	Inlet Velocity (m/s)	Init. Inner Wall Temp. (K)*	Avg. Inner Wall Temp. (K)	Deposit Mass (µg)	Deposit Rate (µg/cm ² -hr)	Avg. Deposit Rate (µg/cm ² -hr)
1-3	Cu	10.1	58	659	659	472	1190	1580
5				665		-	-	
7				662		452	1140	
9				650		951	2400	
2-3	Ni	10.4	30	685	623	115	284	1281
5				621		481	1190	
7				596		885	2180	
9				590		596	1470	
3-3	Cu	10.2	30	666	668	26	67	164
5				670		227	584	
7				654		3	7	
9				680		0	0	
4-3	Cu	9.9	29	745	709	25	64	345
5				717		81	209	
7				714		377	973	
9				662		52	134	

ORIGINAL PAGE IS
OF POOR QUALITY

*Mean value

TABLE X

DEPOSIT BURNOFF DATA FOR COMMERCIAL-GRADE PROPANE

Run-Section	Tube Material	Duration (min)	Inlet Velocity (m/s)	Init. Inner Wall Temp. (K)*	Avg. Inner Wall Temp. (K)	Deposit Mass (μg)	Deposit Rate ($\mu\text{g}/\text{cm}^2\text{-hr}$)	Avg. Deposit Rate ($\mu\text{g}/\text{cm}^2\text{-hr}$)
5-3	Cu	10.2	49	541	547	18	46	234
5				528		72	184	
7				544		208	531	
9				574		68	173	
6-3	Ni	9.0	34	495	554	43	122	161
5				551		99	281	
7				581		57	162	
9				586		27	77	
7-3	Ni	10.5	30	415	458	114	278	243
5				425		76	186	
7				454		129	315	
9				537		79	193	
8-3	Ni	24.0	32	495	547	9	10	32
5				538		31	33	
7				578		39	42	
9				576		39	42	
9-3	Ni	10.0	32	557	614	0	0	12
5				591		0	0	
7				644		0	0	
9				665		18	46	

TABLE X (Cont'd)

DEPOSIT BURNOFF DATA FOR COMMERCIAL-GRADE PROPANE

Run-Section	Tube Material	Duration (min)	Inlet Velocity (m/s)	Init. Inner Wall Temp. (K)*	Avg. Inner Wall Temp. (K)	Deposit Mass (μg)	Deposit Rate ($\mu\text{g}/\text{cm}^2\text{-hr}$)	Avg. Deposit Rate ($\mu\text{g}/\text{cm}^2\text{-hr}$)
10-3	Ni	10.2	31	391	483	73	184	97
5				461		56	141	
7				514		15	38	
9				567		10	25	
11-3	Cu	9.6	30	546	573	0	0	3
5				568		0	0	
7				585		0	0	
9				592		5	13	
12-3	Ni	10.1	30	536	619	5	13	71
5				680		0	0	
7				615		80	204	
9				644		26	66	

*Mean value

TABLE XI

DEPOSIT BURNOFF DATA FOR NATURAL GAS

Run-Section	Tube Material	Duration (min)	Inlet Velocity (m/s)	Init. Inner Wall Temp. (K)*	Avg. Inner Wall Temp. (K)	Deposit Mass (μg)	Deposit Rate ($\mu\text{g}/\text{cm}^2\text{-hr}$)	Avg. Deposit Rate ($\mu\text{g}/\text{cm}^2\text{-hr}$)
13-3	Ni	10.3	31	481	533	72	180	128
5				519		65	162	
7				548		45	112	
9				583		25	60	
14-3	Ni	10.2	32	533	595	40	100	73
5				581		56	140	
7				619		20	51	
9				649		0	0	
15-3	Cu	10.4	31	545	624	0	0	0
5				683		0	0	
7				612		0	0	
9				655		0	0	
16-3	Cu	9.8	31	761	714	0	0	0
5				685		0	0	
7				700		0	0	
9				710		0	0	
17-3	Cu	10.3	65	552	620	0	0	79
5				611		127	316	
7				645		0	0	
9				670		0	0	

TABLE XI (Cont'd)

DEPOSIT BURNOFF DATA FOR NATURAL GAS

Run-Section	Tube Material	Duration (min)	Inlet Velocity (m/s)	Init. Inner Wall Temp. (K)*	Avg. Inner Wall Temp. (K)	Deposit Mass (μg)	Deposit Rate ($\mu\text{g}/\text{cm}^2\text{-hr}$)	Avg. Deposit Rate ($\mu\text{g}/\text{cm}^2\text{-hr}$)
18-3	Cu	10.3	98	588	619	0	0	26
5				573		42	105	
7				643		0	0	
9				670		0	0	
19-3	Ni	10.3	32	656	736	16	40	19
5				720		0	0	
7				771		8	20	
9				799		6	15	
20-3	Ni	24.5	32	520	570	144	151	67
5				555		32	33	
7				584		9	9	
9				620		72	75	
21-3	Ni	10.0	34	295	343	111	284	318
5				310		122	313	
7				331		131	336	
9				436		132	338	
22-3	Ni	8.2	35	251	313	71	222	325
5				278		289	905	
7				310		0	0	
9				415		55	172	

TABLE XI (Cont'd)

DEPOSIT BURNOFF DATA FOR NATURAL GAS

Run-Section	Tube Material	Duration (min)	Inlet Velocity (m/s)	Init. Inner Wall Temp. (K)*	Avg. Inner Wall Temp. (K)	Deposit Mass (μg)	Deposit Rate ($\mu\text{g}/\text{cm}^2\text{-hr}$)	Avg. Deposit Rate ($\mu\text{g}/\text{cm}^2\text{-hr}$)
23-3	Cu	10.0	32	270	354	128	328	188
5				306		40	103	
7				336		102	261	
9				502		24	62	
24-3	Cu	10.0	33	225	302	79	203	182
5				254		113	290	
7				283		62	159	
9				446		29	74	
220-3	Ni	10.4	29	271	355	118	291	267
5				308		110	272	
7				338		123	304	
9				504		82	202	

*Mean value

TABLE XII

FORCED-CONVECTION HEAT TRANSFER CORRELATION ANALYSES FOR HYDROCARBON ROCKET FUELS

$$\text{Correlation Equation: } Nu = A Re^b Pr^c \left(\frac{\rho}{\rho_w} \right)^d \left(\frac{\mu}{\mu_w} \right)^e \left(\frac{k}{k_w} \right)^f \left(\frac{\bar{C}_p}{C_p} \right)^g \left(\frac{P}{P_{crit}} \right)^h \left(1 + \frac{2}{x/D} \right)$$

Fuel	Coefficient/Exponent										No. of Points	Std. Dev.	Correl. Coeff.
	A	b	c	d	e	f	g	h					
RP-1	0.0095 0.0068	0.99 0.94	0.4* 0.4*	0.37 0*	0.60 0*	-0.20 0*	-6.0 0*	-0.36 0*	274 274	0.16 0.20	0.97 0.96		
Chem. Pure Propane	0.011 0.020	0.87 0.81	0.4* 0.4*	-9.6 0*	2.4 0*	-0.57 0*	0.26 0*	-0.23 0*	79 79	0.098 0.15	0.99 0.97		
Commercial Propane	0.034 0.028	0.80 0.80	0.4* 0.4*	-0.24 0*	0.098 0*	-0.48 0*	2.1 0*	-0.38 0*	285 285	0.27 0.29	0.94 0.93		
Natural Gas	0.00069 0.0028 3.7	1.1 1.0 0.42	0.4* 0.4* 0.4*	1.4 1.5 0*	-6.5 -6.5 0*	6.3 6.4 0*	2.6 2.4 0*	0.087 0* 0*	130 130 130	0.16 0.16 0.38	0.92 0.92 0.30		
Note (1)	0.019	0.81	0.4*	-0.059	0.0019	0.083	0.52	0.11	768	0.28	0.97		
Note (2)	0.044	0.76	0.4*	0*	0*	0*	0*	0*	638	0.26	0.98		

*Denotes exponent held constant in analysis

Notes

- (1) Commingled correlation for RP-1, chemically-pure propane, commercial-grade propane, and natural gas
- (2) Commingled correlation for RP-1, chemically-pure propane, and commercial-grade propane

ORIGINAL PAGE IS
OF POOR QUALITY

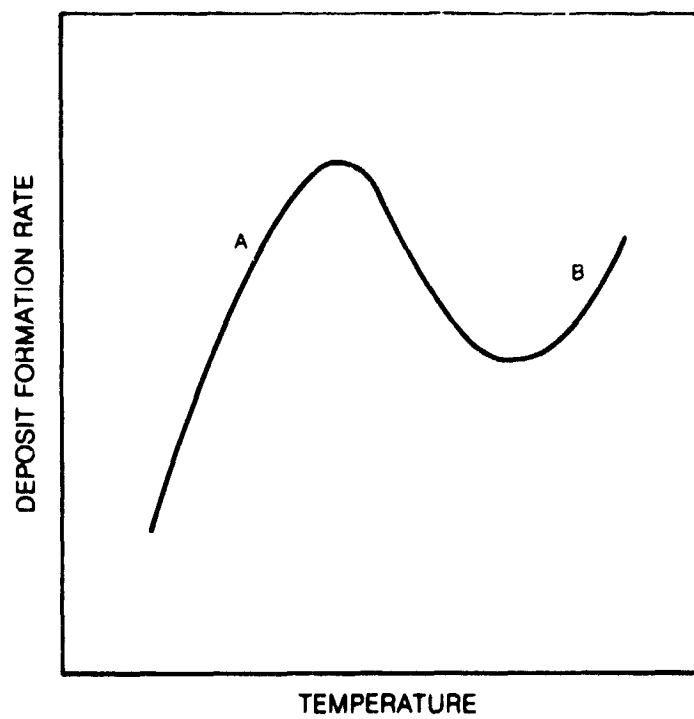


Figure 1. Carbon Deposition for Hydrocarbon Fuels in Contact with a Hot Surface

ORIGINAL PAGE IS
OF POOR QUALITY



Figure 3. Deposit Formation Test Facility

ORIGINAL PAGE IS
OF POOR QUALITY

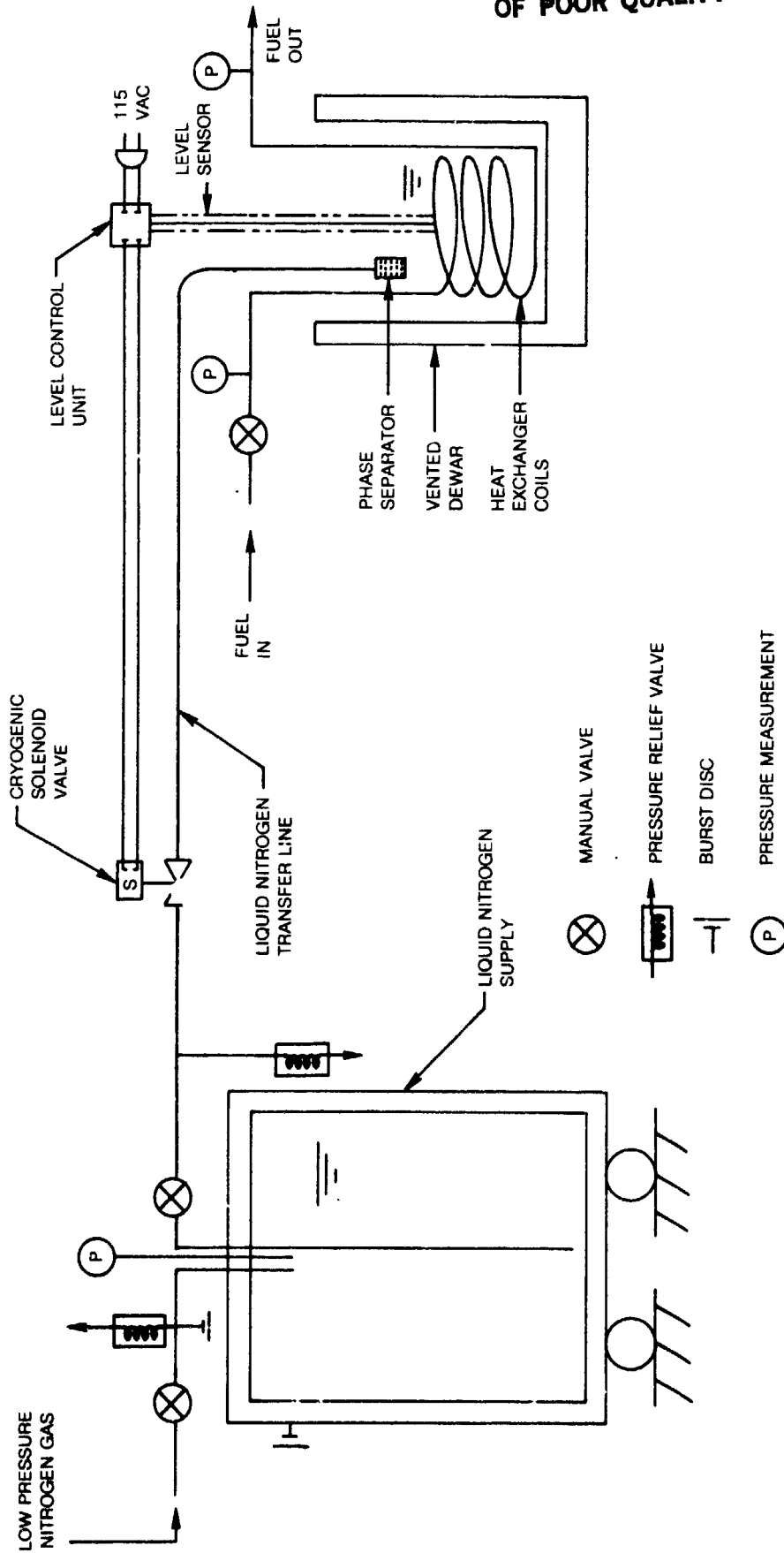


Figure 4. Cryogenic Fuel Delivery System

ORIGINAL PAGE IS
OF POOR QUALITY

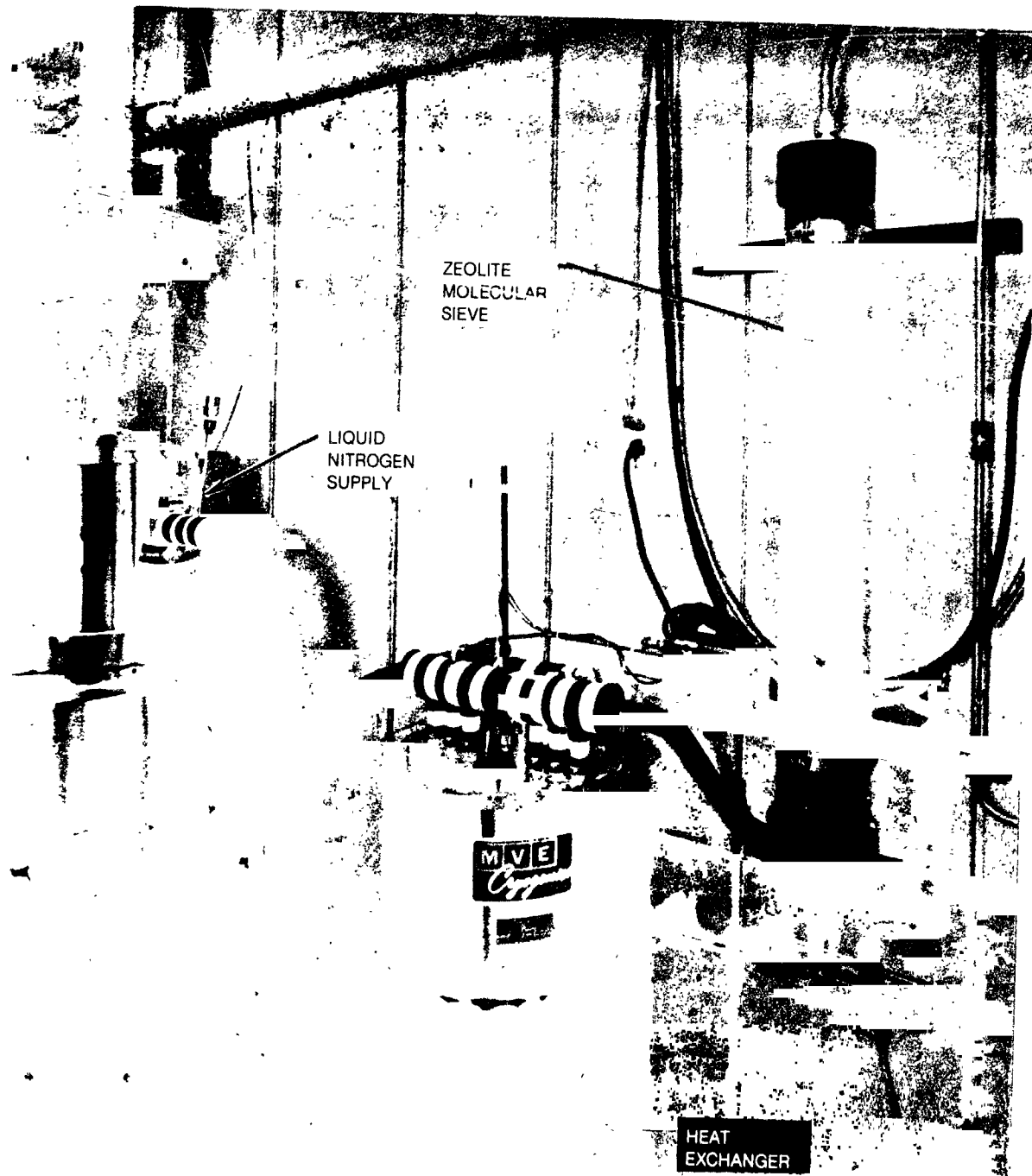


Figure 5. Cryogenic Heat Exchanger

ORIGINAL PAGE IS
OF POOR QUALITY

ALL DIMENSIONS IN CENTIMETERS

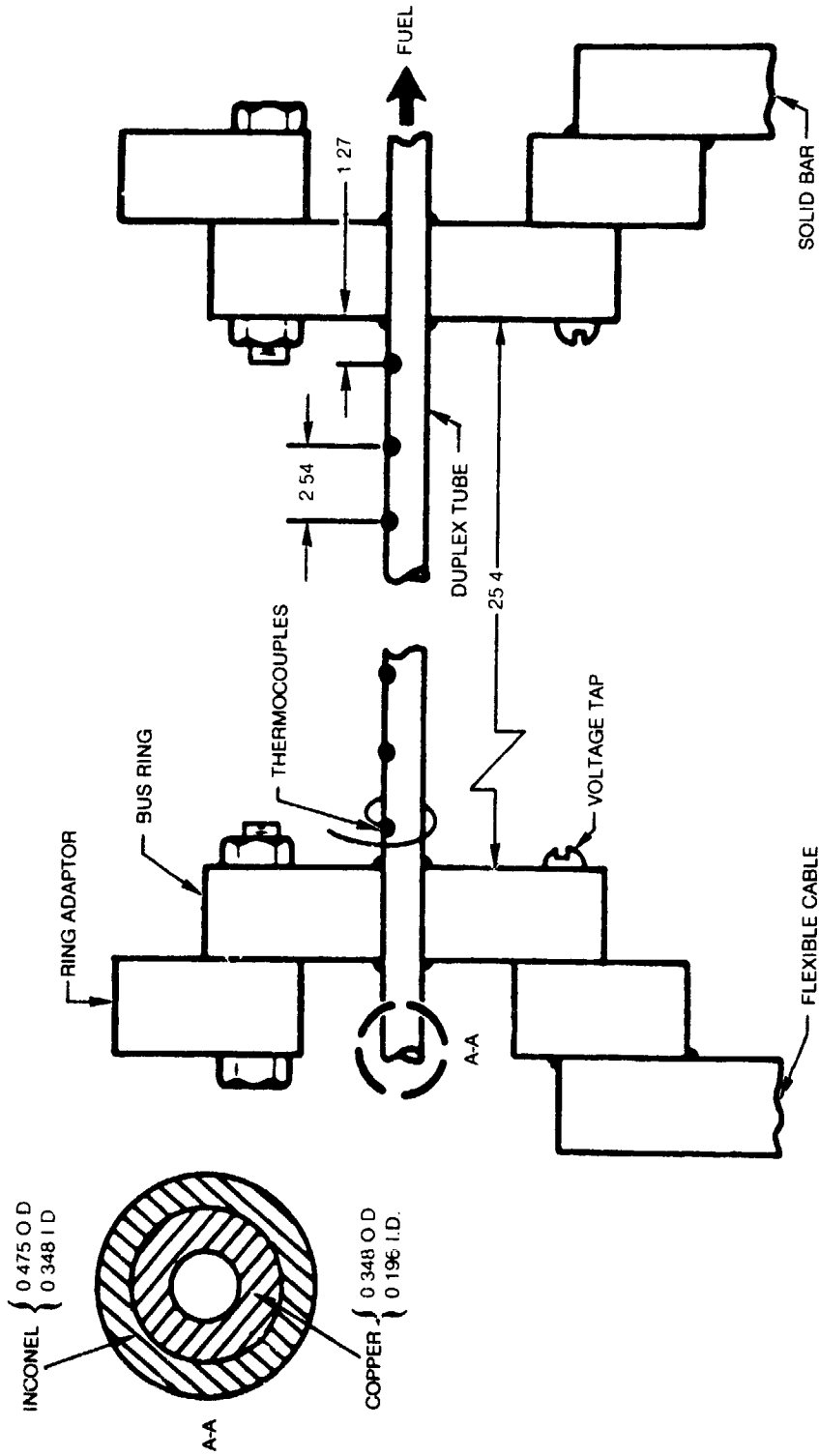


Figure 6. Test Tube Assembly

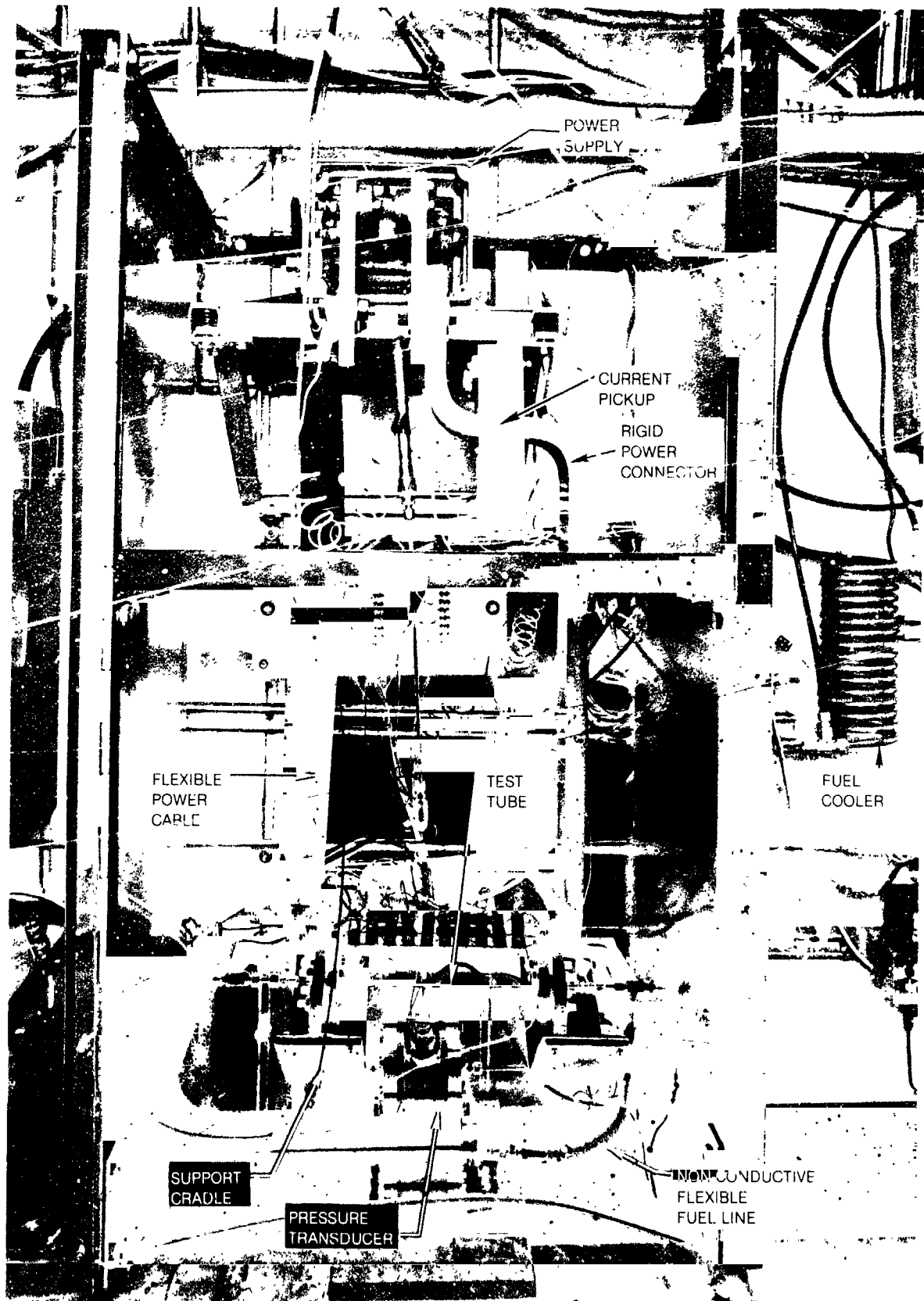


Figure 7. Test Section Mounting Arrangement

ORIGINAL PAGE IS
OF POOR QUALITY

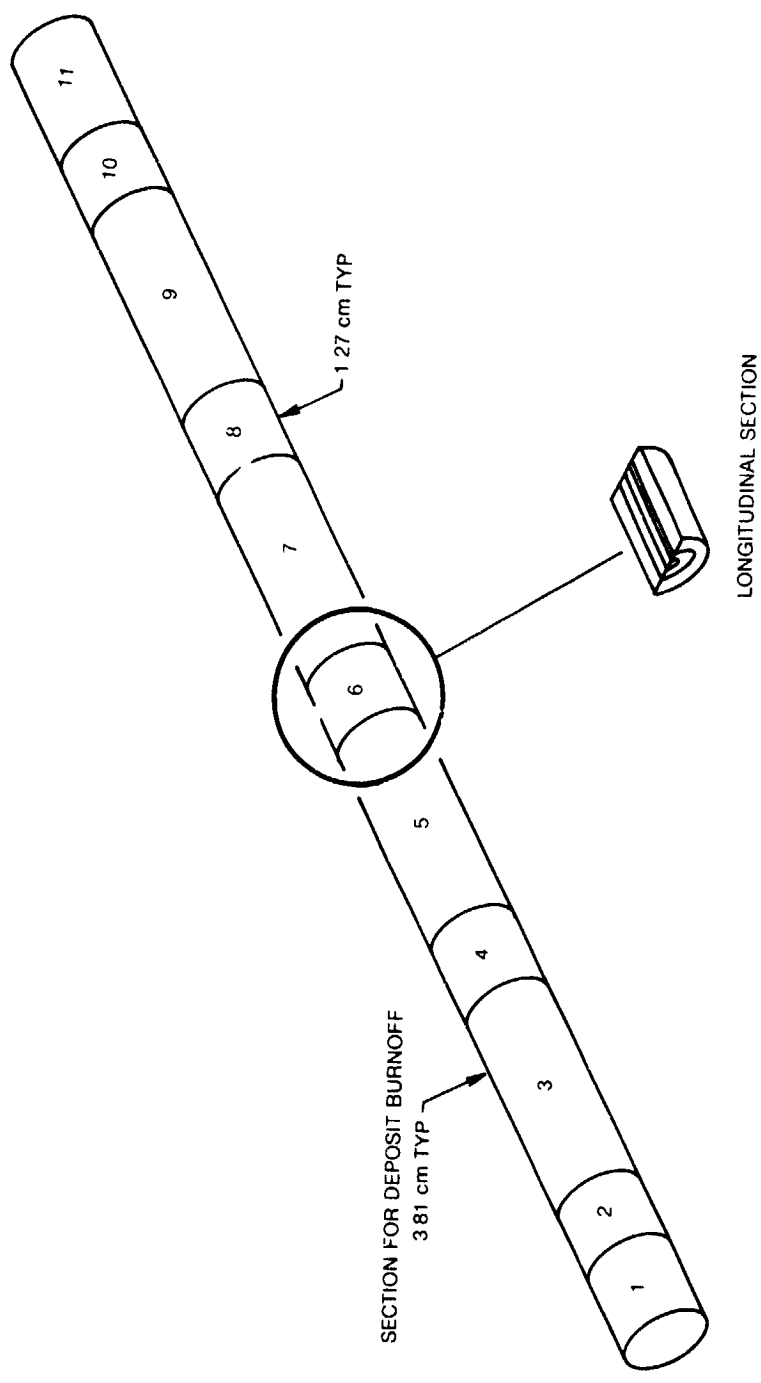
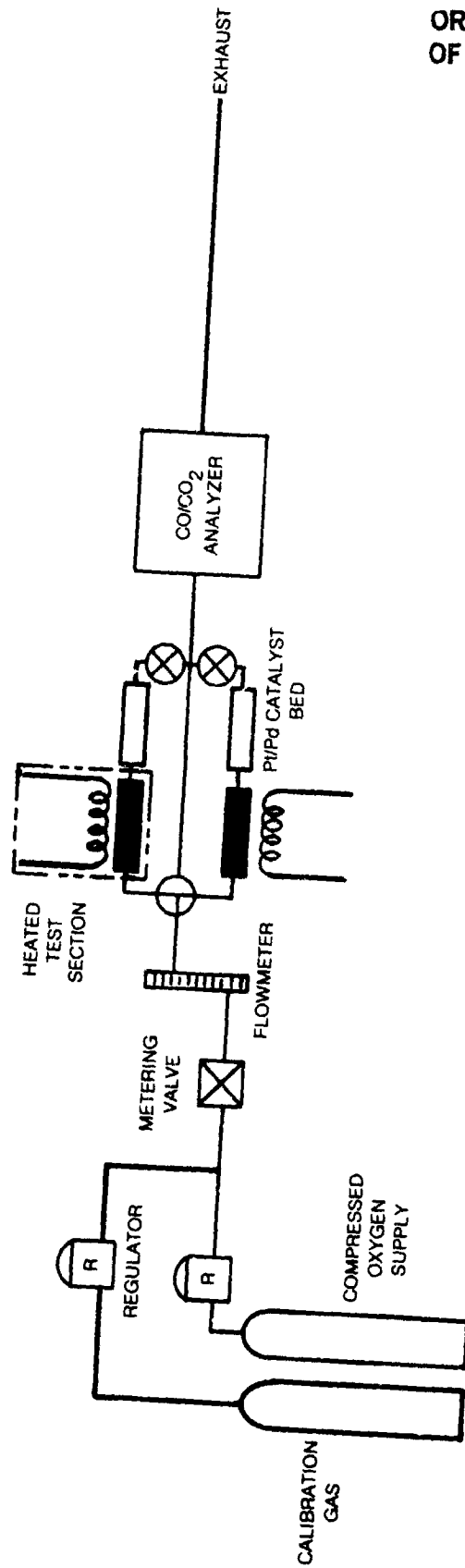


Figure 8. Tube Sectioning



ORIGINAL PAGE IS
OF POOR QUALITY

Figure 9. Deposit Burnoff Apparatus

ORIGINAL PAGE 13
OF POOR QUALITY

RP-1
COPPER TUBE
P = 13.8 MPa

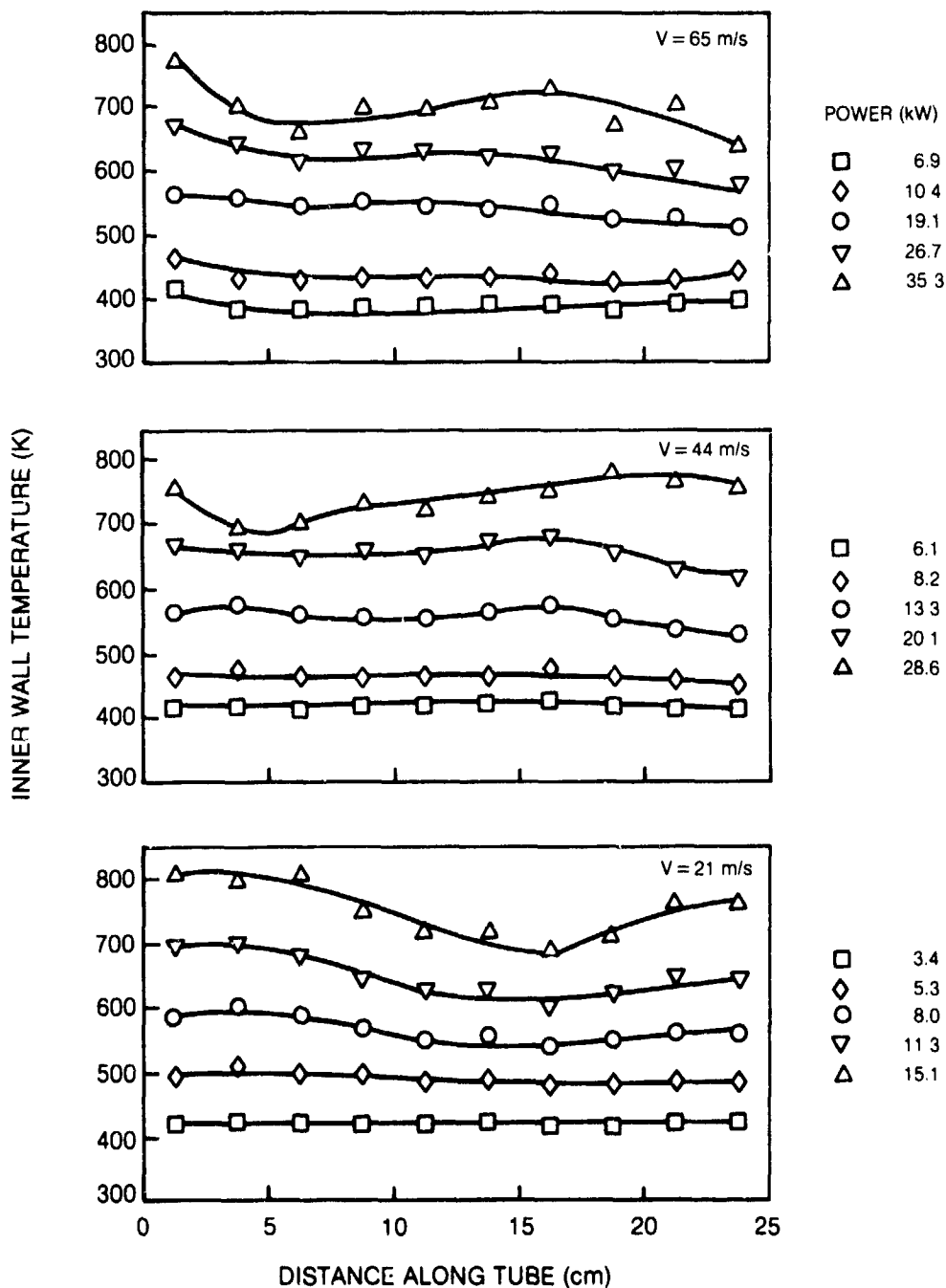


Figure 10. Variation of Axial Wall Temperature with Power

ORIGINAL PAGE IS
OF POOR QUALITY

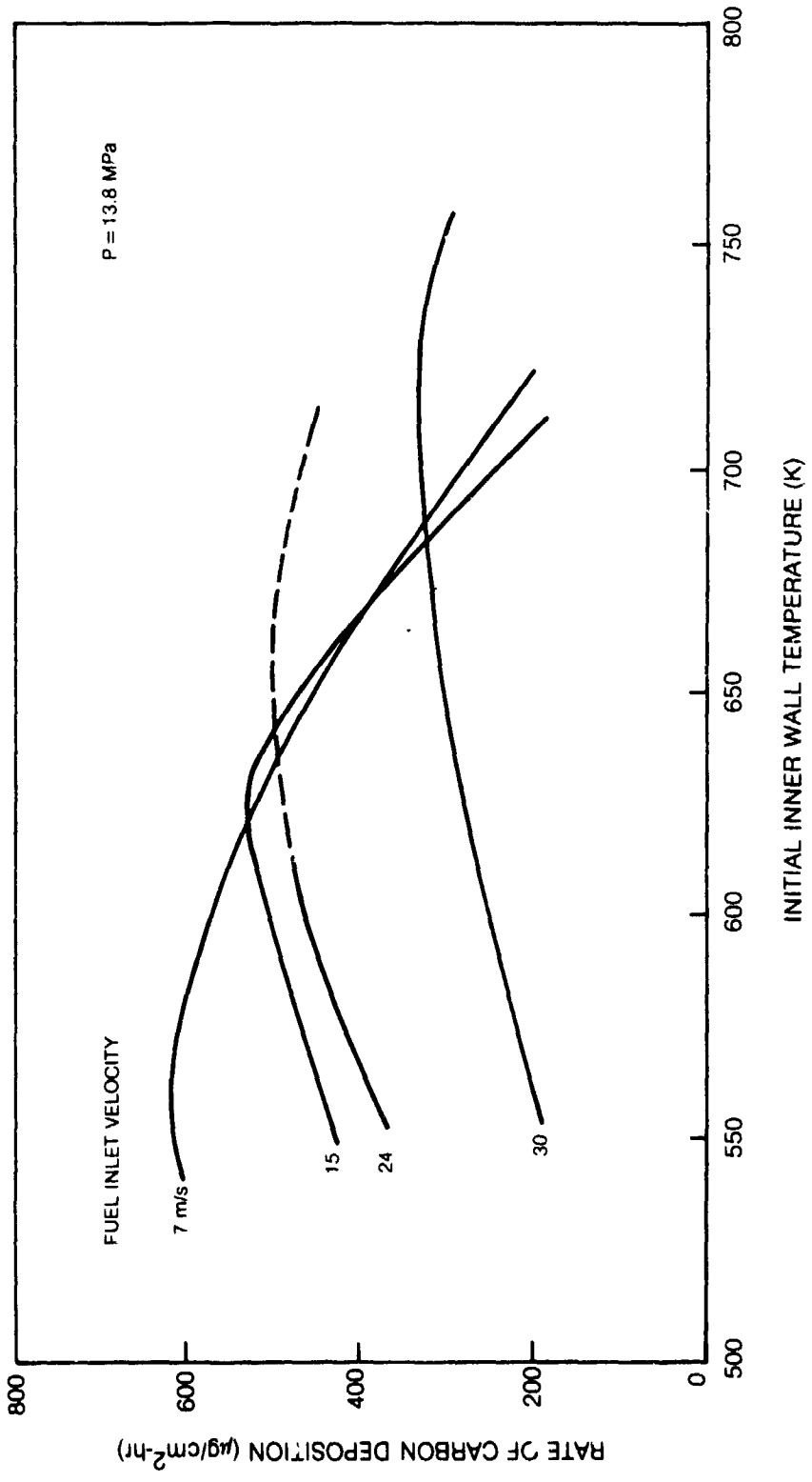


Figure 11. Rate of Carbon Deposition for RP-1 in Copper Tubes

ORIGINAL PAGE IS
OF POOR QUALITY

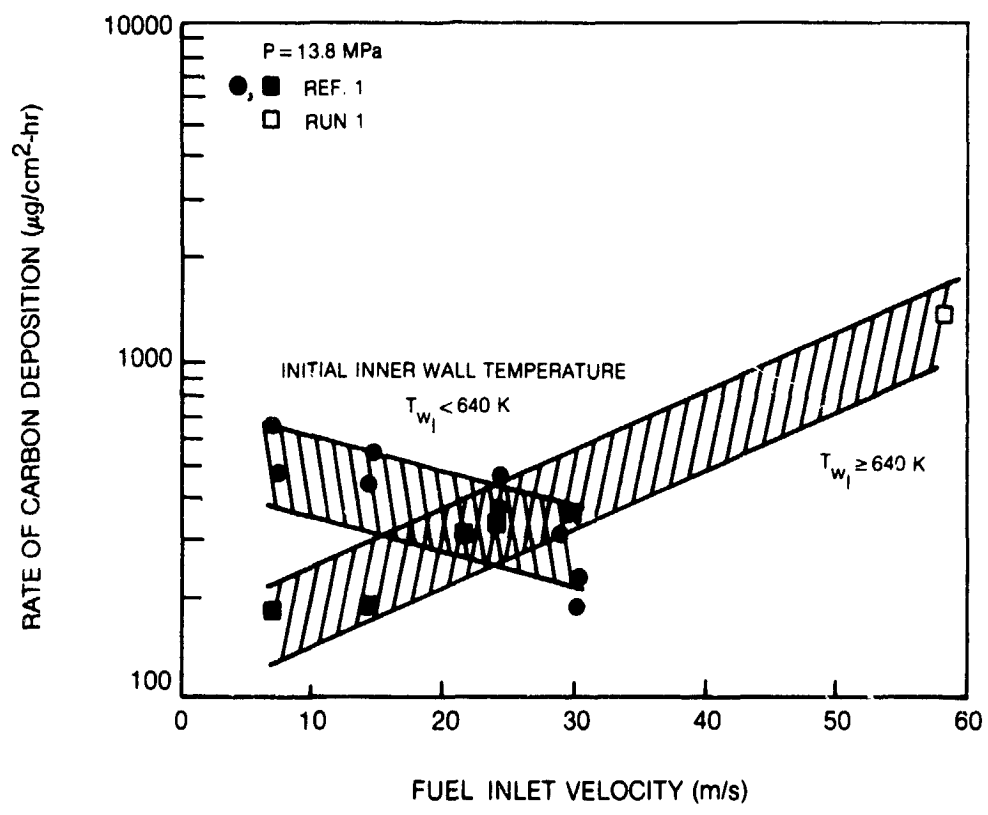


Figure 12. Effect of Fuel Velocity on Carbon Deposition for RP-1 in Copper Tubes

ORIGINAL PAGE IS
OF POOR QUALITY

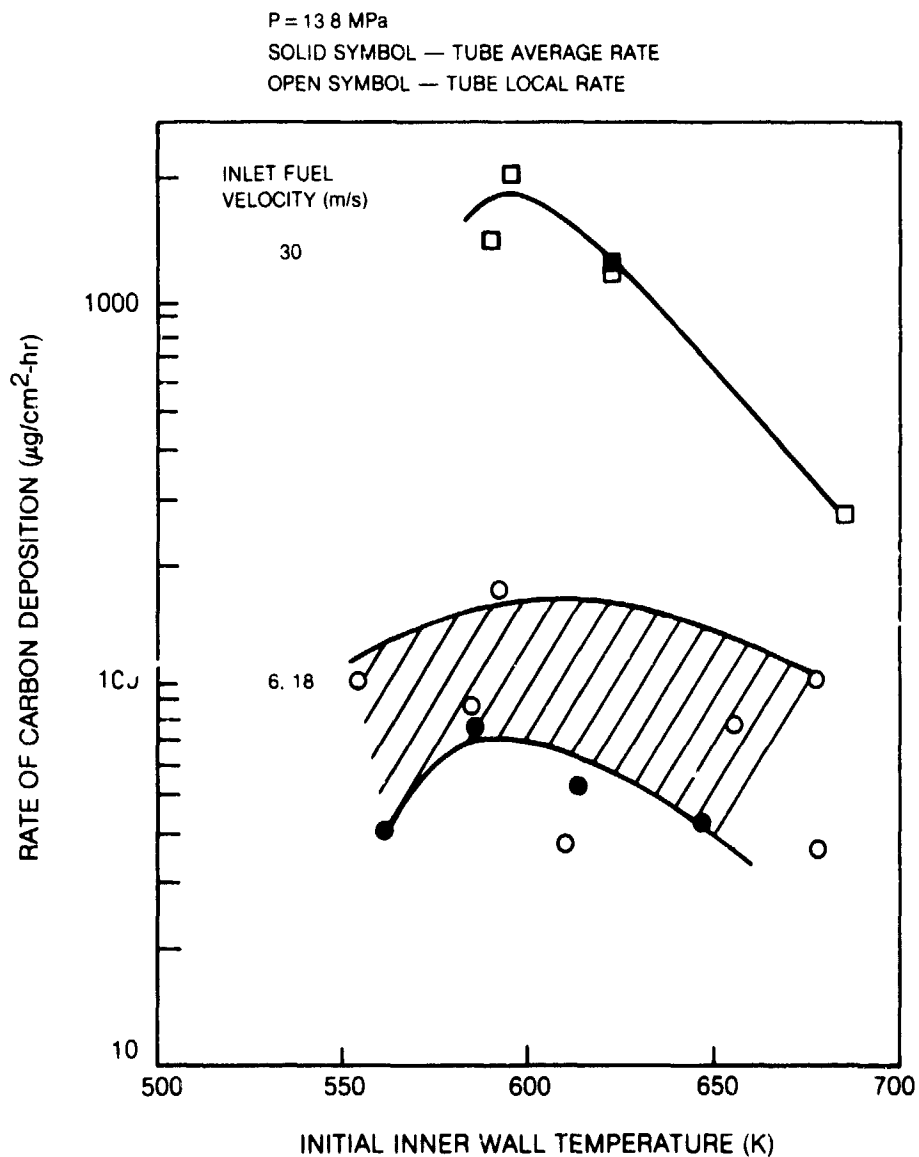


Figure 13. Effect of Fuel Velocity on Carbon Deposition for RP-1 in Nickel Tubes

ORIGINAL PAGE IS
OF POOR QUALITY

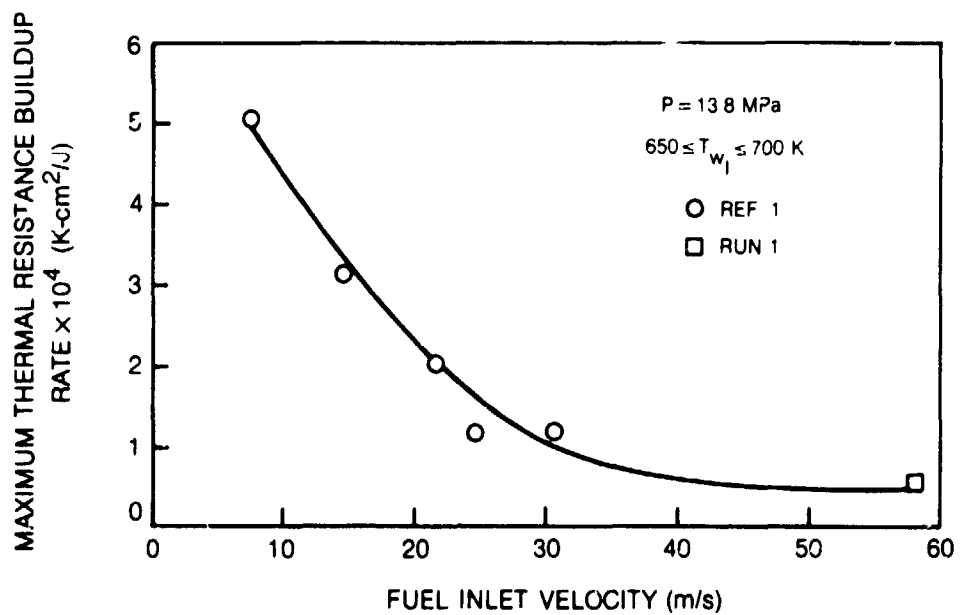


Figure 14. Effect of Fuel Velocity on Thermal Resistance Buildup Rate for RP-1 in Copper Tubes

ORIGINAL PAGE IS
OF POOR QUALITY

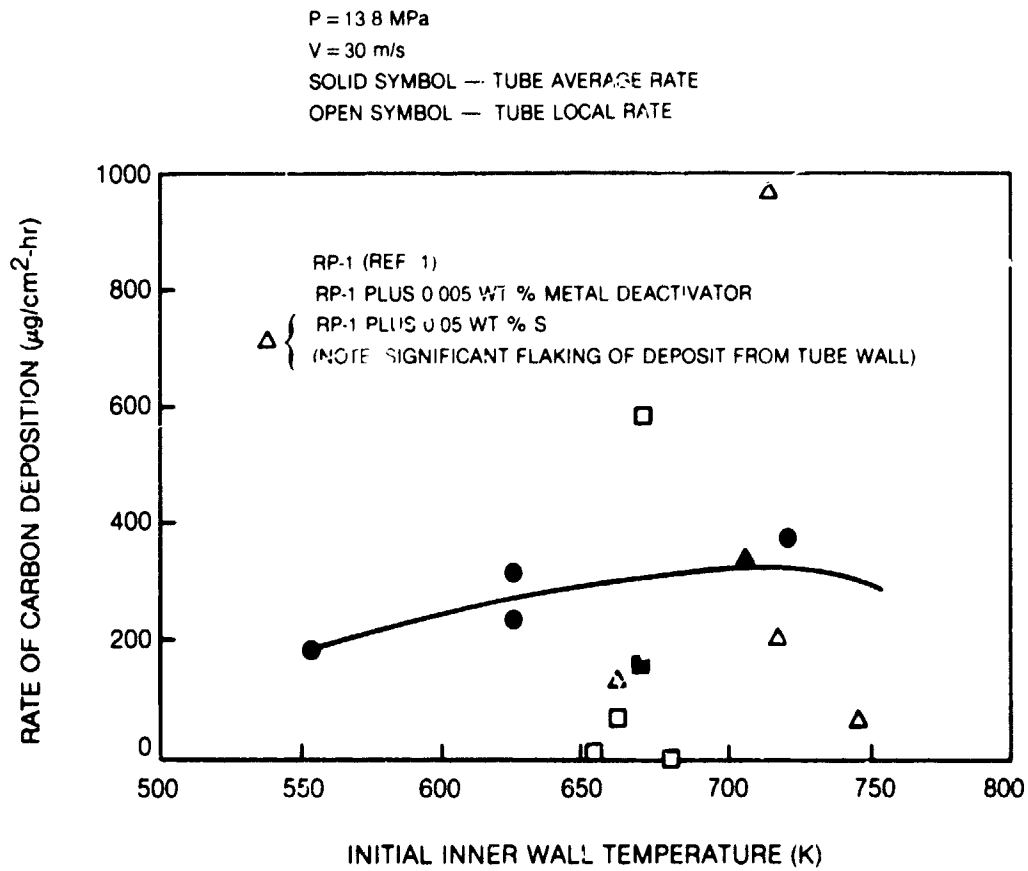


Figure 15. Effect of Fuel Composition on Carbon Deposition for RP-1 Fuel
in Copper Tubes

ORIGINAL PAGE IS
OF POOR QUALITY

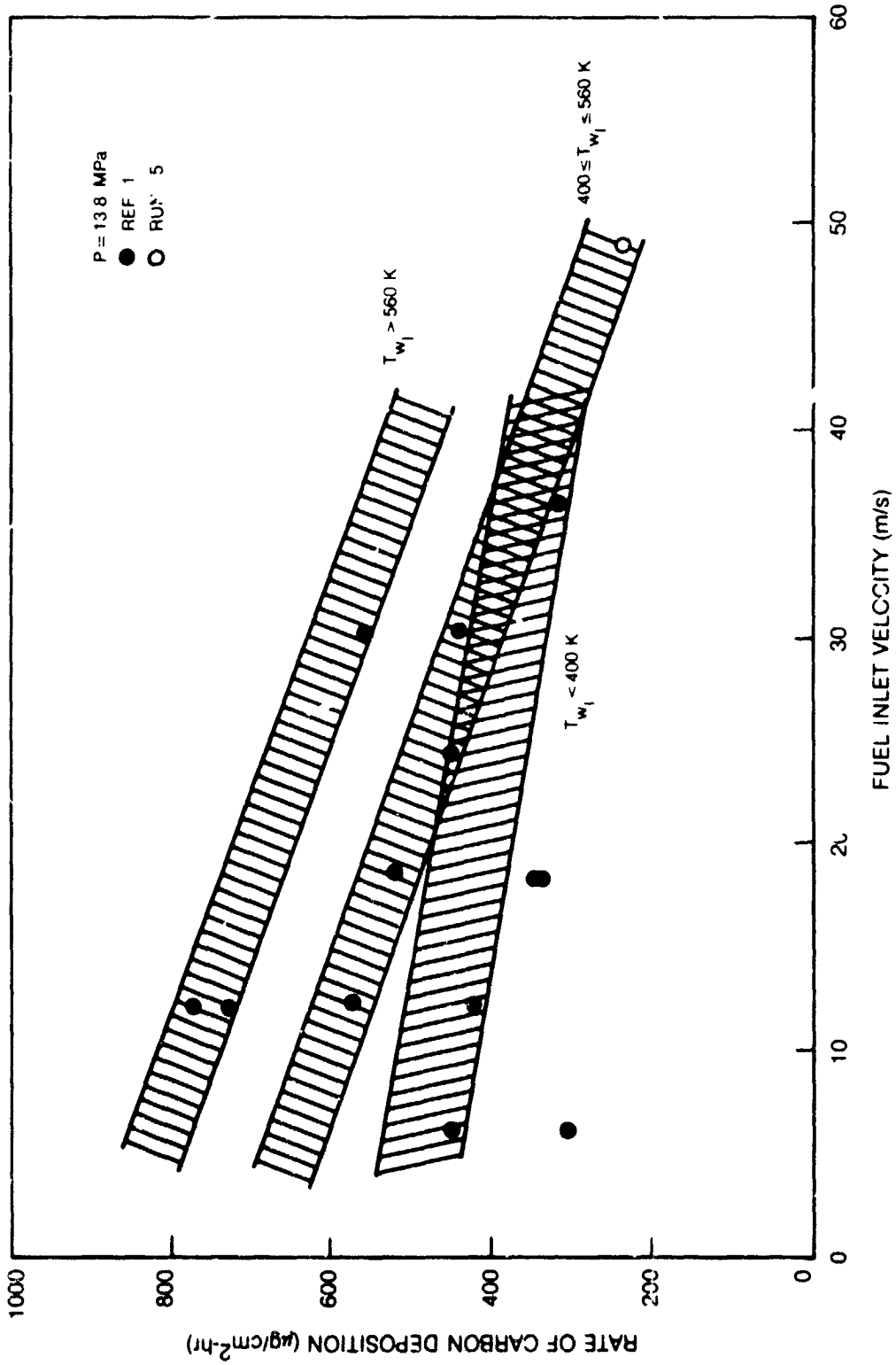


Figure 16. Effect of Fuel Velocity on Carbon Deposition for Commercial-Grade Propane in Copper Tubes

PRESSURE = 13.8 MPa $T_{WALL} \cong 700K$ VELOCITY = 30.5 m/sec

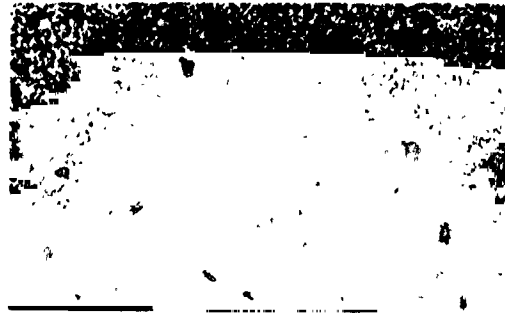
DENDRITE



COPPER



CARBON



SULFUR



ORIGINAL FILED
OF POOR QUALITY

Figure 17. Scanning-Electron-Microprobe Analysis of Deposits Showing Tube Corrosion for Commercial Propane (Ref. 1)

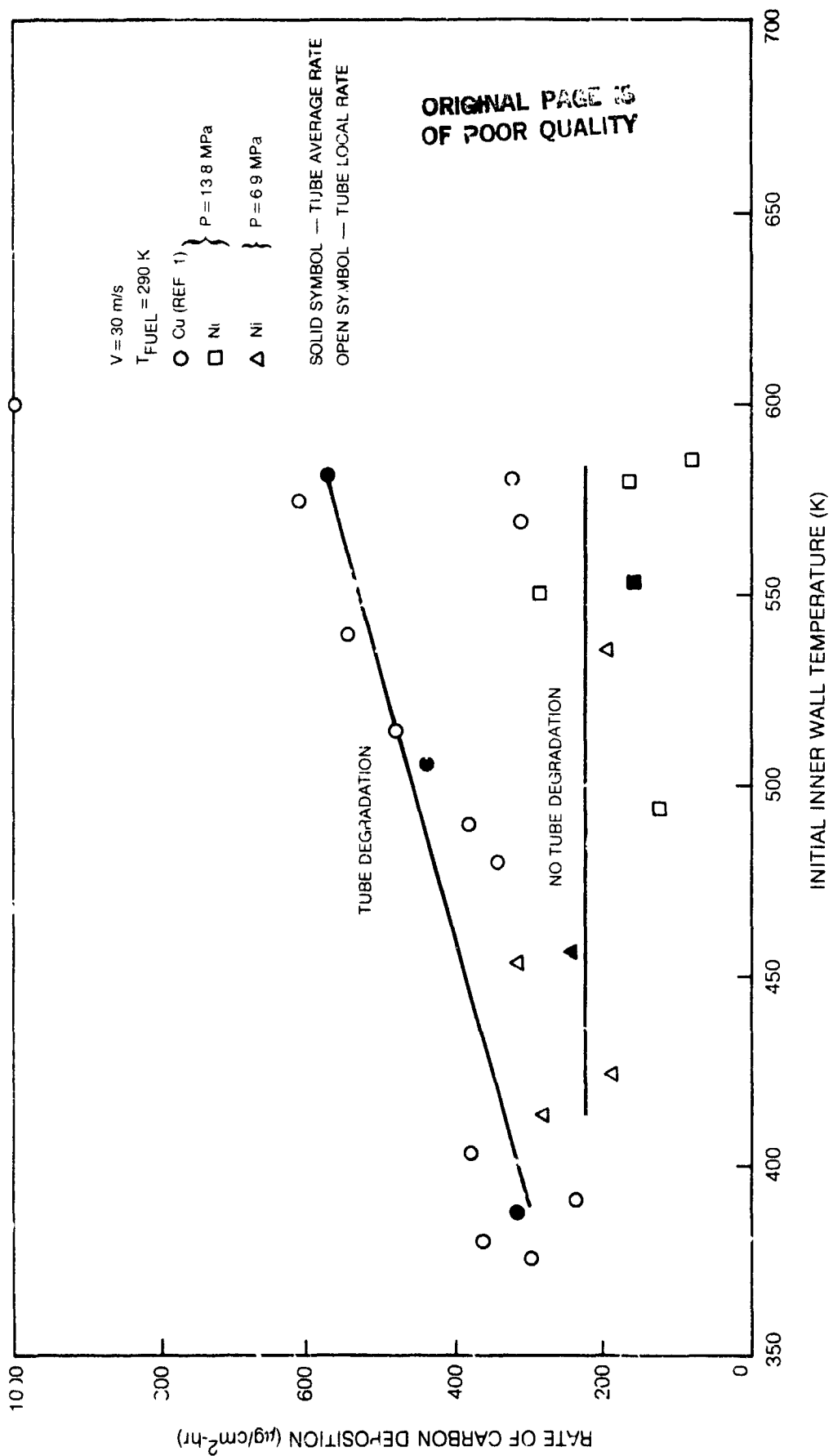


Figure 18. Rate of Carbon Deposition for Commercial-Grade Propane in Copper and Nickel Tubes

ORIGINAL TITLE IS
OF POOR QUALITY

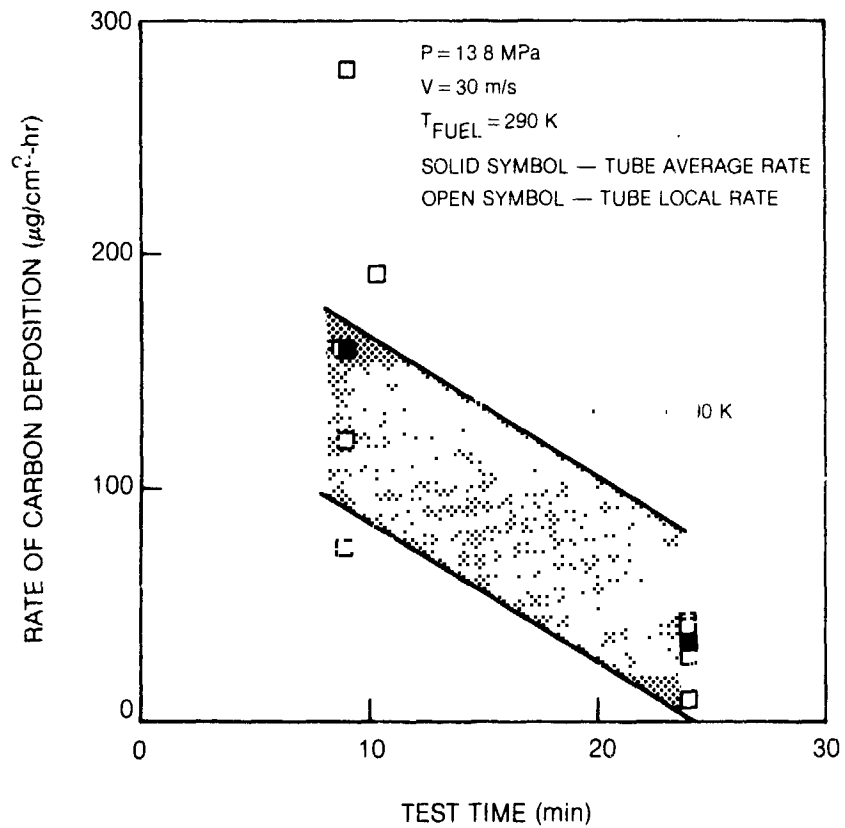


Figure 19. Effect of Intermittent Operation and Test Time on Carbon Deposition for Commercial-Grade Propane in Nickel Tubes

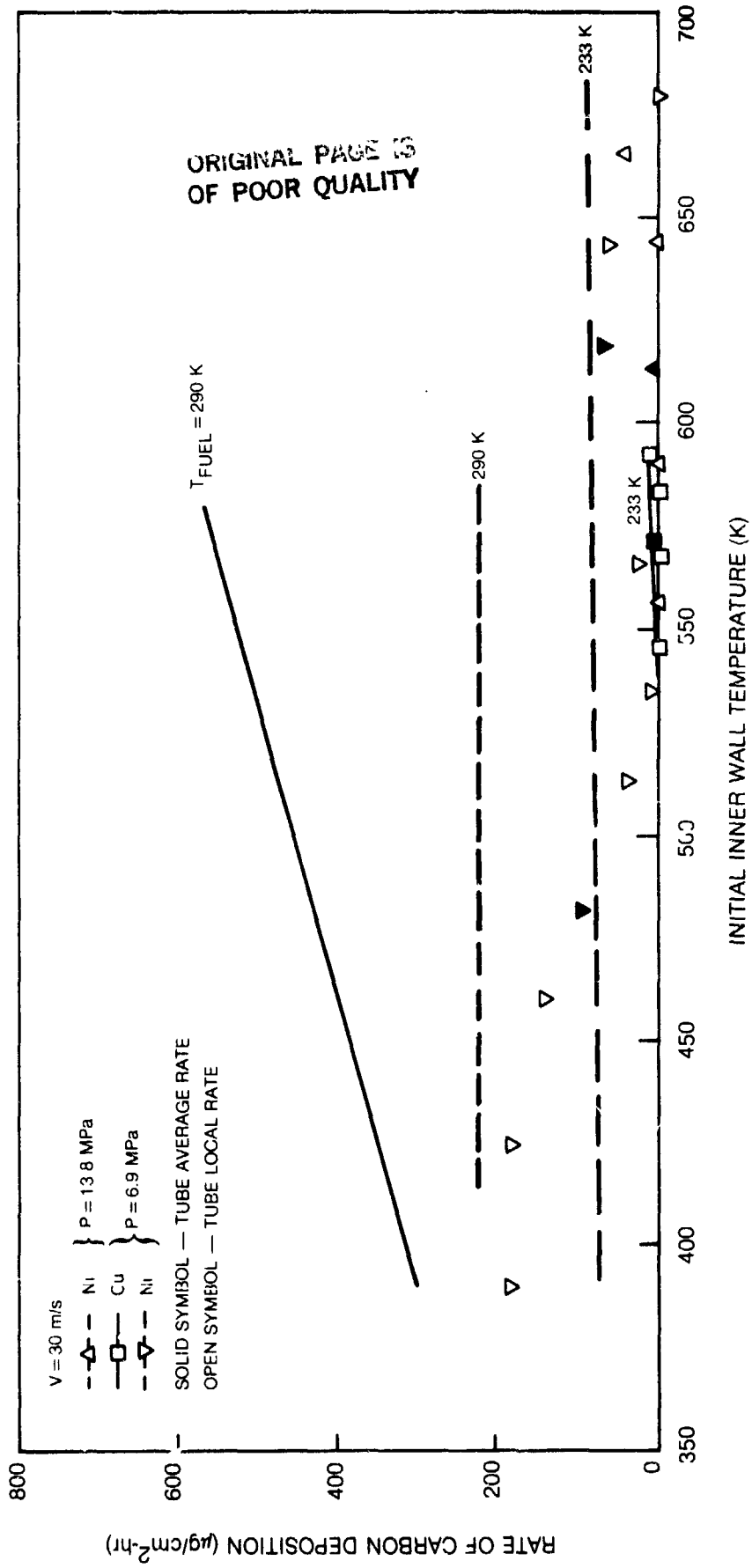


Figure 20. Effect of Fuel Chilling on Carbon Deposition for Propane in Copper and Nickel Tubes

ORIGINAL PAGE IS
OF POOR QUALITY

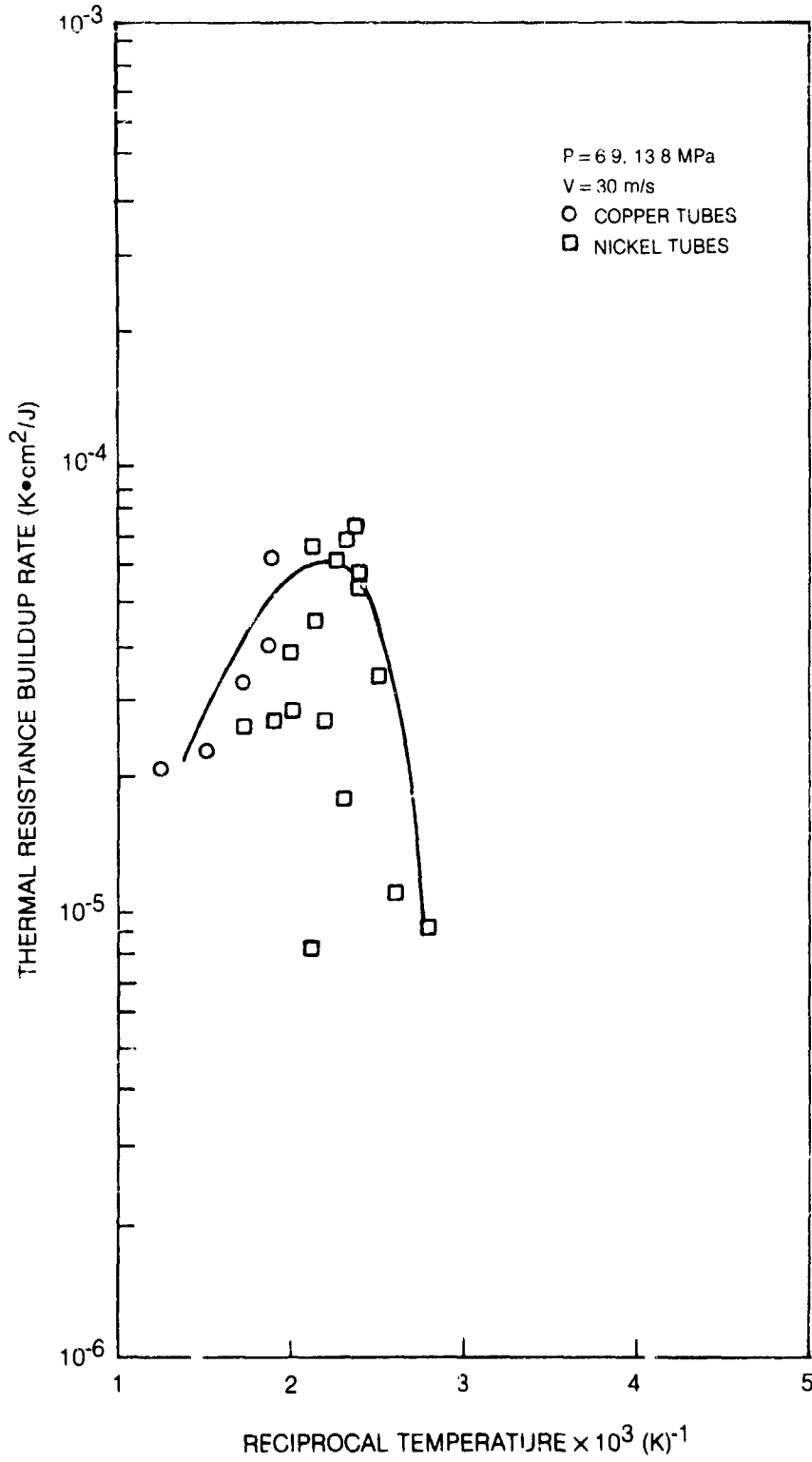


Figure 21. Deposit Thermal Resistance Buildup Rate for Commercial-Grade Propane

ORIGINAL PAGE IS
OF POOR QUALITY

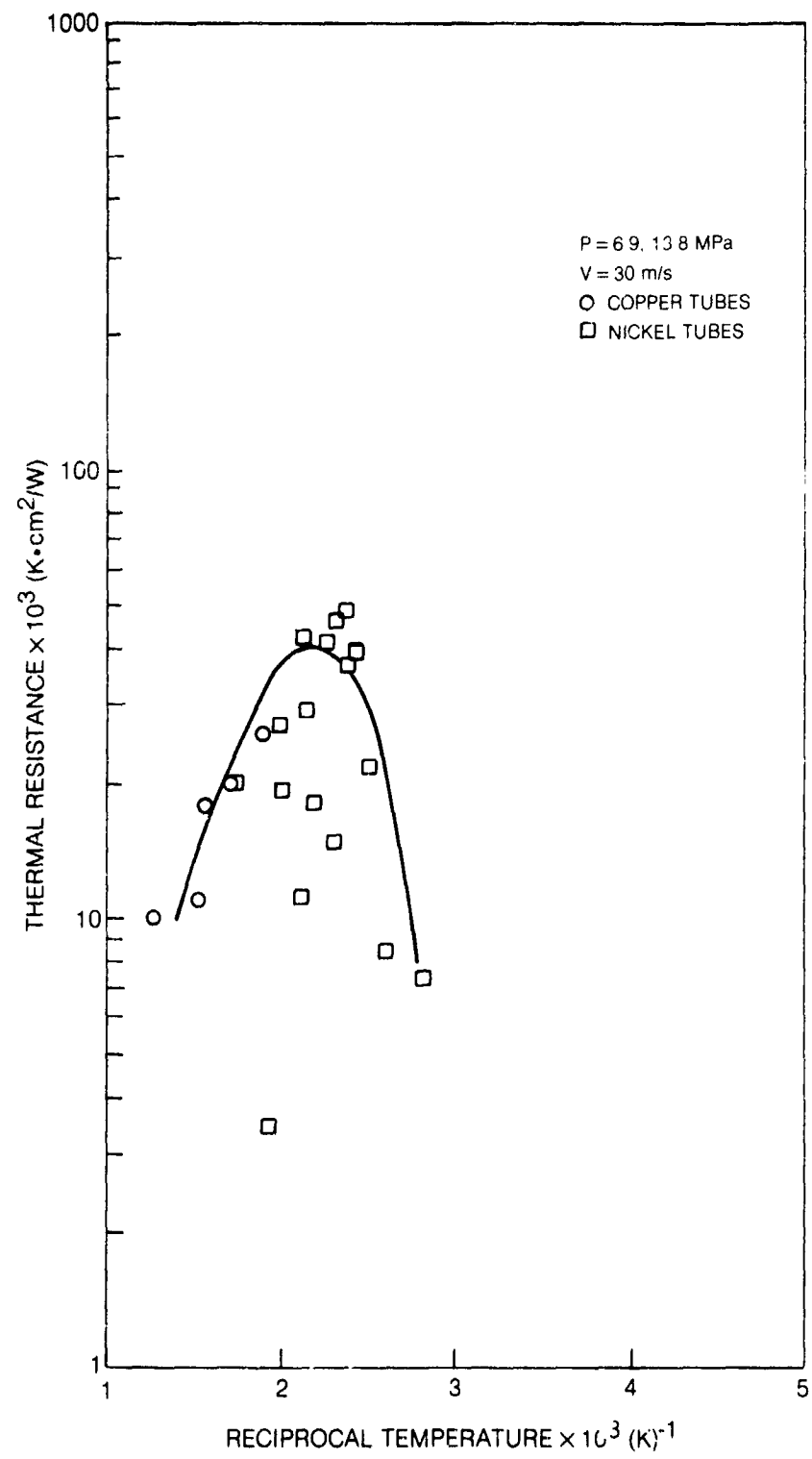


Figure 22. Deposit Thermal Resistance for Commercial-Grade Propane

P = 13.8 MPa
V = 30 m/s
□ 0 min
○ 10 min

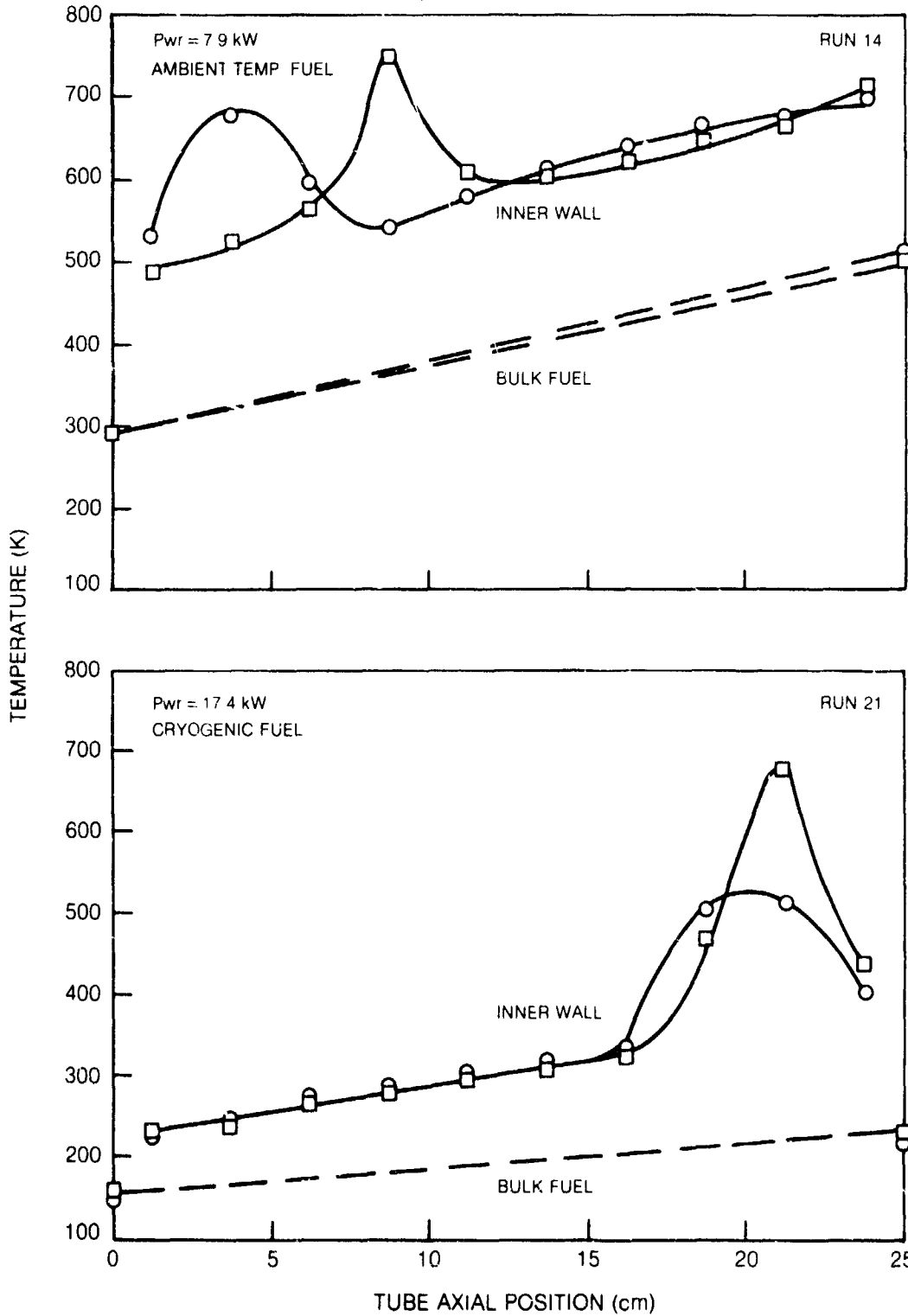


Figure 23. Wall and Bulk Fuel Temperature Profiles for Ambient Temperature and Cryogenic Natural Gas in Copper Tubes

ORIGINAL PROFILE
OF POOR QUALITY

P = 13.8 MPa
V = 30 m/s
□ 0 min
○ 10 min

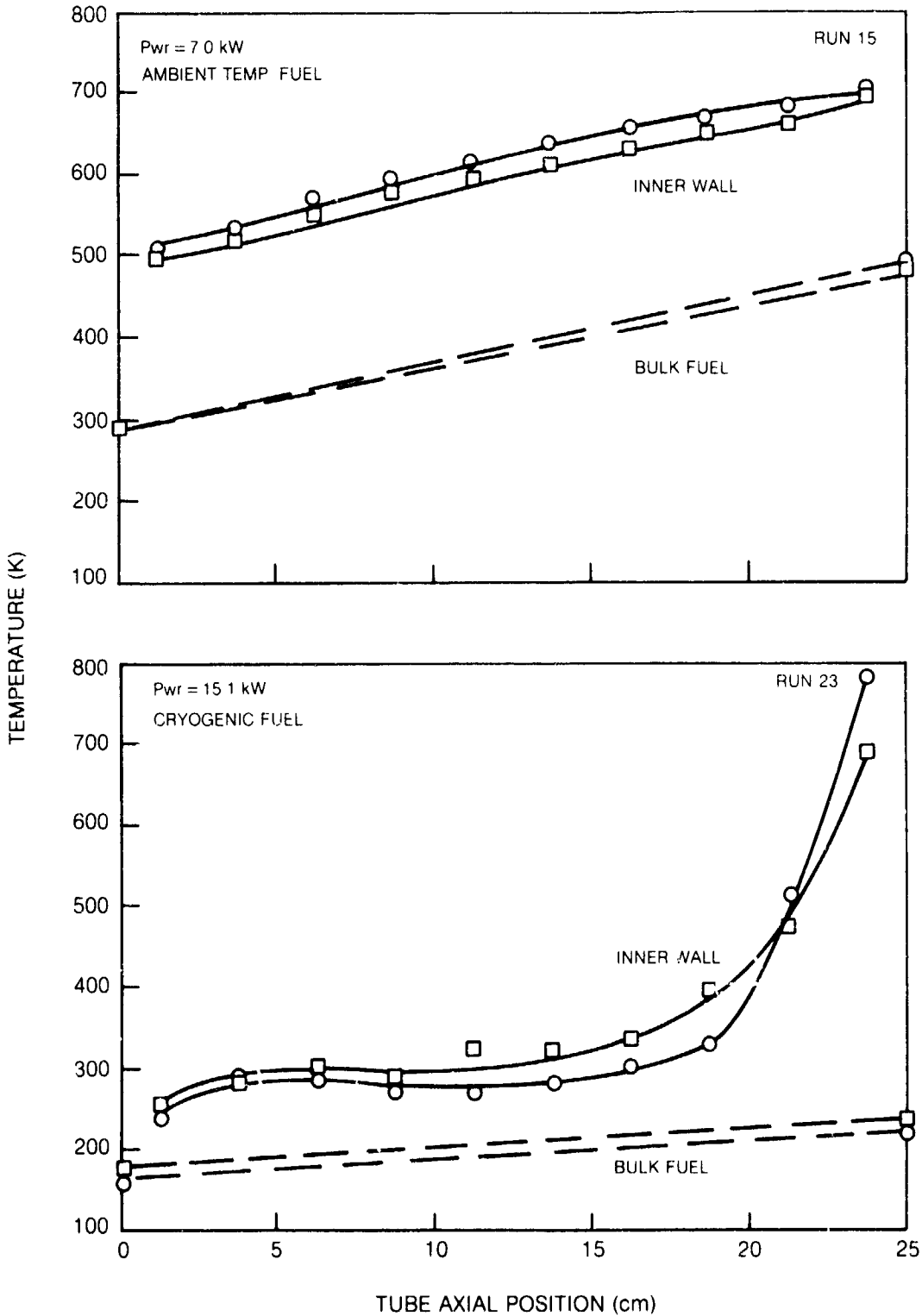


Figure 24. Wall and Bulk Fuel Temperature Profiles for Ambient Temperature and Cryogenic Natural Gas in Nickel Tubes

ORIGINAL PAGE IS
OF POOR QUALITY

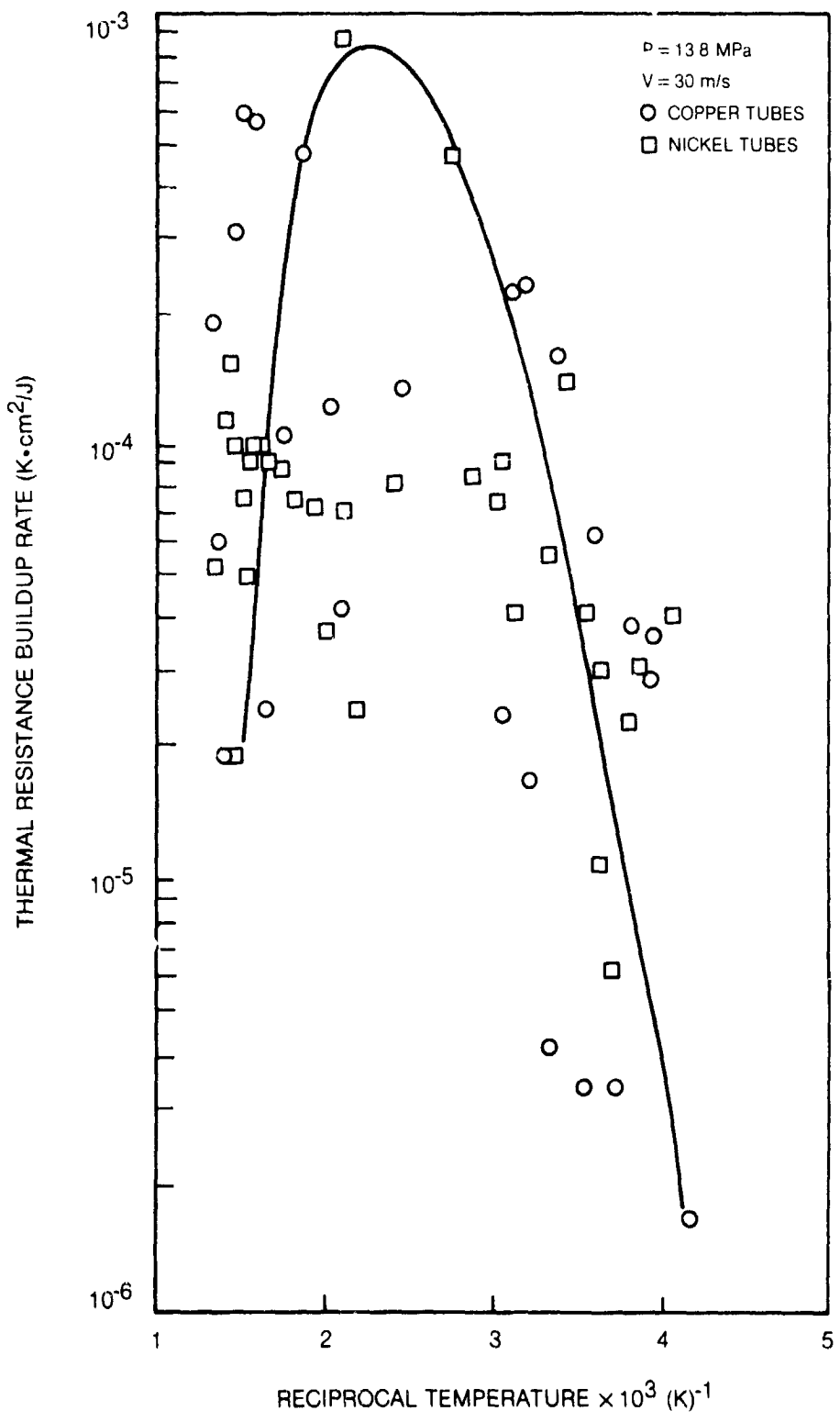


Figure 25. Deposit Thermal Resistance Buildup Rate for Natural Gas

ORIGINAL PAGE IS
OF POOR QUALITY

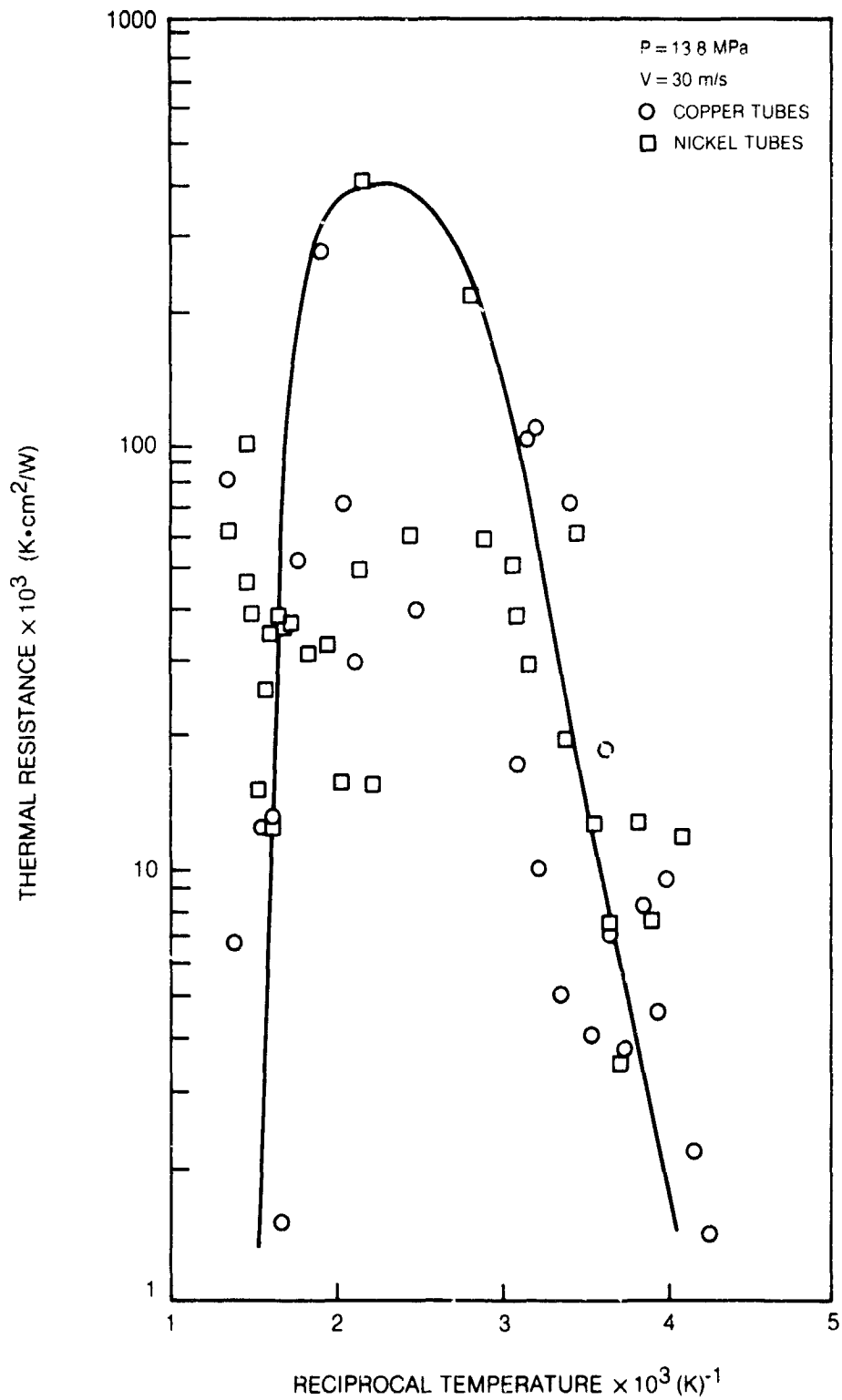


Figure 26. Deposit Thermal Resistance for Natural Gas

ORIGINAL PAPER
OF POOR QUALITY

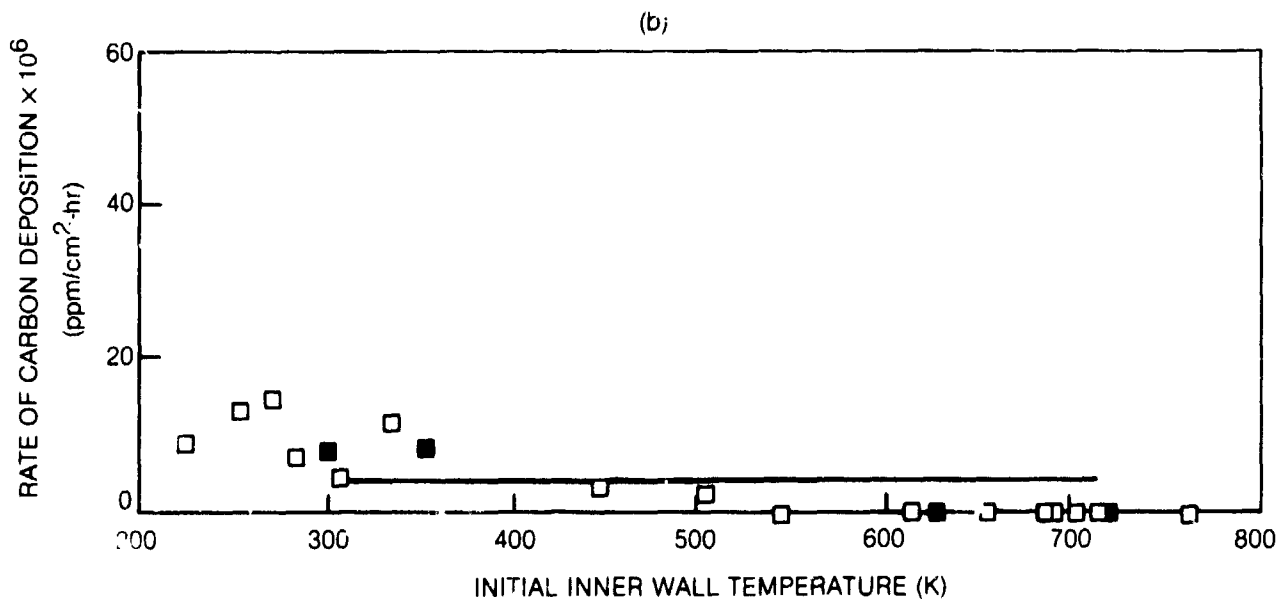
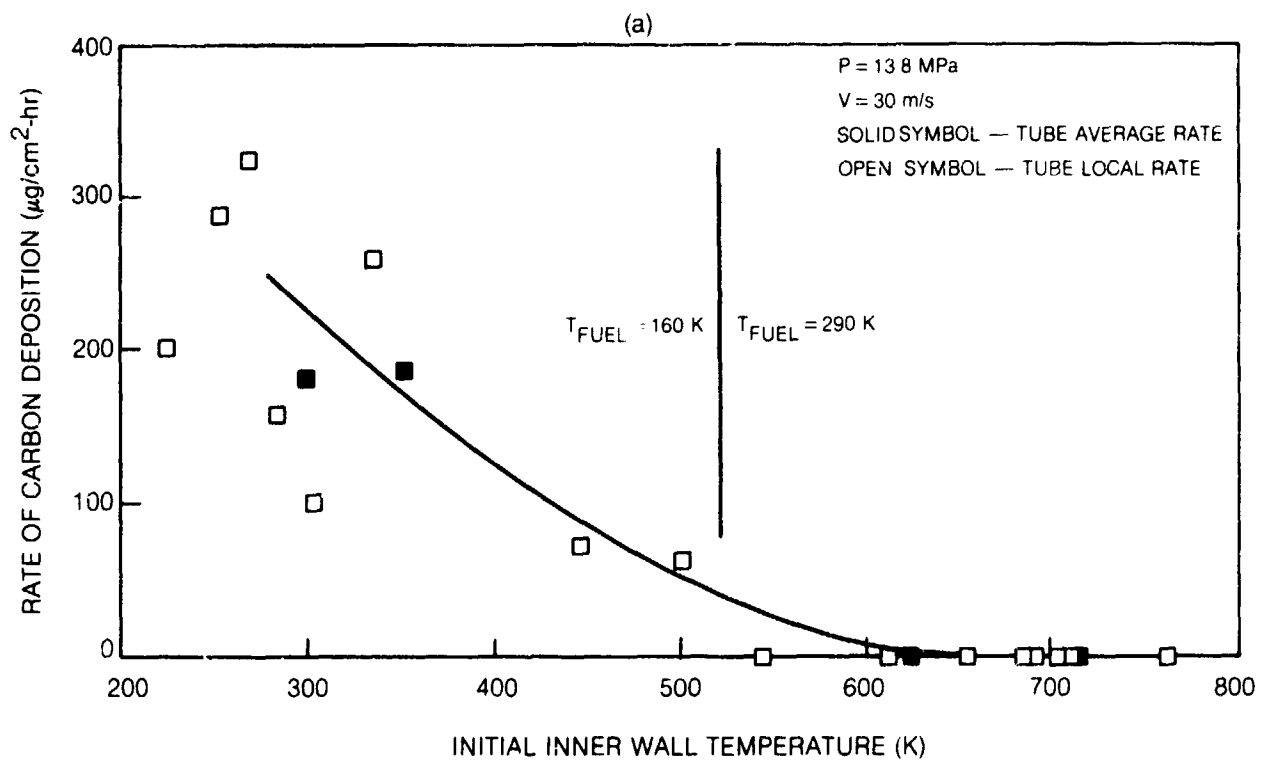


Figure 27. Absolute and Normalized Rates of Carbon Deposition for Natural Gas in Copper Tubes

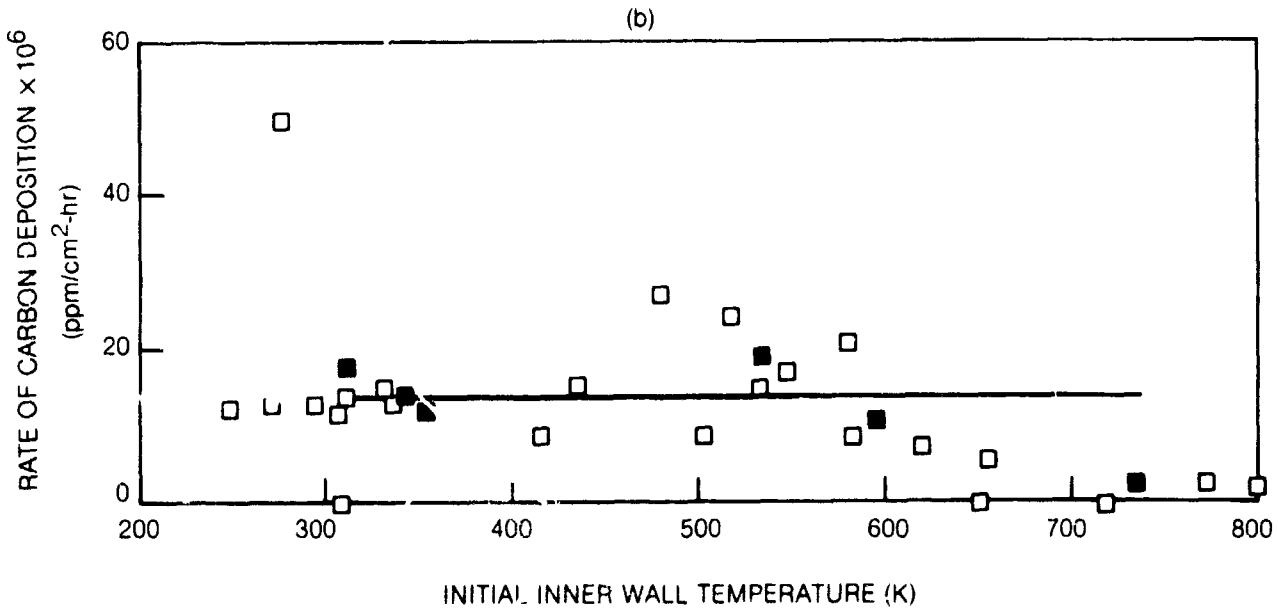
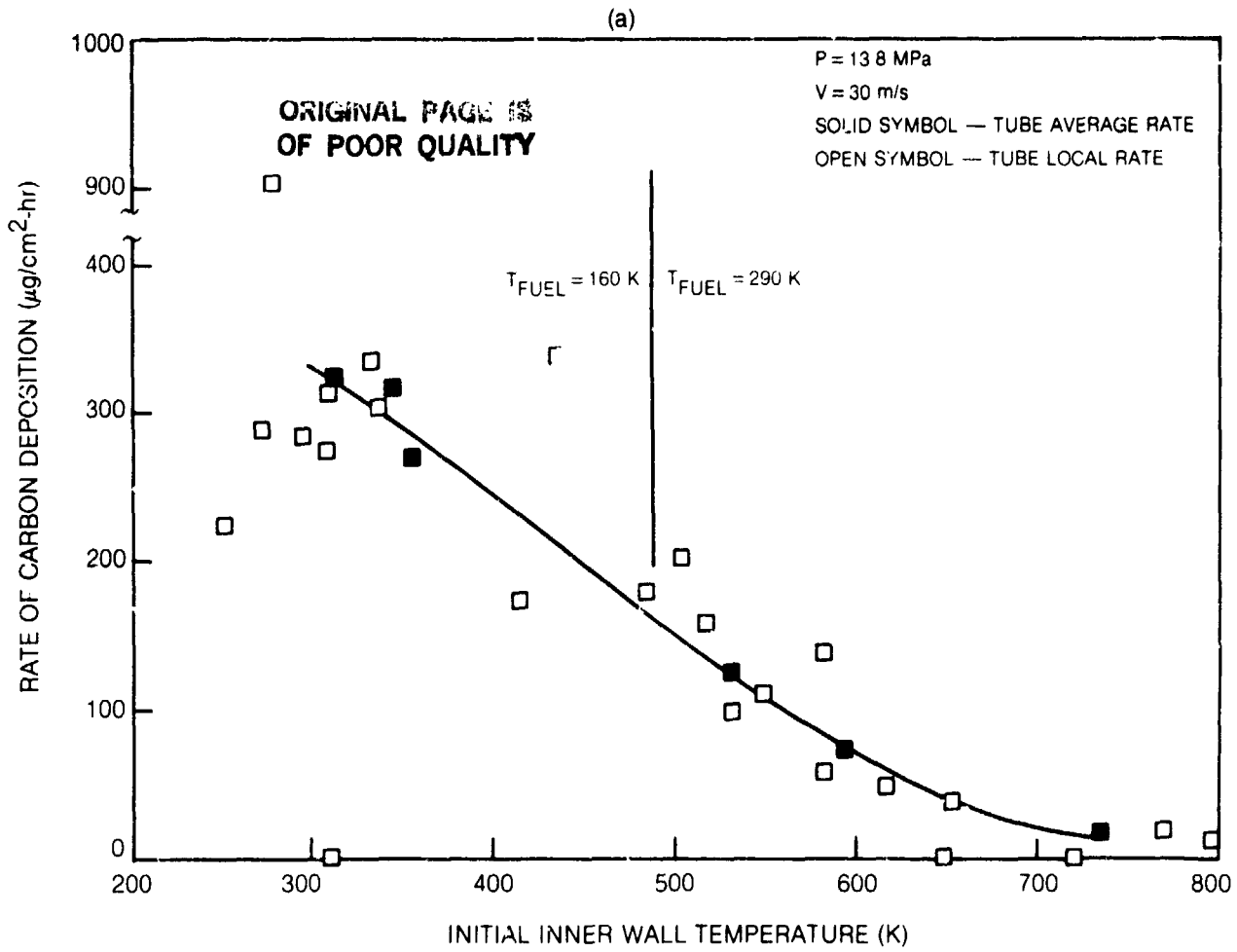


Figure 28. Absolute and Normalized Rates of Carbon Deposition for Natural Gas in Nickel Tubes

ORIGINAL PAGE IS
OF POOR QUALITY

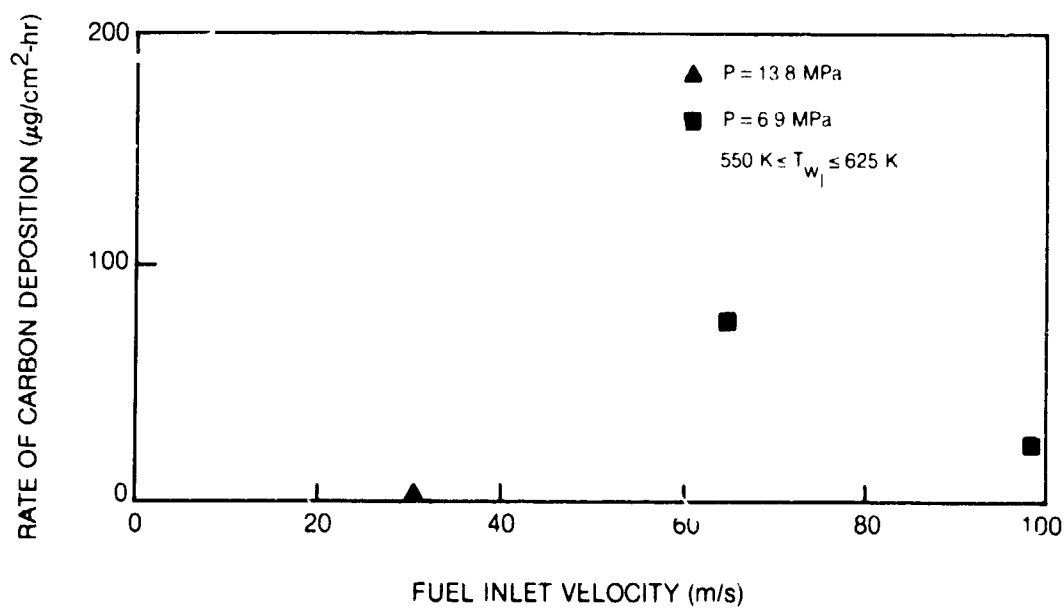


Figure 29. Effect of Fuel Velocity on Carbon Deposition for Natural Gas in Copper Tubes

ORIGINAL PAGE IS
OF POOR QUALITY

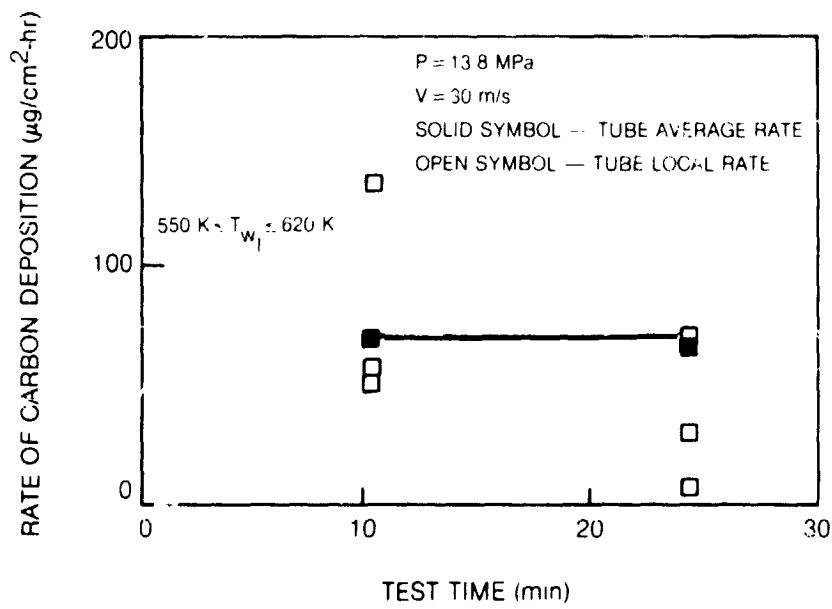


Figure 30. Effect of Intermittent Operation and Test Time on Carbon Deposition for Natural Gas in Nickel Tubes

ORIGINAL PAGE IS
OF POOR QUALITY

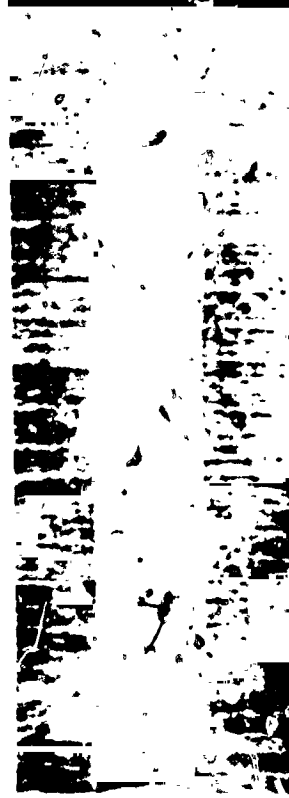
ENTRANCE-SECTION 2



RP-1 (RUN 1)



RP-1 AND SULFUR ADDITIVES (RUN 4)

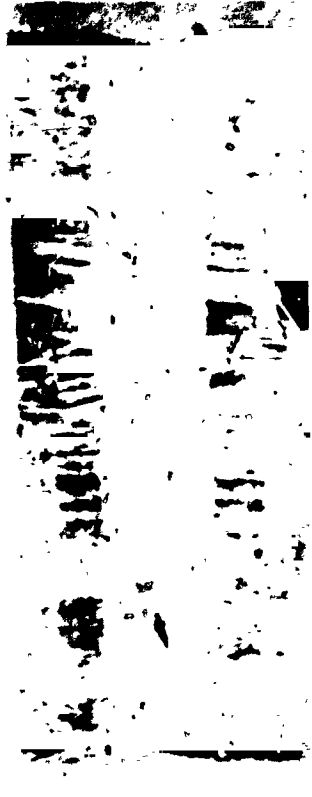


NATURAL GAS (RUN 15)



1 mm

CLEAN TUBE



RP-1 AND METAL DEACTIVATOR (RUN 3)



COMMERCIAL-GRADE PROPANE (RUN 5)

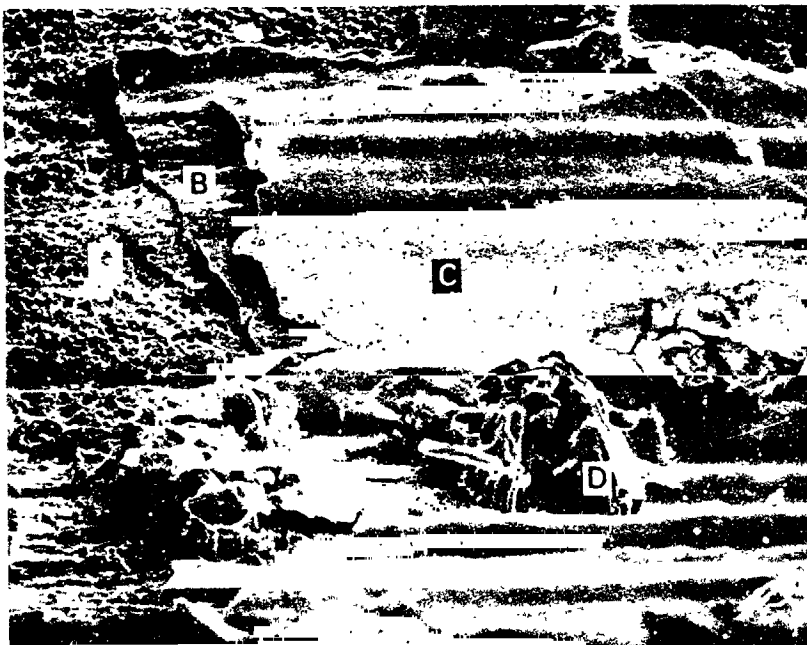
← FLOW

Figure 33. Fuel Deposits on a Heated Copper Tube

ORIGINAL PAGE IS
OF POOR QUALITY

RP-1 AND SULFUR ADDITIVES (RUN 4, SECTION 6)

(a)



0.1 mm

(b)



Figure 32. Deposit Morphology for RP-1 Doped with Sulfur Compounds in a Copper Tube

C-2

ORIGINAL PAGE IS
OF POOR QUALITY

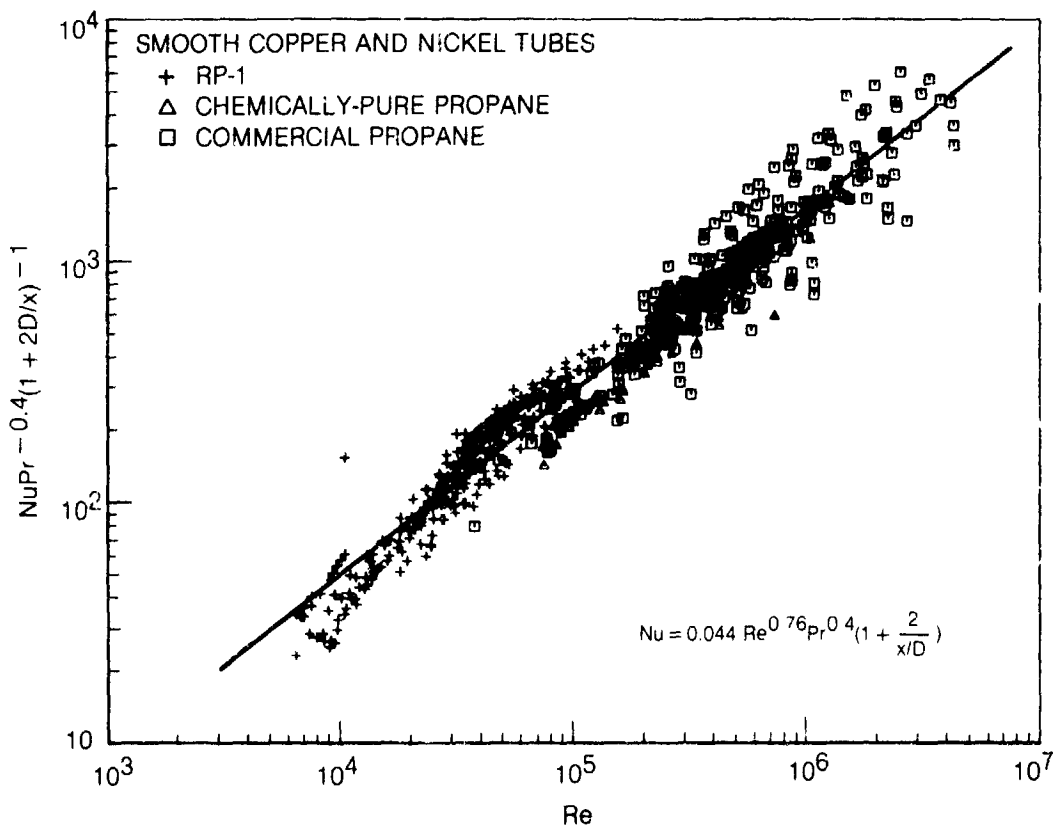


Figure 33. Forced-Convection Heat Transfer for Liquid Hydrocarbons in Clean Tubes

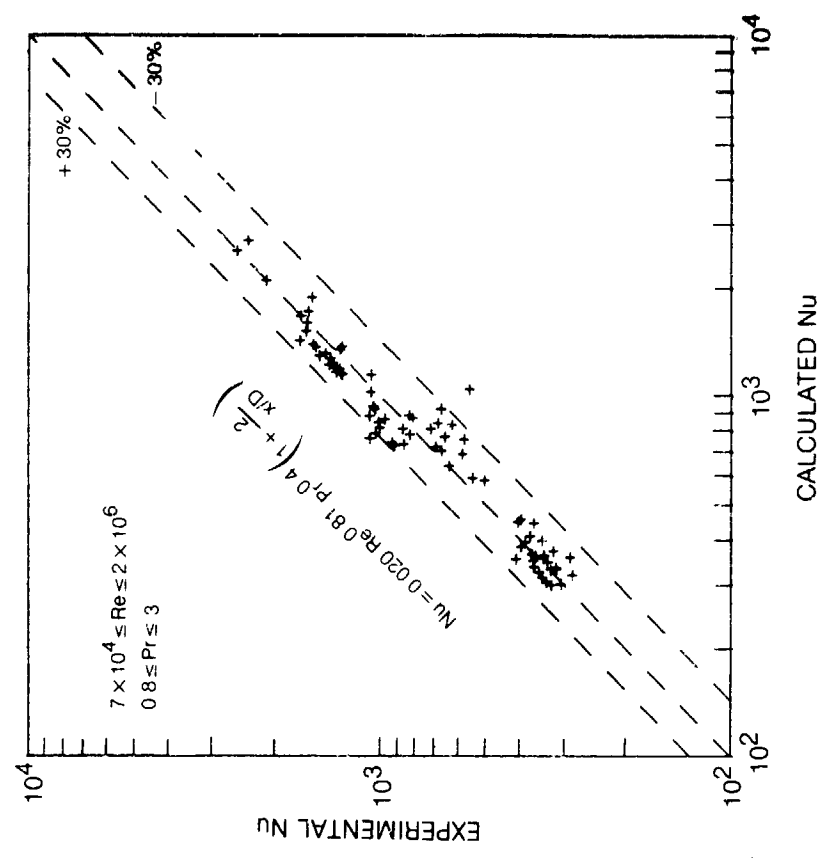


Figure 35. Nusselt No. Evaluation for Chemically-Pure Propane

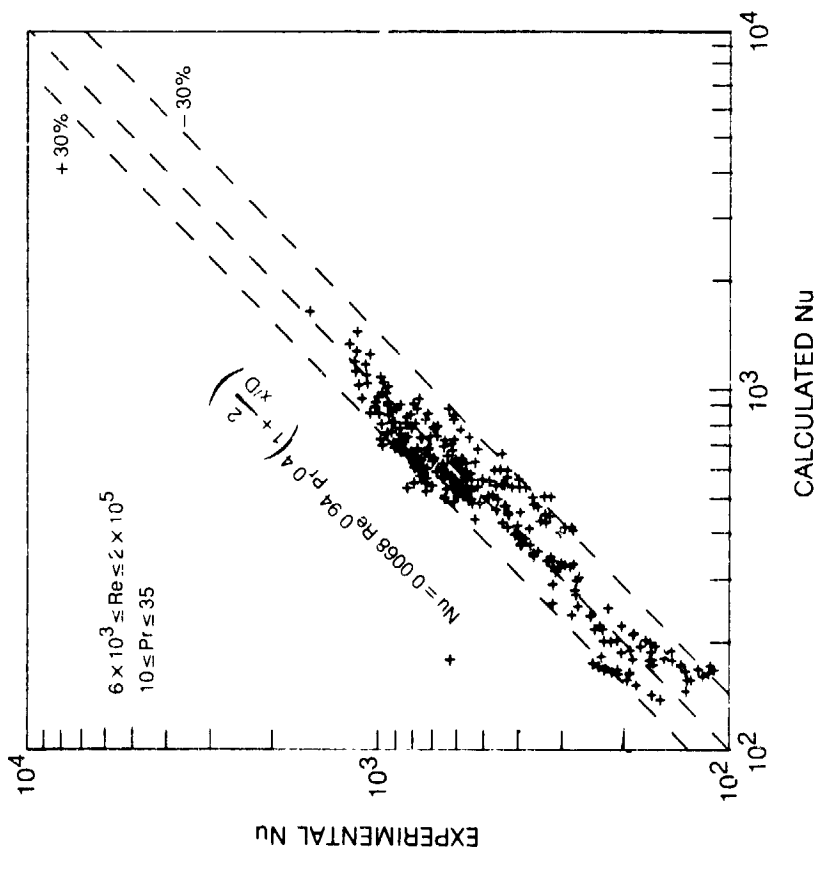


Figure 34. Nusselt No. Evaluation for RP-1

ORIGINAL PAGE IS
OF POOR QUALITY

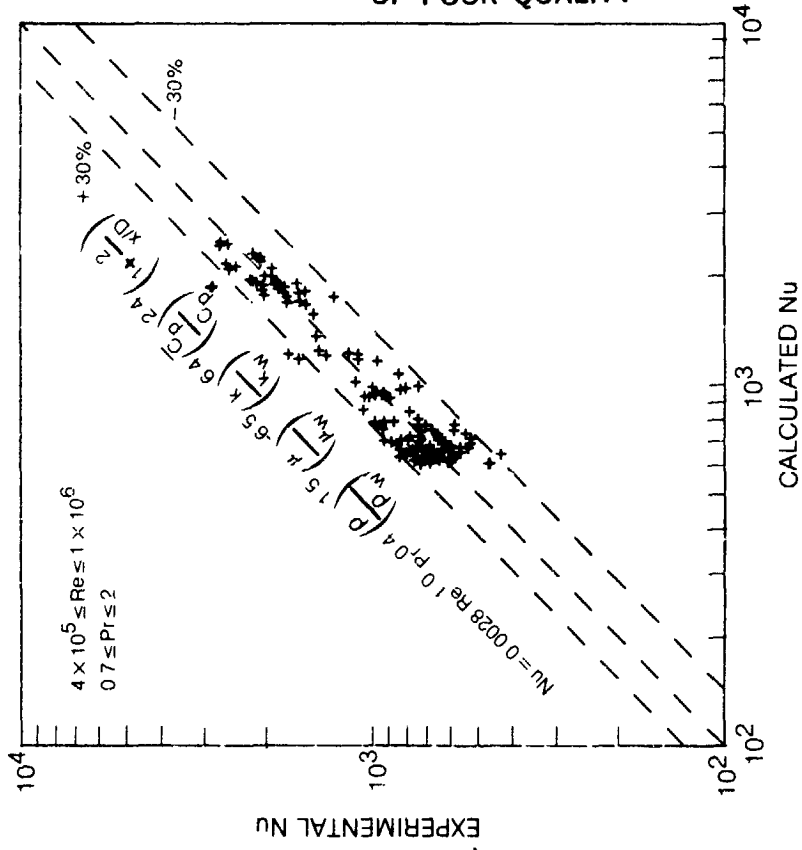


Figure 37. Nusselt No. Evaluation for Natural Gas

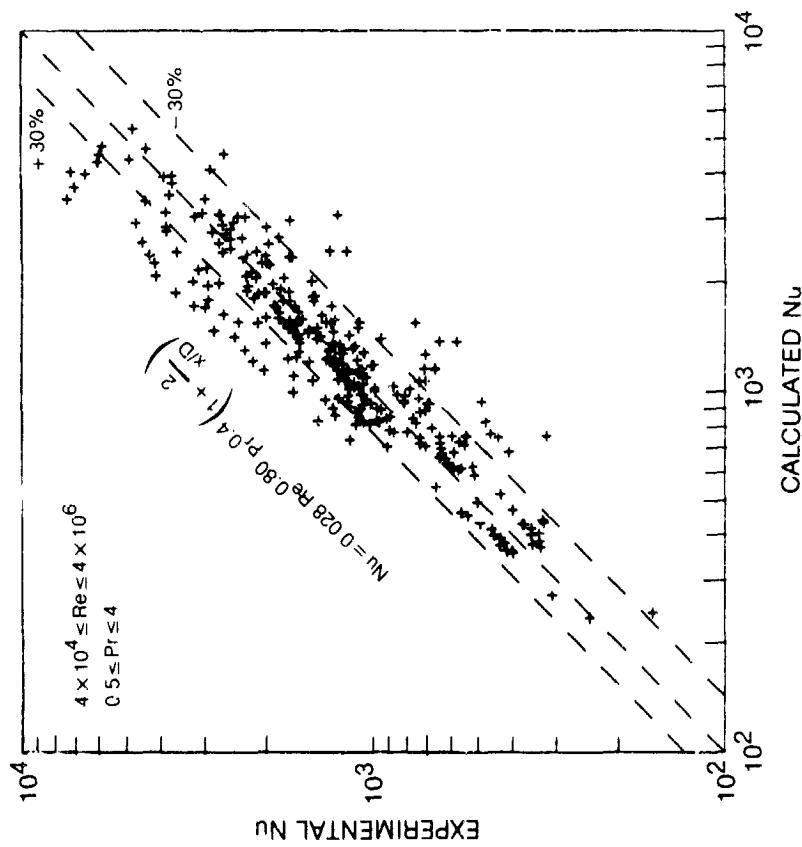


Figure 36. Nusselt No. Evaluation for Commercial-Grade Propane

ORIGINAL PAGE IS
OF POOR QUALITY

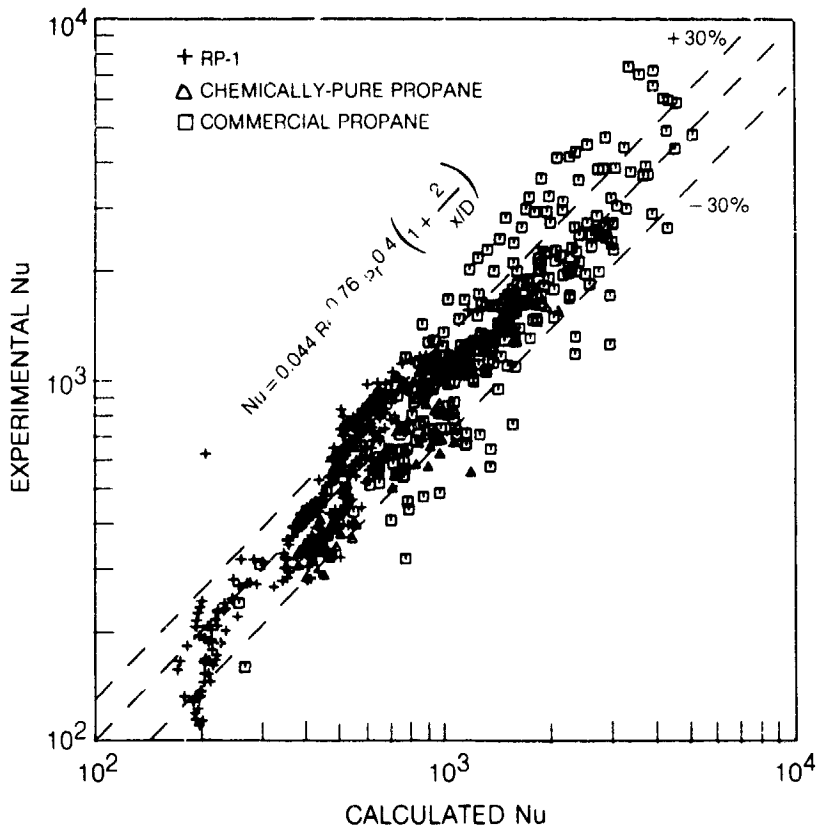


Figure 38. Nusselt No. Evaluation for Several Liquid Hydrocarbon Fuels

ORIGINAL PAGE IS
OF POOR QUALITY

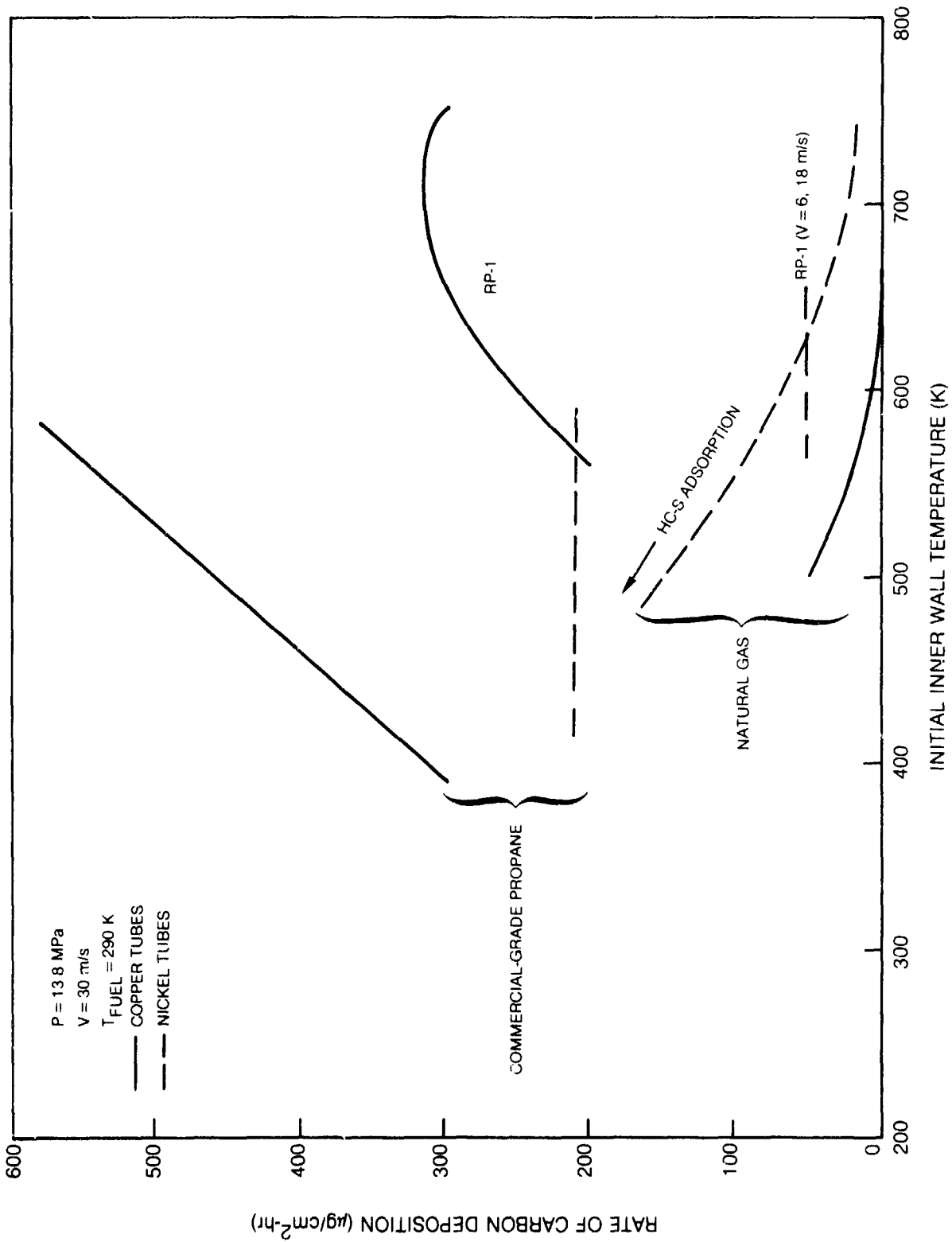


Figure 39. Rates of Carbon Deposition for Three Hydrocarbon Fuels

APPENDIX A
TABULATED TEST DATA

TABLE A-1

SUMMARY OF DATA REDUCTION PARAMETERS

Item	Keyword	Definition and Symbol	Units	Measured	Calculated
1	TW OUT	Outer tube surface temperature, T_{w_o}	K	x	
2	TW IN	Inner tube surface temperature, $T_{w_i}^{(1)}$	K		x
3	FUEL INLET P	Inlet fuel pressure, P_1	MPa	x	
4	FUEL EXIT P	Exit fuel pressure, P_2	MPa	x	
5	FUEL INLET TEMP	Inlet fuel temperature, T_{f_1}	K	x	
6	FUEL EXIT TEMP	Exit fuel temperature, T_{f_2}	K	x	
7	FLOW RATE	Fuel mass flow rate, \dot{m}	kg/s	x	
8	CURRENT	Current through test tube, I	Amps	x	
9	VOLTAGE	Voltage drop across test tube, V	Volts	x	
10	POWER	Electrical power dissipated in test tube, $E = I \cdot V$	kW		x
11	HEAT FLUX	Electrical power E divided by total inside lateral surface area of test tube, (Q/A)	W/cm ²		x
12	INLET FUEL VEL	Inlet fuel velocity as calculated from steady flow continuity, v	m/s		x

TABLE A-1 (Cont'd)

ORIGINAL PAGE IS
OF POOR QUALITY

SUMMARY OF DATA REDUCTION PARAMETERS

Item	Keyword	Definition and Symbol	Units	Measured	Calculated
13	ENERGY BALANCE	Consistency check between electrical power supplied to test tube and thermal power absorbed by fuel, EB ⁽²⁾	percent		x
14	INLET REYNOLDS NO	Reynolds number at test tube entrance based on inside tube diameter, Re _D	-		x
15	AVG FRICTION FACTOR	Tube overall friction factor, f ⁽³⁾	-		x
16	U	Overall inside wall heat transfer coefficient, U	W/cm ² ·K		x
17	T/K	Deposit thermal resistance defined as ratio of deposit thickness to deposit thermal conductivity, t/k	K·cm ² /W		x
18	RC	Thermal resistance build-rate, R _c	K·cm ² /J		x

(1)

$$T_{wi} = T_{wo} - 1.27 E$$

(2)

$$EB = 100 \frac{\bar{m} C_{pb} (T_{f2} - T_{f1}) - E}{E}$$

(RP-1)

$$EB = 100 \frac{\dot{m} (h_2 - h_1) - E}{E}$$

(Propane and Natural Gas)

(3)

$$f = \frac{\pi^2 (P_1 - P_2) \bar{\rho}_b D^5}{32 \bar{m}^2 L}$$

Note: \bar{C}_{pb} and $\bar{\rho}_b$ are evaluated at the bulk mean fuel temperature $(T_{f1} + T_{f2})/2$

ROCKET FUEL DEPOSIT TEST PROGRAM (RP-1 FUEL)
 RUN 1 DECEMBER 13, 1982

TIME	(MIN)	UUUU	1.133	2.133	3.133	4.133	5.133	6.133	7.133	8.133	9.133	10.133
IM OUT	1.3	712.0	722.6	723.6	726.5	728.7	728.2	731.5	727.6	725.9	717.0	719.0
IM OUT	1.4	694.8	685.9	687.0	689.0	681.5	674.8	689.8	665.9	660.9	654.8	653.2
IM OUT	1.5	698.2	689.3	691.5	693.5	685.7	679.4	693.8	668.7	664.3	658.8	657.0
IM OUT	1.6	700.3	692.6	694.8	696.8	688.0	681.9	695.8	672.9	668.9	663.4	662.3
IM OUT	1.7	716.5	703.7	705.9	707.9	699.0	692.8	706.9	682.0	678.0	672.9	671.7
IM OUT	1.8	717.5	708.2	710.4	712.4	703.5	697.3	711.4	686.4	682.4	677.6	676.5
IM OUT	1.9	718.5	709.2	711.4	713.4	704.5	698.3	712.4	687.4	683.4	678.2	677.1
IM IN	2.0	657.1	648.2	650.4	652.4	643.5	637.3	651.4	626.4	622.4	617.2	616.1
IM IN	2.1	658.1	649.2	651.4	653.4	644.5	638.3	652.4	627.4	623.4	618.2	617.1
IM IN	2.2	659.1	650.2	652.4	654.4	645.5	639.3	653.4	628.4	624.4	619.2	618.1
IM IN	2.3	660.1	651.2	653.4	655.4	646.5	640.3	654.4	629.4	625.4	620.2	619.1
IM IN	2.4	661.1	652.2	654.4	656.4	647.5	641.3	655.4	630.4	626.4	621.2	620.1
IM IN	2.5	662.1	653.2	655.4	657.4	648.5	642.3	656.4	631.4	627.4	622.2	621.1
IM IN	2.6	663.1	654.2	656.4	658.4	649.5	643.3	657.4	632.4	628.4	623.2	622.1
IM IN	2.7	664.1	655.2	657.4	659.4	650.5	644.3	658.4	633.4	629.4	624.2	623.1
IM IN	2.8	665.1	656.2	658.4	660.4	651.5	645.3	659.4	634.4	630.4	625.2	624.1
IM IN	2.9	666.1	657.2	659.4	661.4	652.5	646.3	660.4	635.4	631.4	626.2	625.1
IM IN	3.0	667.1	658.2	660.4	662.4	653.5	647.3	661.4	636.4	632.4	627.2	626.1
IM IN	3.1	668.1	659.2	661.4	663.4	654.5	648.3	662.4	637.4	633.4	628.2	627.1
IM IN	3.2	669.1	660.2	662.4	664.4	655.5	649.3	663.4	638.4	634.4	629.2	628.1
IM IN	3.3	670.1	661.2	663.4	665.4	656.5	650.3	664.4	639.4	635.4	630.2	629.1
IM IN	3.4	671.1	662.2	664.4	666.4	657.5	651.3	665.4	640.4	636.4	631.2	630.1
IM IN	3.5	672.1	663.2	665.4	667.4	658.5	652.3	666.4	641.4	637.4	632.2	631.1
IM IN	3.6	673.1	664.2	666.4	668.4	659.5	653.3	667.4	642.4	638.4	633.2	632.1
IM IN	3.7	674.1	665.2	667.4	669.4	660.5	654.3	668.4	643.4	639.4	634.2	633.1
IM IN	3.8	675.1	666.2	668.4	670.4	661.5	655.3	669.4	644.4	640.4	635.2	634.1
IM IN	3.9	676.1	667.2	669.4	671.4	662.5	656.3	670.4	645.4	641.4	636.2	635.1
IM IN	4.0	677.1	668.2	670.4	672.4	663.5	657.3	671.4	646.4	642.4	637.2	636.1
IM IN	4.1	678.1	669.2	671.4	673.4	664.5	658.3	672.4	647.4	643.4	638.2	637.1
IM IN	4.2	679.1	670.2	672.4	674.4	665.5	659.3	673.4	648.4	644.4	639.2	638.1
IM IN	4.3	680.1	671.2	673.4	675.4	666.5	660.3	674.4	649.4	645.4	640.2	639.1
IM IN	4.4	681.1	672.2	674.4	676.4	667.5	661.3	675.4	650.4	646.4	641.2	640.1
IM IN	4.5	682.1	673.2	675.4	677.4	668.5	662.3	676.4	651.4	647.4	642.2	641.1
IM IN	4.6	683.1	674.2	676.4	678.4	669.5	663.3	677.4	652.4	648.4	643.2	642.1
IM IN	4.7	684.1	675.2	677.4	679.4	670.5	664.3	678.4	653.4	649.4	644.2	643.1
IM IN	4.8	685.1	676.2	678.4	680.4	671.5	665.3	679.4	654.4	650.4	645.2	644.1
IM IN	4.9	686.1	677.2	679.4	681.4	672.5	666.3	680.4	655.4	651.4	646.2	645.1
IM IN	5.0	687.1	678.2	680.4	682.4	673.5	667.3	681.4	656.4	652.4	647.2	646.1
IM IN	5.1	688.1	679.2	681.4	683.4	674.5	668.3	682.4	657.4	653.4	648.2	647.1
IM IN	5.2	689.1	680.2	682.4	684.4	675.5	669.3	683.4	658.4	654.4	649.2	648.1
IM IN	5.3	690.1	681.2	683.4	685.4	676.5	670.3	684.4	659.4	655.4	650.2	649.1
IM IN	5.4	691.1	682.2	684.4	686.4	677.5	671.3	685.4	660.4	656.4	651.2	650.1
IM IN	5.5	692.1	683.2	685.4	687.4	678.5	672.3	686.4	661.4	657.4	652.2	651.1
IM IN	5.6	693.1	684.2	686.4	688.4	679.5	673.3	687.4	662.4	658.4	653.2	652.1
IM IN	5.7	694.1	685.2	687.4	689.4	680.5	674.3	688.4	663.4	659.4	654.2	653.1
IM IN	5.8	695.1	686.2	688.4	690.4	681.5	675.3	689.4	664.4	660.4	655.2	654.1
IM IN	5.9	696.1	687.2	689.4	691.4	682.5	676.3	690.4	665.4	661.4	656.2	655.1
IM IN	6.0	697.1	688.2	690.4	692.4	683.5	677.3	691.4	666.4	662.4	657.2	656.1
IM IN	6.1	698.1	689.2	691.4	693.4	684.5	678.3	692.4	667.4	663.4	658.2	657.1
IM IN	6.2	699.1	690.2	692.4	694.4	685.5	679.3	693.4	668.4	664.4	659.2	658.1
IM IN	6.3	700.1	691.2	693.4	695.4	686.5	680.3	694.4	669.4	665.4	660.2	659.1
IM IN	6.4	701.1	692.2	694.4	696.4	687.5	681.3	695.4	670.4	666.4	661.2	660.1
IM IN	6.5	702.1	693.2	695.4	697.4	688.5	682.3	696.4	671.4	667.4	662.2	661.1
IM IN	6.6	703.1	694.2	696.4	698.4	689.5	683.3	697.4	672.4	668.4	663.2	662.1
IM IN	6.7	704.1	695.2	697.4	699.4	690.5	684.3	698.4	673.4	669.4	664.2	663.1
IM IN	6.8	705.1	696.2	698.4	700.4	691.5	685.3	699.4	674.4	670.4	665.2	664.1
IM IN	6.9	706.1	697.2	699.4	701.4	692.5	686.3	700.4	675.4	671.4	666.2	665.1
IM IN	7.0	707.1	698.2	700.4	702.4	693.5	687.3	701.4	676.4	672.4	667.2	666.1
IM IN	7.1	708.1	699.2	701.4	703.4	694.5	688.3	702.4	677.4	673.4	668.2	667.1
IM IN	7.2	709.1	700.2	702.4	704.4	695.5	689.3	703.4	678.4	674.4	669.2	668.1
IM IN	7.3	710.1	701.2	703.4	705.4	696.5	690.3	704.4	679.4	675.4	670.2	669.1
IM IN	7.4	711.1	702.2	704.4	706.4	697.5	691.3	705.4	680.4	676.4	671.2	670.1
IM IN	7.5	712.1	703.2	705.4	707.4	698.5	692.3	706.4	681.4	677.4	672.2	671.1
IM IN	7.6	713.1	704.2	706.4	708.4	699.5	693.3	707.4	682.4	678.4	673.2	672.1
IM IN	7.7	714.1	705.2	707.4	709.4	700.5	694.3	708.4	683.4	679.4	674.2	673.1
IM IN	7.8	715.1	706.2	708.4	710.4	701.5	695.3	709.4	684.4	680.4	675.2	674.1
IM IN	7.9	716.1	707.2	709.4	711.4	702.5	696.3	710.4	685.4	681.4	676.2	675.1
IM IN	8.0	717.1	708.2	710.4	712.4	703.5	697.3	711.4	686.4	682.4	677.2	676.1
IM IN	8.1	718.1	709.2	711.4	713.4	704.5	698.3	712.4	687.4	683.4	678.2	677.1
IM IN	8.2	719.1	710.2	712.4	714.4	705.5	699.3	713.4	688.4	684.4	679.2	678.1
IM IN	8.3	720.1	711.2	713.4	715.4	706.5	700.3	714.4	689.4	685.4	680.2	679.1
IM IN	8.4	721.1	712.2	714.4	716.4	707.5	701.3	715.4	690.4	686.4	681.2	680.1
IM IN	8.5	722.1	713.2	715.4	717.4	708.5	702.3	716.4	691.4	687.4	682.2	681.1
IM IN	8.6	723.1	714.2	716.4	718.4	709.5	703.3	717.4	692.4	688.4	683.2	682.1
IM IN	8.7	724.1	715.2	717.4	719.4	710.5	704.3	718.4	693.4	689.4	684.2	683.1
IM IN	8.8	725.1	716.2	718.4	720.4	711.5	705.3	719.4	694.4	690.4	685.2	684.1
IM IN	8.9	726.1	717.2	719.4	721.4	712.5	706.3	720.4	695.4	691.4	686.2	685.1
IM IN	9.0	727.1	718.2	720.4	722.4	713.5	707.3	721.4	696.4	692.4	687.2	686.1
IM IN	9.1	728.1	719.2	721.4	723.4	714.5	708.3	722.4	697.4	693.4	688.2	687.1
IM IN	9.2	729.1	720.2	722.4	724.4	715.5	709.3	723.4	698.4	694.4	689.2	688.1
IM IN	9.3	730.1	721.2	723.4	725.4	716.5	710.3	724.4	699.4	695.4	690.2	689.1
IM IN	9.4	731.1	722.2	724.4	726.4	717.5	711.3	725.4	700.4	696.4	691.2	690.1
IM IN	9.5	732.1	723.2	725.4	727.4	718.5	712.3	726.4	701.4	697.4	692.2	691.1
IM IN	9.6	733.1	724.2	726.4	728.4	719.5	713.3	7				

ROCKET FUEL DEPOSIT TEST PROGRAM (RP-- FUEL)
 RUN 1 DECEMBER 13, 1962

TIME	(MEM)	.UUDU	1.133	2.133	3.133	4.133	5.133	6.133	7.133	8.133	9.133	10.13
INLET	MEYNOLUS	.UUDU	.UUDU	.UUDU	.UUDU	.UUDU	.UUDU	.UUDU	.UUDU	.UUDU	.UUDU	.UUDU
AV	1.3	5175-002	3639-005	3561-005	3463-005	3355-005	3349-005	3338-005	3345-005	3359-005	3297-002	3349-005
L	1.3	4.441	4.311	4.285	4.209	4.174	4.169	4.149	4.176	4.177	4.222	4.304
U	3.8	4.808	4.793	4.721	4.653	4.727	4.729	4.737	4.762	4.777	4.740	4.827
U	6.9	4.856	4.984	4.962	4.896	4.963	5.061	5.131	5.178	5.249	5.272	5.322
U	11.4	4.956	5.304	5.101	5.048	5.133	5.283	5.372	5.442	5.511	5.548	5.610
U	14.0	4.947	5.112	5.203	5.411	5.265	5.403	5.467	5.518	5.559	5.593	5.650
U	16.5	5.747	5.881	5.872	5.819	5.935	6.059	6.141	6.218	6.292	6.335	6.369
U	19.1	5.523	5.478	5.557	5.814	5.673	5.776	5.839	5.884	5.932	5.971	5.945
U	24.1	7.668	6.792-002	7.256	6.944	6.693	6.477	6.278	6.177	6.070	5.971	5.818
I/K	1.3	.0000	.6792-002	.8180-002	.1240-001	.1418-001	.1355-001	.1604-001	.1430-001	.1368-001	.1169-001	.7164-002
I/K	3.8	.0000	.6344-003	.5820-002	.6931-002	.3547-002	.3599-002	.3111-002	.1990-002	.1379-002	.2984-002	.0000
I/K	6.9	.0000	.0000	.0000	.0000	.0000	.0000	.0000	.0000	.0000	.0000	.0000
I/K	11.4	.0000	.0000	.0000	.0000	.0000	.0000	.0000	.0000	.0000	.0000	.0000
I/K	14.0	.0000	.0000	.0000	.0000	.0000	.0000	.0000	.0000	.0000	.0000	.0000
I/K	16.5	.0000	.0000	.0000	.0000	.0000	.0000	.0000	.0000	.0000	.0000	.0000
I/K	19.1	.0000	.0000	.0000	.0000	.0000	.0000	.0000	.0000	.0000	.0000	.0000
I/K	24.1	.0000	.0000	.0000	.0000	.0000	.0000	.0000	.0000	.0000	.0000	.0000
KC	1.3	.0000	.1483-002	.0000	.0000	.0000	.0000	.0000	.0000	.0000	.0000	.0000
KC	3.8	.0000	.1911-002	.7406-002	.1360-001	.1960-001	.2397-001	.2987-001	.3148-001	.3433-001	.3990-001	.4088-001
KC	6.9	.0000	.8479-004	.4524-004	.4305-004	.3783-004	.2938-004	.2792-004	.2047-004	.1598-004	.4803-005	.0000
KC	11.4	.0000	.0000	.0000	.0000	.0000	.0000	.0000	.0000	.0000	.0000	.0000
KC	14.0	.0000	.0000	.0000	.0000	.0000	.0000	.0000	.0000	.0000	.0000	.0000
KC	16.5	.0000	.0000	.0000	.0000	.0000	.0000	.0000	.0000	.0000	.0000	.0000
KC	19.1	.0000	.0000	.0000	.0000	.0000	.0000	.0000	.0000	.0000	.0000	.0000
KC	24.1	.0000	.1884-005	.4775-004	.5853-004	.6393-004	.6420-004	.6752-004	.6444-004	.6193-004	.6064-004	.5770-004

ORIGINAL PAGE IS
 OF POOR QUALITY

ROCKET FUEL DEPOSIT TEST PROGRAM (RP-1 FUEL)
 RUN 2 FEBRUARY 23, 1963

TIME	(MIN)	.0000	.9000	1.900	2.900	3.900	4.900	5.900	6.900	7.900	8.900	10.40
IN OUT	3.5	690.9	693.7	691.7	692.6	688.7	701.5	701.5	709.3	723.2	729.3	825.9
IN OUT	3.8	718.5	703.8	697.0	672.0	680.9	669.8	662.0	653.2	660.4	657.6	551.9
IN OUT	4.0	698.3	678.7	672.6	642.0	664.3	632.0	627.0	630.4	635.9	634.8	601.5
IN OUT	4.3	623.4	644.8	641.5	619.3	614.3	609.8	605.9	608.7	613.2	612.0	582.0
IN OUT	4.5	611.5	661.4	607.6	608.2	604.3	599.8	595.9	597.6	600.2	602.8	585.9
IN OUT	4.8	605.9	608.3	600.9	601.5	598.2	593.7	594.4	593.7	595.9	595.4	557.5
IN IN	5.0	675.2	603.2	601.5	602.0	583.3	586.5	594.8	591.4	594.8	593.2	557.5
IN IN	5.3	700.8	694.1	681.5	666.5	683.3	672.5	680.7	691.4	707.8	711.9	601.0
IN IN	5.4	699.6	683.1	671.1	656.5	648.7	641.7	640.7	637.9	659.5	652.9	602.1
IN IN	5.6	632.5	653.2	626.0	626.5	621.7	616.7	611.7	615.0	620.6	619.2	569.1
IN IN	5.9	609.7	603.9	591.5	603.7	588.9	594.5	590.6	593.3	597.8	596.7	561.0
IN IN	6.0	596.9	594.8	589.3	592.6	586.7	584.3	580.6	584.9	587.8	586.7	559.9
IN IN	6.3	590.2	588.7	585.4	590.9	586.8	582.3	573.0	582.2	585.0	584.5	555.5
IN IN	6.5	590.2	588.7	585.4	590.9	586.8	582.3	573.0	582.2	585.0	584.5	555.5
FUEL IN	6.8	590.2	588.7	585.4	590.9	586.8	582.3	573.0	582.2	585.0	584.5	555.5
FUEL IN	7.0	590.2	588.7	585.4	590.9	586.8	582.3	573.0	582.2	585.0	584.5	555.5
FUEL IN	7.2	590.2	588.7	585.4	590.9	586.8	582.3	573.0	582.2	585.0	584.5	555.5
FUEL IN	7.4	590.2	588.7	585.4	590.9	586.8	582.3	573.0	582.2	585.0	584.5	555.5
FUEL IN	7.6	590.2	588.7	585.4	590.9	586.8	582.3	573.0	582.2	585.0	584.5	555.5
FUEL IN	7.8	590.2	588.7	585.4	590.9	586.8	582.3	573.0	582.2	585.0	584.5	555.5
FUEL IN	8.0	590.2	588.7	585.4	590.9	586.8	582.3	573.0	582.2	585.0	584.5	555.5
FUEL IN	8.2	590.2	588.7	585.4	590.9	586.8	582.3	573.0	582.2	585.0	584.5	555.5
FUEL IN	8.4	590.2	588.7	585.4	590.9	586.8	582.3	573.0	582.2	585.0	584.5	555.5
FUEL IN	8.6	590.2	588.7	585.4	590.9	586.8	582.3	573.0	582.2	585.0	584.5	555.5
FUEL IN	8.8	590.2	588.7	585.4	590.9	586.8	582.3	573.0	582.2	585.0	584.5	555.5
FUEL IN	9.0	590.2	588.7	585.4	590.9	586.8	582.3	573.0	582.2	585.0	584.5	555.5
FUEL IN	9.2	590.2	588.7	585.4	590.9	586.8	582.3	573.0	582.2	585.0	584.5	555.5
FUEL IN	9.4	590.2	588.7	585.4	590.9	586.8	582.3	573.0	582.2	585.0	584.5	555.5
FUEL IN	9.6	590.2	588.7	585.4	590.9	586.8	582.3	573.0	582.2	585.0	584.5	555.5
FUEL IN	9.8	590.2	588.7	585.4	590.9	586.8	582.3	573.0	582.2	585.0	584.5	555.5
FUEL IN	10.0	590.2	588.7	585.4	590.9	586.8	582.3	573.0	582.2	585.0	584.5	555.5
FUEL IN	10.2	590.2	588.7	585.4	590.9	586.8	582.3	573.0	582.2	585.0	584.5	555.5
FUEL IN	10.4	590.2	588.7	585.4	590.9	586.8	582.3	573.0	582.2	585.0	584.5	555.5
FUEL IN	10.6	590.2	588.7	585.4	590.9	586.8	582.3	573.0	582.2	585.0	584.5	555.5
FUEL IN	10.8	590.2	588.7	585.4	590.9	586.8	582.3	573.0	582.2	585.0	584.5	555.5
FUEL IN	11.0	590.2	588.7	585.4	590.9	586.8	582.3	573.0	582.2	585.0	584.5	555.5
FUEL IN	11.2	590.2	588.7	585.4	590.9	586.8	582.3	573.0	582.2	585.0	584.5	555.5
FUEL IN	11.4	590.2	588.7	585.4	590.9	586.8	582.3	573.0	582.2	585.0	584.5	555.5
FUEL IN	11.6	590.2	588.7	585.4	590.9	586.8	582.3	573.0	582.2	585.0	584.5	555.5
FUEL IN	11.8	590.2	588.7	585.4	590.9	586.8	582.3	573.0	582.2	585.0	584.5	555.5
FUEL IN	12.0	590.2	588.7	585.4	590.9	586.8	582.3	573.0	582.2	585.0	584.5	555.5
FUEL IN	12.2	590.2	588.7	585.4	590.9	586.8	582.3	573.0	582.2	585.0	584.5	555.5
FUEL IN	12.4	590.2	588.7	585.4	590.9	586.8	582.3	573.0	582.2	585.0	584.5	555.5
FUEL IN	12.6	590.2	588.7	585.4	590.9	586.8	582.3	573.0	582.2	585.0	584.5	555.5
FUEL IN	12.8	590.2	588.7	585.4	590.9	586.8	582.3	573.0	582.2	585.0	584.5	555.5
FUEL IN	13.0	590.2	588.7	585.4	590.9	586.8	582.3	573.0	582.2	585.0	584.5	555.5
FUEL IN	13.2	590.2	588.7	585.4	590.9	586.8	582.3	573.0	582.2	585.0	584.5	555.5
FUEL IN	13.4	590.2	588.7	585.4	590.9	586.8	582.3	573.0	582.2	585.0	584.5	555.5
FUEL IN	13.6	590.2	588.7	585.4	590.9	586.8	582.3	573.0	582.2	585.0	584.5	555.5
FUEL IN	13.8	590.2	588.7	585.4	590.9	586.8	582.3	573.0	582.2	585.0	584.5	555.5
FUEL IN	14.0	590.2	588.7	585.4	590.9	586.8	582.3	573.0	582.2	585.0	584.5	555.5
FUEL IN	14.2	590.2	588.7	585.4	590.9	586.8	582.3	573.0	582.2	585.0	584.5	555.5
FUEL IN	14.4	590.2	588.7	585.4	590.9	586.8	582.3	573.0	582.2	585.0	584.5	555.5
FUEL IN	14.6	590.2	588.7	585.4	590.9	586.8	582.3	573.0	582.2	585.0	584.5	555.5
FUEL IN	14.8	590.2	588.7	585.4	590.9	586.8	582.3	573.0	582.2	585.0	584.5	555.5
FUEL IN	15.0	590.2	588.7	585.4	590.9	586.8	582.3	573.0	582.2	585.0	584.5	555.5
FUEL IN	15.2	590.2	588.7	585.4	590.9	586.8	582.3	573.0	582.2	585.0	584.5	555.5
FUEL IN	15.4	590.2	588.7	585.4	590.9	586.8	582.3	573.0	582.2	585.0	584.5	555.5
FUEL IN	15.6	590.2	588.7	585.4	590.9	586.8	582.3	573.0	582.2	585.0	584.5	555.5
FUEL IN	15.8	590.2	588.7	585.4	590.9	586.8	582.3	573.0	582.2	585.0	584.5	555.5
FUEL IN	16.0	590.2	588.7	585.4	590.9	586.8	582.3	573.0	582.2	585.0	584.5	555.5
FUEL IN	16.2	590.2	588.7	585.4	590.9	586.8	582.3	573.0	582.2	585.0	584.5	555.5
FUEL IN	16.4	590.2	588.7	585.4	590.9	586.8	582.3	573.0	582.2	585.0	584.5	555.5
FUEL IN	16.6	590.2	588.7	585.4	590.9	586.8	582.3	573.0	582.2	585.0	584.5	555.5
FUEL IN	16.8	590.2	588.7	585.4	590.9	586.8	582.3	573.0	582.2	585.0	584.5	555.5
FUEL IN	17.0	590.2	588.7	585.4	590.9	586.8	582.3	573.0	582.2	585.0	584.5	555.5
FUEL IN	17.2	590.2	588.7	585.4	590.9	586.8	582.3	573.0	582.2	585.0	584.5	555.5
FUEL IN	17.4	590.2	588.7	585.4	590.9	586.8	582.3	573.0	582.2	585.0	584.5	555.5
FUEL IN	17.6	590.2	588.7	585.4	590.9	586.8	582.3	573.0	582.2	585.0	584.5	555.5
FUEL IN	17.8	590.2	588.7	585.4	590.9	586.8	582.3	573.0	582.2	585.0	584.5	555.5
FUEL IN	18.0	590.2	588.7	585.4	590.9	586.8	582.3	573.0	582.2	585.0	584.5	555.5
FUEL IN	18.2	590.2	588.7	585.4	590.9	586.8	582.3	573.0	582.2	585.0	584.5	555.5
FUEL IN	18.4	590.2	588.7	585.4	590.9	586.8	582.3	573.0	582.2	585.0	584.5	555.5
FUEL IN	18.6	590.2	588.7	585.4	590.9	586.8	582.3	573.0	582.2	585.0	584.5	555.5
FUEL IN	18.8	590.2	588.7	585.4	590.9	586.8	582.3	573.0	582.2	585.0	584.5	555.5
FUEL IN	19.0	590.2	588.7	585.4	590.9	586.8	582.3	573.0	582.2	585.0	584.5	555.5
FUEL IN	19.2	590.2	588.7	585.4	590.9	586.8	582.3	573.0	582.2	585.0	584.5	555.5
FUEL IN	19.4	590.2	588.7	585.4	590.9	586.8	582.3	573.0	582.2	585.0	584.5	555.5
FUEL IN	19.6	590.2	588.7	585.4	590.9	586.8	582.3	573.0	582.2	585.0	584.5	555.5
FUEL IN	19.8	590.2	588.7	585.4	590.9	586.8	582.3	573.0	582.2	585.0	584.5	555.5
FUEL IN	20.0	590.2	588.7	585.4	590.9	586.8	582.3	573.0	582.2	585.0	584.5	555.5
FUEL IN	20.2	590.2	588.7	585.4	590.9	586.8	582.3	573.0	582.2	585.0	584.5	555.5
FUEL IN	20.4	590.2	588.7	585.4	590.9	586.8	582.3	573.0	582.2	585.0	584.5	555.5
FUEL IN	20.6	590.2	588									

ROCKET FUEL DEPOSIT TEST PROGRAM (RP-1 FUEL)
 MUN 2 FEBRUARY 23, 1983

TIME	(MIN)	0.000	1.000	2.000	3.000	4.000	5.000	6.000	7.000	8.000	10.00
AVU	1.0	2262-002	2258-002	2254-002	2646-002	2239-002	2462-002	2250-002	2098-002	2113-002	2089-002
AVU	1.5	2.077	2.040	2.023	1.992	1.970	1.937	1.946	1.860	1.834	1.795
AVU	2.0	1.981	2.063	2.095	2.132	2.189	2.247	2.230	2.149	2.163	2.120
AVU	2.5	2.514	2.537	2.538	2.547	2.575	2.575	2.568	2.531	2.509	2.540
AVU	3.0	2.781	2.825	2.815	2.825	2.860	2.917	2.895	2.811	2.821	2.753
AVU	3.5	3.494	3.025	3.015	3.025	3.060	3.116	3.085	3.005	3.016	3.053
AVU	4.0	3.102	3.146	3.131	3.147	3.184	3.236	3.210	3.133	3.137	3.231
AVU	4.5	3.273	3.300	3.277	3.303	3.333	3.388	3.371	3.296	3.300	3.351
AVU	5.0	3.382	3.402	3.417	3.403	3.393	3.408	3.461	3.426	3.445	3.434
AVU	5.5	0.000	0.000	0.000	0.000	0.000	0.000	0.000	0.000	0.000	0.000
AVU	6.0	0.000	0.000	0.000	0.000	0.000	0.000	0.000	0.000	0.000	0.000
AVU	6.5	0.000	0.000	0.000	0.000	0.000	0.000	0.000	0.000	0.000	0.000
AVU	7.0	0.000	0.000	0.000	0.000	0.000	0.000	0.000	0.000	0.000	0.000
AVU	7.5	0.000	0.000	0.000	0.000	0.000	0.000	0.000	0.000	0.000	0.000
AVU	8.0	0.000	0.000	0.000	0.000	0.000	0.000	0.000	0.000	0.000	0.000
AVU	8.5	0.000	0.000	0.000	0.000	0.000	0.000	0.000	0.000	0.000	0.000
AVU	9.0	0.000	0.000	0.000	0.000	0.000	0.000	0.000	0.000	0.000	0.000
AVU	9.5	0.000	0.000	0.000	0.000	0.000	0.000	0.000	0.000	0.000	0.000
AVU	10.0	0.000	0.000	0.000	0.000	0.000	0.000	0.000	0.000	0.000	0.000

ORIGINAL PAGE IS
 OF POOR QUALITY

ROCKET FUEL DEPOSIT TEST PROGRAM (RP-1 FUEL)
 RUN 3 DECEMBER 16, 1962

TIME	(MIN)	0000	1.167	2.150	3.150	4.150	5.150	6.150	7.150	8.150	9.150	10.15
IN OUT	CM (K)	711.5	712.0	713.7	717.6	724.8	726.5	727.0	735.6	752.4	793.8	773.7
IN OUT	CM (K)	687.0	738.2	742.0	744.4	753.7	760.4	766.5	769.3	802.6	754.8	768.4
IN OUT	CM (K)	680.0	760.4	762.6	765.4	769.9	774.3	777.0	784.3	775.6	770.9	711.3
IN OUT	CM (K)	680.4	760.4	762.6	765.4	769.9	774.3	777.0	784.3	775.6	770.9	711.3
IN OUT	CM (K)	683.7	734.3	744.8	745.9	752.6	755.4	762.6	744.9	732.8	618.2	627.0
IN OUT	CM (K)	703.2	741.5	752.6	754.4	762.6	778.7	789.6	744.9	703.2	625.9	623.4
IN OUT	CM (K)	694.3	749.8	758.7	760.4	767.0	775.9	787.6	744.9	703.2	618.2	627.0
IN OUT	CM (K)	690.9	727.0	751.5	758.4	762.6	775.4	789.6	744.9	703.2	618.2	627.0
IN IN	CM (K)	693.1	692.9	694.6	698.6	705.8	707.6	708.4	717.3	736.0	618.2	627.0
IN IN	CM (K)	668.1	691.8	700.2	700.3	707.7	712.6	713.8	717.3	734.0	618.2	627.0
IN IN	CM (K)	662.0	719.0	723.0	725.8	734.4	741.5	749.8	750.7	765.8	618.2	627.0
IN IN	CM (K)	674.1	741.3	743.0	746.4	750.8	755.4	764.8	765.7	784.0	618.2	627.0
IN IN	CM (K)	662.4	702.9	705.7	709.1	709.8	709.8	709.8	719.0	732.0	618.2	627.0
IN IN	CM (K)	684.8	715.1	725.7	726.9	734.7	746.0	749.5	766.4	714.0	618.2	627.0
IN IN	CM (K)	684.8	732.4	735.5	735.3	743.6	746.0	749.5	766.4	714.0	618.2	627.0
IN IN	CM (K)	675.9	730.7	733.6	734.4	743.6	746.0	749.5	766.4	714.0	618.2	627.0
IN IN	CM (K)	672.6	730.7	733.6	734.4	743.6	746.0	749.5	766.4	714.0	618.2	627.0
FULL INLET P	(MPA)	13.73	13.71	13.70	13.67	13.65	13.62	13.58	13.57	12.58	13.55	12.54
FUEL INLET TEMP	(K)	290.9	290.9	291.5	290.9	290.9	290.9	290.9	290.4	290.4	290.9	290.4
FUEL EXIT TEMP	(K)	380.9	387.0	387.0	385.4	385.4	385.4	385.4	383.2	383.7	384.8	384.8
FLOW RATE	(KG/S)	6592	7231	7218	7231	7281	7231	7218	7256	7244	7294	7294
CURRENT	(VOLTS)	2788	2912	2894	2883	2870	2849	2826	2826	2831	2910	2923
VOLTAGE	(VOLTS)	5.184	5.176	5.194	5.196	5.213	5.220	5.213	5.187	5.180	5.080	5.079
HEAT FLUX	(W/CM ²)	14.45	15.07	15.03	14.98	14.96	14.87	14.33	14.66	14.66	14.78	14.86
INLET FUEL VEL	(M/S)	226.1	226.7	226.3	226.0	226.6	226.8	226.8	226.2	226.2	226.8	226.8
INLET FUEL ANGLE	(DEG)	28.62	29.60	29.57	29.60	29.80	29.60	29.60	29.67	29.62	29.85	29.88
ENERGY BAL. ANGLE	(DEG)	-6.554	-2.544	-2.700	-1.544	-1.7416	-1.6092	-1.405	-1.055	-0.6212	-0.002	-0.790

ORIGINAL PAGE IS
 OF POOR QUALITY

ROCKET FUEL DEPOSIT TEST PROGRAM (RP-1 FUEL)
 RUN 4 DECEMBER 20, 1982

TIME	(MIN)	0000	0800	1.817	2.810	3.800	4.800	5.800	6.600	7.800	8.800	9.933
OUT	0	839.8	827.0	788.7	769.5	725.4	709.9	623.2	678.7	693.7	659.8	657.8
IN	0	739.3	728.7	705.9	683.2	677.0	662.6	643.2	678.3	693.0	659.8	657.8
OUT	0	775.9	692.0	667.6	664.3	660.4	653.7	643.2	640.3	645.0	637.6	637.6
IN	0	740.4	693.7	705.9	683.2	671.5	666.3	654.3	640.3	648.7	634.3	634.3
OUT	0	662.6	620.9	620.4	625.4	620.8	703.2	603.9	687.6	684.3	629.9	629.9
IN	0	659.8	660.4	671.5	699.8	704.8	708.2	691.5	688.2	689.3	590.9	590.9
OUT	0	821.1	735.4	704.8	707.0	704.8	743.2	694.7	696.5	700.4	708.7	714.0
IN	0	720.5	809.1	770.8	768.4	735.4	683.2	733.7	730.9	724.3	738.5	734.0
OUT	0	757.2	670.5	630.8	631.9	627.5	619.9	607.7	601.1	597.9	592.2	592.2
IN	0	676.8	670.5	649.0	665.2	642.3	644.9	632.6	626.7	624.3	620.2	621.3
OUT	0	621.6	675.8	688.0	665.2	653.6	648.8	626.6	623.3	627.9	616.4	616.4
IN	0	705.5	603.0	602.5	607.5	602.5	598.2	585.3	585.5	582.8	580.5	580.5
OUT	0	681.1	734.1	695.2	689.1	691.4	690.5	673.9	670.5	671.8	579.1	576.3
IN	0	651.4	712.5	750.2	747.5	686.4	687.1	681.1	678.9	671.8	691.3	696.9
FUEL INLET P	TEMP	13.42	13.40	13.36	13.35	13.31	13.27	11.48	11.43	11.46	11.47	11.47
FUEL INLET P	TEMP	12.30	12.11	11.96	11.79	11.67	11.62	11.57	11.48	11.46	11.47	11.47
FUEL EXIT	TEMP	286.5	286.5	286.5	286.5	286.5	286.5	286.5	286.5	286.5	286.5	286.5
FUEL EXIT	TEMP	374.8	374.8	374.8	374.8	374.8	374.8	374.8	374.8	374.8	374.8	374.8
FLOW RATE	(KG/S)	2256.8	2256.8	2256.8	2256.8	2256.8	2256.8	2256.8	2256.8	2256.8	2256.8	2256.8
CURRENT	(AMPS)	2918.0	2900.0	2906.0	2907.0	2901.0	2873.0	2860.0	2854.0	2839.0	2830.0	2826.0
VOLTAG	(VOLTS)	5.069	4.864	4.857	4.855	4.861	4.850	4.857	4.861	4.837	4.844	4.855
POWER	(KW)	14.79	14.10	14.12	14.11	14.10	13.94	13.59	13.87	13.73	13.71	13.72
HEAT FLUX	(W/CM ²)	947.7	903.8	904.4	904.3	903.6	892.9	893.2	889.0	880.0	878.2	878.9
INLET FUEL VEL	(M/S)	29.86	29.47	29.58	29.37	29.73	29.06	29.32	29.68	29.63	30.19	30.22
ENERGY BALANCE	(PCT)	-2.592	-3.220	-2.296	-2.9768	-1.027	-2.749	-3.552	-2.956	-2.130	-2.145	-2.6732

ORIGINAL PAGE IS
 OF POOR QUALITY

ROCKET FUEL DEPOSIT TEST PROGRAM (RP-1 FUEL)
 RUN 4
 DECEMBER 20, 1962

TIME	(MIN)	.0000	1.817	2.800	3.800	4.800	5.800	6.800	7.800	8.800	9.933
INLET REYNOLDS FACTOR											
AVG FRICTION FACTOR											
U @ 1.3 CM(W/CM-K)		2107+005	2086+005	2071+005	2096+005	2049+005	2067+005	2093+005	2089+005	2129+005	2133+005
U @ 1.5 CM(W/CM-K)		5365-002	7109-002	1976	2170	8231-002	8369+002	8347-002	8351-002	8455-002	8557
U @ 1.8 CM(W/CM-K)		1788	1885	2725	2759	2790	2889	2948	2949	2996	3000
U @ 2.0 CM(W/CM-K)		2020	2733	2539	2580	2656	2763	2792	2781	2811	2806
U @ 2.5 CM(W/CM-K)		2306	3385	2724	2783	2805	2864	2904	2891	2922	2928
U @ 3.0 CM(W/CM-K)		2717	2502	2676	2765	2771	2844	2904	2891	2922	2928
U @ 3.5 CM(W/CM-K)		2464	2565	2531	2573	2551	2632	2648	2646	2700	2707
U @ 4.0 CM(W/CM-K)		2284	3503	3450	3509	3519	3532	3663	3665	3700	3704
U @ 4.5 CM(W/CM-K)		2593	3011	2777	2671	2647	2765	2790	2727	2741	2767
U @ 5.0 CM(W/CM-K)		3036	2715	2412	2612	2519	2778	2581	2604	2528	2607
U @ 5.5 CM(W/CM-K)		0000	0000	0000	0000	0000	0000	0000	0000	0000	0000
U @ 6.0 CM(W/CM-K)		0000	0000	0000	0000	0000	0000	0000	0000	0000	0000
U @ 6.5 CM(W/CM-K)		0000	0000	0000	0000	0000	0000	0000	0000	0000	0000
U @ 7.0 CM(W/CM-K)		0000	0000	0000	0000	0000	0000	0000	0000	0000	0000
U @ 7.5 CM(W/CM-K)		0000	0000	0000	0000	0000	0000	0000	0000	0000	0000
U @ 8.0 CM(W/CM-K)		0000	0000	0000	0000	0000	0000	0000	0000	0000	0000
U @ 8.5 CM(W/CM-K)		0000	0000	0000	0000	0000	0000	0000	0000	0000	0000
U @ 9.0 CM(W/CM-K)		0000	0000	0000	0000	0000	0000	0000	0000	0000	0000
U @ 9.5 CM(W/CM-K)		0000	0000	0000	0000	0000	0000	0000	0000	0000	0000
U @ 10.0 CM(W/CM-K)		0000	0000	0000	0000	0000	0000	0000	0000	0000	0000
U @ 10.5 CM(W/CM-K)		0000	0000	0000	0000	0000	0000	0000	0000	0000	0000
U @ 11.0 CM(W/CM-K)		0000	0000	0000	0000	0000	0000	0000	0000	0000	0000
U @ 11.5 CM(W/CM-K)		0000	0000	0000	0000	0000	0000	0000	0000	0000	0000
U @ 12.0 CM(W/CM-K)		0000	0000	0000	0000	0000	0000	0000	0000	0000	0000
U @ 12.5 CM(W/CM-K)		0000	0000	0000	0000	0000	0000	0000	0000	0000	0000
U @ 13.0 CM(W/CM-K)		0000	0000	0000	0000	0000	0000	0000	0000	0000	0000
U @ 13.5 CM(W/CM-K)		0000	0000	0000	0000	0000	0000	0000	0000	0000	0000
U @ 14.0 CM(W/CM-K)		0000	0000	0000	0000	0000	0000	0000	0000	0000	0000
U @ 14.5 CM(W/CM-K)		0000	0000	0000	0000	0000	0000	0000	0000	0000	0000
U @ 15.0 CM(W/CM-K)		0000	0000	0000	0000	0000	0000	0000	0000	0000	0000
U @ 15.5 CM(W/CM-K)		0000	0000	0000	0000	0000	0000	0000	0000	0000	0000
U @ 16.0 CM(W/CM-K)		0000	0000	0000	0000	0000	0000	0000	0000	0000	0000
U @ 16.5 CM(W/CM-K)		0000	0000	0000	0000	0000	0000	0000	0000	0000	0000
U @ 17.0 CM(W/CM-K)		0000	0000	0000	0000	0000	0000	0000	0000	0000	0000
U @ 17.5 CM(W/CM-K)		0000	0000	0000	0000	0000	0000	0000	0000	0000	0000
U @ 18.0 CM(W/CM-K)		0000	0000	0000	0000	0000	0000	0000	0000	0000	0000
U @ 18.5 CM(W/CM-K)		0000	0000	0000	0000	0000	0000	0000	0000	0000	0000
U @ 19.0 CM(W/CM-K)		0000	0000	0000	0000	0000	0000	0000	0000	0000	0000
U @ 19.5 CM(W/CM-K)		0000	0000	0000	0000	0000	0000	0000	0000	0000	0000
U @ 20.0 CM(W/CM-K)		0000	0000	0000	0000	0000	0000	0000	0000	0000	0000
U @ 20.5 CM(W/CM-K)		0000	0000	0000	0000	0000	0000	0000	0000	0000	0000
U @ 21.0 CM(W/CM-K)		0000	0000	0000	0000	0000	0000	0000	0000	0000	0000
U @ 21.5 CM(W/CM-K)		0000	0000	0000	0000	0000	0000	0000	0000	0000	0000
U @ 22.0 CM(W/CM-K)		0000	0000	0000	0000	0000	0000	0000	0000	0000	0000
U @ 22.5 CM(W/CM-K)		0000	0000	0000	0000	0000	0000	0000	0000	0000	0000
U @ 23.0 CM(W/CM-K)		0000	0000	0000	0000	0000	0000	0000	0000	0000	0000
U @ 23.5 CM(W/CM-K)		0000	0000	0000	0000	0000	0000	0000	0000	0000	0000
U @ 24.0 CM(W/CM-K)		0000	0000	0000	0000	0000	0000	0000	0000	0000	0000

ORIGINAL PAGE IS
 OF POOR QUALITY

ROCKET FUEL DEPOSIT TEST PROGRAM (COMMERCIAL C3H8 FUEL)
 RUN 5 JANUARY 13, 1983

TIME	(UNIT)	0.0000	1.050	2.050	3.050	4.050	5.050	6.050	7.067	8.050	9.050	10.05
IN OUT	CM (K)	621.5	585.1	577.6	573.4	577.0	577.0	576.4	574.3	569.7	563.0	543.0
IN OUT	CM (K)	624.8	588.4	580.9	567.6	572.0	570.4	575.9	573.2	570.4	563.2	543.0
IN OUT	CM (K)	574.8	569.8	566.5	564.3	570.9	575.4	583.8	582.0	577.9	570.4	563.0
IN OUT	CM (K)	576.3	578.2	580.5	588.7	595.4	597.0	593.7	592.6	585.4	579.3	563.0
IN OUT	CM (K)	589.3	582.0	592.6	590.4	594.8	597.8	603.9	603.2	595.4	587.3	577.6
IN OUT	CM (K)	613.7	623.7	623.4	620.4	644.8	637.0	630.2	630.9	607.6	600.4	577.6
IN OUT	CM (K)	628.7	605.9	623.7	620.4	615.4	637.0	630.2	641.5	623.2	619.3	600.4
IN OUT	CM (K)	626.5	665.9	632.0	633.3	647.8	644.8	630.4	663.0	658.0	649.3	628.7
IN IN	CM (K)	624.2	536.7	529.0	525.3	529.1	529.7	530.8	526.4	513.3	507.0	504.8
IN IN	CM (K)	525.3	540.0	537.9	537.0	549.1	539.1	542.0	539.7	527.3	520.9	518.8
IN IN	CM (K)	527.5	521.7	522.4	519.2	524.6	524.0	523.0	525.3	513.3	508.1	507.1
IN IN	CM (K)	529.2	529.5	527.9	524.9	547.4	543.0	546.9	544.7	531.2	525.1	522.9
IN IN	CM (K)	545.3	539.5	544.0	540.0	549.1	546.9	551.3	548.0	539.5	535.2	532.5
IN IN	CM (K)	545.3	533.3	544.6	536.4	546.9	548.0	551.4	555.3	540.2	535.2	532.7
IN IN	CM (K)	581.4	575.0	576.8	572.0	567.4	582.9	593.0	583.0	570.6	574.0	558.4
IN IN	CM (K)	629.2	572.2	576.8	585.3	567.4	582.9	593.0	583.0	570.6	574.0	558.4
FULL INLET TEMP	(MPA)	14.05	13.81	13.71	13.57	13.44	13.15	13.07	12.92	12.78	12.65	12.51
FULL INLET TEMP	(MPA)	10.04	8.499	8.011	7.029	7.784	7.162	7.981	7.83.7	7.749	7.660	7.557
FULL INLET TEMP	(MPA)	285.9	285.4	285.4	285.4	285.4	283.7	283.7	283.7	283.7	283.7	283.7
FULL INLET TEMP	(MPA)	418.2	408.7	409.8	407.0	403.7	403.7	412.6	418.7	411.5	409.8	413.7
FLOW RATE	(KG/S)	.8995	.9700	.9347	.9070	.8453	.7962	.7395	.7118	.7155	.6992	.6778
VOLTAGE	(VOLTS)	4955.	5200.	5218.	5213.	5181.	5168.	5172.	5186.	5169.	5112.	5079.
POWER	(KW)	37.25	38.37	38.27	38.13	37.293	37.278	37.305	37.276	36.080	35.52	35.38
HEAT FLUX	(W/CM ²)	2387.	2459.	2452.	2444.	2421.	2420.	2421.	2418.	2345.	2276.	2267.
INLET FUEL VLL	(M/S)	55.95	60.27	58.07	56.35	52.52	49.29	45.78	44.06	44.24	43.23	41.91
FUELV BALANCE	(PCT)	-6.740	-10.54	-11.63	-17.21	-24.73	-24.21	-27.24	-25.74	-27.83	-28.51	-27.7.

ORIGINAL PAGE IS
 OF POOR QUALITY

ROCKET FUEL DEPOSIT TEST PROGRAM (COMMERCIAL C3H8 FUEL)
 RUN JANUARY 13, 1983

TIME	(MIN)	0.000	1.050	2.050	3.050	4.050	5.050	6.050	7.050	8.050	9.050	10.05
INLE	1	MEYNOLUS	NO									
AVG	1.5	FRICTION	FAC	10.33	10.33	10.33	10.33	10.33	10.33	10.33	10.33	10.33
U	3.8	CM	(M/CM2-K)	10.49	10.49	10.49	10.49	10.49	10.49	10.49	10.49	10.49
U	6.4	CM	(M/CM2-K)	11.91	11.91	11.91	11.91	11.91	11.91	11.91	11.91	11.91
U	8.9	CM	(M/CM2-K)	12.26	12.26	12.26	12.26	12.26	12.26	12.26	12.26	12.26
U	11.4	CM	(M/CM2-K)	13.04	13.04	13.04	13.04	13.04	13.04	13.04	13.04	13.04
U	14.0	CM	(M/CM2-K)	13.20	13.20	13.20	13.20	13.20	13.20	13.20	13.20	13.20
U	16.5	CM	(M/CM2-K)	14.67	14.67	14.67	14.67	14.67	14.67	14.67	14.67	14.67
U	19.1	CM	(M/CM2-K)	14.72	14.72	14.72	14.72	14.72	14.72	14.72	14.72	14.72
U	21.6	CM	(M/CM2-K)	11.45	11.45	11.45	11.45	11.45	11.45	11.45	11.45	11.45
U	24.1	CM	(M/CM2-K)	0.000	0.000	0.000	0.000	0.000	0.000	0.000	0.000	0.000
I/K	3.8	CM	(K-CM2/M)	0.000	0.000	0.000	0.000	0.000	0.000	0.000	0.000	0.000
I/K	6.4	CM	(K-CM2/M)	0.000	0.000	0.000	0.000	0.000	0.000	0.000	0.000	0.000
I/K	8.9	CM	(K-CM2/M)	0.000	0.000	0.000	0.000	0.000	0.000	0.000	0.000	0.000
I/K	11.4	CM	(K-CM2/M)	0.000	0.000	0.000	0.000	0.000	0.000	0.000	0.000	0.000
I/K	14.0	CM	(K-CM2/M)	0.000	0.000	0.000	0.000	0.000	0.000	0.000	0.000	0.000
I/K	16.5	CM	(K-CM2/M)	0.000	0.000	0.000	0.000	0.000	0.000	0.000	0.000	0.000
I/K	19.1	CM	(K-CM2/M)	0.000	0.000	0.000	0.000	0.000	0.000	0.000	0.000	0.000
I/K	21.6	CM	(K-CM2/M)	0.000	0.000	0.000	0.000	0.000	0.000	0.000	0.000	0.000
I/K	24.1	CM	(K-CM2/M)	0.000	0.000	0.000	0.000	0.000	0.000	0.000	0.000	0.000
M	1.5	CM	(K-CM2/M)	0.000	0.000	0.000	0.000	0.000	0.000	0.000	0.000	0.000
M	3.8	CM	(K-CM2/M)	0.000	0.000	0.000	0.000	0.000	0.000	0.000	0.000	0.000
M	6.4	CM	(K-CM2/M)	0.000	0.000	0.000	0.000	0.000	0.000	0.000	0.000	0.000
M	8.9	CM	(K-CM2/M)	0.000	0.000	0.000	0.000	0.000	0.000	0.000	0.000	0.000
M	11.4	CM	(K-CM2/M)	0.000	0.000	0.000	0.000	0.000	0.000	0.000	0.000	0.000
M	14.0	CM	(K-CM2/M)	0.000	0.000	0.000	0.000	0.000	0.000	0.000	0.000	0.000
M	16.5	CM	(K-CM2/M)	0.000	0.000	0.000	0.000	0.000	0.000	0.000	0.000	0.000
M	19.1	CM	(K-CM2/M)	0.000	0.000	0.000	0.000	0.000	0.000	0.000	0.000	0.000
M	21.6	CM	(K-CM2/M)	0.000	0.000	0.000	0.000	0.000	0.000	0.000	0.000	0.000
M	24.1	CM	(K-CM2/M)	0.000	0.000	0.000	0.000	0.000	0.000	0.000	0.000	0.000

ORIGINAL PAGE IS
 OF POOR QUALITY

ROCKET FUEL DEPOSIT TEST PROGRAM (COMMERCIAL C3HR FUEL)
 RUN 6 JANUARY 21, 1983

TIME	(MIN)	0.000	1.000	2.000	3.000	4.000	4.500	5.500	6.000	7.000	8.000	9.000
INLET VELOCITY NO		3025+006	3203+006	3205+006	3181+006	3167+006	3153+006	3238+006	3181+006	3181+006	3167+006	3136+006
AVG PARTICULATION (ACTOR)		4521+002	4442+002	4411+002	4384+002	4359+002	4307+002	4256+002	4558+002	4552+002	4710+002	5077+002
U 1.3 CM(W/LM-Z-K)		6.104	6.126	6.449	6.446	6.444	6.424	6.247	6.360	6.354	5.989	7.248
U 3.8 CM(W/LM-Z-K)		6.042	6.212	6.359	6.357	6.414	6.438	7.247	7.190	7.251	7.220	6.948
U 6.4 CM(W/LM-Z-K)		5.862	6.204	6.310	6.349	6.348	6.331	6.226	6.948	6.894	6.894	6.352
U 8.9 CM(W/LM-Z-K)		5.280	5.571	5.719	5.815	5.866	5.901	6.244	6.298	6.301	6.301	6.063
U 11.4 CM(W/LM-Z-K)		4.967	5.432	5.586	5.711	5.744	5.844	6.277	6.130	6.144	6.088	6.593
U 14.0 CM(W/LM-Z-K)		5.011	5.477	5.719	5.920	5.983	6.060	6.370	6.380	6.463	6.423	6.226
U 16.5 CM(W/LM-Z-K)		4.933	5.479	5.719	6.024	6.026	6.250	6.288	6.316	6.409	6.389	6.226
U 19.1 CM(W/LM-Z-K)		5.508	6.051	6.223	6.450	6.521	6.442	6.730	6.794	6.752	6.539	6.493
U 21.6 CM(W/LM-Z-K)		6.021	6.526	6.290	6.442	6.473	6.436	6.733	6.755	6.721	6.498	6.493
I/K 1.3 CM(K-LM-Z/W)		0.000	0.000	0.000	0.000	0.000	0.000	0.000	0.000	0.000	0.000	0.197
I/K 3.8 CM(K-LM-Z/W)		0.000	0.000	0.000	0.000	0.000	0.000	0.000	0.000	0.000	0.000	1.106-001
I/K 6.4 CM(K-LM-Z/W)		0.000	0.000	0.000	0.000	0.000	0.000	0.000	0.000	0.000	0.000	0.000
I/K 8.9 CM(K-LM-Z/W)		0.000	0.000	0.000	0.000	0.000	0.000	0.000	0.000	0.000	0.000	0.000
I/K 11.4 CM(K-LM-Z/W)		0.000	0.000	0.000	0.000	0.000	0.000	0.000	0.000	0.000	0.000	0.000
I/K 14.0 CM(K-LM-Z/W)		0.000	0.000	0.000	0.000	0.000	0.000	0.000	0.000	0.000	0.000	0.000
I/K 16.5 CM(K-LM-Z/W)		0.000	0.000	0.000	0.000	0.000	0.000	0.000	0.000	0.000	0.000	0.000
I/K 19.1 CM(K-LM-Z/W)		0.000	0.000	0.000	0.000	0.000	0.000	0.000	0.000	0.000	0.000	0.000
I/K 21.6 CM(K-LM-Z/W)		0.000	0.000	0.000	0.000	0.000	0.000	0.000	0.000	0.000	0.000	0.000
KC 1.3 CM(K-LM-Z/J)		0.000	0.000	0.000	0.000	0.000	0.000	0.000	0.000	0.000	0.000	0.000
KC 3.8 CM(K-LM-Z/J)		0.000	0.000	0.000	0.000	0.000	0.000	0.000	0.000	0.000	0.000	0.000
KC 6.4 CM(K-LM-Z/J)		0.000	0.000	0.000	0.000	0.000	0.000	0.000	0.000	0.000	0.000	0.000
KC 8.9 CM(K-LM-Z/J)		0.000	0.000	0.000	0.000	0.000	0.000	0.000	0.000	0.000	0.000	0.000
KC 11.4 CM(K-LM-Z/J)		0.000	0.000	0.000	0.000	0.000	0.000	0.000	0.000	0.000	0.000	0.000
KC 14.0 CM(K-LM-Z/J)		0.000	0.000	0.000	0.000	0.000	0.000	0.000	0.000	0.000	0.000	0.000
KC 16.5 CM(K-LM-Z/J)		0.000	0.000	0.000	0.000	0.000	0.000	0.000	0.000	0.000	0.000	0.000
KC 19.1 CM(K-LM-Z/J)		0.000	0.000	0.000	0.000	0.000	0.000	0.000	0.000	0.000	0.000	0.000
KC 21.6 CM(K-LM-Z/J)		0.000	0.000	0.000	0.000	0.000	0.000	0.000	0.000	0.000	0.000	0.000
KC 24.1 CM(K-LM-Z/J)		0.000	0.000	0.000	0.000	0.000	0.000	0.000	0.000	0.000	0.000	0.000

ORIGINAL PAGE IS
 OF POOR QUALITY

ROCKET FUEL DEPOSIT TEST PROGRAM (COMMERCIAL C3H8 FUEL)
 RUN JANUARY 25, 1983

TIME	(MIN)	000U	1.000	2.000	3.000	4.000	5.000	6.000	7.000	8.000	9.000	10.50
IN OUT	1.5	449.8	452.0	452.6	454.8	461.2	461.5	452.9	448.2	449.8	464.3	460.6
IN OUT	3.5	436.5	438.2	438.2	439.6	438.2	447.0	449.8	449.3	443.9	468.7	464.3
IN OUT	5.5	430.7	442.8	442.8	454.8	451.5	453.2	449.8	457.0	472.6	479.8	480.4
IN OUT	7.5	447.0	462.6	462.6	469.8	465.9	470.9	475.4	477.9	489.8	482.6	486.5
IN OUT	9.5	455.7	474.3	474.3	487.6	481.5	479.8	485.9	485.9	517.0	525.9	491.5
IN OUT	11.5	487.6	509.6	509.6	518.7	507.6	519.3	528.9	529.3	517.0	535.4	525.7
IN OUT	13.5	517.0	536.5	536.5	540.9	534.8	538.2	550.9	549.9	522.6	535.4	538.7
IN OUT	15.5	709.3	748.2	748.2	618.2	610.2	613.2	614.3	614.8	712.6	628.7	608.7
IN IN	17.5	431.6	434.2	434.2	436.3	443.2	438.2	437.5	429.9	426.6	446.3	418.7
IN IN	19.5	418.3	414.8	414.8	413.3	419.5	423.7	425.8	422.0	421.1	416.3	442.4
IN IN	21.5	412.7	424.2	424.2	429.0	426.5	428.7	431.4	431.0	426.1	410.8	449.6
IN IN	23.5	428.8	431.2	431.2	436.3	433.2	434.9	439.1	438.8	426.1	450.8	446.2
IN IN	25.5	437.7	444.2	444.2	451.3	447.6	452.6	456.9	459.3	471.6	461.7	462.4
IN IN	27.5	465.4	455.9	455.9	462.9	458.2	461.5	467.5	467.6	463.3	469.1	473.5
IN IN	29.5	498.8	491.5	491.5	500.1	489.3	501.9	510.2	511.0	498.9	508.0	507.4
IN IN	31.5	575.5	518.1	518.1	542.4	516.5	519.9	532.5	531.0	504.4	517.4	520.7
IN IN	33.5	691.1	729.8	729.8	599.6	592.1	566.0	595.8	596.5	550.4	595.2	590.7
FUEL INLET P		7.455	7.442	7.442	7.442	7.442	7.442	7.442	7.442	7.255	7.268	7.280
FUEL INLET TEMP		6.510	6.482	6.482	6.489	6.477	6.469	6.470	6.461	6.273	6.285	6.305
FUEL INLET TEMP		286.5	287.0	287.0	286.5	286.5	286.5	287.0	287.0	284.8	287.8	285.8
FUEL RATE		383.2	383.2	383.2	383.2	382.6	381.5	382.0	382.0	380.4	379.3	379.8
CURRENT		4699-U01	4699-U01	4699-U01	4699-U01	4699-U01	4699-U01	4699-U01	4699-U01	4699-U01	4699-U01	4699-U01
VOLTAGE		3199.9	3208.0	3208.0	3225.5	3184.4	3184.4	3188.8	3175.5	3161.8	3156.8	3153.3
POWER		4.486	4.511	4.511	4.535	4.534	4.527	4.563	4.540	4.530	4.580	4.504
INLET FUEL VEL		14.35	14.47	14.47	14.63	14.52	14.42	14.55	14.42	14.32	14.14	14.20
INLET FUEL VEL		928.9	927.3	927.3	937.7	925.2	923.7	932.7	923.7	917.7	905.9	909.8
INLET FUEL VEL		30.51	29.99	29.99	29.99	29.86	29.94	29.99	29.99	29.82	29.98	30.02
INLET FUEL VEL		4.411	4.445	4.445	4.450	4.406	4.268	4.593	4.834	4.608	4.976	4.602

ORIGINAL PAGE IS
 OF POOR QUALITY

ROCKET FUEL DEPOSIT TEST PROGRAM (COMMERCIAL C3H8 FUEL)
 RUN JANUARY 25, 1983

TIME	(MIN)	1.000	2.000	3.000	4.000	5.000	6.000	7.000	8.000	9.000	10.50
INLET REYNOLDS NO		2859+006	2799+006	2823+006	2799+006	2806+006	2822+006	2822+006	2759+006	2774+006	2789+006
AVG FRICTION FACTOR		6.551-002	6.823-002	6.490-002	6.655-002	6.540-002	6.691-002	6.691-002	6.527-002	6.952-002	6.881-002
U 0	1.3	7.819	7.838	7.824	7.978	7.544	7.613	7.613	7.684	7.684	5.976
U 0	3.8	8.009	8.196	7.945	7.978	7.795	7.987	7.987	7.819	7.819	6.065
U 0	6.4	8.387	8.372	8.110	8.186	8.025	7.732	7.732	7.740	7.740	6.322
U 0	8.9	8.576	8.372	8.110	8.186	8.025	7.732	7.732	7.381	7.381	6.472
U 0	11.4	8.463	8.140	7.746	7.850	7.486	7.334	7.334	6.288	6.288	6.884
U 0	14.0	8.353	8.140	7.619	7.728	7.524	7.273	7.198	6.041	6.041	5.666
U 0	16.5	6.641	6.534	6.222	6.554	6.549	5.774	5.696	4.990	4.990	5.532
U 0	19.1	5.680	5.433	5.115	5.859	5.849	5.252	5.350	4.214	4.214	4.034
U 0	21.6	4.755	4.717	4.060	4.833	4.849	4.389	4.019	3.879	3.879	4.034
U 0	24.1	2.535	2.639	3.255	4.263	3.800	3.900	4.214	2.000	2.000	4.034
1/A 0	1.3	5.991-003	8.723-003	16.179-002	11.948-003	11.803-001	13.006-002	13.006-002	16.374-002	22.469-002	37.000-001
1/A 0	3.8	0.000	0.000	0.000	6.433-001	4.666-001	5.068-001	3.971-001	4.974-001	4.554-001	3.920-001
1/A 0	6.4	7.657-002	10.44-001	14.28-001	13.77-001	16.71-001	17.75-001	18.52-001	16.32-001	15.54-001	14.40-001
1/A 0	8.9	6.838-002	9.675-002	13.58-001	12.80-001	14.45-001	17.71-001	18.47-001	18.59-001	19.19-001	18.40-001
1/A 0	11.4	9.601-002	14.30-001	20.50-001	18.83-001	2.502-001	2.780-001	3.164-001	3.815-001	4.304-001	4.595-001
1/A 0	14.0	1.176-001	1.712-001	2.330-001	2.049-001	2.896-001	2.953-001	3.098-001	2.927-001	3.813-001	4.137-001
1/A 0	16.5	1.846-001	2.093-001	2.866-001	1.953-001	2.496-001	4.107-001	4.345-001	3.343-001	4.647-001	4.937-001
1/A 0	19.1	2.219-002	0.000	4.164-001	1.682-001	2.163-001	3.297-001	3.307-001	7.329-001	2.472-001	2.690-001
1/A 0	21.6	8.059-001	0.000	1.935-001	1.500-001	0.000	1.762-001	2.186-001	0.000	2.706-001	2.036-001
1/A 0	24.1	8.441-001	3.661-001	0.000	0.000	0.000	0.000	0.000	0.000	0.000	0.000
1/C 0	1.3	2.987-004	2.496-004	1.964-004	5.254-004	4.210-004	1.921-004	0.000	0.000	2.953-004	1.841-004
1/C 0	3.8	0.000	1.498-004	1.976-004	7.505-005	1.804-004	2.317-004	0.000	6.306-005	0.000	5.815-004
1/C 0	6.4	1.595-003	1.048-003	9.879-004	6.254-004	5.813-004	5.228-004	4.725-004	7.722-004	7.722-004	7.268-004
1/C 0	8.9	1.993-003	9.984-004	9.550-004	8.254-004	5.242-004	5.042-004	4.725-004	7.693-004	8.404-004	6.881-004
1/C 0	11.4	3.580-003	1.647-003	1.515-003	8.506-004	2.650-004	8.942-004	7.976-004	9.711-004	7.268-004	6.202-004
1/C 0	14.0	4.286-003	1.997-003	1.844-003	9.257-004	8.650-004	8.359-003	7.976-004	5.801-004	6.350-004	6.590-004
1/C 0	16.5	0.000	1.747-003	2.601-003	8.006-004	1.143-003	1.255-003	1.074-003	6.684-004	7.656-004	6.590-004
1/C 0	19.1	2.093-003	0.000	1.449-003	7.505-004	0.000	1.015-004	6.305-004	1.261-004	3.948-004	3.780-004
1/C 0	21.6	1.505-002	3.494-003	0.000	0.000	0.000	0.000	5.728-004	0.000	0.000	0.000
1/C 0	24.1	0.000	0.000	0.000	0.000	0.000	0.000	0.000	7.567-005	0.000	0.000

ORIGINAL PAGE IS
 OF POOR QUALITY

ROCKET FUEL DEPOSIT TEST PROGRAM (COMMERCIAL C3H8 FUEL)
 RUN JANUARY 25, 1983

TIME	(PIM)	11.00	12.00	13.00	14.00	15.00	16.00	17.00	18.00	19.00	20.00	21.00
IN OUT		318.27	307.9	319.2	317.0	317.0	316.2	317.0	315.4	316.7	316.0	317.6
IN OUT		330.4	318.2	332.4	318.0	333.7	319.3	335.4	332.6	336.5	335.4	337.4
IN OUT		583.7	568.2	592.5	578.8	593.2	582.0	594.3	588.2	597.0	595.9	603.7
IN OUT		603.7	587.3	622.9	619.3	622.0	619.8	622.0	616.5	617.6	614.8	621.3
IN OUT		607.0	608.2	627.0	625.4	633.7	623.0	633.7	615.4	617.6	614.8	621.3
IN IN		594.3	596.5	603.4	607.6	603.7	605.5	603.3	603.7	605.9	604.3	609.8
IN IN		493.7	483.1	494.8	492.9	491.7	491.7	492.2	490.6	494.1	493.2	493.2
IN IN		505.9	506.4	510.6	509.6	508.0	509.4	510.6	507.9	511.9	510.0	510.4
IN IN		257.2	262.6	271.7	269.6	267.5	268.3	271.7	267.9	264.7	261.5	263.9
IN IN		281.2	282.6	291.5	289.2	287.1	288.1	291.5	288.8	289.0	289.4	289.8
IN IN		282.6	284.2	296.2	294.9	295.2	296.0	297.2	294.5	293.0	290.4	293.9
IN IN		13.61	12.95	12.24	13.31	13.35	13.24	13.44	13.46	13.02	13.01	13.07
FUEL INLET TEMP	(MPA)	12.50	12.22	12.22	12.22	12.22	12.24	12.33	12.28	12.93	13.01	13.07
FUEL INLET TEMP	(MPA)	289.3	289.3	289.3	288.2	288.2	288.2	289.2	288.2	289.7	288.2	288.2
FUEL INLET TEMP	(MPA)	418.2	417.0	417.0	417.0	417.0	417.0	417.0	415.9	417.6	417.6	417.6
FUEL INLET TEMP	(MPA)	507.7	508.4	507.7	507.7	508.4	512.7	510.2	515.9	505.2	507.7	506.4
FUEL INLET TEMP	(MPA)	367.0	369.4	367.0	369.4	369.4	368.5	367.0	366.4	364.9	364.2	363.8
VOLTAGE	(VOLTS)	5.314	5.309	5.314	5.314	5.314	5.338	5.329	5.320	5.303	5.287	5.290
HEAT FLUX	(W/M ²)	19.26	19.26	19.26	19.26	19.26	19.57	19.54	19.49	19.35	19.26	19.23
INLET FLOW VEL	(M/S)	1235	1235	1250	1244	1237	1254	1252	1249	1240	1234	1233
INLET FLOW VEL	(M/S)	31.81	31.65	31.73	31.73	31.65	31.89	31.89	31.65	31.61	31.73	31.65
ENERGY BALANCE	(PCT)	-1.474	-1.194	-1.334	-1.171	-1.171	-1.205	-1.623	-3.132	-1.478	-3.179	-3.155

← CYCLE 7 →

← CYCLE 6 →

← CYCLE 5 →

ORIGINAL PAGE IS
 OF POOR QUALITY

ORIGINAL PAGE
OF POOR QUALITY

ROCKET FUEL DEPOSIT TEST PROGRAM (COMMERCIAL C3HB FUEL)
RUN 8 JANUARY 25, 1983

TIME	(MIN)	22.00	23.00	24.00
IN OUT	LM (K)	499.3	494.1	493.2
IN OUT	LM (K)	519.0	513.8	512.6
IN OUT	LM (K)	537.0	529.8	526.7
IN OUT	LM (K)	587.0	576.5	574.5
IN OUT	LM (K)	616.7	609.9	603.7
IN OUT	LM (K)	619.8	607.0	603.4
IN OUT	LM (K)	636.5	623.9	620.5
IN OUT	LM (K)	611.5	603.2	600.3
IN IN	LM (K)	474.5	470.0	468.8
IN IN	LM (K)	495.1	489.4	488.2
IN IN	LM (K)	512.3	505.5	504.3
IN IN	LM (K)	542.3	533.3	532.1
IN IN	LM (K)	562.8	552.7	550.5
IN IN	LM (K)	593.9	581.6	579.3
IN IN	LM (K)	595.1	582.7	581.0
IN IN	LM (K)	611.7	601.6	602.1
IN IN	LM (K)	586.7	578.8	577.9
FUEL INLET	(MPA)	14.30	14.12	14.41
FUEL EXIT	(MPA)	13.22	13.24	13.26
FUEL INLET TEMP	(K)	285.9	285.9	285.9
FUEL EXIT TEMP	(K)	417.6	414.3	414.3
FLOW RATE	(KG/S)	5064-001	5127-001	5127-001
CURRENT	(AMPS)	3651	3640	3651
VOLTAGE	(VOLTS)	5.37	5.261	5.260
POWER	(KW)	19.52	19.15	19.20
FUEL FLUX	(G/LPZ)	1251.	1227.	1231.
INLET FUEL VEL	(M/S)	31.50	31.89	31.89
EXHAUST MALAISE	(PCT)	-0.2924	-0.3383	-0.6004



ROCKET FUEL DEPOSIT TEST PROGRAM (COMMERCIAL C3H8 FUEL)
 RUN 8 JANUARY 25, 1983

TIME	(MIN)	0.000	1.000	2.000	3.000	4.000	5.000	6.000	7.000	8.000	9.000	10.00
INLET METHOLUS NO		.3104*006	.3096*006	.3081*006	.3066*006	.3066*006	.3066*006	.3086*006	.3146*006	.3120*006	.3104*006	.3212*006
AVG THICKEN FACTOR		.6192-002	.6083-002	.6007-002	.5905-002	.5679-002	.5905-002	.6079-002	.6120-002	.6142-002	.6106-002	.6466-002
U 0 1.3 CM1W/LM2-R)		5.794	6.161	6.669	6.379	6.376	6.428	6.379	6.560	6.025	6.123	6.195
U 0 3.8 CM1W/LM2-R)		6.813	6.308	6.532	6.539	6.631	6.706	6.379	6.708	6.454	6.440	6.831
U 0 6.4 CM1W/LM2-R)		6.714	6.459	6.525	6.533	6.631	6.629	6.379	6.340	6.618	6.503	6.907
U 0 11.4 CM1W/LM2-R)		5.824	5.905	6.079	6.006	6.281	6.324	6.405	6.401	6.340	6.285	6.625
U 0 14.0 CM1W/LM2-R)		5.824	6.055	6.120	6.164	6.196	6.254	6.332	5.984	6.158	6.138	6.482
U 0 16.5 CM1W/LM2-R)		5.757	6.487	6.544	6.617	6.455	6.516	6.564	5.424	5.830	5.294	6.257
U 0 19.1 CM1W/LM2-R)		6.223	7.123	7.241	7.382	7.108	7.182	7.173	6.980	6.833	6.785	6.761
U 0 21.6 CM1W/LM2-R)		7.065	6.664	7.318	6.948	7.554	7.354	7.615	7.508	7.223	7.168	7.119
U 0 24.1 CM1W/LM2-R)		6.825	6.776-301	4.158-001	2.714-001	3.481-002	.0000	.0000	.0000	.0000	.0000	.0000
I/A 0 1.3 CM1A-LM2/W)		.0000	.1175-001	1.113-001	1.004-001	1.004-001	.8778-002	.6302-002	.5651-002	.8167-002	.8484-002	.0000
I/A 0 3.8 CM1A-LM2/W)		.0000	.5879-002	4.310-002	3.953-002	1.853-002	1.622-003	.0000	.0000	.2144-002	.2490-002	.0000
I/A 0 6.4 CM1A-LM2/W)		.0000	.1180-003	.0000	.0000	.0000	.0000	.0000	.0000	.0000	.0000	.0000
I/A 0 11.4 CM1A-LM2/W)		.0000	.0000	.0000	.0000	.0000	.0000	.0000	.0000	.0000	.0000	.0000
I/A 0 16.5 CM1A-LM2/W)		.0000	.0000	.0000	.0000	.0000	.0000	.0000	.0000	.0000	.0000	.0000
I/A 0 19.1 CM1A-LM2/W)		.0000	.0000	.0000	.0000	.0000	.0000	.0000	.0000	.0000	.0000	.0000
I/A 0 21.6 CM1A-LM2/W)		.0000	.0000	.0000	.0000	.0000	.0000	.0000	.0000	.0000	.0000	.0000
I/A 0 24.1 CM1A-LM2/W)		.0000	.1427-002	.0000	.0000	.0000	.0000	.2167-003	.0000	.0000	.0000	.0000
MC 0 1.3 CM1A-LM2/J)		.0000	.1089-002	.3273-003	.1416-003	.5707-005	.0000	.0000	.0000	.0000	.0000	.0000
MC 0 3.8 CM1A-LM2/J)		.0000	.1599-003	.7611-004	.4815-004	.3421-004	.2135-004	.0000	.2133-004	.7241-004	.1918-004	.2986-005
MC 0 6.4 CM1A-LM2/J)		.0000	.6091-004	.1903-004	.1517-004	.0000	.0000	.0000	.8527-005	.1028-004	.8340-005	.0000
MC 0 11.4 CM1A-LM2/J)		.0000	.0000	.0000	.0000	.0000	.0000	.0000	.0000	.0000	.0000	.0000
MC 0 16.5 CM1A-LM2/J)		.0000	.0000	.0000	.0000	.0000	.0000	.0000	.0000	.0000	.0000	.0000
MC 0 19.1 CM1A-LM2/J)		.0000	.0000	.0000	.0000	.0000	.0000	.0000	.0000	.0000	.0000	.0000
MC 0 21.6 CM1A-LM2/J)		.0000	.0000	.0000	.0000	.0000	.0000	.0000	.0000	.0000	.0000	.0000
MC 0 24.1 CM1A-LM2/J)		.0000	.1523-004	.0000	.0000	.0000	.0000	.0000	.0000	.0000	.0000	.0000



ORIGINAL PAGE IS
 OF POOR QUALITY

ORIGINAL PAGE IS
OF POOR QUALITY

ROCKET FUEL DEPOSIT TEST PROGRAM (COMMERCIAL C3H8 FUEL)
RUN 9 JANUARY 28, 1985

TIME	(MIN)	0.000	1.000	2.000	3.000	4.000	5.000	6.000	7.000	8.000	9.000	10.00
IN OUT	3.8	573.5	573.0	573.6	569.3	569.8	569.3	568.7	567.9	570.4	568.3	568.7
IN OUT	6.4	620.9	620.3	603.8	601.5	611.5	601.5	597.8	605.5	603.6	601.5	601.6
IN OUT	14.4	625.4	624.3	621.5	615.7	619.8	615.9	607.0	600.4	600.4	597.4	600.9
IN OUT	16.5	666.5	666.5	645.9	630.4	645.9	615.4	608.7	608.2	608.2	604.3	607.6
IN OUT	19.1	701.5	678.7	653.7	640.9	653.7	628.2	617.3	618.2	616.5	610.9	611.7
IN OUT	21.6	692.6	650.4	665.4	650.9	640.9	622.0	627.8	642.6	612.0	625.4	627.0
IN	24.1	690.9	640.6	682.4	660.9	654.8	639.3	629.8	630.9	629.8	625.4	627.0
IN	3.8	541.7	540.4	541.8	537.9	538.4	537.9	537.5	538.7	537.9	537.3	537.9
IN	6.4	572.8	572.0	588.2	570.5	570.0	570.1	566.6	568.0	571.9	570.3	571.6
IN	8.9	589.4	589.2	589.9	584.4	580.0	579.6	575.8	574.0	576.3	574.2	574.9
IN	11.4	633.0	614.3	614.3	598.8	588.4	584.6	577.5	569.1	569.1	563.9	570.0
IN	14.0	653.9	622.1	622.1	609.8	600.8	596.8	588.0	576.9	585.2	573.1	576.6
IN	16.5	670.0	646.0	646.0	632.7	622.3	620.7	611.4	611.3	610.8	605.9	607.7
IN	19.1	659.4	633.8	633.8	619.4	609.5	607.9	598.6	597.4	598.6	605.9	596.1
IN	21.6	661.1	651.0	651.0	629.5	623.4	627.9	625.6	637.4	643.6	628.1	628.5
FUEL INLET P	(MPA)	14.77	14.64	14.64	14.58	14.53	14.46	14.39	14.34	14.36	14.24	14.21
FUEL INLET T	(MPA)	14.08	13.98	13.98	13.79	13.83	13.79	13.71	13.66	13.60	13.54	13.49
FUEL INLET T	(MPA)	229.3	234.3	234.3	233.7	229.3	233.7	233.7	233.3	232.8	232.5	232.2
FUEL INLET T	(MPA)	398.7	398.2	398.2	399.3	396.3	399.3	397.0	399.3	398.7	398.5	398.2
FUEL INLET T	(MPA)	555.0	563.1	563.1	568.2	566.9	568.0	566.9	565.6	565.6	566.9	565.6
FUEL INLET T	(MPA)	3905.0	3950.6	3950.6	3946.0	3946.0	3935.0	3935.0	3935.0	3935.0	3935.0	3935.0
FUEL INLET T	(MPA)	6.320	6.306	6.306	6.303	6.279	6.271	6.271	6.270	6.268	6.242	6.238
FUEL INLET T	(MPA)	24.97	24.91	24.91	24.88	24.78	24.62	24.62	24.64	24.63	24.56	24.41
FUEL INLET T	(MPA)	1600.0	1596.0	1596.0	1594.0	1588.0	1584.0	1578.0	1578.0	1578.0	1574.0	1564.0
FUEL INLET T	(MPA)	31.91	31.45	31.45	31.55	31.63	31.80	31.75	31.84	31.77	31.75	31.77
FUEL INLET T	(MPA)	1.331	1.011	1.011	.8765	1.200	1.117	1.122	1.155	1.324	.9448	1.790

ROCKET FUEL DEPOSIT TEST PROGRAM (COMMERCIAL C3H8 FUEL)
 RUN 9 JANUARY 28, 1983

TIME	(MIN)	0.000	1.000	2.000	3.000	4.000	5.000	6.000	7.000	8.000	9.000	10.000
INLET REYNOLDS NO		1613+006	1957+006	1848+006	1948+006	1850+006	1940+006	1895+006	1952+006	1921+006	1895+006	1921+006
AVG FRICTION FACTOR		5.3892-002	5.3843-002	5.527-002	5.3729-002	5.3590-002	5.3644-002	5.3613-002	5.3717-002	5.37614-002	5.3606-002	5.3851-002
U @ 3.8 CM/W/CM2-K)		5.283	5.404	5.288	5.399	5.311	5.368	5.336	5.397	5.308	5.289	5.290
U @ 6.9 CM/W/CM2-K)		5.517	5.550	5.330	5.448	5.433	5.501	5.533	5.585	5.533	5.523	5.483
U @ 11.0 CM/W/CM2-K)		5.059	5.181	5.614	5.872	5.845	5.946	5.784	6.058	6.058	6.050	5.958
U @ 16.5 CM/W/CM2-K)		5.072	5.256	5.468	5.803	5.943	6.109	6.190	6.268	6.268	6.274	6.190
U @ 19.1 CM/W/CM2-K)		5.527	5.199	5.505	5.803	5.939	6.200	6.171	6.434	6.459	6.530	6.455
U @ 24.6 CM/W/CM2-K)		5.910	5.964	6.119	6.511	7.969	6.784	6.771	7.012	7.024	7.072	7.024
1/A @ 3.8 CM/W/CM2-M)		0.000	0.000	0.000	0.000	0.000	0.000	0.000	0.000	0.000	0.000	0.000
1/A @ 6.9 CM/W/CM2-M)		0.000	0.000	0.000	0.000	0.000	0.000	0.000	0.000	0.000	0.000	0.000
1/A @ 11.0 CM/W/CM2-M)		0.000	0.000	0.000	0.000	0.000	0.000	0.000	0.000	0.000	0.000	0.000
1/A @ 16.5 CM/W/CM2-M)		0.000	0.000	0.000	0.000	0.000	0.000	0.000	0.000	0.000	0.000	0.000
1/A @ 19.1 CM/W/CM2-M)		0.000	0.000	0.000	0.000	0.000	0.000	0.000	0.000	0.000	0.000	0.000
1/A @ 24.6 CM/W/CM2-M)		0.000	0.000	0.000	0.000	0.000	0.000	0.000	0.000	0.000	0.000	0.000
KL @ 3.8 CM/W/CM2-J)		0.000	0.000	0.000	0.000	0.000	0.000	0.000	0.000	0.000	0.000	0.000
KL @ 6.9 CM/W/CM2-J)		0.000	0.000	0.000	0.000	0.000	0.000	0.000	0.000	0.000	0.000	0.000
KL @ 11.0 CM/W/CM2-J)		0.000	0.000	0.000	0.000	0.000	0.000	0.000	0.000	0.000	0.000	0.000
KL @ 16.5 CM/W/CM2-J)		0.000	0.000	0.000	0.000	0.000	0.000	0.000	0.000	0.000	0.000	0.000
KL @ 19.1 CM/W/CM2-J)		0.000	0.000	0.000	0.000	0.000	0.000	0.000	0.000	0.000	0.000	0.000
KL @ 24.6 CM/W/CM2-J)		0.000	0.000	0.000	0.000	0.000	0.000	0.000	0.000	0.000	0.000	0.000
KL @ 24.6 CM/W/CM2-J)		0.000	0.000	0.000	0.000	0.000	0.000	0.000	0.000	0.000	0.000	0.000

ORIGINAL PAGE IS
 OF POOR QUALITY

ROCKET FUEL DEPOSIT TEST PROGRAM (COMMERCIAL C3H8 FUEL)
 RUN 10 JANUARY 28, 1983

TIME	(MIN)	0000	1.150	2.150	3.150	4.150	5.150	6.150	7.150	8.150	9.150	10.15
FM OUT	1.5	377.6	378.2	377.6	380.9	383.7	381.5	383.7	383.7	383.7	383.7	383.7
FM OUT	1.5	402.6	404.0	403.0	406.9	406.6	406.5	406.6	406.6	406.6	406.6	406.6
FM OUT	6.4	420.4	427.6	431.5	430.9	432.6	431.5	432.6	432.6	432.6	432.6	432.6
FM OUT	11.4	488.2	505.4	510.4	507.3	502.0	504.8	502.0	508.7	502.6	514.3	515.9
FM OUT	14.5	518.2	532.6	535.4	530.7	527.6	527.6	527.6	527.6	527.6	527.6	527.6
FM OUT	19.5	549.6	570.9	569.3	549.8	554.3	559.3	554.3	559.3	559.3	559.3	559.3
FM OUT	24.5	560.4	612.0	609.3	590.9	594.3	593.2	594.3	603.7	603.7	603.7	603.7
FM IN	1.5	613.7	705.9	679.6	653.2	639.8	649.3	639.8	639.8	645.9	642.0	635.2
FM IN	6.4	357.5	358.1	359.2	360.9	363.8	361.6	363.8	367.6	363.8	363.7	363.2
FM IN	11.4	400.3	407.5	411.9	386.5	387.7	411.6	387.7	415.4	388.2	388.2	388.2
FM IN	16.4	454.1	463.1	466.0	464.3	412.7	411.6	412.7	468.8	412.7	419.3	421.0
FM IN	21.4	468.0	465.3	460.3	467.1	458.8	465.0	458.8	468.8	468.8	469.3	471.0
FM IN	26.4	498.0	512.5	515.6	510.9	504.4	507.7	504.4	509.8	513.6	514.4	515.4
FM IN	31.4	529.7	542.5	535.6	529.6	522.1	525.5	522.1	537.9	531.6	534.8	535.6
FM IN	36.4	560.3	550.8	549.2	539.6	534.4	537.2	534.4	539.5	534.4	534.8	535.6
FM IN	41.4	593.6	685.8	689.2	633.2	614.4	629.4	614.4	619.8	625.4	621.0	619.0
FULL INLET P	TEMP	7.244	7.256	7.269	7.219	7.231	7.219	7.231	7.221	7.244	7.244	7.256
FULL INLET TEMP	(K)	233.7	231.5	230.9	229.8	230.9	230.9	230.9	231.5	231.5	231.5	231.5
FULL EXIT TEMP	(K)	343.2	343.2	343.7	341.5	342.0	342.0	341.5	343.2	343.2	343.2	343.2
FLOW RATE	(KG/S)	5505	5417	5417	5442	5442	5442	5442	5442	5442	5442	5442
LOW RATE	(KMP)	3498	3494	3494	3498	3494	3485	3485	3485	3485	3485	3485
VOLTAGE	(VOLTS)	4.533	4.534	4.532	4.532	4.532	4.532	4.532	4.532	4.532	4.532	4.532
PEAK FLUX	(W/CM ²)	15.84	15.84	15.84	15.75	15.68	15.65	15.68	15.74	15.74	15.74	15.74
INLET FUEL VEL	(M/S)	1015	1015	1015	1007	1003	1003	1003	1003	1003	1003	1003
ENERGY BALANCE	(%)	31.28	30.766	30.739	30.200	30.739	30.69	30.739	30.84	30.739	30.739	30.739
		-3.033	-2.766	-1.739	-2.200	-2.199	-2.080	-2.199	-1.884	-1.706	-2.649	-2.097

ORIGINAL PAGE IS
 OF POOR QUALITY

ROCKET FUEL DEPOSIT TEST PROGRAM (COMMERCIAL C3H8 FUEL)
 RUN 10
 JANUARY 28, 1963

TIME	(MIN)	0.000	1.150	2.150	3.150	4.150	5.150	6.150	7.150	8.150	9.150	10.15
IMPT		1888+006	1811+006	1789+006	180L+006	1786+006	1804+006	1797+006	1820+006	1794+006	1815+006	1846+006
AVG		4152-002	4168-002	4228-002	4244-002	4167-002	4202-002	4188-002	4247-002	4325-002	4365-002	4248-002
U 0	1.3	8.59J	7.437	8.357	8.277	8.04U	7.213	7.558	7.247	7.198	7.920	8.085
U 0	3.8	7.678	6.854	7.296	7.295	7.213	6.558	7.144	7.247	6.993	6.931	7.215
U 0	6.4	7.301	5.273	6.737	6.665	6.588	5.228	6.302	6.475	6.371	6.862	6.289
U 0	8.9	5.579	5.273	5.191	5.163	5.186	4.915	5.301	5.199	5.102	4.867	5.729
U 0	11.4	5.470	4.987	4.684	4.865	4.876	4.649	4.720	4.880	4.783	4.507	4.429
U 0	14.0	4.978	4.622	4.584	4.564	4.594	4.510	4.577	4.656	4.438	4.250	4.149
U 0	16.5	4.519	4.257	4.346	4.382	4.449	4.499	4.554	4.518	4.464	4.249	4.145
U 0	19.1	4.527	4.308	4.328	4.343	4.461	4.499	4.554	4.508	4.464	4.249	4.145
U 0	21.6	3.816	3.822	3.904	3.868	4.099	4.045	4.027	3.925	3.754	3.529	3.879
U 0	24.1	2.852	2.915	3.057	3.155	3.395	3.423	3.538	3.578	3.502	3.272	3.630
1/K 0	1.3	0.000	2.776-002	3.245-002	4.397-002	7.964-002	8.375-002	1.084-001	8.973-002	9.422-002	9.873-002	7.276-002
1/K 0	3.8	0.000	4.214-002	6.811-002	6.824-002	8.388-002	6.393-002	9.728-002	7.737-002	8.671-002	1.276-001	8.355-002
1/K 0	6.4	0.000	8.928-002	1.147-001	1.507-001	1.482-001	1.522-001	1.623-001	1.741-001	2.000-001	2.273-001	2.294-001
1/K 0	8.9	0.000	1.040-001	1.341-001	1.444-001	1.433-001	1.207-001	1.935-001	1.310-001	1.624-001	2.495-001	1.891-001
1/K 0	11.4	0.000	1.839-001	2.299-001	2.343-001	2.294-001	2.133-001	1.866-001	2.280-001	2.624-001	3.292-001	2.871-001
1/K 0	14.0	0.000	1.346-001	1.726-001	1.820-001	1.679-001	1.421-001	1.966-001	1.387-001	1.786-001	3.292-001	3.891-001
1/K 0	16.5	0.000	1.362-001	8.792-002	6.946-002	3.498-002	1.421-001	0.000	4.178-004	4.035-002	1.937-001	1.891-001
1/K 0	19.1	0.000	1.121-001	1.016-001	9.354-002	3.275-002	1.398-002	0.000	9.196-003	3.157-002	2.037-001	3.891-001
1/K 0	21.6	0.000	0.000	0.000	0.000	0.000	0.000	0.000	0.000	4.000	2.028-001	0.000
1/K 0	24.1	0.000	0.000	0.000	0.000	0.000	0.000	0.000	0.000	0.000	2.028-001	0.000
1/K 0	1.3	0.000	7.932-005	0.000	8.690-005	1.326-004	1.255-004	1.648-004	1.411-004	1.242-004	1.003-004	9.063-005
1/K 0	3.8	0.000	3.173-004	2.969-004	2.317-004	1.547-004	1.548-004	1.154-004	1.154-004	1.104-004	1.003-004	1.088-004
1/K 0	6.4	0.000	1.031-003	8.483-004	5.792-004	4.270-004	3.586-004	3.298-004	3.463-004	3.499-004	3.471-004	3.719-004
1/K 0	8.9	0.000	1.269-003	8.483-004	6.662-004	3.751-004	2.337-004	1.199-004	2.433-004	2.822-004	2.709-004	3.719-004
1/K 0	11.4	0.000	2.459-003	1.612-003	1.159-003	3.751-004	5.376-004	1.746-004	4.744-004	4.965-004	4.715-004	4.715-004
1/K 0	14.0	0.000	2.062-003	1.188-003	8.980-004	5.044-004	3.648-004	1.648-004	2.693-004	3.184-004	2.809-004	2.809-004
1/K 0	16.5	0.000	1.824-003	5.514-004	3.186-004	0.000	0.000	0.000	0.000	3.386-005	2.007-005	2.007-005
1/K 0	19.1	0.000	1.507-003	6.786-004	4.635-004	0.000	0.000	0.000	0.000	4.551-005	0.000	0.000
1/K 0	21.6	0.000	0.000	0.000	0.000	0.000	0.000	0.000	0.000	2.255-005	0.000	0.000
1/K 0	24.1	0.000	0.000	0.000	0.000	0.000	0.000	0.000	0.000	0.000	0.000	0.000

ORIGINAL PAGE 10
 OF POOR QUALITY

ORIGINAL PAGE IS
OF POOR QUALITY

HOCKET FULL DEPOSIT TEST PROGRAM (COMMERCIAL C3HR FUEL)
RUN 11
FEBRUARY 1, 1983

TIME	(MIN)	0000	1.083	2.083	3.083	4.083	5.083	6.083	7.083	8.083	9.083
IN	3	613.7	622.4	604.8	572.0	535.0	574.8	597.9	615.4	605.9	587.6
OUT	3	613.7	617.0	611.5	568.7	535.0	574.8	597.9	615.4	605.9	587.6
IN	3.8	601.5	595.9	589.3	555.4	522.5	545.4	555.0	571.5	579.3	565.4
OUT	3.8	601.5	595.9	589.3	555.4	522.5	545.4	555.0	571.5	579.3	565.4
IN	6.4	595.4	580.9	564.8	539.8	507.0	529.8	539.8	553.2	557.6	548.2
OUT	6.4	595.4	580.9	564.8	539.8	507.0	529.8	539.8	553.2	557.6	548.2
IN	11.4	629.6	603.9	540.4	530.4	533.4	555.4	524.8	555.4	565.4	560.2
OUT	11.4	629.6	603.9	540.4	530.4	533.4	555.4	524.8	555.4	565.4	560.2
IN	19.6	621.5	600.4	542.6	537.6	539.8	533.4	525.4	564.8	570.4	566.3
OUT	19.6	621.5	600.4	542.6	537.6	539.8	533.4	525.4	564.8	570.4	566.3
IN	24.1	582.4	577.5	552.1	540.6	504.5	523.5	534.8	568.8	570.4	566.3
OUT	24.1	582.4	577.5	552.1	540.6	504.5	523.5	534.8	568.8	570.4	566.3
IN	3.8	522.4	522.4	579.8	573.4	566.2	533.5	545.9	594.7	575.0	570.4
OUT	3.8	522.4	522.4	579.8	573.4	566.2	533.5	545.9	594.7	575.0	570.4
IN	6.4	571.5	564.4	577.5	523.4	526.2	514.1	517.0	540.4	548.3	537.4
OUT	6.4	571.5	564.4	577.5	523.4	526.2	514.1	517.0	540.4	548.3	537.4
IN	11.4	598.5	549.4	533.1	513.4	520.6	498.5	483.6	522.1	526.7	529.4
OUT	11.4	598.5	549.4	533.1	513.4	520.6	498.5	483.6	522.1	526.7	529.4
IN	16.5	572.4	529.4	508.7	508.4	507.9	503.5	493.6	526.5	529.4	530.2
OUT	16.5	572.4	529.4	508.7	508.4	507.9	503.5	493.6	526.5	529.4	530.2
IN	19.6	594.1	533.3	511.9	504.5	509.0	501.9	497.1	527.1	534.3	535.3
OUT	19.6	594.1	533.3	511.9	504.5	509.0	501.9	497.1	527.1	534.3	535.3
IN	24.1	593.0	508.8	510.4	516.9	508.4	503.0	497.6	533.2	539.4	538.3
OUT	24.1	593.0	508.8	510.4	516.9	508.4	503.0	497.6	533.2	539.4	538.3
FUEL INLET P	(MPA)	7.709	7.719	7.719	7.719	7.719	7.719	7.719	7.719	7.719	7.719
FUEL EXIT P	(MPA)	7.702	7.702	7.702	7.702	7.702	7.702	7.702	7.702	7.702	7.702
FUEL INLET TEMP	(K)	2842	2842	2842	2842	2842	2842	2842	2842	2842	2842
FUEL EXIT TEMP	(K)	2842	2842	2842	2842	2842	2842	2842	2842	2842	2842
FLOW RATE	(KG/S)	3815	3793	3782	377.6	373.2	373.2	373.2	360.9	355.9	355.9
VOLTAGE	(VOLTS)	4067	4143	4197	4161	4151	4151	4105	4109	4063	4076
POWER	(KW)	24.66	24.99	24.99	24.78	24.31	24.31	24.54	24.47	24.03	24.41
HEAT FLUX	(W/CM2)	1580	1602	1602	1586	1552	1580	1572	1568	1563	1564
INLET FUEL VEL	(M/S)	29.33	30.00	30.00	30.66	30.68	30.48	29.96	28.29	28.04	28.84
ENERGY BALANCE	(GCI)	-10.18	-12.91	-12.91	-12.98	-12.98	-12.98	-12.98	-12.98	-12.98	-12.98

ROCKET FUEL DEPOSIT TEST PROGRAM (COMMERCIAL C3H8 FUEL)
RUN 11 FEBRUARY 1, 1983

TIME	(MIN)	1.083	2.083	3.083	4.083	5.083	6.083	7.083	8.083	9.083
INLET	HELYNOLUS NO	1726+006	1729+006	1693+006	1648+006	1880+006	1799+006	1689+006	1523+006	1496+006
AVG	FUNCTION	1480-001	1435-001	1415-001	1459-001	1724-001	1770-001	2764-001	3622-001	3748-001
U	1.5	4.997	4.907	5.198	4.727	5.337	5.337	4.483	4.180	4.172
U	3.8	5.122	5.106	5.834	4.431	5.216	5.388	4.578	4.797	5.072
U	8.9	5.635	5.792	6.512	5.134	6.239	6.260	5.445	5.454	5.650
U	11.4	6.304	6.754	7.275	6.052	7.869	6.787	5.764	5.874	5.997
U	14.0	6.610	7.337	8.009	7.173	8.179	8.157	6.766	6.518	6.770
U	16.5	7.860	8.762	9.135	8.409	9.385	8.606	7.020	6.795	7.008
U	19.1	8.995	9.417	9.860	9.070	9.895	9.256	7.527	7.026	7.608
U	21.6	6.718	7.600	9.375	9.520	10.51	10.878	7.529	7.125	7.767
U	24.1	3162-002	3233-001	3116-001	3400-001	3309-002	3196-001	3769-002	3393	4.679
I/A	1.5	7975-002	3233-001	3116-001	3400-001	3309-002	3196-001	3769-002	3393	4.679
I/A	3.8	0000	0000	0000	0000	0000	0000	0000	0000	0000
I/A	8.9	0000	0000	0000	0000	0000	0000	0000	0000	0000
I/A	11.4	0000	0000	0000	0000	0000	0000	0000	0000	0000
I/A	14.0	0000	0000	0000	0000	0000	0000	0000	0000	0000
I/A	16.5	0000	0000	0000	0000	0000	0000	0000	0000	0000
I/A	19.1	0000	0000	0000	0000	0000	0000	0000	0000	0000
I/A	21.6	0000	0000	0000	0000	0000	0000	0000	0000	0000
I/A	24.1	0000	0000	0000	0000	0000	0000	0000	0000	0000
MC	1.5	8586-004	0000	0000	0000	0000	0000	0000	0000	0000
MC	3.8	3218-003	2775-003	1740-003	2054-003	2190-004	4365-004	9170-005	3665-004	1812-001
MC	8.9	1503-003	2775-003	1740-003	2054-003	2190-004	4365-004	1075-003	6890-004	3259-004
MC	11.4	0000	0000	0000	0000	0000	0000	0000	0000	0000
MC	14.0	0000	0000	0000	0000	0000	0000	0000	0000	0000
MC	16.5	0000	0000	0000	0000	0000	0000	0000	0000	0000
MC	19.1	0000	0000	0000	0000	0000	0000	0000	0000	0000
MC	21.6	0000	0000	0000	0000	0000	0000	0000	0000	0000
MC	24.1	0000	0000	0000	0000	0000	0000	0000	0000	0000

ROCKET FUEL DEPOSIT TEST PROGRAM (COMMERCIAL C3H8 FUEL)
 RUN 12 FEBRUARY 10, 1983

TIME	(MIN)	0.067	1.067	2.067	3.067	4.067	5.067	6.067	7.067	8.067	9.067	10.07
IN OUT	0	737.6	677.6	697.0	675.9	729.8	742.9	739.8	741.5	704.3	698.7	675.8
IN OUT	1.3	550.9	673.0	659.3	663.2	635.4	658.0	640.6	643.2	624.3	623.7	603.7
IN OUT	3.8	584.8	678.2	683.9	665.4	635.4	617.6	597.6	583.7	574.6	557.0	543.7
IN OUT	8.4	733.7	678.2	682.0	665.9	635.4	588.2	583.4	560.4	546.5	534.8	523.4
IN OUT	11.4	688.7	678.2	681.0	665.4	635.4	594.3	586.5	557.6	546.5	534.8	523.4
IN OUT	16.0	653.3	678.2	681.0	665.4	635.4	572.0	567.7	580.4	575.9	562.0	553.7
IN OUT	19.1	657.0	678.2	681.0	665.4	635.4	572.0	567.7	580.4	575.9	562.0	553.7
IN OUT	21.6	642.0	678.2	681.0	665.4	635.4	670.8	615.4	603.2	605.9	591.5	574.3
IN OUT	24.1	615.4	678.2	681.0	665.4	635.4	781.2	821.4	809.9	773.0	728.7	684.6
IN IN	3	706.6	646.3	625.9	644.5	696.4	711.2	708.4	709.9	673.0	616.5	578.5
IN IN	3.8	519.9	601.4	625.9	631.8	635.4	627.3	608.9	611.6	621.4	602.1	581.3
IN IN	6.4	553.8	641.8	652.4	624.5	603.4	586.2	568.9	528.1	543.0	523.7	512.0
IN IN	8.4	702.7	646.3	656.8	655.1	640.6	532.3	548.0	528.8	515.2	503.2	488.5
IN IN	11.4	622.7	646.3	656.8	655.1	640.6	562.8	557.3	548.8	544.7	530.4	512.0
IN IN	14.0	608.2	646.3	656.8	655.1	640.6	541.2	530.2	533.6	547.5	526.5	512.0
IN IN	19.1	626.6	646.3	656.8	655.1	640.6	583.4	583.9	571.6	574.7	559.8	542.9
IN IN	21.6	661.0	646.3	656.8	655.1	640.6	639.5	624.8	694.2	679.9	634.8	604.6
IN IN	24.1	744.3	646.3	656.8	655.1	640.6	751.2	742.3	694.2	709.9	634.8	604.6
FUEL INLET P		7.443	7.244	7.456	7.184	7.406	7.140	7.406	7.406	7.414	7.406	7.406
FUEL INLET TEMP		5.831	7.244	7.456	7.184	7.406	7.140	7.406	7.406	7.414	7.406	7.406
FUEL EXIT TEMP		216.5	219.8	224.3	230.9	229.3	229.3	231.5	232.9	235.9	234.6	230.9
FUEL EXIT RATE		378.2	371.0	380.4	380.9	379.3	379.8	380.4	379.9	378.7	374.6	370.5
FLOW RATE	(KG/S)	5266	5354	5379	5367	5329	5367	5329	5404	5358	5320	5293
CURRENT	(VOLTS)	3957	4061	4054	4073	4073	4093	4074	4138	4067	4156	4122
VOLTAGE	(VOLTS)	6.179	6.078	6.054	6.089	6.086	6.055	6.053	6.013	6.054	6.002	5.996
HEAT FLUX	(KW)	24.45	24.68	24.69	24.74	24.79	24.78	24.78	24.88	24.94	24.94	24.72
INLET FULL VEL	(M/S)	1567	1582	1582	1585	1568	1568	1568	1598	1578	1598	1584
INLET FULL VEL	(M/S)	29.01	29.41	30.04	30.34	30.53	30.74	30.74	30.64	30.55	30.91	31.05
ENERGY BALANCE	(BTU)	-6.205	-5.769	-6.760	-9.740	-9.978	-10.26	-11.43	-12.16	-14.20	-14.08	-11.91

ORIGINAL PAGE 1
 OF POOR QUALITY

ROCKET FUEL DEPOSIT TEST PROGRAM (NATURAL GAS)
 RUN 13 MARCH 2, 1963

TIME	(MIN)	0000	.7833	1.783	2.783	3.783	4.793	5.783	6.783	7.783	8.783	10.28
IN	OUT	1.3	460.4	457.6	457.6	458.7	460.9	462.4	463.7	461.5	464.3	465.4
IN	OUT	3.8	497.0	466.5	467.0	468.7	469.3	470.4	471.3	469.3	470.4	470.9
IN	OUT	6.4	516.2	484.3	484.8	487.0	485.0	488.2	489.3	487.6	488.2	488.7
IN	OUT	8.9	533.7	502.0	503.2	504.8	505.4	506.5	507.6	505.0	506.5	507.0
IN	OUT	11.4	549.3	517.6	518.7	520.7	520.9	522.6	523.2	520.8	520.9	522.6
IN	OUT	13.9	559.8	530.9	532.0	533.4	533.4	534.9	537.0	534.9	535.4	537.6
IN	OUT	16.5	567.0	542.0	543.2	544.8	545.9	547.0	547.6	545.7	546.5	547.6
IN	OUT	19.1	582.0	559.4	560.0	563.2	563.7	565.2	566.5	563.3	564.3	565.2
IN	OUT	21.6	592.0	575.4	577.0	579.3	579.8	582.4	583.2	579.3	580.4	582.0
IN	IN	24.1	456.8	451.2	451.2	452.3	454.5	450.2	455.1	455.1	457.8	458.3
IN	IN	26.6	482.9	467.1	468.4	468.0	462.9	463.9	465.1	462.8	463.9	464.3
IN	IN	29.1	501.2	477.6	478.7	480.6	480.6	481.7	482.8	481.2	481.7	482.3
IN	IN	31.6	517.4	495.6	496.4	499.0	499.0	500.1	501.2	498.6	500.1	500.6
IN	IN	34.1	531.7	511.5	512.3	514.5	514.5	516.2	516.7	514.5	514.5	516.2
IN	IN	36.6	542.9	524.5	525.6	527.3	529.0	529.0	530.2	528.9	529.0	530.6
IN	IN	39.1	553.4	535.4	536.7	537.3	537.3	538.9	540.7	537.3	537.3	538.9
IN	IN	41.6	569.0	553.4	554.6	556.7	558.9	558.9	560.7	557.3	557.3	558.9
IN	IN	44.1	585.7	569.0	570.6	572.5	573.4	575.7	576.7	572.8	573.7	575.7
IN	IN	46.6	585.4	580.1	582.3	584.5	585.6	587.3	588.5	585.6	586.7	587.8
IN	IN	49.1	13.42	13.37	13.32	13.27	13.22	13.17	13.15	12.97	12.97	12.97
IN	IN	51.6	13.04	12.96	12.91	12.80	12.81	12.77	12.74	12.55	12.55	12.55
IN	IN	54.1	292.6	292.0	292.0	292.0	291.5	291.5	291.5	290.4	290.4	290.4
IN	IN	56.6	430.9	427.6	428.7	429.8	430.4	432.0	433.1	430.4	430.9	430.9
IN	IN	59.1	1054-001	1081-001	1077-001	1072-001	1068-001	1064-001	1059-001	1073-001	1073-001	1067-001
IN	IN	61.6	1911	1931	1931	1926	1927	1931	1932	1940	1938	1937
IN	IN	64.1	2.626	4.613	2.616	2.618	2.618	2.627	2.624	2.604	2.602	2.603
IN	IN	66.6	3.017	3.046	3.051	3.047	3.047	3.071	3.089	3.071	3.062	3.073
IN	IN	69.1	321.5	323.5	323.2	323.2	323.2	325.0	324.8	324.9	325.0	325.1
IN	IN	71.6	31.03	31.68	31.57	31.43	31.20	31.09	30.94	31.11	31.13	30.82
IN	IN	74.1	-12.33	-12.33	-12.04	-11.71	-11.20	-10.97	-10.66	-10.44	-10.13	-10.27

ORIGINAL PAGE IS
 OF POOR QUALITY

ORIGINAL PRINTED BY
OF POOR QUALITY

ROCKET FUEL USPOSIT II TLST PROGRAM (NATURAL GAS)
RUN 14 MARCH 3, 1963

TIME	(MIN)	0000	0.733	1.733	2.733	3.733	4.733	5.733	6.733	7.733	8.733	10.23
IN	0	503.7	501.5	510.4	509.8	507.9	505.9	504.2	508.7	510.2	512.6	518.3
OUT	1.0	525.7	526.0	540.4	541.5	576.5	574.8	577.6	577.6	578.7	578.7	579.8
IN	2.0	558.7	560.9	574.8	576.5	601.5	600.9	603.2	602.9	603.7	603.9	604.8
OUT	3.0	599.3	582.0	594.8	600.9	622.0	620.7	625.2	623.7	627.8	627.0	627.0
IN	4.0	619.3	623.2	642.0	644.3	642.0	642.0	643.9	643.9	647.0	643.3	643.3
OUT	5.0	649.8	654.0	672.0	675.4	683.7	691.3	694.9	693.7	694.8	697.0	697.0
IN	6.0	664.8	666.7	687.6	689.8	690.9	697.0	697.0	697.0	697.0	697.0	697.0
OUT	7.0	700.4	707.6	710.9	712.0	712.0	708.7	711.2	708.7	708.2	708.3	708.3
IN	8.0	730.4	749.2	751.5	751.0	752.1	750.4	749.2	749.8	751.4	751.4	751.4
OUT	9.0	789.4	817.7	831.5	832.7	832.1	830.4	833.1	832.5	833.7	833.9	833.9
IN	10.0	815.4	852.2	869.8	867.1	867.0	865.9	864.2	864.7	864.8	864.8	864.8
OUT	11.0	870.4	893.0	914.9	913.5	913.7	912.0	911.4	911.4	911.4	911.4	911.4
IN	12.0	897.7	932.1	950.9	953.8	957.0	952.0	952.9	954.8	954.8	954.8	954.8
OUT	13.0	961.0	985.9	998.1	981.0	982.1	978.2	980.9	980.4	980.7	980.8	980.8
IN	14.0	990.0	998.8	1002.0	1000.0	1000.0	999.8	999.8	999.8	999.2	999.3	999.3
OUT	15.0	1020.0	1066.0	1070.0	1068.5	1064.9	1064.9	1064.9	1064.9	1064.9	1064.9	1064.9
IN	16.0	1070.0	1092.0	1107.0	1102.0	1107.0	1107.0	1107.0	1107.0	1107.0	1107.0	1107.0
OUT	17.0	1107.0	1106.6	1109.0	1102.0	1106.4	1107.0	1107.0	1107.0	1107.0	1107.0	1107.0
IN	18.0	1107.0	1092.0	1109.0	1102.0	1106.4	1107.0	1107.0	1107.0	1107.0	1107.0	1107.0
OUT	19.0	1107.0	1092.0	1109.0	1102.0	1106.4	1107.0	1107.0	1107.0	1107.0	1107.0	1107.0
IN	20.0	1107.0	1092.0	1109.0	1102.0	1106.4	1107.0	1107.0	1107.0	1107.0	1107.0	1107.0
OUT	21.0	1107.0	1092.0	1109.0	1102.0	1106.4	1107.0	1107.0	1107.0	1107.0	1107.0	1107.0
IN	22.0	1107.0	1092.0	1109.0	1102.0	1106.4	1107.0	1107.0	1107.0	1107.0	1107.0	1107.0
OUT	23.0	1107.0	1092.0	1109.0	1102.0	1106.4	1107.0	1107.0	1107.0	1107.0	1107.0	1107.0
IN	24.0	1107.0	1092.0	1109.0	1102.0	1106.4	1107.0	1107.0	1107.0	1107.0	1107.0	1107.0
OUT	25.0	1107.0	1092.0	1109.0	1102.0	1106.4	1107.0	1107.0	1107.0	1107.0	1107.0	1107.0
IN	26.0	1107.0	1092.0	1109.0	1102.0	1106.4	1107.0	1107.0	1107.0	1107.0	1107.0	1107.0
OUT	27.0	1107.0	1092.0	1109.0	1102.0	1106.4	1107.0	1107.0	1107.0	1107.0	1107.0	1107.0
IN	28.0	1107.0	1092.0	1109.0	1102.0	1106.4	1107.0	1107.0	1107.0	1107.0	1107.0	1107.0
OUT	29.0	1107.0	1092.0	1109.0	1102.0	1106.4	1107.0	1107.0	1107.0	1107.0	1107.0	1107.0
IN	30.0	1107.0	1092.0	1109.0	1102.0	1106.4	1107.0	1107.0	1107.0	1107.0	1107.0	1107.0
OUT	31.0	1107.0	1092.0	1109.0	1102.0	1106.4	1107.0	1107.0	1107.0	1107.0	1107.0	1107.0
IN	32.0	1107.0	1092.0	1109.0	1102.0	1106.4	1107.0	1107.0	1107.0	1107.0	1107.0	1107.0
OUT	33.0	1107.0	1092.0	1109.0	1102.0	1106.4	1107.0	1107.0	1107.0	1107.0	1107.0	1107.0
IN	34.0	1107.0	1092.0	1109.0	1102.0	1106.4	1107.0	1107.0	1107.0	1107.0	1107.0	1107.0
OUT	35.0	1107.0	1092.0	1109.0	1102.0	1106.4	1107.0	1107.0	1107.0	1107.0	1107.0	1107.0
IN	36.0	1107.0	1092.0	1109.0	1102.0	1106.4	1107.0	1107.0	1107.0	1107.0	1107.0	1107.0
OUT	37.0	1107.0	1092.0	1109.0	1102.0	1106.4	1107.0	1107.0	1107.0	1107.0	1107.0	1107.0
IN	38.0	1107.0	1092.0	1109.0	1102.0	1106.4	1107.0	1107.0	1107.0	1107.0	1107.0	1107.0
OUT	39.0	1107.0	1092.0	1109.0	1102.0	1106.4	1107.0	1107.0	1107.0	1107.0	1107.0	1107.0
IN	40.0	1107.0	1092.0	1109.0	1102.0	1106.4	1107.0	1107.0	1107.0	1107.0	1107.0	1107.0
OUT	41.0	1107.0	1092.0	1109.0	1102.0	1106.4	1107.0	1107.0	1107.0	1107.0	1107.0	1107.0
IN	42.0	1107.0	1092.0	1109.0	1102.0	1106.4	1107.0	1107.0	1107.0	1107.0	1107.0	1107.0
OUT	43.0	1107.0	1092.0	1109.0	1102.0	1106.4	1107.0	1107.0	1107.0	1107.0	1107.0	1107.0
IN	44.0	1107.0	1092.0	1109.0	1102.0	1106.4	1107.0	1107.0	1107.0	1107.0	1107.0	1107.0
OUT	45.0	1107.0	1092.0	1109.0	1102.0	1106.4	1107.0	1107.0	1107.0	1107.0	1107.0	1107.0
IN	46.0	1107.0	1092.0	1109.0	1102.0	1106.4	1107.0	1107.0	1107.0	1107.0	1107.0	1107.0
OUT	47.0	1107.0	1092.0	1109.0	1102.0	1106.4	1107.0	1107.0	1107.0	1107.0	1107.0	1107.0
IN	48.0	1107.0	1092.0	1109.0	1102.0	1106.4	1107.0	1107.0	1107.0	1107.0	1107.0	1107.0
OUT	49.0	1107.0	1092.0	1109.0	1102.0	1106.4	1107.0	1107.0	1107.0	1107.0	1107.0	1107.0
IN	50.0	1107.0	1092.0	1109.0	1102.0	1106.4	1107.0	1107.0	1107.0	1107.0	1107.0	1107.0
OUT	51.0	1107.0	1092.0	1109.0	1102.0	1106.4	1107.0	1107.0	1107.0	1107.0	1107.0	1107.0
IN	52.0	1107.0	1092.0	1109.0	1102.0	1106.4	1107.0	1107.0	1107.0	1107.0	1107.0	1107.0
OUT	53.0	1107.0	1092.0	1109.0	1102.0	1106.4	1107.0	1107.0	1107.0	1107.0	1107.0	1107.0
IN	54.0	1107.0	1092.0	1109.0	1102.0	1106.4	1107.0	1107.0	1107.0	1107.0	1107.0	1107.0
OUT	55.0	1107.0	1092.0	1109.0	1102.0	1106.4	1107.0	1107.0	1107.0	1107.0	1107.0	1107.0
IN	56.0	1107.0	1092.0	1109.0	1102.0	1106.4	1107.0	1107.0	1107.0	1107.0	1107.0	1107.0
OUT	57.0	1107.0	1092.0	1109.0	1102.0	1106.4	1107.0	1107.0	1107.0	1107.0	1107.0	1107.0
IN	58.0	1107.0	1092.0	1109.0	1102.0	1106.4	1107.0	1107.0	1107.0	1107.0	1107.0	1107.0
OUT	59.0	1107.0	1092.0	1109.0	1102.0	1106.4	1107.0	1107.0	1107.0	1107.0	1107.0	1107.0
IN	60.0	1107.0	1092.0	1109.0	1102.0	1106.4	1107.0	1107.0	1107.0	1107.0	1107.0	1107.0
OUT	61.0	1107.0	1092.0	1109.0	1102.0	1106.4	1107.0	1107.0	1107.0	1107.0	1107.0	1107.0
IN	62.0	1107.0	1092.0	1109.0	1102.0	1106.4	1107.0	1107.0	1107.0	1107.0	1107.0	1107.0
OUT	63.0	1107.0	1092.0	1109.0	1102.0	1106.4	1107.0	1107.0	1107.0	1107.0	1107.0	1107.0
IN	64.0	1107.0	1092.0	1109.0	1102.0	1106.4	1107.0	1107.0	1107.0	1107.0	1107.0	1107.0
OUT	65.0	1107.0	1092.0	1109.0	1102.0	1106.4	1107.0	1107.0	1107.0	1107.0	1107.0	1107.0
IN	66.0	1107.0	1092.0	1109.0	1102.0	1106.4	1107.0	1107.0	1107.0	1107.0	1107.0	1107.0
OUT	67.0	1107.0	1092.0	1109.0	1102.0	1106.4	1107.0	1107.0	1107.0	1107.0	1107.0	1107.0
IN	68.0	1107.0	1092.0	1109.0	1102.0	1106.4	1107.0	1107.0	1107.0	1107.0	1107.0	1107.0
OUT	69.0	1107.0	1092.0	1109.0	1102.0	1106.4	1107.0	1107.0	1107.0	1107.0	1107.0	1107.0
IN	70.0	1107.0	1092.0	1109.0	1102.0	1106.4	1107.0	1107.0	1107.0	1107.0	1107.0	1107.0
OUT	71.0	1107.0	1092.0	1109.0	1102.0	1106.4	1107.0	1107.0	1107.0	1107.0	1107.0	1107.0
IN	72.0	1107.0	1092.0	1109.0	1102.0	1106.4	1107.0	1107.0	1107.0	1107.0	1107.0	1107.0
OUT	73.0	1107.0	1092.0	1109.0	1102.0	1106.4	1107.0	1107.0	1107.0	1107.0	1107.0	1107.0
IN	74.0	1107.0	1092.0	1109.0	1102.0	1106.4	1107.0	1107.0	1107.0	1107.0	1107.0	1107.0
OUT	75.0	1107.0	1092.0	1109.0	1102.0	1106.4	1107.0	1107.0	1107.0	1107.0	1107.0	1107.0
IN	76.0	1107.0	1092.0	1109.0	1102.0	1106.4	1107.0	1107.0	1107.0	1107.0	1107.0	1107.0
OUT	77.0	1107.0	1092.0	1109.0	1102.0	1106.4	1107.0	1107.0	1107.0	1107.0	1107.0	1107.0
IN	78.0	1107.0	1092.0	1109.0	1102.0	1106.4	110					

ROCKET FUEL DEPOSIT TEST PROGRAM (NATURAL GAS)
 RUN 15 MARCH 3, 1983

TIME	(MIN)	0.000	1.883	2.883	3.883	4.883	5.883	6.883	7.883	8.883	10.30
INLET REYNOLDS NO		4371+006	4390+006	4392+006	4365+006	4380+006	4406+006	4381+006	4750+006	4372+006	4346+006
AVG FRICTION FACTOR		1287-001	1290-001	1302-001	1309-001	1320-001	1308-001	1344-001	1432-001	1267-001	1509-001
U 3	1.3	2.465	2.599	2.589	2.389	2.336	2.502	2.784	1.594	2.267	2.203
U 4	3.8	2.297	2.128	1.529	1.541	1.582	1.368	1.745	1.858	1.526	1.440
U 5	6.9	1.303	1.782	1.768	1.768	1.982	2.062	2.709	2.831	1.860	2.042
U 6	8.9	2.274	2.307	2.501	2.790	2.632	2.418	2.447	2.493	2.504	2.689
U 7	11.0	2.524	2.607	2.790	2.790	2.835	2.579	2.600	2.625	2.629	2.693
U 8	14.0	2.625	2.634	2.753	2.753	2.778	2.329	2.531	2.534	2.520	2.534
U 9	16.5	2.594	2.616	2.743	2.743	2.758	2.314	2.519	2.520	2.511	2.534
U 10	19.1	2.579	2.690	2.787	2.787	2.787	2.348	2.585	2.589	2.608	2.628
U 11	21.6	2.294	2.423	2.424	2.424	2.488	2.288	2.707	2.696	2.696	2.700
U 12	24.1	0.000	5424-002	6647-002	5076-002	2488-002	1.888-001	4801-001	2.6268-001	6198-001	7371-001
U 13	1.3	0.000	1125-001	1236-001	1306-001	2231-001	9398-001	1549-001	2268-001	2498-001	2887-001
U 14	3.8	0.000	3450-001	1010	2189	2137	2326	1378	1028	6879-001	5431-001
U 15	6.9	0.000	0.000	0.000	0.000	0.000	0.000	0.000	0.000	0.000	0.000
U 16	8.9	0.000	0.000	0.000	0.000	0.000	0.000	0.000	0.000	0.000	0.000
U 17	11.0	0.000	0.000	0.000	0.000	0.000	0.000	0.000	0.000	0.000	0.000
U 18	14.0	0.000	0.000	0.000	0.000	0.000	0.000	0.000	0.000	0.000	0.000
U 19	16.5	0.000	0.000	0.000	0.000	0.000	0.000	0.000	0.000	0.000	0.000
U 20	19.1	0.000	0.000	0.000	0.000	0.000	0.000	0.000	0.000	0.000	0.000
U 21	21.6	0.000	0.000	0.000	0.000	0.000	0.000	0.000	0.000	0.000	0.000
U 22	24.1	0.000	0.000	0.000	0.000	0.000	0.000	0.000	0.000	0.000	0.000
U 23	1.3	0.000	6778-004	5047-004	1867-004	3745-004	1.221-003	1357-003	1371-003	1271-003	1244-003
U 24	3.8	0.000	1259-003	833-004	5661-004	8238-004	2356-003	6016-003	5011-003	4862-003	4749-003
U 25	6.9	0.000	3389-003	6057-003	9435-003	7328-003	6386-003	5679-003	2562-003	1533-003	1040-003
U 26	8.9	0.000	0.000	0.000	0.000	0.000	0.000	0.000	0.000	0.000	0.000
U 27	11.0	0.000	0.000	0.000	0.000	0.000	0.000	0.000	0.000	0.000	0.000
U 28	14.0	0.000	9683-005	0.000	0.000	0.000	0.000	0.000	0.000	0.000	0.000
U 29	16.5	0.000	2076-004	6309-005	0.000	0.000	0.000	0.000	0.000	0.000	0.000
U 30	19.1	0.000	3873-004	0.000	0.000	0.000	0.000	0.000	0.000	0.000	0.000
U 31	21.6	0.000	0.000	0.000	0.000	0.000	0.000	0.000	0.000	0.000	0.000
U 32	24.1	0.000	0.000	0.000	0.000	0.000	0.000	0.000	0.000	0.000	0.000

ORIGINAL PAGE IS
 OF POOR QUALITY

ROCKET FUEL DEPOSIT TEST PROGRAM (NATURAL GAS)
 RUN 16 MARCH 8, 1983

TIME	(MIN)	•0000	1•800	2•800	3•800	4•800	5•800	6•900	7•800	8•800	9•800
OUT	0	920.9	694.7	668.7	669.8	657.6	658.7	661.5	638.0	626.5	619.8
OUT	0	920.3	596.5	593.2	593.2	585.4	585.3	584.2	591.5	590.7	595.2
OUT	0	720.3	704.3	704.8	708.2	703.2	706.5	703.7	698.7	697.4	695.7
OUT	0	696.5	749.3	752.5	757.7	748.2	749.8	749.8	685.4	685.3	668.5
OUT	0	704.4	789.3	784.3	779.3	723.2	717.5	694.8	685.4	688.7	689.5
OUT	0	714.8	729.3	742.0	738.2	720.4	723.7	718.2	719.3	722.2	722.0
OUT	0	744.8	748.6	765.4	763.2	751.5	753.7	750.4	790.9	805.2	814.7
IN	0	744.8	785.4	787.0	785.9	793.2	794.3	794.3	794.3	794.3	801.7
IN	0	812.4	590.3	656.5	657.9	645.4	646.5	645.9	626.0	614.4	607.7
IN	0	599.1	580.3	599.8	580.9	571.6	577.0	575.9	577.1	573.2	566.1
IN	0	709.1	580.2	580.9	580.9	573.2	577.0	575.9	569.6	568.2	566.1
IN	0	684.6	690.3	692.8	695.9	691.0	694.3	691.6	672.7	673.2	663.8
IN	0	684.6	731.0	714.3	744.8	736.0	709.8	677.6	658.8	657.1	656.4
IN	0	692.4	749.6	708.8	686.5	667.7	669.3	663.6	673.2	676.6	677.2
IN	0	708.5	777.6	729.6	767.0	711.0	707.0	682.6	707.1	709.9	710.8
IN	0	711.6	733.6	729.6	725.9	706.2	711.5	705.9	739.9	741.8	738.2
IN	0	717.4	753.3	752.2	750.9	739.3	741.5	738.2	778.8	793.8	802.2
IN	0	735.0	777.1	774.8	773.7	781.0	782.0	782.1	793.8	793.8	793.8
FUEL INLET P		12.15	12.32	13.07	13.04	12.01	12.97	12.95	12.91	12.87	12.80
FUEL INLET TEMP		12.33	12.32	12.37	12.25	12.27	12.18	12.15	12.11	12.07	12.04
FUEL EXIT TEMP		289.3	289.7	288.7	289.3	288.7	288.7	288.7	289.3	289.8	290.4
FLOW RATE		544.3	555.0	554.3	554.8	551.5	553.2	551.5	551.5	554.3	555.4
FLOW RATE (G/GS)		1090.001	1105.001	1081.001	1085.001	1083.001	1080.001	1081.001	1085.001	1075.001	1076.001
CURRENT		2266.0	2311.0	2300.0	2306.0	2295.0	2332.0	2307.0	2313.0	2302.0	2295.0
VOLTAGE		4.226	4.190	4.149	4.188	4.172	4.183	4.170	4.143	4.159	4.152
HEAT FLUX		9.576	9.583	9.614	9.658	9.575	9.629	9.621	9.581	9.575	9.530
HEAT FLUX (W/CM2)		613.6	620.4	617.4	618.6	613.5	617.0	616.4	613.9	613.5	611.9
HEAT FLUX (W/CM2)		311.56	311.67	309.8	311.21	311.05	309.95	309.8	311.21	311.04	311.19
HEAT BALANCE (PCT)		-11.85	-8.601	-9.355	-9.275	-8.564	-8.794	-10.20	-9.736	-9.794	-9.040

ORIGINAL PAGE IS
 OF POOR QUALITY

ROCKET FUEL DEPOSIT TEST PROGRAM (NATURAL GAS)
 RUN 16 MARCH 8, 1963

TIME	REYNOLDS NO	(MIN)	0.000	0.800	1.600	2.800	3.800	4.800	5.000	6.800	7.800	8.800	9.800
INLET													
AVG	1.3	CM14/CM2-K	4434+006	4459+006	4474+006	4377+006	4398+006	4387+006	4372+006	4377+006	4398+006	4361+006	4371+006
U	3.8	CM14/CM2-K	1469-001	1454-001	1456-001	1475-001	1485-001	1509-001	1522-001	1537-001	1527-001	1546-001	1547-001
U	6.4	CM14/CM2-K	1233	1486	2702	2740	2797	2875	2936	2930	2945	2995	3004
U	8.9	CM14/CM2-K	1647	2164	2705	2734	2748	2804	2777	2830	2862	2890	2914
U	11.4	CM14/CM2-K	1121	1116	1882	1862	1864	1865	1771	1984	2010	2028	2031
U	14.0	CM14/CM2-K	2339	2197	1969	1929	2464	2617	2624	2673	2725	2766	2864
U	19.1	CM14/CM2-K	2657	2668	2508	1987	2440	2759	2749	2800	2876	2856	2866
U	21.6	CM14/CM2-K	2789	2668	2556	2586	2623	2700	2706	2800	2776	2767	2766
U	24.1	CM14/CM2-K	2919	2754	2649	2640	2666	2529	2549	2727	2696	2710	2736
U	3.8	CM14/CM2-W	0000	1773	7497-001	7772-001	7722-001	6355-001	6198-001	6711-001	3064-001	1089-001	1524-002
U	6.4	CM14/CM2-W	0000	0000	0000	0000	0000	0000	0000	0000	0000	0000	0000
U	8.9	CM14/CM2-W	0000	0000	0000	0000	0000	0000	0000	0000	0000	0000	0000
U	11.4	CM14/CM2-W	0000	0000	0000	0000	0000	0000	0000	0000	0000	0000	0000
U	14.0	CM14/CM2-W	0000	0000	0000	0000	0000	0000	0000	0000	0000	0000	0000
U	19.1	CM14/CM2-W	0000	0000	0000	0000	0000	0000	0000	0000	0000	0000	0000
U	21.6	CM14/CM2-W	0000	0000	0000	0000	0000	0000	0000	0000	0000	0000	0000
U	24.1	CM14/CM2-W	0000	0000	0000	0000	0000	0000	0000	0000	0000	0000	0000
U	3.8	CM14/CM2-W	0000	0000	0000	0000	0000	0000	0000	0000	0000	0000	0000
U	6.4	CM14/CM2-W	0000	0000	0000	0000	0000	0000	0000	0000	0000	0000	0000
U	8.9	CM14/CM2-W	0000	0000	0000	0000	0000	0000	0000	0000	0000	0000	0000
U	11.4	CM14/CM2-W	0000	0000	0000	0000	0000	0000	0000	0000	0000	0000	0000
U	14.0	CM14/CM2-W	0000	0000	0000	0000	0000	0000	0000	0000	0000	0000	0000
U	19.1	CM14/CM2-W	0000	0000	0000	0000	0000	0000	0000	0000	0000	0000	0000
U	21.6	CM14/CM2-W	0000	0000	0000	0000	0000	0000	0000	0000	0000	0000	0000
U	24.1	CM14/CM2-W	0000	0000	0000	0000	0000	0000	0000	0000	0000	0000	0000
U	3.8	CM14/CM2-J	0000	0000	0000	0000	0000	0000	0000	0000	0000	0000	0000
U	6.4	CM14/CM2-J	0000	0000	0000	0000	0000	0000	0000	0000	0000	0000	0000
U	8.9	CM14/CM2-J	0000	0000	0000	0000	0000	0000	0000	0000	0000	0000	0000
U	11.4	CM14/CM2-J	0000	0000	0000	0000	0000	0000	0000	0000	0000	0000	0000
U	14.0	CM14/CM2-J	0000	0000	0000	0000	0000	0000	0000	0000	0000	0000	0000
U	19.1	CM14/CM2-J	0000	0000	0000	0000	0000	0000	0000	0000	0000	0000	0000
U	21.6	CM14/CM2-J	0000	0000	0000	0000	0000	0000	0000	0000	0000	0000	0000
U	24.1	CM14/CM2-J	0000	0000	0000	0000	0000	0000	0000	0000	0000	0000	0000

ORIGINAL PAGE IS
 OF POOR QUALITY

ROCKET FUEL DEPOSIT TEST PROGRAM (NATURAL GAS)
 RUN 17 MARCH 9, 1983

TIME	(MIN)	0000	0800	1000	1800	2800	3800	4800	5000	6800	7800	8800	1030
IM OUT	1.5	CM	(K)	567.6	571.5	568.2	568.2	568.2	567.8	570.9	571.5	573.7	572.0
IM OUT	3.0	CM	(K)	537.6	535.7	532.6	532.6	532.6	534.2	533.6	533.8	538.7	537.0
IM OUT	6.0	CM	(K)	596.5	591.5	585.9	585.9	585.9	583.7	581.5	580.4	580.4	577.0
IM OUT	8.0	CM	(K)	615.4	606.5	595.9	595.9	595.9	593.7	593.2	593.2	594.8	593.7
IM OUT	11.0	CM	(K)	637.3	610.4	607.0	607.0	607.0	605.7	606.5	606.5	609.5	607.0
IM OUT	14.0	CM	(K)	654.8	635.4	640.9	640.9	640.9	640.3	640.4	640.5	646.5	643.2
IM OUT	16.5	CM	(K)	666.5	666.5	670.4	670.4	670.4	669.3	670.4	670.4	672.0	666.5
IM OUT	19.0	CM	(K)	680.9	685.4	684.6	684.6	684.6	685.9	686.5	686.5	687.6	682.6
IM OUT	21.0	CM	(K)	703.2	703.7	705.4	705.4	705.4	704.8	706.5	706.5	708.2	704.3
IM IN	24.0	CM	(K)	721.5	723.7	728.2	728.2	728.2	725.4	727.0	727.0	728.2	723.3
IM IN	3.0	CM	(K)	558.8	558.8	526.6	526.6	526.6	523.9	523.9	523.9	529.9	523.3
IM IN	6.0	CM	(K)	587.7	586.7	582.7	582.7	582.7	581.4	582.7	582.7	584.9	581.4
IM IN	9.0	CM	(K)	606.6	607.7	591.1	591.1	591.1	589.4	589.4	589.4	586.5	581.4
IM IN	11.0	CM	(K)	624.1	601.6	597.2	597.2	597.2	595.7	597.7	597.7	597.7	586.5
IM IN	14.0	CM	(K)	636.1	626.9	626.8	626.8	626.8	625.0	626.8	626.8	631.6	626.8
IM IN	16.5	CM	(K)	654.4	657.7	658.8	658.8	658.8	657.2	658.8	658.8	661.6	657.7
IM IN	19.0	CM	(K)	658.9	676.6	676.1	676.1	676.1	675.2	676.6	676.6	677.7	673.3
IM IN	21.0	CM	(K)	681.7	694.4	695.0	695.0	695.0	695.1	697.7	697.7	699.9	695.6
IM IN	24.0	CM	(K)	700.0	712.7	715.5	715.5	715.5	716.7	718.3	718.3	719.4	714.9
FULL INLET P			(MPA)	7291	714.9	732.9	732.9	732.9	729.9	730.4	730.4	729.4	729.0
FULL EXIT P			(MPA)	6244	6281	6276	6276	6276	6281	6243	6243	621.8	621.8
FULL FLOW RATE			(K)	291.5	291.5	291.5	291.5	291.5	291.5	290.9	290.9	290.9	290.9
FULL EXIT TEMP			(K)	502.6	507.0	506.5	506.5	506.5	507.6	508.2	508.2	509.8	508.2
FLOW RATE			(K/S)	1014	1018	1017	1017	1017	1014	1014	1017	1015	1015
VOLTAGE			(VOLTS)	2060	2075	2075	2075	2075	2069	2071	2071	2077	2074
POWER			(KW)	3331	3333	3327	3327	3327	3323	3329	3330	3331	3310
HEAT FLUX			(W/CM2)	6863	6915	6901	6901	6901	6876	6890	6914	6919	6867
INLET FLOW VLL			(M/S)	439.7	443.1	442.4	442.4	442.4	440.6	441.8	443.0	443.4	440.0
ENERGY BALANCE			(PCT)	-13.56	-11.93	-11.67	-11.67	-11.67	-11.29	-11.30	-11.32	-10.76	-10.82

ORIGINAL PAGE IS
 OF POOR QUALITY

ROCKET FUEL DEPOSIT TEST PROGRAM (NATURAL GAS)
 RUN 1R MARCH 9, 1963

TIME	(MIN)	00:00	0:783	1:783	2:783	3:783	4:783	5:783	6:783	7:783	8:783	10:28
IM OUT	3	1.5	575.6	578.2	577.6	575.4	577.0	577.0	579.3	541.5	542.0	542.0
IM OUT	8	3.6	605.9	605.4	602.6	602.0	597.0	597.0	597.0	597.0	596.2	597.0
IM OUT	8	8.9	615.4	615.4	613.2	614.3	615.5	615.5	616.5	617.0	618.7	617.6
IM OUT	8	11.4	655.7	655.7	660.4	669.3	668.5	665.9	665.9	665.9	665.9	660.9
IM OUT	8	14.0	674.8	674.8	682.0	691.5	690.2	683.7	685.9	683.7	682.0	675.4
IM OUT	8	16.5	695.4	695.4	703.7	715.4	713.9	705.9	708.7	705.9	705.9	696.5
IM OUT	8	19.1	738.7	738.7	744.8	754.9	753.4	747.8	748.2	746.5	747.8	739.3
IM OUT	8	24.0	744.8	744.8	748.7	754.9	754.9	747.8	748.2	746.5	747.8	739.3
IM IN	8	1.3	523.2	523.2	525.4	523.1	525.4	525.4	527.1	529.9	529.9	529.9
IM IN	8	3.8	565.7	565.7	563.2	563.1	565.7	565.7	566.8	559.3	560.4	558.8
IM IN	8	6.4	593.1	593.1	593.4	589.8	589.8	586.0	584.9	584.9	585.9	583.2
IM IN	8	8.9	593.3	593.3	593.3	593.3	593.3	593.3	593.3	593.3	593.3	593.3
IM IN	8	11.4	601.0	601.0	601.0	605.9	605.9	605.9	604.3	605.4	606.3	605.4
IM IN	8	14.0	643.8	643.8	648.2	655.7	657.0	654.3	653.8	653.7	653.7	648.8
IM IN	8	16.5	662.7	662.7	669.9	678.1	679.2	676.0	673.8	671.5	670.4	663.2
IM IN	8	19.1	683.2	683.2	691.5	701.4	703.1	699.8	696.5	693.7	693.7	684.3
IM IN	8	21.6	726.6	726.6	732.6	743.1	742.0	737.7	736.5	734.4	734.4	725.4
IM IN	8	24.0	732.7	732.7	736.5	742.0	742.0	737.7	736.5	734.4	734.4	727.1
FUEL FILL	P	1.3	742.0	742.0	744.8	744.8	744.8	746.7	745.5	744.1	744.1	740.4
FUEL FILL	P	3.8	744.8	744.8	748.7	754.9	754.9	754.9	753.4	753.4	753.4	748.7
FUEL FILL	P	6.4	754.9	754.9	754.9	754.9	754.9	754.9	754.9	754.9	754.9	754.9
FUEL FILL	P	8.9	754.9	754.9	754.9	754.9	754.9	754.9	754.9	754.9	754.9	754.9
FUEL FILL	P	11.4	754.9	754.9	754.9	754.9	754.9	754.9	754.9	754.9	754.9	754.9
FUEL FILL	P	14.0	754.9	754.9	754.9	754.9	754.9	754.9	754.9	754.9	754.9	754.9
FUEL FILL	P	16.5	754.9	754.9	754.9	754.9	754.9	754.9	754.9	754.9	754.9	754.9
FUEL FILL	P	19.1	754.9	754.9	754.9	754.9	754.9	754.9	754.9	754.9	754.9	754.9
FUEL FILL	P	21.6	754.9	754.9	754.9	754.9	754.9	754.9	754.9	754.9	754.9	754.9
FUEL FILL	P	24.0	754.9	754.9	754.9	754.9	754.9	754.9	754.9	754.9	754.9	754.9
FUEL EXIT	TEMP	1.3	487.6	487.6	489.4	489.4	489.4	489.4	489.4	489.4	489.4	489.4
FUEL EXIT	TEMP	3.8	491.5	491.5	491.5	495.4	495.4	495.4	495.4	495.4	495.4	495.4
FUEL EXIT	TEMP	6.4	495.4	495.4	495.4	495.4	495.4	495.4	495.4	495.4	495.4	495.4
FUEL EXIT	TEMP	8.9	495.4	495.4	495.4	495.4	495.4	495.4	495.4	495.4	495.4	495.4
FUEL EXIT	TEMP	11.4	495.4	495.4	495.4	495.4	495.4	495.4	495.4	495.4	495.4	495.4
FUEL EXIT	TEMP	14.0	495.4	495.4	495.4	495.4	495.4	495.4	495.4	495.4	495.4	495.4
FUEL EXIT	TEMP	16.5	495.4	495.4	495.4	495.4	495.4	495.4	495.4	495.4	495.4	495.4
FUEL EXIT	TEMP	19.1	495.4	495.4	495.4	495.4	495.4	495.4	495.4	495.4	495.4	495.4
FUEL EXIT	TEMP	21.6	495.4	495.4	495.4	495.4	495.4	495.4	495.4	495.4	495.4	495.4
FUEL EXIT	TEMP	24.0	495.4	495.4	495.4	495.4	495.4	495.4	495.4	495.4	495.4	495.4
FLOW RATE	(KG/S)	1.3	1528-001	1528-001	1528-001	1529-001	1529-001	1529-001	1526-001	1528-001	1528-001	1527-001
FLOW RATE	(KG/S)	3.8	2434.0	2434.0	2434.0	2452.0	2452.0	2452.0	2448.0	2451.0	2454.0	2453.0
FLOW RATE	(KG/S)	6.4	3942.0	3942.0	3942.0	3939.0	3939.0	3939.0	3919.0	3922.0	3932.0	3930.0
CURRENT	(AMPS)	11.4	9.596	9.596	9.664	9.657	9.657	9.657	9.594	9.612	9.649	9.582
VOLTAGE	(VOLTS)	16.5	614.9	614.9	619.4	618.8	618.8	613.9	614.7	615.9	618.3	613.9
POWER	(W)	21.6	97.45	97.45	97.81	97.81	97.81	97.53	97.57	97.45	96.61	96.62
HEAT FLUX	(W/CM ²)	24.0	-11.63	-11.63	-10.53	-10.53	-10.53	-10.53	-10.68	-10.20	-10.08	-10.55
IMPELLER FULL	VLL	1.3	1528-001	1528-001	1528-001	1528-001	1528-001	1528-001	1528-001	1528-001	1528-001	1528-001
IMPELLER FULL	VLL	3.8	1528-001	1528-001	1528-001	1528-001	1528-001	1528-001	1528-001	1528-001	1528-001	1528-001
IMPELLER FULL	VLL	6.4	1528-001	1528-001	1528-001	1528-001	1528-001	1528-001	1528-001	1528-001	1528-001	1528-001
IMPELLER FULL	VLL	8.9	1528-001	1528-001	1528-001	1528-001	1528-001	1528-001	1528-001	1528-001	1528-001	1528-001
IMPELLER FULL	VLL	11.4	1528-001	1528-001	1528-001	1528-001	1528-001	1528-001	1528-001	1528-001	1528-001	1528-001
IMPELLER FULL	VLL	14.0	1528-001	1528-001	1528-001	1528-001	1528-001	1528-001	1528-001	1528-001	1528-001	1528-001
IMPELLER FULL	VLL	16.5	1528-001	1528-001	1528-001	1528-001	1528-001	1528-001	1528-001	1528-001	1528-001	1528-001
IMPELLER FULL	VLL	19.1	1528-001	1528-001	1528-001	1528-001	1528-001	1528-001	1528-001	1528-001	1528-001	1528-001
IMPELLER FULL	VLL	21.6	1528-001	1528-001	1528-001	1528-001	1528-001	1528-001	1528-001	1528-001	1528-001	1528-001
IMPELLER FULL	VLL	24.0	1528-001	1528-001	1528-001	1528-001	1528-001	1528-001	1528-001	1528-001	1528-001	1528-001
ENERGY BALANCE	(PCT)	1.3	-13.14	-13.14	-12.61	-12.61	-12.61	-12.61	-12.61	-12.61	-12.61	-12.61

ORIGINAL PAGE IS
OF POOR QUALITY

ROCKET FUEL DEPOSIT TEST PROGRAM (NATURAL GAS)
 RUN 18 MARCH 9, 1983

TIME	(MIN)	.783	1.783	2.783	3.783	4.783	5.783	6.783	7.783	8.783	10.28
INLE F	REYNOLDS NU	8047-006	8033-006	8032-006	8039-006	8012-006	8033-006	8055-006	8041-006		
AVG	FRICTION FACTOR	1341-001	1350-001	1376-001	1398-001	1406-001	1493-001	1479-001	1471-001		
U 8	1.3 CM/W/CM2-K	2.748	2.733	2.742	2.742	2.720	2.585	2.568	2.569		
U 9	3.8 CM/W/CM2-K	2.497	2.535	2.562	2.576	2.590	2.585	2.568	2.569		
U 4	6.4 CM/W/CM2-K	2.413	2.467	2.498	2.510	2.529	2.531	2.516	2.526		
U 5	8.9 CM/W/CM2-K	3.424	3.439	3.447	3.457	3.480	3.473	3.462	3.454		
U 6	11.4 CM/W/CM2-K	2.799	2.777	2.776	2.770	2.771	2.762	2.745	2.733		
U 7	14.0 CM/W/CM2-K	2.545	2.452	2.440	2.438	2.453	2.455	2.454	2.479		
U 8	16.5 CM/W/CM2-K	2.620	2.435	2.423	2.426	2.453	2.481	2.497	2.540		
U 9	19.1 CM/W/CM2-K	2.670	2.408	2.391	2.403	2.453	2.484	2.465	2.531		
U 8	21.6 CM/W/CM2-K	2.411	2.424	2.418	2.426	2.454	2.467	2.463	2.532		
U 9	24.1 CM/W/CM2-K	2.430	2.406	2.409	2.421	2.441	2.467	2.463	2.530		
I/A 8	1.3 CM/W/CM2-M	0.000	0.000	0.000	0.000	0.000	0.000	0.000	0.000		
I/A 9	3.8 CM/W/CM2-M	0.000	0.000	0.000	0.000	0.000	0.000	0.000	0.000		
I/A 4	6.4 CM/W/CM2-M	0.000	0.000	0.000	0.000	0.000	0.000	0.000	0.000		
I/A 5	8.9 CM/W/CM2-M	0.000	0.000	0.000	0.000	0.000	0.000	0.000	0.000		
I/A 6	11.4 CM/W/CM2-M	0.000	0.000	0.000	0.000	0.000	0.000	0.000	0.000		
I/A 7	14.0 CM/W/CM2-M	0.000	0.000	0.000	0.000	0.000	0.000	0.000	0.000		
I/A 8	16.5 CM/W/CM2-M	0.000	0.000	0.000	0.000	0.000	0.000	0.000	0.000		
I/A 9	19.1 CM/W/CM2-M	0.000	0.000	0.000	0.000	0.000	0.000	0.000	0.000		
I/A 8	21.6 CM/W/CM2-M	0.000	0.000	0.000	0.000	0.000	0.000	0.000	0.000		
I/A 9	24.1 CM/W/CM2-M	0.000	0.000	0.000	0.000	0.000	0.000	0.000	0.000		
KL 8	1.3 CM/W/CM2-J	0.000	0.000	0.000	0.000	0.000	0.000	0.000	0.000		
KL 9	3.8 CM/W/CM2-J	0.000	0.000	0.000	0.000	0.000	0.000	0.000	0.000		
KL 4	6.4 CM/W/CM2-J	0.000	0.000	0.000	0.000	0.000	0.000	0.000	0.000		
KL 5	8.9 CM/W/CM2-J	0.000	0.000	0.000	0.000	0.000	0.000	0.000	0.000		
KL 6	11.4 CM/W/CM2-J	0.000	0.000	0.000	0.000	0.000	0.000	0.000	0.000		
KL 7	14.0 CM/W/CM2-J	0.000	0.000	0.000	0.000	0.000	0.000	0.000	0.000		
KL 8	16.5 CM/W/CM2-J	0.000	0.000	0.000	0.000	0.000	0.000	0.000	0.000		
KL 9	19.1 CM/W/CM2-J	0.000	0.000	0.000	0.000	0.000	0.000	0.000	0.000		
KL 8	21.6 CM/W/CM2-J	0.000	0.000	0.000	0.000	0.000	0.000	0.000	0.000		
KL 9	24.1 CM/W/CM2-J	0.000	0.000	0.000	0.000	0.000	0.000	0.000	0.000		

ORIGINAL PAGE IS
 OF POOR QUALITY

ROCKET FUEL DEPOSIT TEST PROGRAM (NATURAL GAS)
 RUN 19 MARCH 9, 1963

TIME	(MIN)	0.7500	1.750	2.750	3.750	4.750	5.750	6.750	7.750	8.750	10.25
IN OUT	CM (K)	658.2	649.3	624.8	628.6	627.0	628.2	629.3	632.0	636.5	635.4
IN OUT	CM (K)	652.0	656.9	654.0	651.0	651.5	662.6	664.3	672.0	672.5	671.5
IN OUT	CM (K)	712.0	726.5	734.3	740.4	749.6	752.6	752.0	752.3	762.5	756.5
IN OUT	CM (K)	750.5	767.0	778.2	780.3	782.0	781.5	783.7	785.9	783.2	770.9
IN OUT	CM (K)	794.6	806.2	809.2	800.4	793.2	781.5	774.3	775.9	776.5	764.8
IN OUT	CM (K)	815.4	804.8	803.2	795.4	788.2	777.6	771.5	775.3	773.7	769.3
IN IN	CM (K)	816.6	805.9	802.0	799.8	795.8	784.8	782.0	787.0	787.6	773.2
IN IN	CM (K)	840.2	837.3	812.7	816.9	814.9	810.5	817.1	819.8	824.3	823.3
IN IN	CM (K)	671.9	646.9	639.9	644.9	649.3	650.5	652.1	657.6	660.3	659.2
IN IN	CM (K)	700.2	714.5	722.2	728.1	737.6	738.2	742.9	747.1	744.3	744.7
IN IN	CM (K)	739.1	757.0	766.1	772.1	779.9	774.9	771.6	773.7	771.0	758.7
IN IN	CM (K)	759.5	777.3	788.1	787.1	783.2	767.3	763.8	766.0	764.3	752.6
IN IN	CM (K)	783.0	796.2	797.7	789.2	781.0	769.6	762.1	764.8	764.3	752.6
IN IN	CM (K)	794.1	795.0	791.1	783.2	776.0	762.7	759.4	763.7	761.6	752.1
IN IN	CM (K)	803.5	792.8	787.2	782.7	777.6	765.5	763.2	767.1	766.6	757.0
FUEL INLET	TEMP (K)	14.27	14.24	14.23	14.23	14.23	14.23	14.22	14.22	14.22	14.21
FUEL EXIT	TEMP (K)	13.98	13.95	13.93	13.92	13.91	13.90	13.89	13.89	13.89	13.86
FUEL EXIT	TEMP (K)	294.8	295.4	295.4	295.4	295.4	295.4	295.4	295.4	295.4	295.4
FLOWMETER	(MPS)	543.9	550.9	550.4	552.6	555.4	547.8	553.7	557.0	559.3	554.3
VOLTAG	(VOLTS)	1058-001	1057-001	1016-001	1017-001	1013-001	1087-001	1080-001	1070-001	1052-001	1087-001
POWER	(KW)	2131	2138	2132	2193	2200	2210	2207	2209	2196	2220
INLET FUEL	WLL (M/S)	4.263	4.358	4.352	4.358	4.3563	4.329	4.330	4.353	4.356	4.331
INLET FUEL	WLL (M/S)	9.344	9.455	9.536	9.558	9.601	9.568	9.558	9.616	9.567	9.615
ENERGY	BALANCE (MCT)	601.3	605.8	611.0	612.5	615.2	613.1	612.4	616.1	613.0	616.1
		31.91	31.69	32.30	32.30	32.16	32.60	32.37	32.07	31.54	32.60
		-13.91	-13.41	-12.21	-12.12	-11.94	-12.39	-11.52	-11.70	-11.95	-11.23

ORIGINAL PAGE IS
 OF POOR QUALITY

ROCKET FUEL DEPOSIT TEST PROGRAM (NATURAL GAS)
 RUN 20 MARCH 10-11, 1963

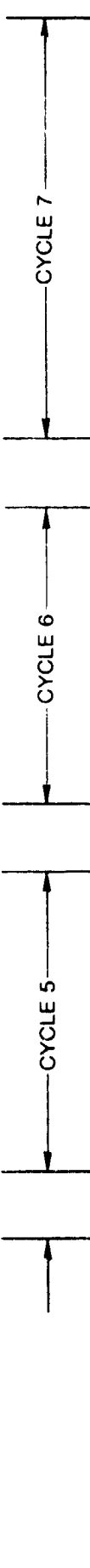
TYPE	(MIN)	0.0000	1.000	2.500	3.000	4.000	5.000	6.000	7.000	7.500	8.000	9.000
12	OUT	563.4	551.5	552.0	601.0	602.0	550.2	654.9	607.6	602.0	604.8	613.3
12	OUT	530.7	550.4	547.6	552.6	553.2	568.7	573.9	572.6	552.6	557.8	554.8
12	OUT	553.4	562.9	562.6	569.8	589.6	585.4	593.7	598.7	572.6	578.2	574.8
12	OUT	575.4	587.6	584.3	614.3	614.6	606.7	619.2	612.6	613.2	620.4	614.4
12	OUT	609.7	625.0	618.7	650.5	650.7	644.6	654.8	649.3	649.8	657.4	650.9
12	OUT	627.6	633.6	631.6	672.6	671.7	665.4	673.9	670.4	671.5	674.6	672.8
12	OUT	707.0	643.7	649.8	675.7	674.8	670.4	693.4	693.7	692.0	697.0	690.9
12	OUT	553.8	543.0	542.6	591.4	592.6	589.3	601.2	597.4	592.4	595.1	604.0
12	IN	518.2	533.1	528.2	542.4	543.5	541.4	545.1	543.0	542.4	547.3	544.6
12	IN	521.5	550.5	551.1	563.0	563.5	559.2	569.2	563.0	563.0	566.4	565.1
12	IN	543.8	556.5	574.8	604.7	580.2	575.8	584.5	579.1	579.7	586.8	581.8
12	IN	566.0	578.1	579.2	609.1	604.7	599.2	603.5	606.9	607.4	610.6	609.0
12	IN	591.5	542.6	601.1	641.9	640.8	635.3	612.4	606.9	607.4	615.1	610.2
12	IN	618.7	610.8	621.6	663.0	661.9	655.3	643.1	639.7	640.2	649.0	641.2
12	IN	674.8	638.2	625.6	666.3	665.2	656.8	669.2	660.8	661.9	669.0	662.3
12	IN	697.6	689.2	625.6	666.3	665.2	656.8	669.2	660.8	661.9	669.0	662.3
12	IN	14.13	689.2	625.6	666.3	665.2	656.8	669.2	660.8	661.9	669.0	662.3
12	IN	13.68	689.2	625.6	666.3	665.2	656.8	669.2	660.8	661.9	669.0	662.3
12	IN	295.4	14.15	14.18	14.21	14.21	14.23	14.24	14.25	14.24	14.28	14.29
12	IN	486.5	13.69	13.72	13.73	13.73	13.75	13.77	13.78	13.76	13.79	13.80
12	IN	2037	295.4	295.4	295.4	295.4	293.7	293.2	293.2	293.2	293.2	293.2
12	IN	1076-001	491.5	491.5	499.3	499.3	496.5	498.7	497.0	497.0	499.3	497.0
12	IN	1076-001	1076-001	1076-001	1076-001	1076-001	1080-001	1077-001	108-001	1082-001	1087-001	1093-001
12	IN	2056	2108	2108	2108	2108	2104	2117	2109	2112	2124	2121
12	IN	3.559	3.591	3.591	3.591	3.592	3.575	3.608	3.588	3.586	3.609	3.608
12	IN	7.462	7.564	7.564	7.564	7.571	7.521	7.637	7.567	7.573	7.665	7.651
12	IN	474.0	485.0	479.0	485.0	485.1	481.9	481.3	484.8	485.3	491.2	490.2
12	IN	32.15	32.22	32.26	32.22	32.31	32.01	31.81	31.92	31.92	32.11	32.30
12	IN	-15.54	-12.89	-15.15	-12.89	-12.61	-12.33	-12.63	-12.24	-12.22	-11.90	-12.20



ORIGINAL P. 1. 15
 OF POOR QUALITY

ROCKET FUEL DEPOSIT TEST PROGRAM (NATURAL GAS)
 RUN 20 MARCH 10-11, 1963

TIME	(MIN)	10.00	11.00	12.00	12.50	13.00	14.00	15.00	16.00	17.00	18.00	19.50
IN OUT		620.4	622.0	622.0	620.9	598.3	605.9	599.3	570.4	578.7	578.7	608.9
IN IN		557.6	561.5	563.7	562.6	540.4	539.8	529.3	537.6	538.7	538.7	572.6
IN OUT		593.5	597.6	598.7	597.6	553.7	553.7	556.5	575.4	558.7	557.5	557.5
IN IN		516.5	620.9	621.5	620.9	573.7	577.6	583.4	602.6	599.3	601.1	559.3
IN OUT		619.8	624.8	625.4	624.8	603.9	606.5	609.8	632.6	634.3	634.3	624.8
IN IN		674.3	674.8	674.3	674.3	625.9	625.9	624.8	654.3	654.3	654.3	632.6
IN OUT		681.5	681.5	682.0	681.5	629.3	630.4	633.2	657.5	659.8	659.8	632.6
IN IN		697.0	697.0	697.0	697.0	667.0	669.3	673.2	688.2	689.8	689.8	632.6
IN IN		612.4	612.4	612.3	611.9	589.8	596.7	583.6	600.6	605.2	605.2	632.6
IN IN		551.8	551.8	554.0	552.9	517.8	516.7	523.0	528.0	529.1	529.1	632.6
IN IN		571.9	571.9	572.8	571.8	531.2	534.5	537.2	547.4	549.1	549.1	632.6
IN IN		587.9	587.9	589.0	587.9	544.5	544.5	547.2	565.8	567.9	567.9	632.6
IN IN		611.2	611.2	611.7	611.2	564.5	564.5	567.8	571.1	574.6	574.6	632.6
IN IN		647.4	647.4	647.8	647.4	567.8	568.4	571.1	583.0	589.6	589.6	632.6
IN IN		670.1	670.1	670.8	670.1	596.7	596.7	597.3	603.0	604.6	604.6	632.6
IN IN		671.8	671.8	672.3	671.8	620.1	621.2	623.9	644.6	644.6	644.6	632.6
IN IN		687.4	687.4	687.3	687.4	620.1	621.2	623.9	644.6	644.6	644.6	632.6
FULL INLET		14.12	14.12	14.09	14.08	13.99	13.96	13.93	14.12	14.12	14.12	14.09
FUEL INLET		13.64	13.63	13.61	13.63	13.52	13.49	13.46	13.64	13.64	13.64	13.61
FUEL EXIT		293.7	293.7	294.3	294.3	292.6	292.6	292.6	295.4	295.4	295.4	295.9
FUEL EXIT		499.3	503.7	503.7	503.7	485.9	487.0	487.8	495.9	497.6	497.6	499.9
FLOW RATE		1077-001	1075-001	1075-001	1075-001	1075-001	1068-001	1066-001	1077-001	1077-001	1071-001	1081-001
CURRENT		2116	2116	2106	2106	2008	2019	2024	2076	2077	2070	2099
VOLTAGE		3.619	3.619	3.616	3.616	3.614	3.618	3.604	3.652	3.650	3.638	3.649
FUEL INLET		3.636	3.636	3.632	3.632	3.634	3.633	3.629	3.652	3.651	3.638	3.651
HEAT FLOW		489.3	489.3	490.3	490.3	464.4	464.4	467.3	485.3	485.8	485.8	485.8
INLET FUEL VEL		31.86	31.87	31.87	31.87	31.84	31.83	31.84	32.30	32.32	32.31	32.39
ENERGY BALANCE		-11.65	-12.09	-12.09	-11.89	-13.69	-13.63	-12.91	-14.31	-13.76	-13.75	-13.91

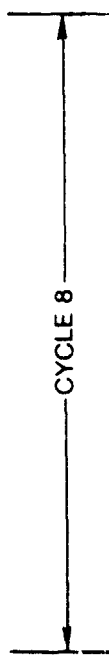


ORIGINAL PAGE IS
 OF POOR QUALITY

ORIGINAL PAGE IS
OF POOR QUALITY

ROCKET FUEL DEPOSIT TEST PROGRAM (NATURAL GAS)
RUN 20 MARCH 10-11, 1963

TIME	(MIN)	20.00	21.00	22.00	23.00	24.50
OUT	1.3	573.7	570.4	573.2	574.3	575.4
OUT	3.0	536.5	536.5	541.2	540.9	540.4
OUT	6.9	555.5	573.7	562.6	561.5	560.4
OUT	11.4	604.3	595.9	580.4	578.2	577.0
OUT	16.5	608.2	600.9	603.2	600.9	599.8
OUT	19.1	641.4	631.3	637.3	637.0	604.3
OUT	21.6	663.6	653.7	661.5	659.3	655.7
OUT	24.1	694.3	685.9	685.9	663.2	662.0
IN	1.3	564.1	560.7	563.5	562.0	565.8
IN	3.0	553.5	526.8	531.8	531.3	530.8
IN	6.9	571.3	546.8	552.9	551.9	550.8
IN	11.4	594.6	564.0	570.7	568.5	567.4
IN	16.5	598.5	580.3	593.5	591.3	590.2
IN	19.1	630.6	591.3	597.9	596.3	594.7
IN	21.6	653.5	621.8	627.6	627.4	625.6
IN	24.1	650.3	647.4	651.8	649.6	646.5
IN	29.1	684.6	676.3	685.2	683.5	682.4
FUEL INLET TEMP (MPA)	14.11	14.07	14.04	14.11	14.11	13.89
FUEL INLET TEMP (MPA)	13.63	13.57	13.56	13.52	13.41	13.41
FUEL EXIT TEMP (K)	295.4	295.4	295.4	295.4	295.4	295.4
FUEL EXIT TEMP (K)	500.4	495.4	500.4	499.4	499.3	499.3
FLOW METER (CM ³ /S)	1068-U01	1093-U01	1068-U01	1073-U01	1072-U01	1072-U01
VOLTAGE (VOLTS)	2077	2091	2082	2079	2077	2077
CURRENT (AMPS)	1.646	1.642	1.652	1.649	1.647	1.647
HEAT FLUX (W/CM ²)	1.578	1.615	1.603	1.587	1.576	1.576
FUEL FLOW VEL (M/S)	485.5	488.0	487.3	486.1	485.4	485.4
ENERGY BALANCE (FCI)	-13.44	-13.37	-13.04	-12.96	-12.96	-12.96



ORIGINAL PAGE IS
OF POOR QUALITY

ROCKET FUEL DEPOSIT TEST PROGRAM (NATURAL GAS)
RUN 20 MARCH 10-11, 1983

TIME	(MIN)	20.00	21.00	22.00	23.00	24.50
INLET REYNOLDS NO		4370+006	4480+006	4376+006	4397+006	4392+006
AVG PARTICULATION FACTOR		1.001-001	1.004-001	1.016-001	1.012-001	1.022-001
U 0 1.3 CM(W/CM2-K)		1.883	1.911	1.890	1.877	1.866
U 0 3.8 CM(W/CM2-K)		2.352	2.424	2.370	2.369	2.375
U 0 6.4 CM(W/CM2-K)		2.582	2.459	2.564	2.412	2.419
U 0 8.9 CM(W/CM2-K)		2.389	2.432	2.396	2.344	2.391
U 0 11.4 CM(W/CM2-K)		2.554	2.432	2.570	2.579	2.594
U 0 14.0 CM(W/CM2-K)		2.405	2.489	2.572	2.441	2.454
U 0 16.5 CM(W/CM2-K)		2.377	2.462	2.409	2.420	2.424
U 0 19.1 CM(W/CM2-K)		2.602	2.688	2.618	2.637	2.642
U 0 21.6 CM(W/CM2-K)		2.497	2.564	2.505	2.621	2.533
U 0 24.1 CM(W/CM2-K)		2.188-002	2.000-002	5086-002	8611-002	1196-001
U 0 3.8 CM(K-CM2/W)		1.383-001	2.585-002	1.189-001	1.215-001	1.162-001
U 0 6.4 CM(K-CM2/W)		4.967-001	3.687-001	4.742-001	4.678-001	4.541-001
U 0 8.9 CM(K-CM2/W)		3.755-001	2.451-001	3.517-001	3.246-001	3.120-001
U 0 11.4 CM(K-CM2/W)		2.609-001	2.240-001	3.318-001	3.070-001	2.956-001
U 0 14.0 CM(K-CM2/W)		3.741-001	2.477-001	3.335-001	3.216-001	2.995-001
U 0 16.5 CM(K-CM2/W)		4.666-001	2.336-001	3.321-001	3.117-001	2.910-001
U 0 19.1 CM(K-CM2/W)		3.719-001	2.827-001	3.710-001	3.530-001	3.449-001
U 0 21.6 CM(K-CM2/W)		0.000	2.489-001	3.493-001	3.213-001	3.139-001
U 0 24.1 CM(K-CM2/W)		0.000	0.000	0.000	0.000	0.000
U 0 1.3 CM(K-CM2/J)		1.811-004	1.175-004	1.554-004	1.656-004	1.713-004
U 0 3.8 CM(K-CM2/J)		2.383-004	1.355-004	2.073-004	1.905-004	1.713-004
U 0 6.4 CM(K-CM2/J)		5.530-004	4.156-004	4.922-004	4.554-004	4.126-004
U 0 8.9 CM(K-CM2/J)		4.767-004	3.343-004	4.232-004	3.726-004	3.347-004
U 0 11.4 CM(K-CM2/J)		4.958-004	3.343-004	4.318-004	3.809-004	3.425-004
U 0 14.0 CM(K-CM2/J)		5.053-004	3.614-004	4.491-004	4.057-004	3.581-004
U 0 16.5 CM(K-CM2/J)		5.433-004	3.704-004	4.750-004	4.223-004	3.737-004
U 0 19.1 CM(K-CM2/J)		6.104-004	4.246-004	5.268-004	4.730-004	4.242-004
U 0 21.6 CM(K-CM2/J)		5.816-004	4.066-004	5.268-004	4.637-004	4.204-004
U 0 24.1 CM(K-CM2/J)		0.000	0.000	0.000	0.000	0.000



ROCKET FUEL DEPOSIT TEST PROGRAM (NATURAL GAS)
 RUN 21 MARCH 24, 1983

TIME	(MIN)	.0000	1.0000	2.0000	3.0000	4.0000	5.0000	6.0000	7.0000	8.0000	9.0000	10.0000
IN OUT	8	285.9	284.8	289.3	290.4	291.8	279.6	277.6	277.0	278.2	273.7	279.8
IN OUT	8	304.8	304.8	311.7	316.5	322.0	320.9	309.9	304.3	304.4	305.9	310.9
IN OUT	8	324.8	324.8	330.9	335.4	341.7	338.2	327.8	320.8	314.8	315.4	319.3
IN OUT	8	344.5	344.5	350.9	355.7	361.7	358.7	347.8	333.7	330.9	332.8	339.8
IN OUT	8	358.7	358.7	364.3	369.3	374.7	372.0	361.5	345.4	344.8	348.7	354.8
IN OUT	8	417.6	417.6	423.6	428.3	433.7	430.0	419.5	402.6	398.7	390.9	396.4
IN OUT	8	494.5	494.5	500.5	505.4	510.4	506.7	495.5	472.6	473.2	486.9	502.9
IN IN	8	266.1	266.1	272.1	277.1	282.1	278.4	267.5	258.2	259.0	254.6	254.7
IN IN	8	285.6	285.6	291.6	296.6	301.6	297.9	288.4	285.2	285.7	286.9	280.7
IN IN	8	305.6	305.6	311.6	316.6	321.6	317.9	309.7	301.4	295.7	296.3	291.2
IN IN	8	325.6	325.6	331.6	336.6	341.6	337.9	329.7	327.4	328.5	329.5	321.2
IN IN	8	339.5	339.5	345.5	350.5	355.5	351.8	344.4	342.3	343.6	344.6	337.4
IN IN	8	398.5	398.5	404.5	409.5	414.5	410.8	402.6	387.5	389.5	390.9	381.9
IN IN	8	475.9	475.9	481.9	486.9	491.9	488.2	477.0	473.5	474.6	479.6	473.3
IN IN	8	693.9	693.9	699.9	704.9	709.9	706.2	695.0	695.2	696.2	701.9	707.9
FULL INLET P	(MPA)	15.80	15.86	15.80	15.86	15.89	15.86	15.80	15.82	15.82	15.82	15.82
FUEL INLET P	(MPA)	11.89	11.94	11.89	11.94	11.97	11.94	11.89	11.91	11.91	11.91	11.91
FUEL EXIT TEMP	(K)	168.2	168.2	168.2	168.7	169.3	168.2	168.7	168.7	170.4	167.6	167.0
FUEL EXIT TEMP	(K)	235.4	235.4	235.7	235.7	235.7	235.7	235.7	235.7	232.0	231.5	231.5
FLOW RATE	(KG/S)	3.65	3.65	3.65	3.65	3.65	3.65	3.65	3.65	3.65	3.65	3.65
CURRENT	(AMPS)	392.1	392.1	392.1	392.1	392.1	392.1	392.1	392.1	392.1	392.1	392.1
VOLTAGE	(VOLTS)	3.871	3.874	3.860	3.860	3.873	3.864	3.872	3.860	3.864	3.844	3.863
POWER	(KW)	15.17	15.16	15.07	14.98	15.05	15.11	15.08	15.05	15.06	15.03	15.03
HEAT FLOW	(W/CM2)	972.2	971.6	965.8	959.9	967.0	968.4	966.3	964.6	964.9	963.2	963.3
INLET FUEL VLL	(M/S)	34.34	34.31	34.27	34.03	34.51	34.24	34.22	34.33	34.55	34.20	34.31
ENERGY BALANCE	(PCT)	-29.28	-29.96	-30.28	-31.71	-31.89	-32.56	-33.10	-33.45	-34.35	-34.28	-32.77

ORIGINAL PAGE 12
 OF POOR QUALITY

ROCKET FUEL DEPOSIT TEST PROGRAM (NATURAL GAS)
 RUN 21 MARCH 24, 1983

TIME	(MIN)	1.000	2.000	3.000	4.000	5.000	6.000	7.000	8.000	9.000	10.000
INLET REYNOLDS NO		4329+006	4369+006	4360+006	4442+006	4365+006	4384+006	4398+006	4490+006	4380+006	4329+006
AVG FRICTION FACTOR		10.33	9.786	9.647	10.38	10.91	11.16	11.21	11.28	11.79	11.28
U 3	1.3 CM(W/UM2-K)	9.038	8.285	8.044	8.692	8.751	8.854	8.213	8.097	8.584	8.286
U 4	3.8 CM(W/UM2-K)	8.001	7.590	7.696	8.181	8.234	8.242	9.015	8.825	8.504	8.840
U 5	6.4 CM(W/UM2-K)	9.318	8.996	9.084	9.550	9.673	9.682	9.643	10.29	10.00	10.59
U 6	11.4 CM(W/UM2-K)	7.780	7.780	7.821	8.298	8.433	8.593	8.200	9.307	10.00	10.35
U 7	14.0 CM(W/UM2-K)	8.215	8.176	8.243	8.606	8.795	8.748	8.619	10.25	10.36	12.05
U 8	16.5 CM(W/UM2-K)	7.808	7.767	7.951	8.143	8.352	8.188	8.262	7.774	7.994	9.712
U 9	19.1 CM(W/UM2-K)	5.533	5.554	5.740	5.774	5.925	5.917	5.810	5.922	6.162	8.251
U 10	21.6 CM(W/UM2-K)	4.010	4.207	4.503	4.207	4.183	3.948	3.837	3.354	2.965	3.255
U 11	24.1 CM(W/UM2-K)	2.177	2.653	3.221	2.461	2.237	2.343	2.067	1.811	1.880	1.733
U 12	24.1 CM(W/UM2-K)	0.000	5.424-002	6.902-002	0.000	0.000	0.000	0.000	0.000	0.000	0.000
U 13	3.8 CM(W/UM2-K)	7.362-003	1.080-001	1.442-001	5.151-002	4.374-002	3.334-002	1.051-004	2.081-004	3.842-002	0.000
U 14	6.4 CM(W/UM2-K)	1.373-002	8.131-002	6.320-002	0.000	0.000	0.000	0.000	0.000	0.000	0.000
U 15	8.9 CM(W/UM2-K)	1.420-002	5.254-002	4.184-002	0.000	0.000	0.000	0.000	0.000	0.000	0.000
U 16	11.4 CM(W/UM2-K)	0.000	0.000	0.000	0.000	0.000	0.000	0.000	0.000	0.000	0.000
U 17	14.0 CM(W/UM2-K)	0.000	0.000	0.000	0.000	0.000	0.000	0.000	0.000	0.000	0.000
U 18	16.5 CM(W/UM2-K)	0.000	0.000	0.000	0.000	0.000	0.000	0.000	0.000	0.000	0.000
U 19	19.1 CM(W/UM2-K)	0.000	0.000	0.000	0.000	0.000	0.000	0.000	0.000	0.000	0.000
U 20	21.6 CM(W/UM2-K)	0.000	0.000	0.000	0.000	0.000	0.000	0.000	0.000	0.000	0.000
U 21	24.1 CM(W/UM2-K)	0.000	0.000	0.000	0.000	0.000	0.000	0.000	0.000	0.000	0.000
U 22	24.1 CM(W/UM2-K)	0.000	0.000	0.000	0.000	0.000	0.000	0.000	0.000	0.000	0.000
U 23	3.8 CM(W/UM2-K)	9.529-005	7.669-004	6.752-004	1.915-004	9.560-005	4.791-005	0.000	0.000	0.000	0.000
U 24	6.4 CM(W/UM2-K)	2.676-004	5.272-004	1.429-005	0.000	0.000	0.000	0.000	0.000	0.000	0.000
U 25	8.9 CM(W/UM2-K)	0.000	0.000	0.000	0.000	0.000	0.000	0.000	0.000	0.000	0.000
U 26	11.4 CM(W/UM2-K)	0.000	0.000	0.000	0.000	0.000	0.000	0.000	0.000	0.000	0.000
U 27	14.0 CM(W/UM2-K)	0.000	0.000	0.000	0.000	0.000	0.000	0.000	0.000	0.000	0.000
U 28	16.5 CM(W/UM2-K)	0.000	0.000	0.000	0.000	0.000	0.000	0.000	0.000	0.000	0.000
U 29	19.1 CM(W/UM2-K)	0.000	0.000	0.000	0.000	0.000	0.000	0.000	0.000	0.000	0.000
U 30	21.6 CM(W/UM2-K)	0.000	0.000	0.000	0.000	0.000	0.000	0.000	0.000	0.000	0.000
U 31	24.1 CM(W/UM2-K)	0.000	0.000	0.000	0.000	0.000	0.000	0.000	0.000	0.000	0.000
U 32	24.1 CM(W/UM2-K)	0.000	0.000	0.000	0.000	0.000	0.000	0.000	0.000	0.000	0.000
U 33	3.8 CM(W/UM2-K)	8.056-001	3.879-002	4.101-001	7.711-001	8.881-002	0.000	0.000	0.000	0.000	0.000
U 34	6.4 CM(W/UM2-K)	5.404-001	1.435-001	0.000	0.000	0.000	0.000	0.000	0.000	0.000	0.000
U 35	8.9 CM(W/UM2-K)	2.136-005	0.000	0.000	0.000	0.000	0.000	0.000	0.000	0.000	0.000
U 36	11.4 CM(W/UM2-K)	0.000	0.000	0.000	0.000	0.000	0.000	0.000	0.000	0.000	0.000
U 37	14.0 CM(W/UM2-K)	0.000	0.000	0.000	0.000	0.000	0.000	0.000	0.000	0.000	0.000
U 38	16.5 CM(W/UM2-K)	0.000	0.000	0.000	0.000	0.000	0.000	0.000	0.000	0.000	0.000
U 39	19.1 CM(W/UM2-K)	0.000	0.000	0.000	0.000	0.000	0.000	0.000	0.000	0.000	0.000
U 40	21.6 CM(W/UM2-K)	0.000	0.000	0.000	0.000	0.000	0.000	0.000	0.000	0.000	0.000
U 41	24.1 CM(W/UM2-K)	0.000	0.000	0.000	0.000	0.000	0.000	0.000	0.000	0.000	0.000
U 42	24.1 CM(W/UM2-K)	0.000	0.000	0.000	0.000	0.000	0.000	0.000	0.000	0.000	0.000
U 43	3.8 CM(W/UM2-K)	1.378-003	2.742-004	0.000	0.000	0.000	0.000	0.000	0.000	0.000	0.000
U 44	6.4 CM(W/UM2-K)	8.437-003	1.463-003	0.000	0.000	0.000	0.000	0.000	0.000	0.000	0.000
U 45	8.9 CM(W/UM2-K)	7.556-004	0.000	0.000	0.000	0.000	0.000	0.000	0.000	0.000	0.000
U 46	11.4 CM(W/UM2-K)	0.000	0.000	0.000	0.000	0.000	0.000	0.000	0.000	0.000	0.000
U 47	14.0 CM(W/UM2-K)	0.000	0.000	0.000	0.000	0.000	0.000	0.000	0.000	0.000	0.000
U 48	16.5 CM(W/UM2-K)	0.000	0.000	0.000	0.000	0.000	0.000	0.000	0.000	0.000	0.000
U 49	19.1 CM(W/UM2-K)	0.000	0.000	0.000	0.000	0.000	0.000	0.000	0.000	0.000	0.000
U 50	21.6 CM(W/UM2-K)	0.000	0.000	0.000	0.000	0.000	0.000	0.000	0.000	0.000	0.000
U 51	24.1 CM(W/UM2-K)	0.000	0.000	0.000	0.000	0.000	0.000	0.000	0.000	0.000	0.000
U 52	24.1 CM(W/UM2-K)	0.000	0.000	0.000	0.000	0.000	0.000	0.000	0.000	0.000	0.000

ORIGINAL PAGE IS
 OF POOR QUALITY

ORIGINAL PART 77
OF POOR QUALITY

ROCKET FUEL DEPOSIT TEST PROGRAM (NATURAL GAS)
RUN 22 MARCH 28, 1983

TIME	(MIN)	•HUUU	1.183	2.183	3.183	4.183	5.183	6.183	7.183	8.183
IN OUT	1.3	307.6	368.7	354.3	362.6	351.5	374.8	374.7	373.2	371.5
IN OUT	3.8	268.3	313.8	296.5	294.9	279.8	292.6	293.2	279.8	283.2
IN OUT	6.4	275.9	334.8	310.5	310.9	294.3	292.6	293.2	264.3	290.4
IN OUT	8.9	292.7	362.0	327.0	327.6	311.9	309.8	311.9	312.6	307.6
IN OUT	11.4	294.3	383.7	347.6	349.8	322.0	320.4	321.5	322.6	318.2
IN OUT	14.0	314.8	424.3	374.2	349.8	346.3	343.2	347.3	349.5	330.4
IN OUT	16.5	343.2	487.0	451.7	393.7	383.7	387.6	387.6	389.5	385.3
IN OUT	19.1	377.6	567.0	527.0	472.0	450.9	490.4	490.4	517.6	502.6
IN OUT	21.6	490.9	683.2	615.9	699.8	686.5	798.2	890.9	933.7	887.6
IN IN	24.1	662.0	737.6	815.9	860.4	849.8	732.6	552.0	496.5	444.8
IN IN	3.8	288.7	350.5	335.9	344.1	333.1	356.4	355.8	354.8	355.3
IN IN	6.4	247.0	295.5	275.9	263.6	261.4	259.7	260.2	261.5	264.8
IN IN	8.9	274.6	316.6	292.5	278.0	275.9	274.2	274.7	275.9	272.1
IN IN	11.4	280.4	343.8	314.2	296.3	293.1	291.4	292.7	293.7	289.3
IN IN	14.0	292.9	365.5	329.2	296.3	293.0	303.0	303.0	303.3	299.8
IN IN	16.5	292.9	406.0	359.8	308.6	305.9	324.7	325.8	328.1	322.1
IN IN	19.1	328.7	468.8	413.3	331.2	325.3	327.0	327.1	328.1	322.6
IN IN	21.6	358.7	548.8	508.6	375.2	353.5	397.0	397.1	399.3	387.6
IN IN	24.1	472.0	664.9	700.3	453.6	432.5	457.0	471.9	499.3	527.6
FUEL INLET P	1.3	845.1	719.3	797.5	681.9	668.1	714.2	833.6	917.1	974.3
FUEL INLET P	3.8	13.76	13.73	13.50	13.33	13.17	13.00	12.87	12.71	12.49
FUEL INLET TEMP	6.4	12.55	12.45	12.32	12.20	12.00	11.92	11.80	11.69	11.53
FUEL EXIT TEMP	8.9	163.2	194.3	162.0	173.7	173.7	172.6	173.9	174.8	173.8
FUEL EXIT TEMP	11.4	225.9	259.3	246.5	238.2	237.6	236.6	235.9	236.5	235.4
FLOW RATE	14.0	3600-U01	3663-U01	3655-U01	3663-U01	3662-U01	3626-U01	3591-U01	3572-U01	3547-U01
CUMULATIVE	16.5	3569	3563	3653	3721	3714	3708	3736	3755	3697
VOLTAGE	19.1	4.011	4.011	3.968	3.914	3.903	3.914	3.898	3.901	3.904
POWER	21.6	14.38	14.38	14.50	14.56	14.50	14.51	14.55	14.45	14.43
HEAT FLUX	24.1	921.6	921.6	928.8	933.2	928.8	930.0	932.3	926.0	924.7
INLET FUEL VEL		40.06	40.06	36.95	35.40	35.39	34.84	35.67	35.68	35.34
ENERGY BALANCE		-21.22	-24.19	-26.97	-27.35	-27.35	-27.85	-29.13	-29.33	-29.90

ORIGINAL PAGE IS
OF POOR QUALITY

ROCKET FUEL DEPOSIT TLST PROGRAM (NATURAL GAS)
RUN 22 MARCH 28, 1983

TIME	(MIN)	0.000	1.183	2.183	3.183	4.183	5.183	6.183	7.183	8.183
INLET REYNOLDS NO		4000+006	6329+006	5331+006	4748+006	4746+006	4624+006	4784+006	4839+006	4790+006
AVG FRICTION FACTOR		.9804-002	6.027-002	7.819-002	8.134-002	8405-002	5.151	5.210	5.235	5.253
U @ 1.3 CM/W/CM2-K		13.12	10.08	11.04	11.64	11.89	12.01	12.08	11.96	11.29
U @ 3.8 CM/W/CM2-K		12.21	8.692	9.842	10.576	10.78	10.88	10.92	10.81	11.15
U @ 6.9 CM/W/CM2-K		10.65	7.271	8.475	8.817	9.181	9.664	9.615	9.518	9.839
U @ 8.9 CM/W/CM2-K		10.73	6.494	7.861	8.179	8.959	9.268	9.204	9.108	9.400
U @ 11.0 CM/W/CM2-K		9.720	5.237	6.529	6.819	7.959	7.970	7.911	7.756	8.081
U @ 14.5 CM/W/CM2-K		7.938	3.964	4.854	5.847	6.190	6.100	6.017	5.812	6.012
U @ 16.5 CM/W/CM2-K		6.473	3.014	3.538	4.031	4.405	3.941	3.707	3.329	3.438
U @ 19.1 CM/W/CM2-K		5.737	2.061	2.604	2.961	2.111	1.684	1.444	1.346	1.438
U @ 21.6 CM/W/CM2-K		1.539	1.989	1.676	1.538	1.559	1.936	3.100	3.784	4.317
U @ 24.1 CM/W/CM2-K		0.000	3.773-001	3.394-001	5.093-001	3.922-001	6.596-001	6.375-001	6.283-001	6.234-001
U @ 1.3 CM/W/CM2-M		0.000	2.297-001	1.437-001	9.678-002	7.865-002	7.060-002	6.962-002	7.351-002	1.231-001
U @ 3.8 CM/W/CM2-M		0.000	3.318-001	1.973-001	1.261-001	1.089-001	1.002-001	9.736-002	1.065-001	1.285-002
U @ 6.9 CM/W/CM2-M		0.000	4.361-001	2.407-001	1.330-001	1.051-001	9.560-002	1.008-001	1.114-001	7.716-002
U @ 8.9 CM/W/CM2-M		0.000	6.083-001	3.404-001	2.025-001	1.575-001	1.474-001	1.549-001	1.663-001	1.332-001
U @ 11.0 CM/W/CM2-M		0.000	8.805-001	5.028-001	2.803-001	2.307-001	2.258-001	2.353-001	2.605-001	2.086-001
U @ 14.5 CM/W/CM2-M		0.000	1.262	1.441	4.505-001	3.556-001	3.795-001	4.023-001	4.608-001	4.036-001
U @ 16.5 CM/W/CM2-M		0.000	1.830	2.314	9.257-001	7.154-001	9.628-001	1.143	1.444	4.277
U @ 19.1 CM/W/CM2-M		0.000	0.000	0.000	2.061	2.061	3.263	0.000	0.000	4.279
U @ 21.6 CM/W/CM2-M		0.000	0.000	0.000	6.001-003	0.000	0.000	0.000	0.000	0.000
U @ 24.1 CM/W/CM2-M		0.000	9.338-003	3.835-003	3.045-003	1.842-003	2.324-003	1.227-003	1.643-003	1.407-003
U @ 1.3 CM/W/CM2-J		0.000	7.555-003	2.495-003	9.973-004	6.871-004	4.802-004	4.176-004	3.897-004	4.180-004
U @ 3.8 CM/W/CM2-J		0.000	8.998-003	3.196-003	1.153-003	7.862-004	5.762-004	4.779-004	3.181-004	3.181-004
U @ 6.9 CM/W/CM2-J		0.000	1.044-002	3.192-003	1.184-003	7.624-004	5.700-004	4.779-004	3.039-004	3.039-004
U @ 8.9 CM/W/CM2-J		0.000	1.290-002	3.972-003	1.558-003	9.768-004	7.298-004	6.424-004	4.584-004	4.160-004
U @ 11.0 CM/W/CM2-J		0.000	1.672-002	5.205-003	1.963-003	1.263-003	9.795-004	8.212-004	7.933-004	5.628-004
U @ 14.5 CM/W/CM2-J		0.000	2.195-002	7.442-003	2.836-003	1.739-003	1.460-003	1.285-003	1.233-003	9.471-004
U @ 16.5 CM/W/CM2-J		0.000	2.895-002	1.426-002	5.208-003	3.145-003	3.380-003	3.260-003	3.507-003	4.775-003
U @ 19.1 CM/W/CM2-J		0.000	2.937-002	1.872-002	1.172-002	8.366-003	1.062-002	1.156-002	1.100	8.736-003
U @ 21.6 CM/W/CM2-J		0.000	0.000	0.000	0.000	0.000	0.000	0.000	0.000	0.000
U @ 24.1 CM/W/CM2-J		0.000	0.000	0.000	0.000	0.000	0.000	0.000	0.000	0.000

ROCKET FUEL DEPOSIT TEST PROGRAM (NATURAL GAS)
 RUN 23 MARCH 25, 1983

TITLE	(MIN)	(NO)	1.000	2.000	3.000	4.000	5.000	6.000	7.000	8.000	9.000	10.00
INLET FUEL FLOW (G/S)	1.3	256.5	255.4	263.2	253.2	254.3	253.2	253.9	254.5	256.5	256.5	257.0
INLET FUEL TEMP (°C)	3.8	290.4	292.0	263.2	262.0	262.0	260.9	263.9	262.0	263.2	262.6	262.6
INLET FUEL PRESS (PSIA)	6.9	304.8	307.0	292.0	292.0	292.0	291.5	292.0	292.0	293.7	292.6	292.6
INLET FUEL BALANCE (PCT)	11.4	320.4	323.6	306.5	306.5	306.5	306.5	306.5	306.5	308.2	307.0	307.0
INLET FUEL VELOCITY (M/S)	16.5	334.8	335.9	322.6	322.6	322.6	322.6	322.6	322.6	324.3	323.8	323.8
INLET FUEL BALANCE (PCT)	19.1	349.8	355.9	335.6	335.6	335.6	335.6	335.6	335.6	337.6	336.0	336.0
INLET FUEL VELOCITY (M/S)	21.0	370.0	370.0	350.9	350.9	350.9	350.9	350.9	350.9	352.6	352.6	352.6
INLET FUEL BALANCE (PCT)	24.0	405.4	413.3	381.5	381.5	381.5	381.5	381.5	381.5	384.5	384.5	384.5
INLET FUEL VELOCITY (M/S)	3.8	449.8	433.3	425.4	425.4	425.4	425.4	425.4	425.4	432.2	427.6	427.6
INLET FUEL BALANCE (PCT)	1.3	238.8	238.8	239.9	239.9	239.9	238.9	238.9	238.9	241.6	240.7	240.7
INLET FUEL VELOCITY (M/S)	6.9	268.3	269.9	269.9	269.9	269.9	269.9	269.9	269.9	271.8	270.7	270.7
INLET FUEL BALANCE (PCT)	11.4	298.3	299.9	284.4	284.4	284.4	284.4	284.4	284.4	286.3	285.1	285.1
INLET FUEL VELOCITY (M/S)	16.5	312.7	313.9	300.5	300.5	300.5	300.5	300.5	300.5	302.3	301.2	301.2
INLET FUEL BALANCE (PCT)	19.1	327.7	333.8	313.9	313.9	313.9	313.9	313.9	313.9	316.8	315.9	315.9
INLET FUEL VELOCITY (M/S)	24.0	387.7	390.9	330.9	330.9	330.9	330.9	330.9	330.9	332.7	330.9	330.9
INLET FUEL BALANCE (PCT)	1.3	617.2	617.2	490.9	490.9	490.9	490.9	490.9	490.9	507.9	507.9	507.9
INLET FUEL VELOCITY (M/S)	3.8	427.7	427.7	391.6	391.6	391.6	391.6	391.6	391.6	405.7	405.7	405.7
INLET FUEL BALANCE (PCT)	6.9	13.83	13.83	13.37	13.37	13.37	13.37	13.37	13.37	13.37	13.31	13.28
INLET FUEL VELOCITY (M/S)	11.4	10.69	10.69	10.34	10.34	10.34	10.34	10.34	10.34	10.34	10.31	10.28
INLET FUEL BALANCE (PCT)	16.5	155.9	156.5	156.5	156.5	156.5	155.4	155.4	155.4	158.2	157.6	157.6
INLET FUEL VELOCITY (M/S)	23.3	233.2	233.2	230.9	230.9	230.9	230.9	230.9	230.9	230.9	230.9	230.9
INLET FUEL BALANCE (PCT)	36.42	363.9	363.9	363.9	363.9	363.9	363.9	363.9	363.9	364.1	364.1	364.2
INLET FUEL VELOCITY (M/S)	43.04	430.4	432.4	432.4	432.4	432.4	432.4	432.4	432.4	431.6	431.6	431.6
INLET FUEL BALANCE (PCT)	4.047	4.047	4.047	4.047	4.047	4.047	4.047	4.047	4.047	4.047	4.047	4.047
INLET FUEL VELOCITY (M/S)	17.42	17.45	17.45	17.45	17.45	17.45	17.45	17.45	17.45	17.45	17.45	17.45
INLET FUEL BALANCE (PCT)	11.8	11.8	11.8	11.8	11.8	11.8	11.8	11.8	11.8	11.8	11.8	11.8
INLET FUEL VELOCITY (M/S)	32.46	32.51	32.49	32.49	32.49	32.49	32.49	32.49	32.49	32.47	32.47	32.47
INLET FUEL BALANCE (PCT)	30.78	31.97	33.72	33.76	33.83	33.83	33.83	33.83	33.83	34.01	34.01	34.01

ORIGINAL PAGE IS
 OF POOR QUALITY

ROCKET FUEL DEPOSIT TEST PROGRAM (NATURAL GAS)
 RUN 23 MARCH 25, 1983

TIME	(MIN)	0.000	1.000	2.000	3.000	4.000	5.000	6.000	7.000	8.000	9.000	10.00
INLET REYNOLDS NO		3700+006	3659+006	3665+006	3662+006	3667+006	3630+006	3606+006	3640+006	3754+006	3731+006	3725+006
AVG FRICTION FACTOR		2471-001	2498-001	2542-001	2570-001	2582-001	2590-001	2593-001	2594-001	2594-001	2568-001	2575-001
U 3	1.5	15.32	15.08	13.85	15.30	15.51	15.60	15.37	15.30	15.24	15.11	14.99
U 4	3.0	15.91	15.65	15.29	15.34	15.43	15.52	15.41	15.34	15.24	15.11	15.35
U 5	6.0	12.24	11.00	11.85	11.78	11.76	11.74	11.61	11.56	11.36	11.69	11.68
U 6	9.0	11.40	11.13	11.05	10.91	10.96	10.88	10.82	10.71	10.80	10.81	10.87
U 7	11.0	10.56	10.38	10.24	10.06	10.10	10.03	9.934	9.839	9.946	10.01	10.09
U 8	14.0	9.555	9.755	9.639	9.464	9.495	9.523	9.484	9.339	9.346	9.212	9.099
U 9	16.0	9.323	9.191	9.902	9.665	9.695	9.827	9.322	9.816	8.513	8.270	8.140
U 10	19.0	4.440	4.076	3.920	4.016	3.867	3.750	3.769	3.843	3.755	3.750	3.605
U 11	21.0	2.440	2.822	3.520	3.621	3.867	3.477	3.591	3.723	3.699	3.607	3.778
U 12	24.0	5.350	5.626	6.410	6.797	7.000	6.000	6.174	6.474	6.593	6.207	6.262
T/K 1	1.5	0.000	1.032-002	6.905-002	9.173-004	0.000	0.000	0.000	5.727-004	3.498-003	9.017-003	1.483-002
T/K 2	3.0	0.000	1.017-002	2.521-002	2.316-002	1.927-002	1.554-002	2.111-002	2.331-002	2.222-002	2.221-002	2.262-002
T/K 3	6.0	0.000	1.633-002	2.708-002	3.165-002	3.299-002	3.455-002	4.000-002	4.831-002	4.382-002	3.648-002	3.898-002
T/K 4	9.0	0.000	2.169-002	2.835-002	3.944-002	3.589-002	4.252-002	4.095-002	5.694-002	4.664-002	4.285-002	4.339-002
T/K 5	11.0	0.000	1.715-002	2.967-002	4.728-002	4.383-002	5.057-002	5.995-002	7.068-002	5.860-002	5.239-002	5.296-002
T/K 6	14.0	0.000	4.266-002	4.084-002	5.998-002	5.661-002	5.348-002	8.365-002	8.774-002	7.332-002	8.672-002	8.024-001
T/K 7	16.0	0.000	1.402-001	1.930-001	1.176-001	1.452-001	3.535-001	3.222-001	2.892-001	1.281-001	1.712-001	1.819-001
T/K 8	19.0	0.000	0.000	0.000	0.000	0.000	0.000	0.000	0.000	0.000	0.000	0.000
T/K 9	21.0	0.000	0.000	0.000	0.000	0.000	0.000	0.000	0.000	0.000	0.000	0.000
T/K 10	24.0	0.000	0.000	0.000	0.000	0.000	0.000	0.000	0.000	0.000	0.000	0.000
KC 1	1.5	0.000	0.000	4.969-004	0.000	0.000	0.000	0.000	0.000	0.000	0.000	8.366-005
KC 2	3.0	0.000	0.000	1.242-004	5.525-005	2.075-005	0.000	0.000	0.000	3.133-005	1.858-005	1.673-005
KC 3	6.0	0.000	0.000	1.242-004	8.288-005	6.224-005	3.324-005	4.153-005	4.760-005	6.266-005	3.716-005	3.346-005
KC 4	9.0	0.000	0.000	1.242-004	1.1361-004	8.299-005	6.649-005	6.922-005	8.331-005	7.310-005	4.646-005	4.183-005
KC 5	11.0	0.000	0.000	2.070-004	1.934-004	1.245-004	6.649-005	5.238-005	8.331-005	9.399-005	1.022-004	1.171-004
KC 6	14.0	0.000	0.000	4.969-004	4.420-004	3.112-004	1.662-004	1.246-004	1.071-004	1.984-004	2.509-004	2.426-004
KC 7	16.0	0.000	0.000	1.408-003	7.735-004	4.357-004	0.000	0.000	0.000	6.161-004	5.482-004	0.000
KC 8	19.0	0.000	0.000	0.000	0.000	0.000	0.000	0.000	0.000	0.000	0.000	0.000
KC 9	21.0	0.000	0.000	0.000	0.000	0.000	0.000	0.000	0.000	0.000	0.000	0.000
KC 10	24.0	0.000	0.000	0.000	0.000	0.000	0.000	0.000	0.000	0.000	0.000	0.000

ORIGINAL PAGE IS
 OF POOR QUALITY

ROCKET FULL DEPOSIT TEST PROGRAM (NATURAL GAS)
 RUN 24 MARCH 25, 1963

TIME	(MIN)	0000	1.000	2.000	3.000	4.000	5.000	6.000	7.000	8.000	9.000	10.00
IN	OUT	IN	OUT	IN	OUT	IN	OUT	IN	OUT	IN	OUT	IN
1.3	1.3	274.5	285.9	291.4	293.2	293.7	296.5	294.4	303.9	318.2	314.8	309.8
1.4	1.4	283.7	286.5	290.4	293.2	293.7	296.5	294.4	303.9	318.2	314.8	309.8
1.5	1.5	298.6	299.3	305.2	304.3	307.6	308.7	311.4	312.5	315.9	317.8	316.8
1.6	1.6	319.9	320.4	325.8	327.6	329.4	335.9	335.2	341.5	346.5	349.3	350.9
1.7	1.7	333.7	343.4	354.8	360.4	372.6	378.2	388.7	402.9	421.9	439.3	450.5
1.8	1.8	339.3	393.0	423.7	464.3	510.9	538.2	553.2	555.9	553.2	545.4	524.8
1.9	1.9	426.5	487.0	524.3	588.7	560.4	586.5	587.0	573.2	553.2	529.3	524.8
2.0	2.0	572.6	407.6	437.6	543.2	542.0	592.6	594.3	575.2	555.2	541.7	522.6
2.1	2.1	883.7	427.6	475.4	603.7	579.8	595.9	594.3	575.2	555.2	541.7	522.6
2.2	2.2	252.6	262.9	267.0	266.5	266.9	268.8	271.5	275.5	290.5	287.4	277.1
2.3	2.3	261.5	272.7	278.6	277.5	286.8	285.0	287.4	287.4	290.5	287.4	277.1
2.4	2.4	273.7	276.8	280.8	277.5	286.8	285.0	287.4	287.4	290.5	287.4	277.1
2.5	2.5	293.7	321.8	300.8	300.2	307.5	308.3	311.4	313.4	316.9	322.0	323.0
2.6	2.6	311.5	370.1	399.2	437.2	445.2	510.5	525.4	528.2	528.3	517.9	499.0
2.7	2.7	317.0	463.5	499.7	560.9	533.1	538.3	520.5	512.1	501.8	501.8	497.3
2.8	2.8	404.4	384.0	413.1	516.5	515.3	554.9	550.3	548.2	527.0	516.2	514.5
2.9	2.9	661.5	404.0	450.8	577.0	553.1	568.3	560.5	548.2	527.0	516.2	514.5
3.0	3.0	13.91	13.93	13.91	13.95	13.81	13.71	13.62	13.51	13.41	13.32	13.24
3.1	3.1	10.46	10.40	10.45	10.43	10.33	10.08	9.728	9.718	9.713	9.717	9.711
3.2	3.2	167.6	164.8	162.9	160.4	158.7	157.0	157.0	156.5	157.9	158.2	158.7
3.3	3.3	241.5	244.8	249.5	258.2	258.2	261.5	262.0	260.4	259.3	259.3	258.7
3.4	3.4	363.3	363.3	362.7	361.6	362.4	363.7	363.7	364.3	363.8	364.6	364.3
3.5	3.5	4248.	4384.	4374.	4364.	4398.	4398.	4375.	4403.	4379.	4370.	4370.
3.6	3.6	4.121	4.235	4.420	4.819	4.795	4.956	4.975	4.955	4.964	4.954	4.946
3.7	3.7	17.51	18.57	19.34	21.03	21.04	21.80	21.87	21.82	21.74	21.65	21.68
3.8	3.8	1122.	1190.	1239.	1348.	1351.	1397.	1401.	1398.	1393.	1387.	1389.
3.9	3.9	34.06	33.63	33.25	32.83	32.68	32.56	32.56	32.54	32.52	32.80	32.85
4.0	4.0	-31.79	-30.48	-27.74	-25.63	-24.58	-23.36	-22.52	-22.75	-22.50	-24.96	-25.84

ORIGINAL PAGE IS
 OF POOR QUALITY

ROCKET FUEL DEPOSIT TEST PROGRAM (NATURAL GAS)
 RUN 24 MARCH 25, 1983

TIME	(MIN)	0000	1.000	2.000	3.000	4.000	5.000	6.000	7.000	8.000	9.000	10.000
INLET	HELYMOLUS	4.322+000	4.143+006	3.995+006	3.851+006	3.767+006	3.651+006	3.601+006	3.669+006	3.721+006	3.759+006	3.787+004
AVG	1.5	13.584	12.772	12.119	11.312	10.604	10.000	9.493	9.000	8.689	8.378	8.051
U	3.8	15.46	13.822	13.733	15.11	14.68	15.06	14.95	14.54	13.94	13.78	13.17
U	6.9	14.47	13.09	13.73	12.53	13.90	14.27	14.11	13.52	13.23	13.07	12.80
U	11.4	13.60	11.44	11.48	12.68	11.89	12.18	12.02	11.56	11.08	10.77	10.20
U	14.0	10.87	9.835	11.629	10.38	9.492	9.502	8.944	8.171	7.311	6.667	6.322
U	16.5	11.06	7.376	6.559	6.033	4.992	4.719	4.511	4.444	4.425	4.552	4.869
U	19.1	11.89	4.824	3.944	4.000	4.333	4.458	4.652	4.853	4.942	4.933	5.077
U	21.6	6.189	4.561	4.553	4.106	4.500	4.319	4.331	4.495	4.749	4.955	4.947
U	24.1	1.799	7.969	7.008	4.938	4.969	4.377	4.376	4.608	4.909	5.099	4.937
I/K	1.5	0.000	6.634-002	8.719-002	10.92-002	4.420-002	4.477-002	4.721-002	9.191-002	1.981-001	1.548-001	1.48-001
I/K	3.8	0.000	6.649-002	6.918-002	2.807-002	2.331-002	5.293-002	9.769-002	2.893-002	6.372-002	2.671-002	4.890-002
I/K	6.9	0.000	9.147-002	8.919-002	1.581-002	4.733-002	2.851-002	3.682-002	5.643-002	8.352-002	2.956-002	4.652-002
I/K	11.4	0.000	1.388-001	1.957-001	5.349-002	1.082-001	8.573-002	9.703-002	1.299-001	1.622-001	1.350-001	1.506-001
I/K	16.5	0.000	1.890-001	2.108-001	1.356-001	2.256-001	2.246-001	2.903-001	3.961-001	5.400-001	6.722-001	1.739-001
I/K	19.1	0.000	4.354-001	6.042-001	7.371-001	1.083	1.199	1.296	1.330	1.339	1.271	1.333
I/K	21.6	0.000	1.760-001	5.806-001	8.200-001	1.546	1.339	1.246	1.157	1.119	1.099	1.066
I/K	24.1	0.000	0.000	0.000	0.000	0.000	0.000	0.000	0.000	0.000	0.000	0.000
K	1.5	0.000	1.634-003	1.158-003	7.785-004	5.995-004	5.303-004	4.756-004	4.919-004	6.563-004	5.133-004	3.666-004
K	3.8	0.000	2.179-003	1.046-003	6.640-004	5.481-004	4.375-004	3.455-004	3.592-004	4.823-004	3.559-004	2.333-004
K	6.9	0.000	3.113-003	1.831-003	8.472-004	7.365-004	9.016-004	5.286-004	4.822-004	4.923-004	4.233-004	3.333-004
K	11.4	0.000	4.124-003	2.616-003	1.214-003	1.113-003	1.439-003	7.372-004	7.372-004	7.228-004	6.893-004	6.190-004
K	16.5	0.000	8.404-003	6.053-003	1.855-003	1.747-003	1.879-003	1.350-003	1.664-003	1.329-003	1.249-003	1.570-003
K	19.1	0.000	2.070-002	1.468-002	5.381-003	5.468-003	4.879-003	4.350-003	3.784-003	3.323-003	2.829-003	2.226-003
K	21.6	0.000	1.159-002	6.576-003	1.024-002	6.868-003	5.409-003	4.262-003	3.419-003	2.899-003	2.335-003	1.866-003
K	24.1	0.000	0.000	0.000	0.000	0.000	0.000	0.000	0.000	0.000	0.000	0.000
K	24.1	0.000	0.000	0.000	0.000	0.000	0.000	0.000	0.000	0.000	0.000	0.000

ORIGINAL FILED
 OF POOR QUALITY

ROCKET FUEL DEPOSIT TEST PROGRAM (RP-1 FUEL)
 RUN D NOVEMBER 24, 1962

TYPE	(MIN)	0.0000	1.0033	2.0033	3.0017	4.0017	5.0017	6.0017	7.0017	8.0017	9.0017	10.002
OUT	1.0	698.7	658.2	611.5	610.4	614.8	690.4	694.7	638.2	651.5	664.6	665.9
OUT	1.0	682.6	680.6	690.4	710.4	717.0	710.4	717.0	724.4	715.0	702.6	710.4
OUT	1.0	675.0	679.8	683.2	649.8	660.5	649.8	660.5	669.8	667.0	667.0	675.0
OUT	1.0	672.0	670.9	673.2	631.0	647.8	631.0	647.8	652.0	652.0	652.0	662.0
OUT	1.0	652.6	655.4	656.5	648.2	648.2	642.0	642.0	633.2	632.0	628.2	633.0
OUT	1.0	635.4	640.9	647.6	646.2	651.5	646.2	652.0	646.5	638.0	640.4	635.0
OUT	1.0	648.2	639.6	647.0	663.2	670.8	663.2	673.7	678.4	682.0	683.7	685.9
OUT	1.0	680.0	662.4	672.0	591.8	596.4	591.8	610.0	619.4	632.0	646.5	646.5
OUT	1.0	664.0	664.0	664.0	671.8	698.0	671.8	680.0	665.0	696.0	683.9	669.5
OUT	1.0	660.0	661.0	664.0	656.8	641.0	656.8	650.0	651.0	678.0	651.2	661.5
OUT	1.0	660.0	672.0	656.8	631.0	641.0	631.0	631.0	633.0	637.0	637.0	651.0
OUT	1.0	650.0	661.0	657.0	622.0	622.0	622.0	622.0	624.0	623.0	624.0	626.0
OUT	1.0	639.0	636.8	647.0	623.0	641.0	623.0	618.0	614.0	623.0	616.0	620.0
OUT	1.0	621.8	621.0	638.0	627.0	629.0	627.0	629.0	610.0	610.0	609.0	612.0
OUT	1.0	616.8	622.0	629.2	629.6	630.8	629.6	633.0	627.8	619.0	621.7	620.0
OUT	1.0	620.6	629.6	628.7	644.6	653.0	628.7	655.0	660.0	663.0	665.1	666.1
OUT	1.0	14.35	14.33	14.29	14.21	14.25	14.21	14.18	14.15	14.11	14.08	14.03
OUT	1.0	13.21	13.19	13.16	13.10	13.06	13.10	13.06	13.04	13.00	12.97	12.93
OUT	1.0	29.03	29.43	29.43	29.37	29.43	29.37	29.37	29.37	28.98	29.37	29.49
OUT	1.0	380.9	380.4	379.3	379.3	379.3	379.3	381.5	381.5	381.5	381.5	381.5
OUT	1.0	280.0	280.0	278.0	283.9	279.3	283.9	283.2	286.2	287.2	287.2	287.2
OUT	1.0	5.112	5.157	5.195	5.197	5.210	5.197	5.152	5.150	5.134	5.107	5.138
OUT	1.0	14.62	14.61	14.49	14.62	14.55	14.62	14.74	14.74	14.74	14.84	14.84
OUT	1.0	936.9	936.2	928.3	936.6	932.3	936.6	944.6	944.4	944.6	941.8	951.1
OUT	1.0	30.52	30.49	30.46	30.41	30.44	30.41	30.36	30.28	30.08	30.25	30.31
OUT	1.0	-5.188	-5.857	-6.474	-6.670	-6.958	-6.670	-5.162	-5.388	-1.621	-5.218	-4.667

ORIGINAL COPY
 OF POOR QUALITY

ROCKET FUEL DEPOSIT TEST PROGRAM (NATURAL GAS)
 RUN 220 MARCH 24, 1983

TIME	(MIN)	0.000	0.883	1.883	2.883	3.883	4.883	5.883	6.883	7.883	8.883	10.38
IN OUT	0	282.0	287.0	289.9	298.7	298.7	274.0	274.0	30.9	317.0	305.4	297.0
IN OUT	0	289.3	286.5	278.0	292.6	292.6	265.0	265.0	33.3	316.0	305.4	293.0
IN OUT	0	294.0	286.5	285.5	295.5	295.5	286.5	286.5	35.1	332.0	315.6	301.0
IN OUT	0	320.9	313.9	311.5	322.9	322.9	312.0	312.0	37.6	354.8	335.4	314.0
IN OUT	0	356.5	334.3	329.8	340.9	340.9	290.4	290.4	42.0	457.6	385.4	363.5
IN OUT	0	347.5	334.3	345.4	343.2	343.2	317.6	317.6	48.0	503.2	421.5	405.5
IN OUT	0	369.2	352.0	401.5	423.2	423.2	348.2	348.2	51.8	575.9	537.0	526.5
IN OUT	0	432.0	419.3	488.2	511.5	511.5	420.4	420.4	62.4	654.3	614.0	593.7
IN OUT	0	813.2	619.3	576.7	520.9	520.9	434.3	434.3	69.5	695.0	666.1	653.7
IN OUT	0	266.7	266.7	269.8	272.7	272.7	242.5	242.5	72.1	729.7	729.7	729.7
IN OUT	0	274.5	260.3	256.7	272.7	272.7	242.5	242.5	72.1	729.7	729.7	729.7
IN OUT	0	274.5	260.3	256.7	272.7	272.7	242.5	242.5	72.1	729.7	729.7	729.7
IN OUT	0	300.0	293.9	291.4	302.9	302.9	269.7	269.7	84.3	835.7	813.2	795.9
IN OUT	0	316.2	305.1	308.1	321.3	321.3	270.8	270.8	94.3	930.5	902.2	882.0
IN OUT	0	327.5	314.9	309.8	331.3	331.3	298.0	298.0	102.2	1022.2	1002.2	982.0
IN OUT	0	349.5	331.7	325.3	363.3	363.3	308.6	308.6	115.2	1152.2	1135.2	1115.0
IN OUT	0	415.0	390.7	381.4	433.3	433.3	347.0	347.0	149.9	1499.9	1484.0	1466.8
IN OUT	0	592.5	518.5	468.1	491.8	491.8	400.6	400.6	205.4	2055.4	2005.4	1947.3
IN OUT	0	792.8	599.1	502.5	501.3	501.3	440.8	440.8	276.5	276.8	276.5	276.3
FUEL INLET P	(MPA)	14.70	14.70	14.52	14.45	14.23	14.23	14.07	14.19	14.03	13.96	13.76
FUEL INLET TEMP	(K)	13.03	12.98	12.98	12.61	12.61	12.20	12.20	11.91	11.85	11.79	11.63
FUEL INLET TEMP	(K)	162.0	155.4	154.8	160.9	160.9	133.2	133.2	200.9	190.4	179.8	170.9
FUEL EXIT TEMP	(K)	239.0	231.5	227.0	233.6	233.6	203.3	203.3	274.3	260.9	248.2	238.2
FUEL EXIT TEMP	(K)	363.9	359.5	362.3	370.1	370.1	338.9	338.9	357.0	342.9	332.7	325.0
CURRENT	(AMPS)	0.010	0.102	0.169	0.109	0.109	0.330	0.330	0.617	0.663	0.957	1.365
VOLTAGE	(VOLTS)	3.990	3.878	3.790	3.779	3.779	3.401	3.401	4.101	4.049	3.963	3.840
POWER	(KW)	16.04	15.91	15.80	15.41	15.41	15.41	15.41	14.84	15.06	15.20	15.11
HEAT FLUX	(W/CM ²)	1026.0	1019.7	1012.0	993.7	993.7	967.1	967.1	950.6	965.2	973.7	968.3
INLET FUEL VEL	(M/S)	33.37	31.97	32.23	33.68	33.68	29.42	29.42	40.82	38.99	36.50	34.78
ENERGY BALANCE	(PCT)	-23.50	-26.62	-29.41	-26.10	-26.10	-27.00	-27.00	-18.52	-18.83	-23.82	-27.48

ORIGINAL PAGE IS
 OF POOR QUALITY

ROCKET FUEL DEPOSIT TEST PROGRAM (NATURAL GAS)
 RUN 220 MARCH 24, 1983

TIME	(MIN)	0.000	1.883	2.883	3.883	4.883	5.883	6.883	7.883	8.883	10.38
AVG FUEL	AVG FUEL	40.00	35.65	32.75	30.74	29.75	29.84	29.25	29.27	29.17	29.17
AVG FUEL	AVG FUEL	13.33	10.97	8.725	8.676	8.366	8.366	8.444	8.279	8.417	8.417
U 3	U 3	10.71	10.90	9.645	9.816	10.00	10.00	9.285	10.01	10.14	10.14
U 3	U 3	11.82	11.09	9.777	10.26	10.91	10.91	9.384	10.201	9.818	10.42
U 3	U 3	8.231	8.401	7.724	8.501	9.066	9.066	7.193	8.002	8.262	9.571
U 3	U 3	11.4	8.019	8.019	9.196	10.44	11.77	5.580	5.726	6.270	6.835
U 3	U 3	16.5	8.725	6.915	8.220	10.02	9.784	3.792	4.612	5.270	5.831
U 3	U 3	19.1	5.718	5.566	6.372	8.319	8.177	3.145	3.895	4.468	5.160
U 3	U 3	21.6	3.416	4.073	5.264	8.044	6.473	2.779	3.079	3.397	3.946
U 3	U 3	24.1	2.745	3.372	3.681	7.253	5.359	2.107	2.502	2.725	3.459
I/K	I/K	1.221	1.655	2.123	2.333	2.615	2.62	1.968	1.478	1.281	1.353
I/K	I/K	0.000	0.000	1.127	1.461	1.741	0.000	1.528	1.747	1.150	1.353
I/K	I/K	0.000	1.362	1.193	0.710	1.269	0.000	2.672	1.833	1.198	1.303
I/K	I/K	0.000	1.442	2.115	0.931	1.981	0.000	3.070	1.663	4.198	0.000
I/K	I/K	0.000	3.028	0.864	0.000	0.000	0.000	6.321	5.862	7.040	3.029
I/K	I/K	0.000	0.000	2.524	0.000	0.000	0.000	1.123	0.974	4.369	5.212
I/K	I/K	0.000	0.000	4.610	2.339	0.000	0.000	1.302	1.232	7.028	6.026
I/K	I/K	0.000	0.000	5.503	0.000	0.000	0.000	1.275	1.343	10.39	6.291
I/K	I/K	0.000	0.000	0.000	0.000	0.000	0.000	4.738	4.348	11.51	0.000
I/K	I/K	0.000	0.000	0.000	0.000	0.000	0.000	0.000	0.000	0.000	0.000
I/K	I/K	0.000	6.312	2.078	6.953	0.000	2.002	1.233	7.504	4.48	2.348
K 3	K 3	0.000	0.000	1.458	1.440	0.000	0.000	1.118	5.963	3.104	2.348
K 3	K 3	0.000	0.000	1.458	2.399	0.000	0.000	1.118	5.963	3.104	2.348
K 3	K 3	0.000	0.000	1.912	7.198	0.000	0.000	1.443	8.143	3.960	6.446
K 3	K 3	0.000	0.000	1.134	0.000	0.000	0.000	2.200	7.422	4.236	1.05
K 3	K 3	0.000	0.000	2.042	0.000	0.000	0.000	3.382	1.606	9.419	4.236
K 3	K 3	0.000	0.000	3.176	5.758	0.000	0.000	3.774	2.920	1.424	7.551
K 3	K 3	0.000	0.000	3.532	0.000	0.000	0.000	3.594	3.068	1.766	8.564
K 3	K 3	0.000	0.000	0.000	0.000	0.000	0.000	2.977	9.128	3.211	0.000
K 3	K 3	0.000	0.000	0.000	0.000	0.000	0.000	0.000	0.000	0.000	0.000

ORIGINAL PAGE IS
 OF POOR QUALITY